SEISMIC PERFORMANCE AND DISASTER MANAGEMENT OF INTERDEPENDENT CRITICAL INFRASTRUCTURES

MAHDI FARAJI

2012

SUMMARY

Modern societies are becoming increasingly dependent on critical infrastructure systems specially lifelines to provide essential services that support economic prosperity and quality of life. Water distribution systems, electrical power transmission systems, and other lifeline systems are not alone but interdependent at multiple levels. Interdependencies enhance the overall system performance while also increasing the potential for cascading failures and amplifying the impact of small failures into catastrophic events. For instance, the recent Fukushima nuclear power plant catastrophe on March 11, 2011, initially triggered by small functional problem in water cooling system which attacked by tsunami.

To understand the cascading failures among infrastructure systems under random incidents, man made attacks and natural hazards, many researchers have proposed different methods for modeling and simulation of interdependent infrastructure systems. Notable examples include Agent Based Methods (ABM), Inoperability Input output Methods (IIM), System Dynamics Methods (SDM), Network or Graph Based Methods (NBM) and Data Driven Methods (DDM).

In this study, at first the characteristics of critical infrastructures are illustrated and damage scales for network components are defined. Then the approaches for critical infrastructure modeling are investigated and network properties based on graph theory are described. As a next step, seismic hazard analysis of distributed infrastructure is done by using the regional siesmicity data. After that the concept of reliability modeling of infrastructure is described and some network performance properties are introduced. By using the individual infrastructure performance, the reliability of interdependent infrastructures is illustrated based on probabilistic model. Finally, the results are summarized to manage the interdependent infrastructure disaster and predict the restoration period and necessary number of repair man-power. All of the theories and algorithms are applied on a case study.

In order to better understand the critical infrastructure role in a society and also learn more about components of interdependent critical infrastructure and their seismic performance, this research illustrates the characteristics of critical infrastructures and presents a literature review on the recent advances in the fields of complex networks, network topology, network dynamics, and interconnected systems.

The approaches for critical infrastructure modeling are illustrated and the graph based method is considered which uses nodes to represent different types of system components and links to mimic the physical and relational connections among them, provides affordable and intuitive system representations along with detailed descriptions of their topology and flow patterns. This method can analyze the effects of system topology, element physical fragility, and

attack intensity on system performance levels which are measured by connectivity and flow delivery.

For seismic risk assessment of a facility or a building is generally specified by one of two basic approaches: through a probabilistic seismic hazard analysis (PSHA) and a stipulated scenario earthquake (SE). A PSHA has been widely accepted as a basis for design and evaluation of individual buildings, bridges and other facilities. However, the vulnerability assessment of distributed infrastructure facilities requires a model of spatial intensity of earthquake ground motion. Since the ground motions from a PSHA represent an aggregation of earthquakes, they cannot model the spatial variation in intensity. For these purposes, alternatives for characterizing the seismic demands on infrastructure systems are illustrated. Attenuation equations for the peak ground acceleration and the peak ground velocity, the local soil amplification factors and the spatial correlation of seismic intensities are introduced. The applicability of the probabilistic seismic hazard analysis approach is considered to a spatially distributed infrastructure system and the hazard map is illustrated. Therefore fragility curves of different infrastructure components are used for seismic vulnerability analysis of individual network components.

Based on the above results, the fundamental concepts of reliability are introduced and the reliability analysis of individual infrastructure systems subjected to spatially correlated seismic demands is done which its results are used for next step.

For modeling the interdependency between critical infrastructures, two important issues of modern interdependent critical infrastructure systems are studied in this research. First the network response under seismic hazard is assessed; then the increased vulnerability due to coupling between networks is analyzed.

The probability reliability model is developed encompasses the spatial distribution of the network structures using a Geographic Information System (GIS) and a probabilistic assessment of the damage performance of a network subjected to an earthquake hazard is provided when coupled to a second network. The seismic risk assessment of individual network facilities is applied based on seismic hazard micro zoning and structural mechanical fragility curves. The results in the form of the system fragility curves of the independent and dependant network are presented in terms of performance measures.

In order to evaluate the impact of seismic disruption of the coupled networks on the water supply to the population, various parameters for measuring network performance are defined. These parameters, based upon topological properties taken from graph theory, are computed for different hazard levels and then visualized on a GIS. The coupling behavior among networks is characterized as a physical dependency of the potable water network on the electricity grid

through the water wells and pump stations. The dependence of one network on the other is modeled with an interoperability matrix, which is defined in terms of the strength of coupling; additionally it is considered how the mechanical structural fragility of the substations and poles of the electric power supply contributes to this dependence.

It is clear that following an earthquake, loss of infrastructure system functionality can significantly disrupt normal economic activity. The duration of this loss of service is a critical determinant of the ultimate magnitude of economic disruption. Therefore, quantitative models of the post earthquake restoration process spatially restoration period and optimum number of repair man-power for restoration are important in evaluating the total economic loss caused by an earthquake. In this research different restoration models are described and a simple model is considered for restoration analysis.

As an application, Bam city in south east of Iran is considered as a case study. The 2003 Bam earthquake with magnitude $M_W = 6.5$ destroyed most of the city. The earthquake was by far the most devastating earthquake in the history of the region around Bam. The earthquake mainly affected power, water, and communication networks in the epicentral regions. Bam infrastructures data (potable water and electric power network) is used for evaluating the functionality of infrastructure systems considering interaction among the systems.

ACKNOWLEDGMENTS

The research was carried out in Graduate School of Engineering, Kyoto University, Japan. I am very grateful to Kyoto University. I wish to express my profound gratitude to the members of dissertation committee, namely, professor Junji Kiyono, Professor Takeshi Koike and Associate professor Aiko Furukawa for their invaluable comments and suggestions.

Foremost, I would like to convey my heartfelt gratitude to my unique academic advisor, Professor Junji Kiyono for accepting me to accomplish my doctoral program in his laboratory and for frequent and helpful guidance and training. He has shown great patience towards my shortcomings and this dissertation might not have been written without his advice and support.

Also I would like to thank Professor Koike who encouraged me during several meetings in my entire doctoral program. My discussion with him have enhanced my understanding on lifeline engineering, and greatly influenced my research work. I thank him very much.

I thank very much for Dr. Yusuke Ono, ex-Assisstant Professor, Aiko Furukawa and Freddy Duran, Associate Professor. For contribute their knowledge to my understanding about the subject matter.

I am very grateful to Eri Miyamoto, ex-secretary, and Sayuri Furukawa, secretary, for providing me various helps in administrative procedures.

To all those who have helped me in our way or another, I should have better expressed my appreciation. However, due to the limitation in language, I could not have done it earlier. Hereby, I would like to sincerely convey my thankfulness to all members and my fellow students of the Earthquake and Lifeline Engineering Laboratory for their advice and friendship during my time on campus.

I would like to express our sincere gratitude to the Japanese Ministry of Education (MEXT) for the vital and useful Monbukagakusho scholarship.

Last but not least, without the support and the encouragement of my parents and parent-in-laws, my study in Japan would not have been so smooth. Not forgetting my beloved wife and my lovely daughter, who have prepared a suitable environment for my study and progress. To them, no words of thank is not enough.

TABLE OF CONTENTS

Contents Page

LIST OF TABLES

Table Page

LIST OF FIGURES

Figure Page

CHAPTER 3

CHAPTER 4

CHAPTER 5

CHAPTER 6

CHAPTER 7

CHAPTER 1

INTRODUCTION

1.1 Background

The current industrial and technology development of a country relies on availability and correct operation of multiple infrastructures. If we take the Oxford dictionary, an infrastructure is defined as "*the basic physical and organizational structures and facilities (e.g., buildings, roads, and power supplies) needed for the operation of a society or enterprise*".

Even though most of dictionaries have a similar definition, the political institutions have often changed and modified their own definition in the last twenty years. This is principally due to the fact that it has seen an escalation of *man-made* disasters especially in regard to destructive effects. During such disasters most of infrastructures have been seriously affected either directly or indirectly. So, if at the beginning engineers as well as politicians were concerned about the quality and adequacy of an infrastructure, today they are more interesting in their protection. Protection today does not mean only to prevent to be damaged, but, especially, to ensure a continuous flow of services for every single infrastructure and to mitigate the risk that if an infrastructure cannot offer the standard level of service, all other infrastructure are minimally affected and can keep operating.

The society is becoming more dependent upon the reliable function of a number of vital infrastructure systems, including electrical power transmission, water and gas distribution, public transportation, banking and finance, and information technology systems. These systems are often being referred to as critical infrastructure systems or lifeline systems, indicating their importance for supporting the functioning of all economic and social activity of an industrialized nation.

The functional loss of these systems due to an external perturbation can cause severe impact on a community in numerous ways (**Fig 1.1**). This loss has the potential to cut water supplies, reduce or eliminate electrical system capacity, and sever gas links. Specifically, seismic hazards cause significant damage to these systems. The 2011 Tohuku earthquake (Mw=9.0) caused extensive damage to lifeline systems. Portions of major highways and freeways in east Japan were closed due to the extensive damage or failure of bridges, inducing widespread disruption after the event. Several cities suffered a blackout, and approximately so

many peoples lost water services immediately following the earthquake. Therefore, understanding the influence of hazards on these systems is critical to mitigate damage and to perform effective response efforts.

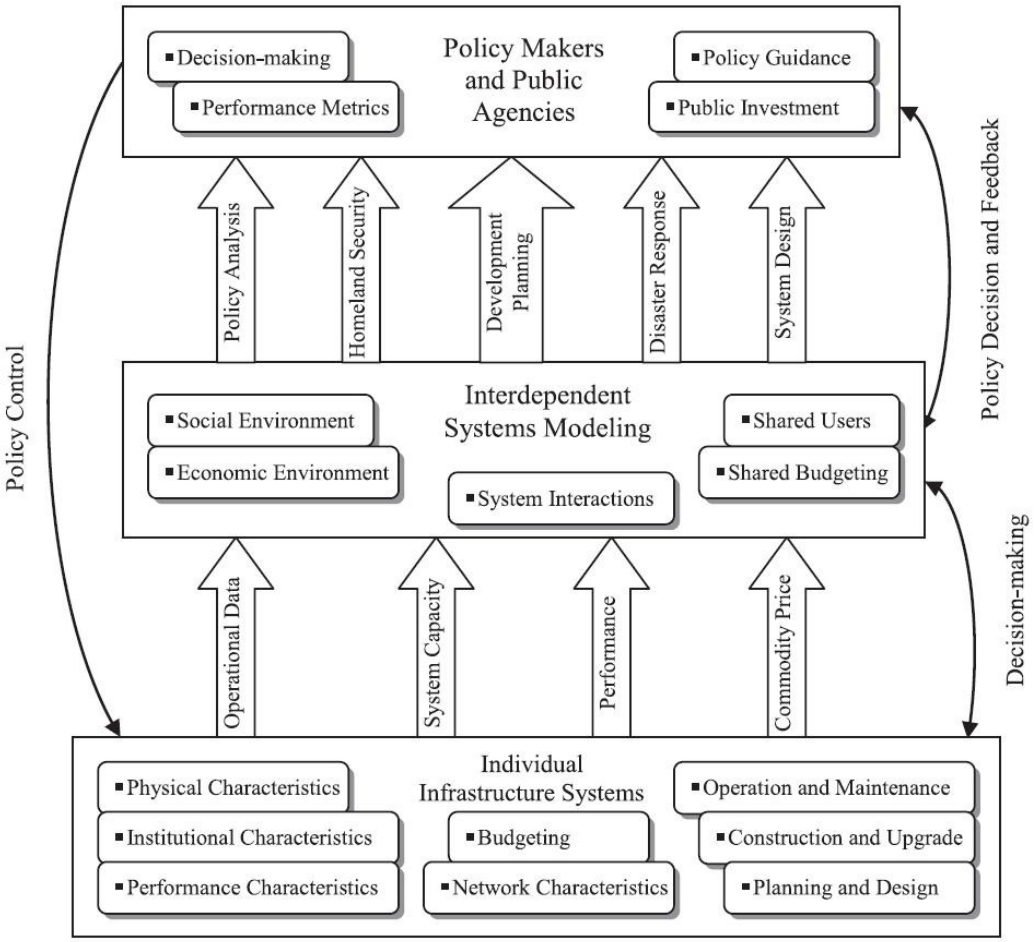

Fig 1.1 Infrastructures interdependencies in the real world (Zhang et al., 2011)

It is clear that real networks do not operate in isolation, and that a larger problem needs to be addressed. Attempting to recognize and quantify the effects of network interdependencies in their response to disturbances constitutes the fundamental challenge of this research study. However, it must be recognized that these networks have also been growing independently very fast. This growth increases their structural complexity and reduces the possibility to trace their dynamics, and the dynamics of their interconnecting systems. Fundamental approaches need to be implemented to understand the properties of these complex entities. Statistical methods for the study of average properties not of single systems, but of large ensembles of systems and their constituent parts are a promising approach to provide the basic tools for this ongoing research. This statistical approach offers a reasonable framework to discover emergent behavior

and universality among systems that are composed of collections of sub-elements. That knowledge is used to understand the correlation between disturbances, network flow, topology, network response or performance, and effects of alternative improvements to prevent large scale failures.

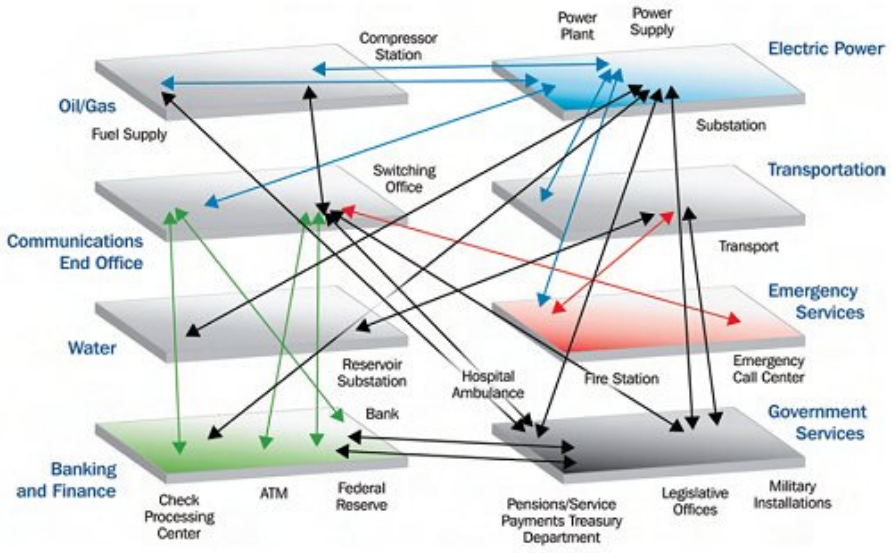

Fig 1.2 Schematic infrastructures interdependencies (Source: www.dhs.gov)

In fact, infrastructure systems are generally mutually dependent. They are frequently connected through a wide variety of mechanisms, such that a mutual relationship exists between the states of any given pair of components in the systems (**Fig 1.2**). The need of accounting for this *interdependency effect* is seen by looking at the importance of functioning of each of them on other performance. For instance, power grids depend on gas networks to fuel generation units. Water networks provide cooling and help to control emissions from coal-based power generators. Water and gas networks are heavily dependent on power for operating pumping stations and control systems. If a particular system is damaged, this damage is propagated to other systems due to the interdependent nature of the systems. Therefore, an emerging need exists for modeling complex and interdependent critical infrastructure to better understand their susceptibility to potential hazards.

The accompanying chart represent (**Table 1.1**) illustrates examples of interdependent relationship between electric, water/wastewater, gas and oil, communications, and transportation infrastructures. These complex relationships are characterized by multiple connections that create an intricate web which, depending on the characteristics of its linkages,

can result in a cascading effect across multiple infrastructures that impact a community's economy and security.

Table 1.1 Interdependent relationships among critical infrastructures

Type of Interdependency	Energy - Electric	Energy - Gas/Oil	Water	Communication	Transportation
Energy - Electric	Highly connected and interdependent infrastructure for business and economic security	Power for control systems, pumping stations, storage, compressors, and batteries	Power for control systems, pumps, It's stations and facilities	Power for switches and communication facilities	Power for signals, switches and public transportation
Energy - Gas/Oil	Fuel for heat generators and lubricants for electric facilities	Highly connected and interdependent infrastructure for business and economic security	Fuel for treatment, heat, pumps, It's stations and facilities	Fuel for heat, generators and facilities	Fuel and lubrications for vehicles and facilities
Water	Water for cooling and emissions control	Water for production, cooling and emissions control	Essential and highly dependent infrastructure for health and safety	Water for cooling facilities	Water transport for emergency response and construction
Communication	automation EMS and SCADA; customer service; and crew repair communication	SCADA communication, customer service	Control system and SCADA, customer service; and crew repair communication	Highly connected and interdependent infrastructure for business and economic security	Signal and control system , and crew repair communication
Transportation	Transport of fuel, shipping of goods and materials, and inspection	Transport of fuel, shipping of goods and materials, and inspection	Transport of water and inspection	Transport of goods and materials, and inspection	Highly connected and interdependent infrastructure for business and economic security

For a given a geographically bounded system, determination of what constitutes interdependencies among infrastructures is a nontrivial problem because factors of different nature contribute to the observed coupling characteristics. Ideally, interdependencies could be quantified by weighting each of the following dimensions: type of interdependency, coupling and response behavior, infrastructure characteristics, infrastructure environment, type of failure, and network state of operation (Rinaldi et al., 2001).

1.2 Literature Reviews

To understand the interdependency and cascading failures among infrastructure systems under random incidents, manmade attacks and natural hazards, many researchers have proposed different methods for modeling and simulation of interdependent infrastructure systems. Notable examples include Agent Based Methods (ABM), Inoperability Input–output Methods (IIM), System Dynamics Methods (SDM), Network or Graph Based Methods (NBM) and Data Driven Methods (DDM). Although these approaches are important advances in the understanding of the seismic response of a lifeline system, consideration of interdependencies in modeling and analyzing lifeline systems accordingly is still a significant challenge.

Rinaldi et al. (2001), Peerenboom et al. (2002), Gillette et al. (2002), NERC (2004) and Fedora (2004) noted the importance of infrastructure interdependencies on economic, industrial and social activities. Rinaldi et al. (2001) and Peerenboom et al. (2002) classified infrastructure interdependencies based on relationships among infrastructure systems. A generalized multi-ordered implication of infrastructure failure was proposed by Little (2002). Axelrod and Cohen (1999) proposed using complex-adaptive systems model for dealing with interconnected infrastructures. Chang et al. (1996) also noted the potential importance of infrastructure interdependency among the water distribution, the gas distribution and the electrical power transmission systems.

In the Agent Based Method, agents represent components in an infrastructure system (such as electric transformers or generators) or some important players (such as government or weather) related to system operation (North 2001, Ehlen 2005, Eusgeld 2009). Different types of agents have different sets of rules that determine the actions the agents take in response to the actions by other agents. This method can analyze system responses to different attack scenarios, (Basu 1998).

Using the energy system context, a group of authors from the Argonne National Laboratory (North, 2001; Macal and North, 2002; Thomas et al., 2003) focus on the decision-making of various players from a market perspective using agent-based simulation (ABS). Other ABS tools (Brown et al., 2004; Tolone et al., 2004; Dudenhoeffer et al., 2006) also mostly focus on the economic interactions between decision makers in the infrastructure systems by using differential equations, discrete events, and rules of operation. In addition to these ABS models, Bush et al. (2005) integrate several existing simulation models and/or tools available for various individual infrastructure systems, and simulate the input–output commodity flows across these systems through a common interface.

The inoperability input–output method (IIM) based on the 1973 Nobel laureate Wassily Leontief's input–output economic model (Leontief 1951) uses a linear matrix equation to capture the inoperability of infrastructure systems, where inoperability is defined as the inability of a system to perform its intended function. The IIM method can analyze how perturbations propagate among interconnected infrastructure systems and how to implement effective mitigation efforts (Haimes 2001, Santos 2004, Crowther 2010). Many studies (e.g., Chang and Seligson et al., 1996; FEMA, 1997 and 2003; Rose, et al., 1997; Shinozuka, et al., 1997 and 1998) have considered financial losses incurred due to loss of serviceability arising from system interdependency effects using Input-Output analysis (Haimes et al, 2005). This approach is necessary to compute the total monetary losses to industries damaged by an earthquake. However, none of the studies to date using IIM analysis have considered the additional serviceability loss due to infrastructure interdependency. Accordingly, such studies may underestimate the total monetary loss.

The System Dynamics (SD) approach studies interdependent complex systems by using feedback loops, stocks, and flows. Feed- back loops indicate connections and directions of effects between system objects, while stocks represent quantities or states of the system, the levels of which are controlled over time by flow rates between stocks. An SD-based model called Critical Infrastructure Protection Decision Support System (CIPDSS) allows for rapid production of scenarios to compare different types of disruptive events and their impacts across multiple infrastructure systems (Conrad 2006, Santella 2009).

The study by Robert (2004) is one of the first that attempted to assess network serviceability considering system interdependency effects directly. Interdependency among systems was modeled by direct links and indirect links.

The network or graph based method, which uses nodes to represent different types of system components and links to mimic the physical and relational connections among them, provides affordable and intuitive system representations along with detailed descriptions of their topology and flow patterns. In the graph theory approach of Duenas-Osorio et al. (2006), the probability that a node or an edge is removed is determined by not only the component fragility or the leakage or break ratio of a distribution element but also the probability that a facility did not receive commodities which are needed to maintain the function of the nodes or the edges. For example, the edge representing a water pumping station was removed when the electrical power was lost. This method can analyze the effects of system topology, element physical fragility, and attack intensity on system performance levels which are measured by connectivity (Ouyang 2011, Adachi 2008, Kim 2009) and flow delivery (Ouyang 2009,

Johansson 2010, Rosato 2008). The data driven methods, which characterize infrastructure system failure interdependencies based on the data from media reports and official ex post assessments of the events, can complement probabilistic, systems-based and simulation methods and provide empirical understanding on how extreme events within or external to one infrastructure system lead to the failures in other infra- structure systems (McDaniels 2007, Chou 2010).

Nozick et al. (2005) develop Markov-based algorithms to estimate system performance and make optimized investment decisions for interdependent infrastructure systems. They illustrate their approach using electric power and gas systems. Jeong et al. (2006) and Qiao et al. (2007) develop network-based models to address security issues in water systems. These models treat water systems as networks composed of a plant, transmission pipelines, storage stations, and distribution lines.

Pederson et al. (2006) provide a systematic survey of studies conducted in the realm of infrastructure interdependencies up to 2006. The survey identifies around thirty models related to this area, and briefly reviews their characteristics and capabilities.

Nagurney and Dong (2002) propose the concept of ‘‘super network” to capture the interactions among transportation, telecommunication, energy, and financial networks. Though the modeling framework is well-defined using generalized network theory and the variational inequality technique, calibration and application issues are not sufficiently addressed.

Friesz et al. (2001) introduce the notion of a multilayer infrastructure network using the concepts of a generalized transportation network and system of systems. Using this framework, Zhang et al. (2005) present a preliminary dynamic network flow equilibrium model in the form of a differential game involving two time scales.

Apart from the above methods, there are still some other hybrid approaches for interdependency studies, such as system of systems approaches (Kroger 2008, Eusgeld 2009) which can capture the complexities of the interdependencies and model the impacts of human factors, multilayer infrastructure network approach which can capture the interdependencies among various infrastructure systems with disparate physical and operational characteristics (Zhang 2011). However, these studies are almost all based on fixed interdependent topologies or relationships. There are only a few studies on how to design interface topologies (physical connections) across infrastructure systems to minimize the cascading failure effects. To tackle this problem, different interface design strategies is proposed (Winkler 2012) based on infrastructure topological properties. In that work, the connectivity loss of just the interface topology was used as a proxy for entire intersystem performance.

Overall, the above mentioned studies can be summarized as follows considering various methodological approaches used to address infrastructure interdependencies, or related problems, by identifying their strengths and limitations.

1.2.1 Surveys and descriptive studies

Some researchers provide a systematic survey of studies and made reports related to infrastructure interdependencies. However, they do not provide a modeling/methodological approach, and mainly focus on discussing potential frameworks or providing policy-oriented guidelines.

1.2.2 Simulation-based approach

Due to the level of complexity involved in modeling large-scale infrastructure systems, simulation is a natural candidate to address interdependency problems. The modeling aspects include the selection of the agents' objectives, the pricing and bidding strategies, learning and adaptation regarding market evolution, and capacity expansion decisions. A preliminary prototype was developed to explore the interdependencies between energy and power systems.

1.2.3 Input–output approach

To address the lack of theoretical capabilities of the simulation approaches, economic theory has been used to develop mathematical formulations and models, especially through the input–output approach. This approach borrows well-defined economic theory to capture cascading risk dependencies across multiple systems. These studies demonstrate that input–output modeling is a natural choice for studying the risk transmission among interdependent infrastructure systems. The approach enables the theoretical analysis of mathematical properties, probability of disruption and risk transmission, and cascading impacts.

1.2.4 Network-based approach

A network modeling approach is used where the nodes represent the supply or demand locations for some utility services, and the arcs, with capacity constraints, represent components or subsystems of an infrastructure system or the connection between infrastructure systems. The methodology is based on the topological characteristics of the infrastructure networks such as connectivity, vertex degree, path length, clustering coefficient, and

redundancy ratio. Two small-scale networks representing electric power and water systems are used to illustrate the ability of the method to capture network interdependencies.

1.2.5 Generalized network and system-of-systems approach

The models reviewed heretofore focus on issues related to security, risk, and vulnerability of infrastructure systems. In contrast to the other approaches, generalized networks and system-of-systems approach represent conceptual paradigms rather than specific theoretical constructs. Their implementation entails drawing from a broad range of methodological domains such as graph theory, network modeling, operations research, mathematical programming, nonlinear science, and behavioral science.

1.3 Research Goal and Objectives

In summary, the existing approaches to address infrastructure interdependencies lack one or more key capabilities in a real-world context. First, most approaches focus on risk modeling and security-related aspects. Very few enable the analysis of business-as-usual scenarios. Hence, there is a need for a unified modeling framework that can analyze both equilibrium and disruption scenarios for interdependent infrastructure systems. Second, the disparate operational, economic, and physical characteristics of the various infrastructure systems preclude the seamless modeling of their interdependencies using most existing approaches. Third, many models do not leverage the network and spatial characteristics of the infrastructure systems, and those that consider the network structure do not capture the market and functional aspects. Fourth, few of these models are capable of holistic ‘‘what-if’’ analysis of policy changes, especially from a prescriptive perspective. Fifth, most approaches can address only a subset of the various types of interdependencies. They are not generalized enough to model all sources of interdependencies in the same framework, and are not flexible enough to incorporate a subset of infrastructure systems at different geographical/spatial scales. Sixth, most existing models are static, and cannot consider the temporal interactions across systems and/or the system evolution over time. Seventh, systematic calibration methods are lacking, and the difficulty in obtaining the required data or its non-availability represent key deployment barriers. Eighth, descriptive and simulation models lack theoretical constructs. For some of the proposed theoretical models, their mathematical properties are not analyzed. Finally, systematic solution approaches or tools are not specified for some models.

In order to address these limitations, it is desirable to have a generalized modeling framework that can incorporate the equilibrium and disruption aspects, static and dynamic capabilities, descriptive and prescriptive analysis, theoretical and implementation capabilities, various types of infrastructure interdependencies, flexible number of systems, different geographical or institutional scales, network characteristics, disparate operational and physical characteristics, realistic data availability, market and engineering perspectives, and a convenient solution platform.

In addition, these approaches shed light on the issue of modeling interdependent networks in the context of earthquake engineering; certain issues require further refinement such as:

- ✓ The probabilistic model for interdependency in this study needs further clarification to consider the failure due to interdependency properly;
- ✓ Instead of taking into account the failure of individual links in a network, the failure probabilities of links that are adjacent to a node is lumped to the node. This simplification may result in a more efficient analysis, but it is at the expense of the seismic reliability of the network being overestimated; and
- ✓ Interdependent failure mechanisms need to be improved to more accurately reflect the physical situation (e.g., existence of a back up supply).

In this research, it is tried to assess the seismic performance of interdependent lifeline systems. A probabilistic model is developed to characterize network interdependency. This probabilistic model is then incorporated into network flow algorithms to assess the seismic performance of the interdependent lifeline systems. Example analyses validate the proposed approach and show the effect of various interdependency levels on the performance of these systems under seismic conditions. The results provide important information to mitigate seismic damage on lifeline systems.

Although topological structure determines the function of networks, recent studies showed that connectivity models alone cannot provide sufficient information about the flow performance of real infrastructure systems (Hines 2010). In addition, an optimum strategy that is the best under one hazard type may not be the most effective under other types, so it requires some global strategy assessment metric. To solve this conflicting objective problem and monitor the response of entire interdependent systems, this study tries to propose an approach to design new interdependent topologies (or enhance existing ones) and finds a global optimum strategy under a hazard across interconnected networks.

1.4 Thesis Organization

This thesis is divided into eight chapters (**Fig 1.3**). Chapter 1 introduces the subject and identifies the major research issues, and presents the research objectives.

In order to better understand the critical infrastructure role in a society and also learn more about components of interdependent critical infrastructure and their seismic performance, the characteristics of critical infrastructures are illustrated in chapter 2 and a literature review on the recent advances is presented in the fields of complex networks, network topology, network dynamics, and interconnected systems.

Chapter 3 presents the approaches for critical infrastructure modeling, illustrating the theories and algorithms that are used in the following chapters with the application in the Bam city infrastructures as a case study. The graph based method is considered which uses nodes to represent different types of system components and links to present the physical and relational connections among them, provides affordable and intuitive system representations along with detailed descriptions of their topology and flow patterns.

Chapter 4 illustrates alternatives for characterizing the seismic demands on infrastructure systems. Probabilistic seismic hazard analysis and the scenario based seismic hazard analysis are introduced, in the context of describing the earthquake threat on a distributed system. Attenuation equations for the peak ground acceleration and the peak ground velocity, the local soil amplification factors and the spatial correlation of seismic intensities are introduced. It considers the applicability of the probabilistic seismic hazard analysis approach to a spatially distributed infrastructure system. The case study networks models are used to identify situations in which probabilistic seismic hazard analysis can reasonably be applied and to explain its limitations through quantitative examples.

Chapter 5 provides an introduction to fundamental concepts of reliability concept that is used throughout the document. The reliability analysis methodology of interdependent infrastructure systems subjected to spatially correlated seismic demands, through a case study involving the water distribution system and the electrical power transmission system in Bam. Easily computed upper and lower bounds on serviceability ratio under the spatially correlated seismic intensities are developed.

Chapter 6 presents a comprehensive analysis of the response of networked systems when subjected to intentional element removal, or when subjected to seismic hazards. The effect of network interdependencies is demonstrated by comparing the response of these systems under different coupling strengths. For modeling the interdependency between critical infrastructures, two important issues of modern interdependent critical infrastructure systems are studied; First

the network response under seismic hazard is assessed; then the increased vulnerability due to coupling between networks is analyzed.

Chapter 7 provides ideas for critical infrastructure management and decision making in disasters, such as optimal mitigation actions, which maximize individual network stability and minimize interdependent network instabilities. The quantitative model of the post-earthquake restoration process is modeled for Bam interdependent critical infrastructure and emergency water supply is described to achieve the customer's acceptance criteria.

Chapter 8 contains the conclusions of this research and presents relevant issues for future research.

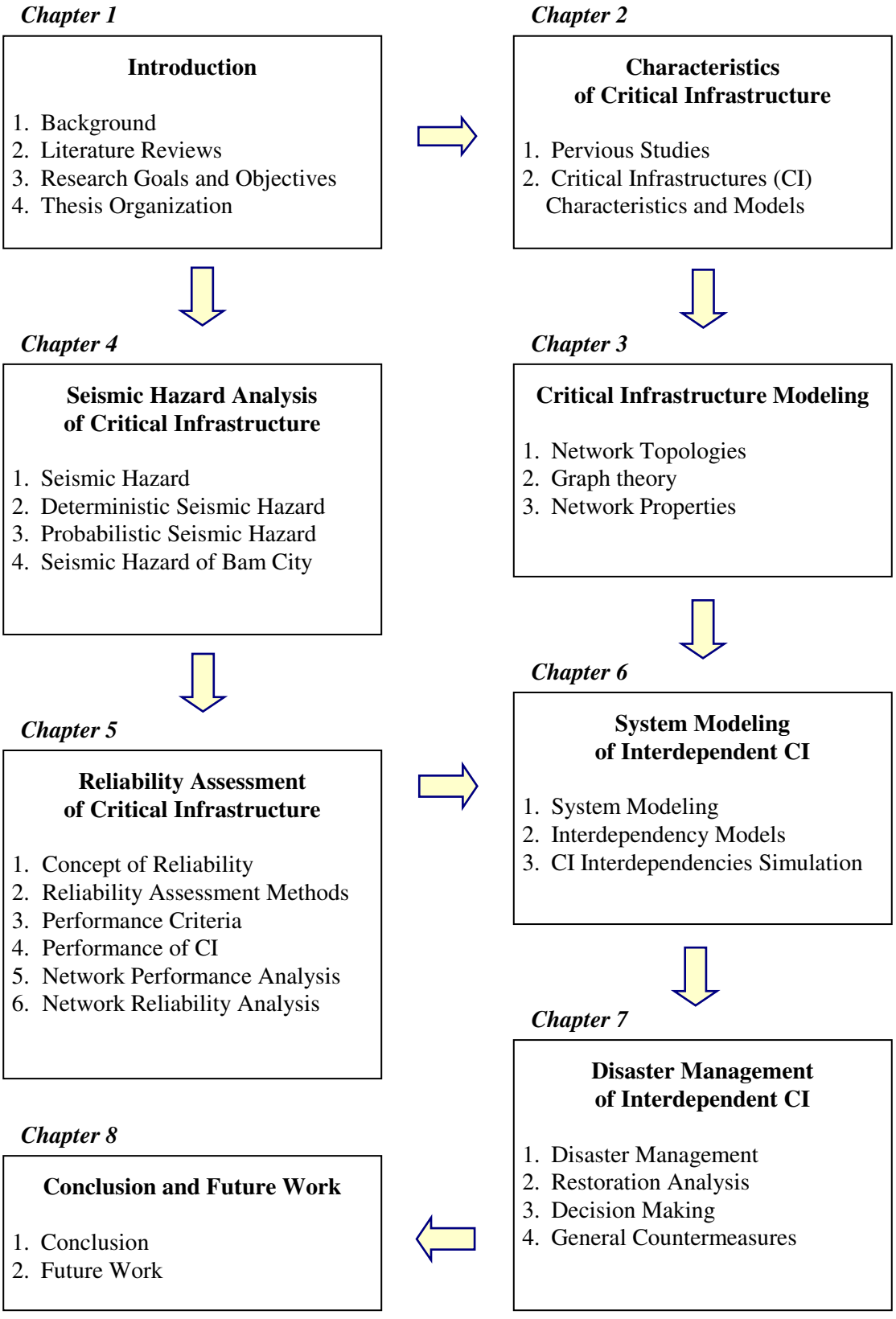

Fig. 1.3 Research flow

CHAPTER 2

CHARACTERISTICS OF CRITICAL INFRASTRUCTURES

2.1 Introduction

An infrastructure system is a collection of many components such as facilities and distribution elements. Each facility or distribution element has its own structural characteristics and its own independent role to maintain a function of the infrastructure system. While an office building or a bridge is also a collection of components, the major characteristic of an infrastructure system not shared by an office building or bridge is that its components are spatially distributed over a large region, and key components may located at some distance from one another. For example, a hydro-power generation station is located close to a water dam in a valley; electrical power is transmitted through transmission lines and substations to urban areas located some distance from the hydropower generation plant. Thus, the modeling approach must take these distinct features into account.

To address this modeling problem, Satyanarayana and Wood (1985), Wagner et al. (1988a and 1988b) and Quimpo et al. (1997) used graph theory to model an infrastructure system. In these studies, an infrastructure system was modeled using edges and vertices. The edge represents components of an infrastructure system such as a facility or a distribution element, and the vertex represents a connecting point which has perfect reliability. When two components such as water pumping station and a water pipe are physically connected, the two edges, which represent the water pumping station and the water pipe, are connected at a vertex. Conversely, when two components (e.g., an electrical power substation and a water dam) are not physically connected, the two edges representing the two components do not share a vertex. Later, Yang and Shaoping (2003) also used a graph to model an infrastructure system although the methodology was not clearly mentioned (Adachi, 2007).

Recently, Duenas-Osario et al. (2006) also modeled an infrastructure system using graph theory. In contrast with the earlier studies mentioned above, a vertex represented a facility such as an electrical power substation, water pumping station or a water storage tank, and an edge represented a distribution element such as a water pipe or an electrical power transmission line. When a distribution element and a facility are physically connected, the vertex and one end of the edge are connected. Compared with the modeling approach proposed by Satyanarayana and Wood (1985), Wagner et al. (1988) and Quimpo et al. (1997), the modeling approach proposed

by Duenas-Osario et al. (2006) is more realistic since an infrastructure system in the real world is composed of vertices (facilities) and edges (distribution elements) in broad perspective.

2.2 Critical Infrastructures

2.2.1 Potable water network

A potable water supply is necessary for drinking, food preparation, sanitation, fire extinguishing etc. Water which may be non potable is also required for cooling equipment. A potable water system consists of transmission and distribution systems. Transmission system stores raw water and delivers it to treatment plants. Such a system is made up of canals, tunnels, elevated aqueducts and buried pipelines, pumping plant and reservoirs. Distribution system delivers treated water to customers. The most important components of potable water system are; Water source, Treatment plant, Pumping station, Reservoir, Supervisory Control and Data Acquisition (SCADA), Transmission Conduits and Distribution Pipes.

2.2.1.1 Water source

The typical water sources are spring or deep wells, rivers, natural lakes, and impounding reservoirs. Water can get from lake or river by intakes, **Fig 2.1**. Wells are used in many cities as both a primary and supplementary source of water. Wells include a pump to bring the water up to the surface, various electromechanical equipments and a building to enclose the well and the equipment.

2.2.1.2 Water treatment plant

Water treatment plants are complex facilities, **Fig 2.2**, generally composed of connected physical and chemical unit processes, whose purpose is to improve the water quality. Treatment processes used depend on the raw water source and the quality of finished water desired. A conventional water treatment plant consists of a coagulation process, followed by a sedimentation process, and finally a filtration process. Components in the treatment process include pre-sedimentation basins, aerators detention tanks, flocculators, clarifiers, backwash tanks, conduit and channels, coal sand or sand filters, mixing tanks, settling tanks, clear wells, and chemical tanks. Alternatively, a water treatment plant can be regarded as a system of interconnected pipes, basins, and channels through which the water moves, and where the flow is governed by hydraulic principles. It is assumed that there is no back-up power in case of loss of electric power as a worst case scenario.

Fig 2.1 Water source intake (myalucardster, 2011)

Fig 2.2 Water treatment plant (wetland)

Water treatment plants are divided to three sizes, due to its increasing redundancy and importance factor for design (HAZUS; NIBS, 2004). Small water treatment plants (≤50 M Gallons or 189.500 m^3/day), are assumed to gallery with flocculation tanks (composed of paddles and baffles) and settling (or sedimentation) basins as main components, chemical tanks (needed in the coagulation and other destabilization processes), chlorination tanks, electrical and mechanical equipment, and elevated pipes. Medium water treatment plants are simulated by adding more redundancy to small treatment plants (i.e. twice as many flocculation, sedimentation, chemical and chlorination tanks) and, Large water treatment plants (i.e. three times as many flocculation, sedimentation, chemical and chlorination tanks/basins) have the capacity more than 200 M Gallons or 758.000 m^3/day .

2.2.1.3 Pumping station

A pumping station is a facility that boosts water pressure in both transmission and distribution systems. In general, pumping stations include larger stations adjacent to reservoirs and rivers, and smaller stations distributed throughout the water system intended to raise head. Pumping stations typically comprise building (**Fig 2.3**), intake structures, pump and motor units, pipes, valves (**Fig 2.4**), and associated electrical and control equipment (ATC-25, ALA 2001a).

Pumping station may be described (HAZUS; NIBS, 2004) with respect to: its size (small, medium or large), Anchored or Unanchored, The subcomponent (equipment and back-up power) considered. A small pumping station boost less than 10 M Gallons (37.900 m^3/day) to transmission and distribution systems, according to HAZUS (NIBS 2004). It is also assumed that there is no back-up power in case of loss of electric power.

Fig 2.3 Pump station building (fucuanind)

Fig 2.4 Pumps, piping and valves (colourbox)

2.2.1.4 Reservoir

Reservoirs can be located at the start, along the length or at the end of a water transmission and distribution system. Their function may be to hold water for operational storage, provide surge relief volumes, provide detention times for disinfection, and other uses.

Fig 2.5 Reinforced water reservoir (elevated and at grade)

Most water systems include various types of storage reservoirs in their transmission and distribution systems. Reservoirs can be either tanks or open cut reservoirs. Reservoir important parameters may be the material, size, anchorage, position (at grade or elevated) (**Fig 2.5**), roof type, seismic design, foundation type, and construction technique.

2.2.1.5 Supervisory Control and Data Acquisition (SCADA)

Various types of in-line components exist along water transmission pipelines, including portions of the Supervisory Control and Data Acquisition (SCADA) system located along the conveyance system and various flow control mechanisms (e.g., valves and gates).

2.2.1.6 Transmission conduits

Transmission conduits are typically large size pipes (more than 400mm in diameter) or channels that convey water from its source (reservoirs, lakes, rivers) to the treatment plant. Transmission pipelines are commonly made of concrete, ductile iron, cast iron, or steel. These could be elevated, at grade or buried.

Fig 2.6 Water transmission main

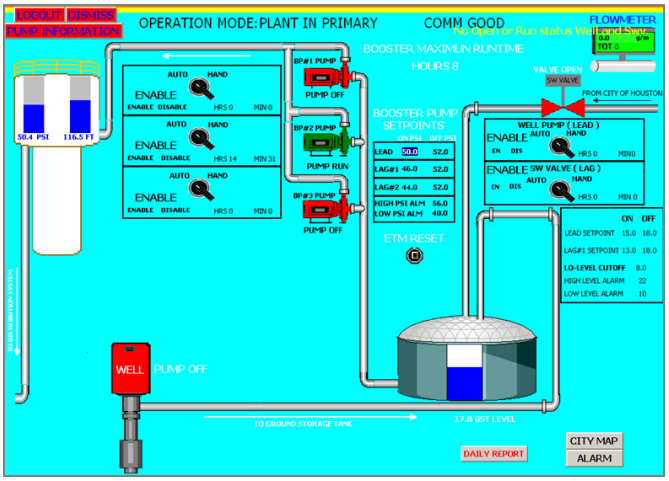

Fig 2.7 Water network SCADA system (dmn, 2011)

Distribution of water through conduits can be accomplished by gravity, or by pumps in conjunction with on-line storage. Except for storage reservoirs located at a much higher altitude than the area being served, distribution of water would necessitate, at least, some pumping along the way. Typically, water is pumped at a relatively constant rate, with flow in excess of consumption being stored in elevated storage tanks. The stored water provides a reserve for fire flow and may be used for general purpose flow should the electric power fail, or in case of pumping capacity loss.

2.2.1.7 Distribution pipes

Distribution pipes can be free flow or pressure conduits, buried or elevated. Several materials can be used. In order to avoid contamination of treated water, potable water pipes are most of the time pressurized. The most important parameters of pipe are; Location (buried or elevated), Material (type, strength), Geometry (diameter, wall thickness), Type of joints (continuous or segmented pipes), Corrosiveness (age and soil conditions), Appurtenances and branches. Distribution pipes represent the network that delivers water to consumption areas. Distribution pipes may be further subdivided into primary lines, secondary lines and small distribution mains. The primary mains carry flow from the pumping station to and from

elevated storage tanks, and to the consumption areas, whether residential, industrial, commercial, or public. These lines are typically laid out in interlocking loops. Secondary lines have smaller loops within the primary mains and run from one primary line to another. They serve primarily to provide a large amount of water for fire fighting without excessive pressure loss. Small distribution lines represent the mains that supply water to the user and to the fire hydrants.

2.2.2 Electric power network

An Electric Power Network is a complex interconnected system that can be subdivided into four major parts; Generation, Transformation, Transmission, Distribution and loads.

2.2.2.1 Generation

Generation of electric power is carried out in power plants. A power plant (**Fig. 2.8**) is composed of several three-phase AC (Alternate Current) generators known as synchronous generators or alternators. Synchronous generators (**Fig 2.9**) have two synchronously rotating fields, one of which is produced by the rotor driven at synchronous speed and excited by DC (Direct Current), while the second one is produced in the stator windings by the three-phase armature currents. The DC current for the rotor windings is provided by the excitation systems, which maintain generator voltage and control the reactive power flow. Because of the absence of the commutator, AC generators can generate high power at high voltage, typically 30 kV. In a power plant, the size of generators can vary from 50 MW to 1500 MW.

Fig 2.8 Power plant cooling towers (Southasiarev)

Fig 2.9 Power plant generators facilities (IDG)

At the time when the first electric power network were established in the world, individual electric companies were operating at different frequencies anywhere, in US ranging from 25 Hz

to 133 Hz. As the need for interconnection and parallel operation became evident, a standard frequency of 60 Hz was adapted throughout the US and Canada, while most European countries and Iran selected the 50 Hz system. In this way, there is some spatial case such as Japan which use both, 50 Hz in east and 60 Hz in west of the country.The source of the mechanical power, commonly named "prime mover", may be hydraulic turbines at waterfalls, steam turbines whose energy comes from the burning of coal, gas and nuclear fuel, gas turbines are occasionally internal combustion engines burning oil. Many alternative energy sources, like solar power, geothermal power, wind power, tidal power and biomass, are also employed.

2.2.2.2 Transformation

One of the major components of a power transmission system (**Fig 2.10**) or substation (**Fig 2.11**) is the transformer (**Fig 2.12**), which transfers power with very high efficiency from one level of voltage to another level.

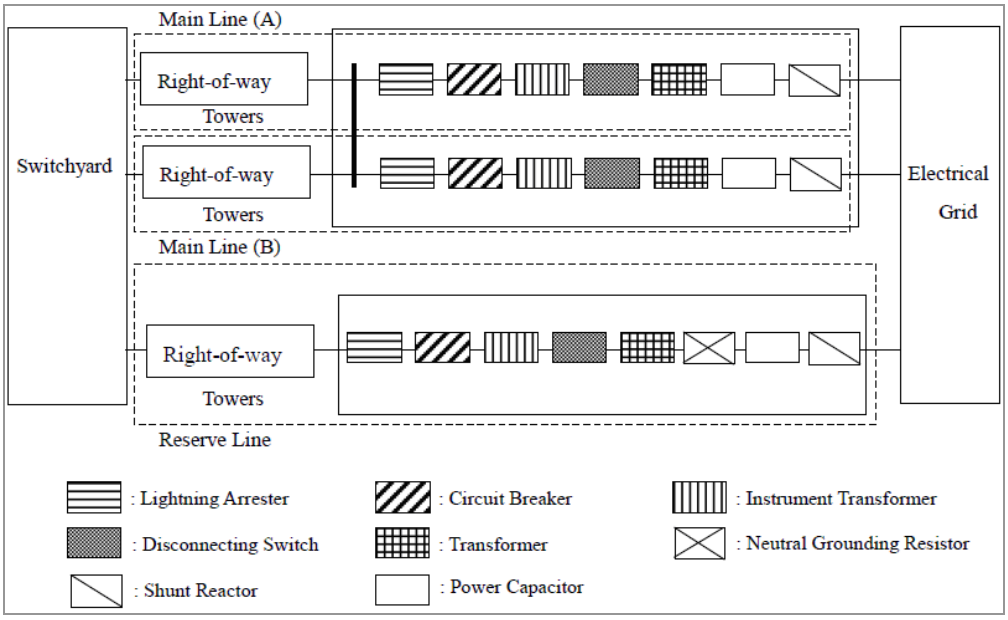

Fig 2.10 Model of Electrical Transmission System, substation, (Oikawa et.al., 2001)

The power transferred to the secondary winding is almost the same as the primary, except for losses in the transformer. Therefore, using a step-up transformer of voltage ratio a will reduce the secondary current of ratio $1/a$, reducing losses in the line, which are inversely proportional to voltage and directly proportional to distance. This makes the transmission of power over long distances possible. At the receiving end of the transmission lines step-down transformers are used to reduce the voltage to suitable values for distribution or utilization.

Fig 2.11 Power electric substation

Fig 2.12 Power electric transformer

2.2.2.3 Transmission and distribution

The purpose of a power delivery system (**Fig 2.13**), also known as transmission and distribution system, is to transfer electric energy from generating units at various locations to the customers demanding the loads. A transmission and distribution system is divided into two general tiers: a transmission system that spans long distances at high voltages on the order of hundred of kilovolts (kV), usually between 60 and 750 kV, and a more local distribution system at intermediate voltages. The latter is further divided into a medium voltage distribution system at voltages in the low tens of kV, and a low voltage distribution system, which consists of the wires that directly connect most domestic and small commercial customers, at voltages in the 110 V for US and Japan, 220-240 V range for Europe and Iran.

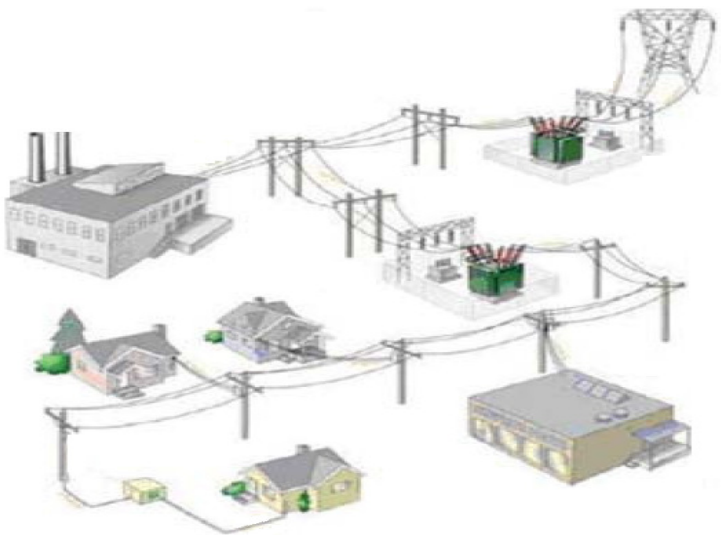

Fig 2.13 Schematic model of power electrical transmission and distribution System (geospatial)

The transmission and distribution systems are generally characterized by two different topological structures: the transmission system is an interconnected redundant grid, composed of stations as nodes and transmission lines as edges while the distribution system is a tree-like network, following the main streets in a city and reaching the end users. **Fig 2.14** shows the two topological structures. The lines at different voltages are terminated in substations.

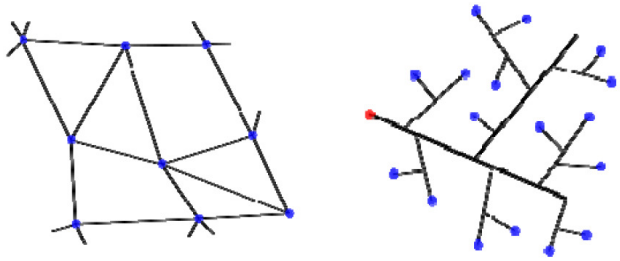

Fig 2.14 Typical topological network structures, grid-like (left) and tree-like (right)

Substations can be entirely enclosed in buildings where all the equipment is assembled into one metal clad unit. Other substations have step-down transformers, high voltage switches, oil circuit breakers, and lighting arresters located outside the substation building. The electric power is delivered to the single customers through distribution circuit, that include poles, wires, in-line equipment, utility-owned equipment at customer sites, above ground and underground conductors. Distribution circuits either consist of anchored or unanchored components.

2.2.2.4 Loads

Loads of power systems are divided into industrial, commercial and residential. Industrial loads are served directly from the high voltage transmission system or medium voltage distribution system. Commercial and residential loads consist largely of lighting, voltage distribution system. These loads are independent of frequency and consume negligibly small reactive power. The real power of loads is expressed in terms of kilowatts (kW) or megawatts (MW). The magnitude of load varies throughout the day and power must be available to consumers on demand. The greatest value of load during a 24-hr period is called peak demand. Smaller peaking generators may be commissioned to meet the peak load that occurs for only a few hours. In order to assess the usefulness of the generating plant the load factor is defined, which is the ratio of average load over a designated period of time to the peak load occurring in that period. Load factors may be given for a day, a month or a year.

2.3 Main Topologies for Network Components

Considering the main topologies for the components is important for network modeling. Usually the network component model to single topology and most researchers do not explicitly distinguish between micro and macro components. This distinction is useful in terms of reliability analysis of electric power network when the approach to network modeling is capacitive and the internal logic of substations is modeled, i.e., partial functioning is accounted for. In this latter case the modeling effort, which is much higher than when a substation is considered as a single component with a binary state (fail/safe), can be reduced by assembling subsets of micro components that are serially arranged within the station in order to reduce them to single element characterized by a single fragility; the macro component. The substation layout is then composed of general arrangement of macro components which can lead to partial functioning states, depending on damage distribution.

2.3.1 Potable water network

The potable water network components can be grouped on the base of four different analysis levels of the network. The main topologies are listed in **Table 2.1**.

Table 2.1 Main topologies of potable water network components

Topology	Analysis Level	Topology	Analysis Level
Water source 1- Electric Power 2- Well pump 3- Building 4- Electric equipment	Station	Water Treatment Plant 1- Electric Power 2- Chlorination Equipment 3- Sediment flocculation 4- Basins 5- Baffles, Paddles, Scrapers 6- Chemical Tanks 7- Electric Equipment 8- Elevated Pipe 9- Filter Gallery	Station
Pumping Station 1- Electric Power 2- Pump 3- Building 4- Equipment	Station		
Reservoir	Station	SCADA 1- Instrumentation 2- Power supply 3- Communication systems 4- Weather enclosures	Station
Transmission Conduit 1- Tunnels 2- Canals 3- Large Diameter Pipes	Distribution	Distribution Pipes	Network

2.3.2 Electric power network

The electric power systems components can be grouped on the base of four different analysis levels of the network. The main topologies are listed in **Table 2.2**.

Table 2.2 Main topologies of electric power network components

Topology	Analysis Level	Topology	Analysis Level
Generation Plant	Station	Distribution circuits	Distribution
Substation	Station	Electric Power grid	Network
Macro components 1- Autotransformer line 2- Line without transformer 3- Bars-connecting line 4- Bars 5- Cluster	Substation component	Micro components 1- Circuit breakers 2- Lighting arrester 3- H Disconnect switch 4- V Disconnect switch 5- Autotransformer 6- Current transformer 7- Voltage transformer 8- Box or Control house 9- Power supply 10- Coil support 11- Bar support, Pothead 12- Regulator 13- Bus 14- Capacitor bank	Substation component

2.4 Damage Scales for Network Components

This section investigates damage scales for different networks components. For each of the main typologies, the different damage states are related to serviceability of the whole network or the single component, depending on the considered analysis level. In particular, for the network and distribution system levels, the tables refer to the serviceability of the single component. The damage scales below do not quantify the reduction of flow corresponding to each damage state. Actually, however, the performance of the network and even of a single component such as electric substation can not be predicted without a flow analysis, continued serviceability resulting from the interaction between various components, both inside the individual substation and within the neighboring ones, as well as from the spread of damage to other parts of the station and to the remaining parts of the network.

2.4.1 Potable water network

2.4.1.1 Water source

Wells are complex components that include several subcomponents. HAZUS (NIBS, 2004) gives fragility curves for anchored and for unanchored subcomponents, (**Table 2.3**).

Table 2.3 Damage scale for water source

Damage State	Description	Serviceability	
Minor	Malfunction of well pump and motor for a short time (less than three days) due to loss of electric/ backup power if any, or light damage to buildings	Nominal water flow and pressure	Operational after limited repairs
Moderate	Malfunction of well pump and motor for about a week due to loss of electric/backup power if any, considerable damage to mechanical and electrical equipment, or moderate damage to buildings	Reduced Water flow and pressure	Operational after repairs
Extensive	The building being extensively damaged or the well pump and vertical shaft being badly destroyed and non-functional		Partially operational after extensive repairs
Complete	Building Collapsing	No water available	Not repairable

2.4.1.2 Water treatment plant

HAZUS (NIBS, 2004) gives fragility curves for anchored and for unanchored sub-components for different sizes of water treatment plants (**Table 2.4**).

Table 2.4 Damage scale for water treatment plant

Damage State	Description	Serviceability	
Minor	Malfunction of plant for a short time (less than three days) due to loss of electric power, considerable damage to various equipments, light damage to chlorination or chemical tanks, Loss of water quality may occur.	Nominal water flow and pressure	Operational after limited repairs
Moderate	Malfunction of plant for about a week due to loss of electric/backup power if any, extensive damage to various equipments, considerable damage to chlorination or chemical tanks with no loss of contents. Loss of water quality is imminent.	Reduced water flow and pressure	Operational after repairs
Extensive	The pipes connecting the different basins and chemical units being extensively damaged. It will likely result in the shutdown of the plant		Partially operational after extensive repairs
Complete	The complete failure of all piping or extensive damage to the filter gallery	No water available	Not repairable

2.4.1.3 Pumping station

Pumping stations are complex components that include several subcomponents. HAZUS (NIBS, 2004) gives fragility curves for anchored and for unanchored subcomponents for different sizes. The description of their damage states is provided in **Table 2.5**.

Table 2.5 Damage scale for pumping station

Damage State	**Description**	**Serviceability**	
Minor	Malfunction of station for a short time (less than three days) due to loss of electric power or slight damage to buildings	Nominal water flow and pressure	Operational after limited repairs
Moderate	The loss of electric power for about a week, considerable damage to mechanical and electrical equipment, or moderate damage to buildings	Reduced water flow and pressure	Operational after repairs
Extensive	The building being extensively damaged or the pumps being badly damaged beyond repair		Partially operational after extensive repairs
Complete	The building collapsing	No water available	Not repairable

2.4.1.4 Reservoirs

Reservoirs are in various types depending on their material, size, anchorage, position, roof type, seismic design, foundation type, and construction technique. Different fragility curves are illustrated by ALA (2001a, b) and HAZUS (NIBS, 2004) for anchored and for unanchored subcomponents for different sizes. The description of damage states is provided in **Table 2.6**.

Table 2.6 Damage scale for water reservoir

Damage State	**Description**	**Serviceability**	
None	None	Operational	Nominal water flow
Failure	Failure of components in one of its failure modes.	Operational after repairs	No water available

2.4.2 Electric power network

2.4.2.1 Generation plant

The FEMA-HAZUS Technical Manual presents fragility curves related to generation plants. The proposed damage scale for this type of station is displayed in **Table 2.7**.

Table 2.7 Damage scale for generation plants

Damage State	Description	Serviceability	
None	None	Operational without repair	Nominal power flow
Minor	Turbine tripping, or light damage to diesel generator, or building being in minor damage state.		Reduced power flow
Moderate	Chattering of instrument panels and racks, considerable damage to boilers & pressure vessels, or the building being in moderate damage state.		
Extensive	Considering damage to motor driven pumps, or considerable damage to large vertical pumps, or the building being in extensive damage state.	Operational after repair	No power available
Complete	Extensive damage to large horizontal vessels beyond repair, extensive damage to large motor operated valves, or the building being in complete damage state.	Not repairable	

2.4.2.2 Substation

In **Table 2.8** is reported the damage scale for substations. It is based on the classification and definition of damage states given by FEMA-HAZUS Technical Manual. The four damage states are linked to the percentage of components which fail under the seismic action or to the building damage.

Table 2.8 Damage scale for substations

Damage State	Description	Serviceability	
None	None	Operational without repair	Nominal power flow
Minor	Failure of 5% of the disconnect switches, or circuit breakers, or building being in minor damage state.		Reduced power flow
Moderate	Failure of 40% of the disconnect switches, or circuit breakers, or current transformers, or the building being in moderate damage state.		
Extensive	Failure of 70% of disconnect switches (e.g, misalignment), 70% of circuit breakers, 70% of current transformers (e.g., oil leaking from transformers, porcelain cracked), or failure of 70% of transformers (e.g., leakage of transformer radiators), or the building being in extensive damage state.	Operational after repair	No power available
Complete	Failures of all disconnect switches, all circuit breakers, all transformers, or all current transformers, or the building being in complete damage state.	Not repairable	

2.4.2.3 Distribution circuits

Table 2.9 reports the damage scale for distribution circuits. It is based on the classification and definition of damage states given by FEMA-HAZUS Technical Manual. The four damage states are linked to the percentage of circuits which fail under the seismic action.

Table 2.9 Damage scale for distribution circuits

Damage State	**Description**	**Serviceability**	
None	None	Operational without repair	Nominal power flow
Minor	Failure of 4% of all circuits		Reduced power flow
Moderate	Failure of 12% of all circuits		
Extensive	Failure of 50% of all circuits	Operational after repair	No power available
Complete	Failure of 80% of all circuits	Not repairable	

2.4.2.4 Electric power grids

The fragility curves related to the whole electric power grid which is presented by Osorio, 2007, composed of the different types of stations, transmission and distribution lines. The proposed damage scale for electric power grids is illustrated in **Table 2.10**. It should be noted how the definition of nominal and reduced power flow is not quantitative and hence, not operational.

Table 2.10 Damage scale for electric power grids

Damage State	**Description**	**Serviceability**	
Minor	Connectivity loss of the distribution nodes to generation nodes is less than 20% (CL<20%)	Operational without repair	Nominal power flow
Moderate	Connectivity loss of the distribution nodes to generation nodes is between 20 to 80%		Reduced power flow
Extensive	Connectivity loss of the distribution nodes to generation nodes is more than 80% (CL=80%)	Operational after repairs	No power available

2.4.2.5 Macro-components

Table 2.11 and **Table 2.12** present the proposed damage scales for electric macro-components, according to their definitions given in the works by Vazni, 1996, and Hwang and

Chou, 1998, and reported below for reference. All macro-components are considered as series systems of several micro-components.

The failure of some macro-components involves the failure of the entire substation, since they constitute the minimal cut sets of the system. The failure of some other macro-components only involves a reduction of the power flow outgoing from the substation.

1. Autotransformer line (autotransformer + discharger + current transformer + circuit breakers + bearing)
2. Line without transformer (voltage transformer + coil support + sectionalizing switch + current transformer + circuit breaker + bearing)
3. Bars connecting line (sectionalizing switch + current transformer + circuit breaker + bearings)
4. Bars (voltage transformer + bearings)
5. Cluster (pothead, lighting arresters, switch structure [bus])

Table 2.11 Damage scales for macro-components no. 1 and 2.

Damage State	**Description**	**Serviceability**	
None	None	Operational without repair	Nominal power flow
Failure	Failure of any of the micro-components (in one of their failure modes) composing the macro-components (series system).		Reduced power flow

Table 2.12 Damage scales for macro-components no 3, 4 and 5.

Damage State	**Description**	**Serviceability**	
None	None	Operational	Nominal power flow
Failure	Failure of any of the micro-components (in one of their failure modes) composing the macro-components (series system).	Operational after repair	Reduced power flow

2.4.2.6 Micro-components

Some of electric micro-components stand alone inside the substation, being physically and logically separated from the rest of the components, while some others are assembled in series in macro-components. **Table 2.13** deals with the micro-components whose failure involves a reduction of the power flow outgoing from the substation. While **Table 2.14** refers to micro-

components whose failure of the entire substation, since either they though standing alone are vital for the performing of the substation or they are parts of the macro-components that are considered minimal cut sets of the system. In order to make this distinction, the substation's logic scheme proposed by Vazni is adopted, since it appears to be the most appropriate in the general context.

Table 2.13 Damage scale for micro-components no. 2, 5, 8, 12 and 14.

Damage State	**Description**	**Serviceability**	
None	None	Operational without repair	Nominal power flow
Failure	Failure of the micro-components in one of its failure modes.		Reduced power flow

Table 2.14 Damage scale for micro-components no. 1, 3, 4, 6, 7, 9, 10, 11 and 13.

Damage State description		**Serviceability**	
None	None	Operational	Nominal power flow
Failure	Failure of the micro-components in one of its failure modes.	Operational after repairs	No power available

2.5 Bam City Critical Infrastructures

As a case study for this research, the city of Bam in south east of Iran is considered where is affected by an earthquake in 2003 (**Fig 2.15**). Based on the Iran State Statistics Centre report, 26,271 people died in the quake that flattened most of the city on December 26. Officials had previously said more than 41,000 people were killed. A big reason for this discrepancy is that some of the dead were counted twice due to the confusion following the quake, 525 people were missed and more than 9,000 people injured. The earthquake left 60,000 homeless and destroyed much of the city of Bam.

The USGS National Earthquake information center is reported a magnitude of 6.5 for the quake, which was located just southeast of the city. About 60 percent of the buildings in Bam were destroyed (**Fig 2.16**). The old quarter and the 2000 years old citadel (Arg-e-Bam) were built primarily of mud brick**,** severely damaged by the earthquake**.**

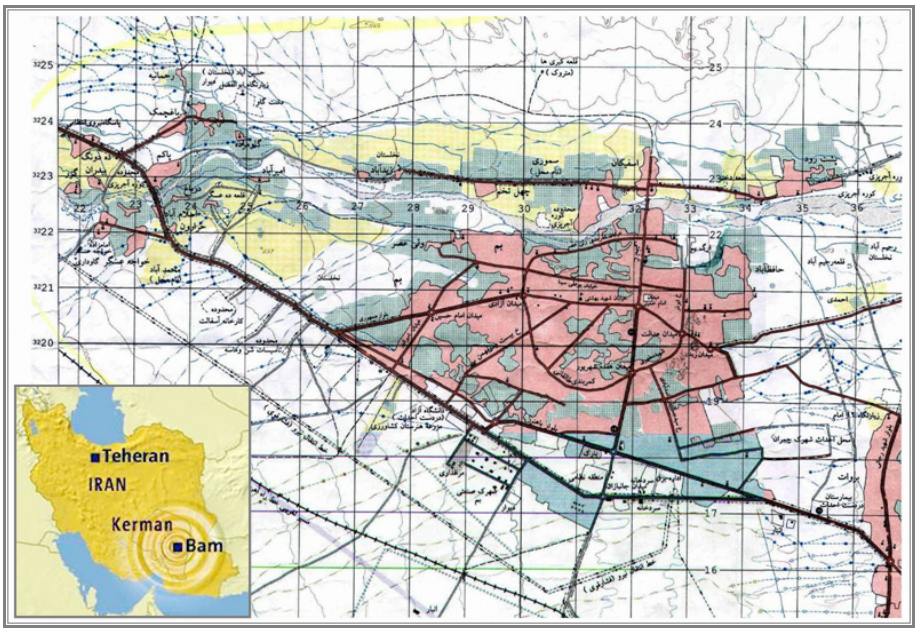

Fig 2.15 The regional map of Bam city in south east of Iran as a case study (INGO, 2001)

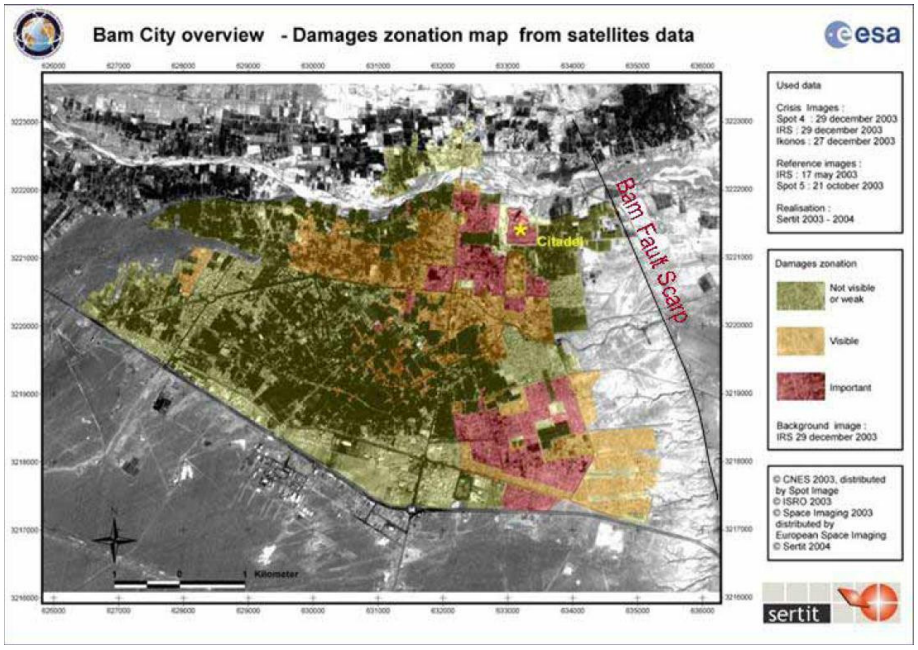

Fig 2.16 Building damage zonation map of Bam city after the 2003 earthquake (Sertit, 2004)

In order to the detailed analysis of Bam city as a case study, the city is modeled in GIS by grid mesh 500 m dimension (**Fig 2.17**). Totally the city is modeled by 217 grid meshes. Using this type of modeling, the mesh analysis can be done for the city.

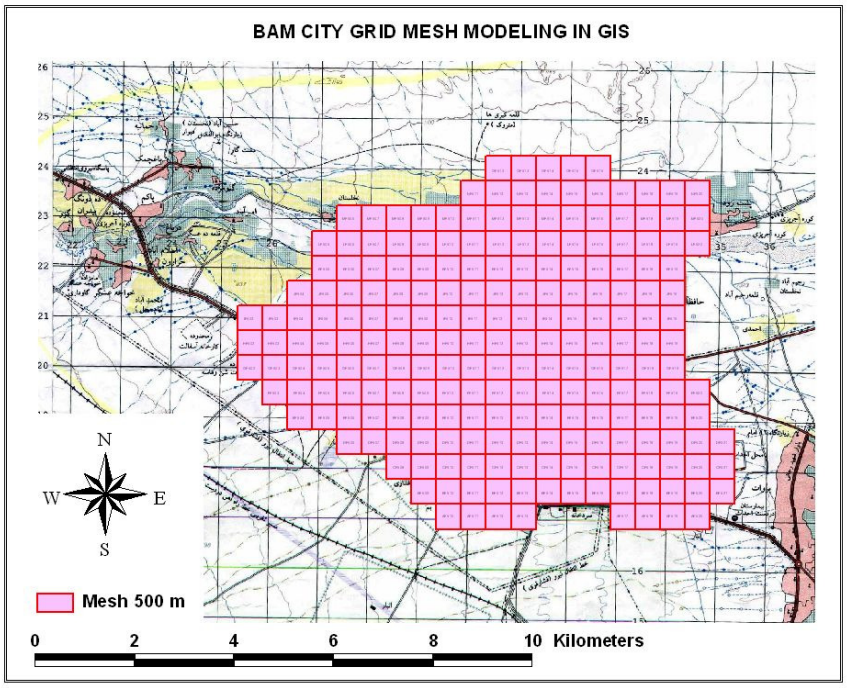

Fig 2.17 The grid mesh (500 meter) modeling of Bam city in GIS

2.5.1 Potable water network

The city uses drinking water from about 12 deep wells. The water is distributed to residential, commercial, industrial and other users via a water distribution system. The system is made of buried pipelines, mostly concrete cement pipes, and several underground and above ground water storage tanks. There is no water treatment plant in Bam. At the locations of several storage tanks chlorine mixture is added to water for chemical treatment.

2.5.2 Electric power network

There are no electric generating plants in Bam or the affected area. Bam and its vicinity are connected to the countrywide electric grid system. Main transmission lines bring electricity from this grid to Bam area. There are four substations in the area: two in Bam, one in Baravat, and one in New Arg. The two substations in Bam are 230kV and 132kV. Transformers are used to reduce the voltage to 220V for residential and commercial use. There was no damage to main 230kV transmission lines.

2.5.3 Gas and petroleum

There is no petroleum pipelines installed in the affected area. Even though a large number of small and large cities in Iran have natural gas distribution system, Bam and the affected area

did not have a gas transmission and distribution system at the time of the quake. The gas stations and heating gas suppliers bring their material via tankers to the city. Fortunately, there was no gas station in the old section of the city, which experienced severe shaking.

2.5.4 Telecommunications

The telecommunication central offices had mostly nonstructural damage as well as damage to unanchored equipment. The main telecom towers mostly survived the quake. Some communication towers located on the roofs of collapsed buildings were also damaged.

2.6 Critical Infrastructures Performance after the 2003 Bam Earthquake

The 2003 Bam earthquake destroyed most of the city of Bam and nearby villages. The earthquake was by far the most devastating earthquake in the history of the region around Bam. The maximum uncorrected accelerations recorded at Bam station were 0.82g, 1.01g and 0.65g in the longitudinal, vertical and transverse directions, respectively. The earthquake mainly affected power, water, and communication networks in the epicentral regions.

Water systems in Bam experienced heavy damage and the water supply was cut off for a long duration due to extensive pipe breaks. Bam water system, on the other hand, experienced major damage mainly because of the old asbestos cement distribution lines in Bam water network (**Fig. 2.18**). Due to collapse of the buildings and breakage of connecting pipes, at user's ends, water had to be brought by tanker trucks to the tents and shelters and other users after the earthquake (**Fig 2.19**).There were several breaks in the water distribution systems and minor damage to deep wells (**Fig 2.20**). However the chlorination unit was damaged (**Fig 2.21**).

Fig 2.18 Damaged asbestos cement water pipe (IEEE)

Fig 2.19 Collapse of the buildings

Overall the storage tanks performed well. The elevated water tank has located near the old section of the city close to the earthquake rupture where the damage was high. The tank experienced severe stress and deformation at the column-beam connections (**Fig 2.5**). However as it can be seen in Fig 2.20, the water deep wells and their building are minor damaged but they were out of service because of power shortage. This is the interdependency effect.

Fig 2.20 Damaged water deep well house

Fig 2.21 Damaged chlorination unit

Damaged substation of the power transmission system and numerous electrical transmission concrete poles in the Bam electric distribution system, caused blackouts in city within hours following the earthquake and power had not been restored for several days. There was however damage to concrete poles in the distribution power electric system and streetlights (**Fig 2.22**). Damage to transformers on distribution poles was reported. Part of the damage to the concrete poles was due to collapse of adjacent walls and buildings (**Fig 2.19**).

Fig 2.22 Damaged electric transmission concrete poles, distribution concrete and wooden poles

It is observed series of poles to be out of plumb. The 230kV substation in Bam experienced some damage. There was some damage to porcelain insulators and bushings at the substation, foundation of 230 kV transformers was also damaged (**Fig 2.23**). The wall around the substation collapsed but office/control building in substation structurally performed well.

Fig 2.23 Damaged porcelain insulators and bushings, damaged foundation of 230 kV transformer

One should note that, fires following earthquakes are very common and existence of underground gas pipelines and their ruptures due to earthquakes could lead to major conflagration. Even though there were reports of at least seven fires after the earthquake, lack of a natural gas system and wood constructions did prevent a conflagration in the city.

The damage to roads, bridges, railway and airport was minor. Many streets and most of the alleys were blocked after the earthquake due to debris from the damaged buildings. The airport was out of operation for a few hours after the earthquake due to damage to the airport control tower but later played a major role in the rescue and relief operations.

2.7 Summary and Conclusion

In order to better understand the critical infrastructure role in a society and also learn more about components of interdependent critical infrastructure and their seismic performance, the characteristics of critical infrastructures are illustrated in this chapter and a literature review on the recent advances is presented in the fields of complex networks, network topology, network dynamics, and interconnected systems. For each of the main typologies, the different damage states are related to serviceability of the whole network or the single component, depending on the considered analysis level. Therefore damage scales for network components are defined here for using in seismic performance analysis.

As a case study, the city of Bam in south east of Iran is considered where is affected by an earthquake in 2003. The earthquake was by far the most devastating earthquake in the history of the region around Bam which destroyed most of the city and nearby villages.

In order to compare the real situation with analytical results which obtain in next chapters, the characteristics of Bam city infrastructures and their performance during the earthquake are investigated. Water network in Bam experienced heavy damage and the water supply was cut off for a long duration due to extensive pipe breaks. Power electric substation and numerous electrical concrete poles are damaged which caused blackouts in city within hours following the earthquake and power had not been restored for several days.

CHAPTER 3

CRITICAL INFRASTRUCTURE MODELLING

3.1 Introduction

The advancement in science and technology has made the critical infrastructures of a society tightly interconnected and mutually dependent. Some aspects of this interdependency include physical factors, human behavior and information sharing; however, all these are vulnerable to disasters. Natural or man-made disasters happen and can cause thousands of severe casualties. These disasters have made the protection and restoration of critical infrastructures, such as health care, utilities, transportation and communication, a serious national concern.

In fact, individual critical infrastructure elements are a part of the whole interconnected system. The system functionality changes when one of the components does not work properly (much in the same way as organs in the human body) and the consequences of the failure of one facility may spread through the whole system. All of a sudden it is not talking only about the vulnerability of one facility, but also about the vulnerability of the system (Poljansek, 2010). Furthermore, it is clear that systems do not work in isolation. On the contrary, they are interdependent with other critical infrastructure systems. What does this mean? The propagation of the failure in one system can spread among systems; therefore such behavior introduces an extra vulnerability into the functioning of each particular system by virtue of its dependence on others.

However, society expects that the infrastructure service will continue with minimal disruptions, even during and after the emergency situation. Such expectations have probably been reinforced by reliable availability of the infrastructure service in the past where small disturbances have been successfully locally absorbed by the system. This perception may be eroded as large-scale accidents may become more frequent and the repercussions more complicated. Interdependencies enhance the overall system performance while also increasing the potential for cascading failures and amplifying the impact of small failures into catastrophic events. For instance, the major North American power blackout on August 14, 2003, initially triggered by some overhead transmission lines contacting with trees, lasted up to 4 days and affected several other infrastructure systems, where the estimated direct costs ranged from US$4 to US$10 billion (U.S.–Canada Power System Outage Task Force, 2006).

The most likely trigging factors are probably due to increasing demands combined with constant growth, imposed upon aging processes and equipment, and stressed by unusual environmental and operating conditions. These are probably only the symptoms of the fact that the management of critical infrastructure systems is not completely controllable for any contingency. (Poljansek, 2010).

Rinaldi, (2001) has defined four primary classes of interdependencies: the physical, cyber, geographical and logical. Two infrastructures are physically interdependent if the state of each is dependent on the material output(s) of the other. An infrastructure has cyber interdependency if its state depends on data transmitted through the information system. Infrastructures are geographically interdependent if a local environmental event can create state changes in all of them. Two infrastructures are logically interdependent if the state of each depends on the state of the other via a mechanism that is not a physical, cyber, or geographical connection. The emphasis in this thesis is on the physical layer.

.

3.2 Network Properties

As was stated in chapter 2, civil infrastructure systems are modeled as consisting of facilities and distributing elements. A water distribution system consists of dams, storage tanks and pumping stations as facilities and pipes as distributing element. An electrical power transmission system involves generating plants, substations and transmission towers as facilities and transmission lines as distributing elements.

The body of knowledge on the new science of networks is strengthening its fundamental basis and this is allowing an expansion of applications. Statistical network characterization is providing important evidence about the universality of network class properties. Also, when these properties are reproduced by analytical or algorithmic models, researchers are able to obtain significant insights on the mechanisms that produce them. Engineering is providing relevant experimental information regarding the fragility of individual and interacting network elements. Sophistication in specific network system models is increasing network response prediction. Loss estimation methods now allow for dynamic decision-making and realistic representation of the social impacts induced by network malfunctions. In the infrastructure interaction area, there are significant advances to allow moving from conceptual recognition of the problem to the development of models that account for these coupling effects. Interacting economic sectors provide evidence of the relevance of accounting for infrastructure coupling, and complex adaptive systems show the potential to become the future tool for dynamic representation of evolving interacting networks.

Despite these advances in less than a decade, statistical characterization of infrastructure networks still needs parameters to quantify network performance and the impact on society if malfunctions occur. Parameters to measure network redundancy or to quantify their service flow reduction need to be investigated. Refinement of the probabilities of failure of network elements given different hazards needs to be included in the calculation of network response to disturbances. Explicit accounting of the effects of network topology should also be considered in the development of engineering reliability assessment and mitigation plans.

The topology and flow pattern characteristics of interdependent systems also require more investigation. This will provide the understanding of the role that each network element has in maintaining individual and interdependent network connectivity and flow. Further analysis of this type of information will lead to optimal strategies to improve the performance of modern multi-infrastructure systems (Duenus-Osorio et al., 2005). **Fig 3.1** sketches an expanded version of this evolving interdependent network. The figure illustrates that individual network growth occurs from core of the existing network to the peripheries proportional to population growth, and that the interdependencies increase uniformly throughout the entire space.

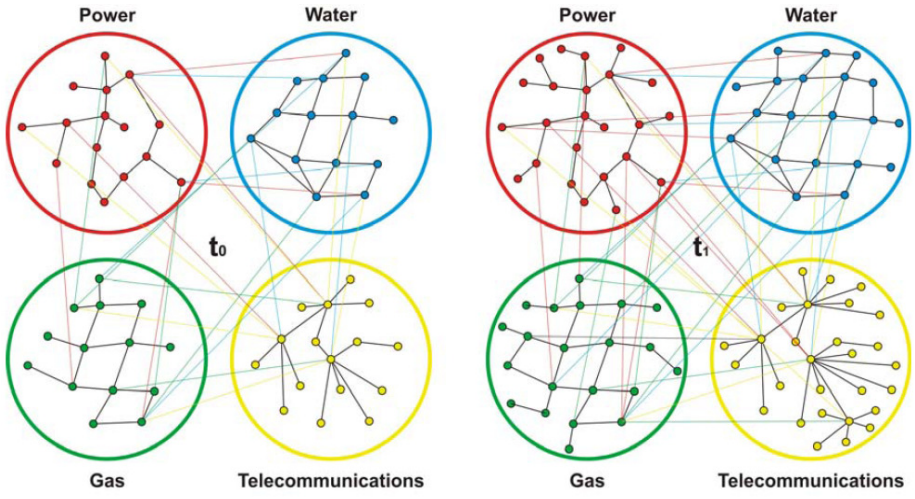

(a) at time t_0 (b) at time t_1

Fig 3.1 Interdependent networks in the same spatial domain at times $t_0 < t_1$ (Duenus-Osorio, 2005)

Additional ongoing research is expanding the understanding of the effects that network disturbances, network topology and optimal engineered service flow patterns have on interdependent response. Specific tasks of this research examine the static properties of networks, identify consistent performance measures useful for characterizing generic network functionality, and investigate approaches for efficient mitigation actions that account for

network flow type, topology, spatial interconnection, strength of coupling, and direction of the interconnectedness.

Every networked system exhibits a distinct topology or physical layout. Depending on the nature of the network, its structural configuration usually evolves to optimize the type of flow to be transported. In the case of civil infrastructure, transportation networks exhibit a mesh-like structure (**Fig 3.2a**); telecommunication networks display a decentralized topology (**Fig 3.2b**); the World Wide Web (WWW) shows an disproportionate case of decentralization in which a few highly connected vertices are responsible for network stability (**Fig 3.2c**); and the power grid at the transmission level displays a sparse mesh-like structure due to its geographical extent while at distribution level it exhibits a radial tree-like structure (**Fig 3.2d**)

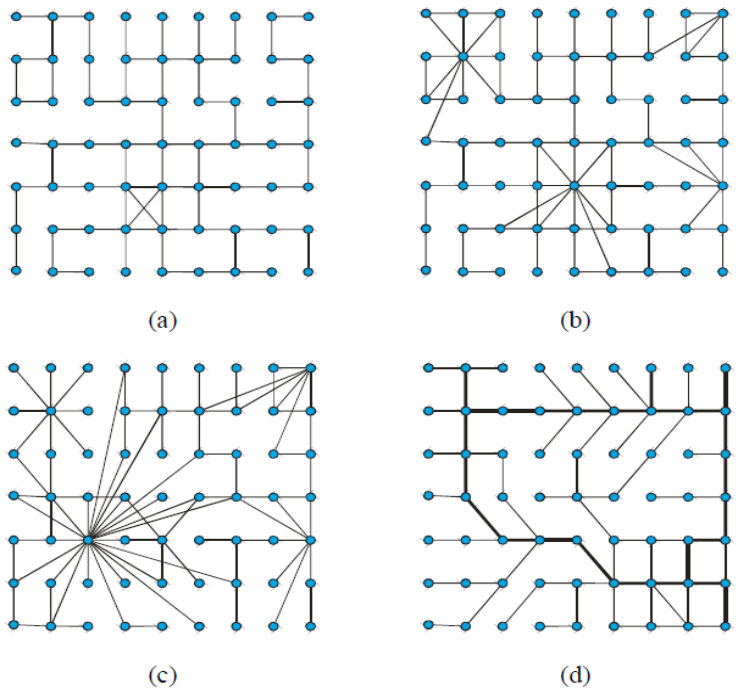

Fig 3.2 Sample of network topology diversity:
(a) transportation, (b) telecommunications, (c) WWW, (d) electric power (Duenus-Osorio, 2005)

Other utility networks such as potable water and natural gas if gas has widespread consumption have a less sparse mesh-like structure within urban centers, and a very sparse (e.g., minimally connected) topology for interurban transmission. Oil networks also have a minimally connected tree structure (Duenus-Osorio, 2005).

In addition to topological differences, networks display distinctive features in terms of their mechanisms for flow dynamics. In most civil infrastructure networks the flow process has a fixed destination from a particular origin, and it tends to happen along the most efficient route

which named the shortest path. This need for optimal flow traversal sets the basis for determining and proposing measurable network properties that simultaneously account for their physical topology and their flow processes along the routes of least resistance. Examples of flow processes different from transmission of goods starting at node i and ending at node j are the kinds of traffic exhibited by broadcasting and e-mail.

These processes allow movement of data packets from node to node, but at some point certain nodes make flow diffusion by replication, as opposed to flow diffusion by transfer. They take their incoming packet and replicate it for massive distribution. When social networks are analyzed, a larger variety of flow processes is observed (Borgatti, 2005; Newman, 2005). Money traverses a social network via random walks (i.e., a bill can move in any direction from person to person, and it is allowed to revisit nodes and links). A particular private rumor, unlike dollar bills, can simultaneously flow in several places. However, one person does not tell the same person the same story twice, even though a person can hear the same rumor from several other people. This makes the flow a trail rather than a walk. Infections flow like gossip, from person to person, but do not re-infect anyone who already has had it and survived because they became immune. If immunization did not take place, the person can be re-infected, making the flow a trek which is a walk that does not backtrack (Duenus-Osorio, 2005).

Concepts from modern graph theory are fundamental to enable measuring of these observable differences in network topology and flow types. Their unambiguous characterization is essential for classification and establishment of correlations between performance, network structure, and flow patterns. This chapter presents a discussion of the concepts of graph theory that are necessary to build up tools for network characterization. It also introduces strategies to identify the importance of network. Additionally, chapter 5 presents network performance measures which provide different levels of detail to estimate network functionality and impact on end users after internal or external disruptions.

3.3 Graph Theory

Standard graph theory terminology used throughout the following chapters is introduced in this section. A set $A' = \{A_1, \cdots, A_k\}$ of disjoint subsets of a set A is a partition of A if $A = \bigcup_{i=1}^{k} A_i$. A set of all *k-element* subsets of A is denoted by $[A]^k$. A graph or *network* is a pair $G = (V, E)$ of sets satisfying $E \subseteq [V]^2$; thus, the elements of E are 2-element subsets of V (**Fig 3.3**). The elements of V are the *vertices* (i.e. nodes) of the graph G, whereas the elements of E are its

edges (i.e., links). The number of vertices of a graph G is its order denoted by $|G|$ or n, and the number of edges is its size denoted by $\|G\|$ or m (Bollobas, 1998; Diestel, 2000).

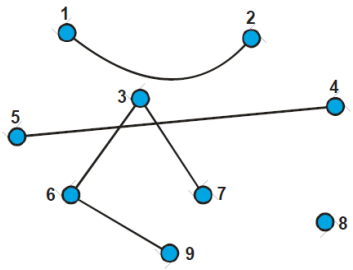

Fig 3.3 A graph on $V = \{1, \ldots, 9\}$ with $E = \{ [1,2], [3,6], [3,7], [4,5], [6,9] \}$ (Duenus-Osorio)

A vertex v is incident with an edge e if $v \in e$; then e is an edge at v. The set of all the edges in E at a vertex v is denoted by $E(v)$. Two vertices x, y of G are adjacent, or neighbors, if xy is an edge of G. If all the vertices of G are pair-wise adjacent, then G is complete. A complete graph on n vertices is K^n; for example K^3 is a triangle. If $V' \subseteq V$ and $E' \subseteq E$, then G' is a sub-graph of G, written as $G' \subseteq G$. A sub-graph $G' \subseteq G$ is a spanning sub-graph of G if V' spans all of G, i.e., if $V' = V$.

A *path* is non-empty graph $P = (V, E)$ with $V = \{x_0, x_1, \cdots, x_k\}$, $E = \{x_0x_1, x_1x_2, \cdots, x_{k-1}x_k\}$ where the all x_i are distinct. The vertices x_0 and x_k are linked by P and are called its ends. The number of edges of a path is its length, and a path of length k is denoted by P^k. In paths, k is allowed to be zero, thus $P_0 = K_1$. If $P = \{x_0x_1 \cdots x_{k-1}\}$ is a path and $k \geq 3$, then the graph $C := P + x_{k-1}x_0$ is called a *cycle*. The length of a cycle is its number of edges or vertices and is denoted by C^k (**Fig 3.4**).

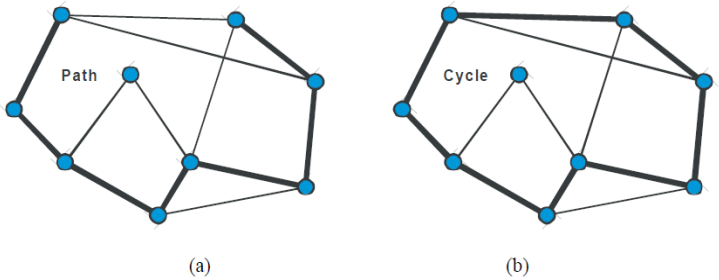

Fig 3.4 Paths and cycles in bold: (a) a path P = P7, and (b) a cycle C8 (Duenus-Osorio, 2005)

The *distance* $d_G(x, y)$ in G of two vertices x, y is the length of a shortest xy path in G; if no such path exists, $d_G(x, y) := \infty$. The greatest distance between any two vertices in G is the

diameter of G denoted by $diam(G)$. A vertex is *central* in G if its greatest distance from any other vertex is as small as possible. This distance is the *radius* of G, denoted by $rad(G)$. These distance measures are *topological parameters* that do not include network performance information such as the rate of flow transmission (Duenus-Osorio, 2005).

A non-empty graph G is called *connected* if any two of its vertices are linked by a path in G. A maximal connected sub-graph of $G=(V,E)$ is called a component of G (**Fig 3.5**). A component, being connected, is always non-empty.

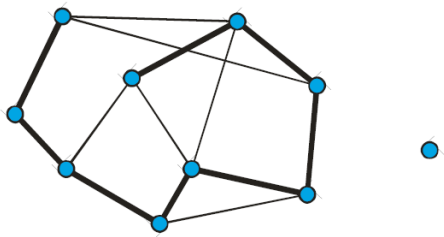

Fig 3.5 A graph with two components and minimal spanning connected sub-graphs (Duenus-Osorio)

An *acyclic* graph is a graph that does not contain any cycles, and it is called a forest. A connected forest is called a tree; a *forest* is thus a graph whose components are trees. The vertices of a tree that have only 1 incident edge are its leaves.

The *adjacency matrix* $A=(a_{ij})_{n\times n}$ of G, which constitutes its more fundamental mathematical representation, is defined by:

$$a_{ij} := \begin{cases} 1 & v_i v_j \in E \\ 0 & v_i v_j \notin E \end{cases} \tag{3.1}$$

Finally, the *incidence matrix* $B=(b_{ij})_{n\times m}$ of a graph G with $V=\{v_1,\cdots,v_n\}$ and $E=\{e_1,\cdots,e_m\}$ is defined by:

$$b_{ij} := \begin{cases} 1 & v_i \in e_j \\ 0 & v_i \notin e_j \end{cases} \tag{3.2}$$

3.4 Network Fundamental Properties

Several parameters can be calculated to characterize the topology (i.e., geometric configuration) of a network. This section presents some of the most relevant parameters currently used in the field, and introduces a proposed parameter that will be used to estimate the potential resilience of a network.

3.4.1 Mean distance, *L*

The network mean distance, *L*, has become one of the fundamental parameters in complex network analysis. Its importance is due to its ability to measure whether or not a network has the *small-world effect* that is; most pairs of vertices are connected by a short path through the network. *L* for graphs is defined as **Eq. 3.3**:

$$L = \frac{1}{n(n-1)} \sum_{i \neq j} d(i, j) \tag{3.3}$$

where $d(i, j)$ is the shortest distance from vertex *i* to vertex *j*, and *n* the order of the graph.The definition of *L* is problematic in networks that have more than one component. In such cases, there exist vertex pairs that have no connecting path, and hence d is assigned with an infinite distance, which drives the value of *L* to also be infinite. An alternative is to define L' as the average of the reciprocals or reciprocal harmonic mean in **Eq. 3.4** (Newman, 2003).

$$L' = n(n-1) \Big/ \sum_{i \neq j} \frac{1}{d(i, j)} \tag{3.4}$$

where the infinite values of $d(i, j)$ contribute nothing to the sum. In essence, these parameters measure the effectiveness of the network elements to communicate at a global scale on the order of *n*.

3.4.2 Vertex degree, *d(v)*

The degree $d_G(v) = d(v)$ of a vertex *v* is the number $|E(v)|$ of edges at *v*. This is equal to the number of neighbors of *v*. The number $\delta(G) := \min\{d(v) | v \in V\}$ is the *minimum* degree of *G*,

while the number $\Delta(G) := \max\{d(v) | v \in V\}$ is the *maximum* degree. If all vertices of *G* have the same degree *k*, then *G* is *k-regular*. The *average degree* of *G* is simply in **Eq. 3.5**.

$$d(G) = \frac{1}{|V|}\sum_{v \in V} d(v) \tag{3.5}$$

Analysis of the vertex degree for theoretical and real graphs has revealed that the distribution of their vertex degree plays a crucial role in determining the fate of a network when subjected to random or targeted attacks (Albert et al., 2000). If the vertex degree distribution is Poisson with short thin tails, then the network is equally vulnerable to random or malicious disruptions because all vertices have a typical degree. If the vertex degree distribution follows a power law with long thick tails (i.e., distribution in which most vertices have a typical degree, but that a few vertices have a disproportionately large degree), then the networks show a significant resilience to random disruptions. However, they also exhibit a dramatically vulnerable response if the disturbance is directed to vertices with highest degree.

3.4.3 Clustering coefficient, γ_v

In order to define the clustering coefficient of a graph, it is necessary to first introduce the concept of neighborhood. The neighborhood, $\Gamma(v)$ of a vertex *v* is the sub-graph that consists of vertices adjacent to *v* without including *v* itself. The clustering coefficient γ_v uses $\Gamma(v)$ to characterize the extent to which vertices adjacent to any vertex *v* are adjacent to each other (Watts, 1999). The clustering coefficient γ_v can obtain by **Eq. 3.6**.

$$\gamma_v = \frac{2|E(\Gamma_v)|}{d(v)(d(v)-1)} \tag{3.6}$$

where $|E(\Gamma_v)|$ is the number of edges in the neighborhood of *v* and the denominator represents the expansion of a binomial coefficient which amounts to the total number of possible edges in $\Gamma(v)$. This clustering coefficient can be regarded as a local measure of connectivity. It measures how connected the network is in local scales (Duenus-Osorio, 2005).

3.4.4 Redundancy ratio, R_R

Large scale complex networks, such as the power grid, may be sporadically subjected to infrequent natural disasters (e.g., earthquake, hurricanes, tornadoes, etc.), or to malicious attacks. However, these networks are also constantly subjected to direct disturbances of their elements, either by frequent natural hazards (e.g., windstorms, ice, fire, lightning, etc.), vandalism, or simple malfunction due to aging or improper operating conditions. Most of the frequent disturbances are locally absorbed by the networks, and the end-users remain unaware of their occurrence (Institute of Electrical and Electronics Engineers, 2004). This fact results from the ability of the networks to redistribute the flow at the location of the disturbance. In other words their global stability depends on the capacity to manage and redistribute local disturbances. When this does not work, the various infrastructure networks can head to imminent cascading failures, traffic congestions, or widespread pressure losses. This local disturbance absorption motivated to propose a parameter named redundancy ratio that captures the redundancy of the network at local levels (Duenus-Osorio, 2005).

Then, if *G* is a graph, the redundancy ratio of a vertex, R_{R_v} is a parameter that counts the number of independent paths from a vertex $v \in V(G)$, to each of the vertices of the set of the neighbors of its neighbors $V\left(\Gamma^2(v)\right)$. This count is normalized by the maximum possible number of node-independent paths from v to the vertices of $V_S\left(\Gamma^2(v)\right)$, where the graph $S = \left\{v \cup \Gamma(v) \cup \Gamma^2(v)\right\}$ is a complete graph. Let $I(i, j)$ denote the maximum number of node independent paths between each pair of distinct vertices (i, j) in *G*. This counting can be efficiently computed using approximating algorithms (White and Newman, 2001), mentioned that $I(i, j) = \min\{d(i), d(j)\}$, which is true for any graph. The redundancy ratio of a vertex *v* in a graph *G* is defined by **Eq. 3.7**.

$$R_{R_v} = \frac{1}{\left(|S| - 1\right)^2} \sum_{j \in V\left(\Gamma_v^2\right)} I(v, j) \tag{3.7}$$

where $\left(|S| - 1\right)^2$ is the number of independent paths between a vertex *v* and the vertices of the vertex set $V_S\left(\Gamma^2(v)\right)$ in a complete graph on $|S|$ vertices. The most redundant simple graph is a complete graph. Hence, the median of R_{R_v} for all $v \in V(G)$ results in a measure of the redundancy ratio for the graph *G*, where $0 \le R_R \le 1$. Values close to 1 identify highly redundant

networks and $R_R = 0$ indicates completely fragmented graph (i.e., no edges left), which implies that the number of components equals the order *n*. $R_R = 1$ indicates a complete graph. For large *n*, paths (i.e., transmission line) have $R_R \to 1/8$, and stars (i.e., graphs with n-1 leaves and 1 vertex connecting them all) have $R_R \to 0$.

If a large scale disturbance occurs and the number of disturbed vertices is comparable to the order n of the network G, then it can be expected that graphs with high R_R will still display a higher global redundancy. This correlation comes from the fact that in most graphs the number of vertices reachable from a vertex v increases exponentially with the distance from it, and therefore the likelihood of path existence between vertices far apart is also high.

3.5 Bam City Network Modeling

Each infrastructure system can be described as an abstract network. For example, for the pipeline systems, nodes describe pipeline intersections or point facilities while links model pipeline segments. This research takes the potable water network and power main distribution grid in Bam city, Iran as an example to illustrate the proposed approach. The original infrastructure systems raw data is obtained from Bam water and power electric companies just after the 2003 Bam earthquake and then converted to GIS format.

3.5.1 Potable water network

For the potable water network, nodes represent water sources (e.g. wells), water storage facilities, water delivery facilities and water pipeline junctions. They are classified into three types: source nodes (water sources and water storage facilities), transmission nodes (connection point), and demand nodes (water delivery facilities), which are, respectively, included in sets S_W , T_W and D_W so that $S_W \cup T_W \cup D_W \subset V_W$. Links represent the pipelines, and are included in set E_W whose ends belong to V_W . **Fig 3.6** presents the geographical representation of the potable water network based on the Kerman Province Water and Wastewater Company (KPWWC) map in 2004. One example sheet of the map is put in **Appendix A**.

There are 162 nodes in total, and among them 5 are source nodes, 64 are transmission nodes and 93 are load nodes. These nodes are connected by 229 links; with a total length of 139.42 km. It is assumed that source type of water nodes require power to keep their normal operation, which means each water source node needs to connect to at least one power node.

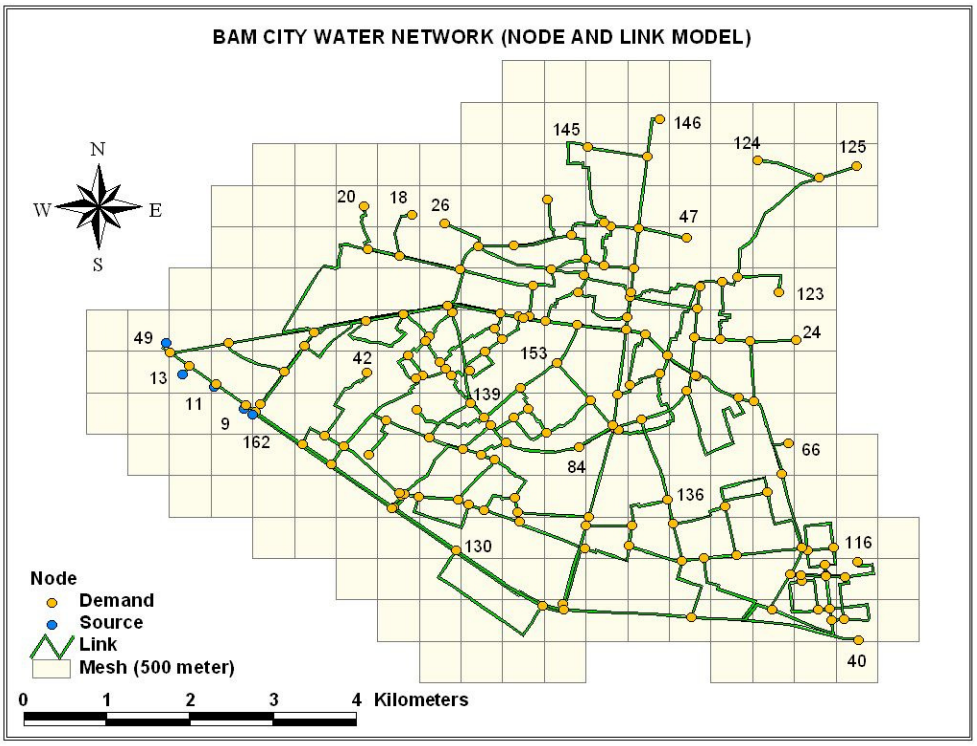

Fig 3.6 The geographical representation of the Bam city potable water network

The diameter of the network is 10939 m between nodes 49 (source) and 66 (demand), the radius is 299 m between nodes 69 and 120. The maximum shortest paths between 5 available source nodes (9, 11, 13, 49 and 162) and demand nodes are related to demand node 66. On the other words the demand node 66 is the farthest node to the sources which is the critical point in the network especially after earthquake. The maximum vertex degree is 6 in node number 139 which is located in center of the network and it has important role in network serviceability. The mean distance, degree, clustering coefficient and redundancy ratio of the Bam water network vertices are illustrated in **Figs 3.8 to 3.11** respectively.

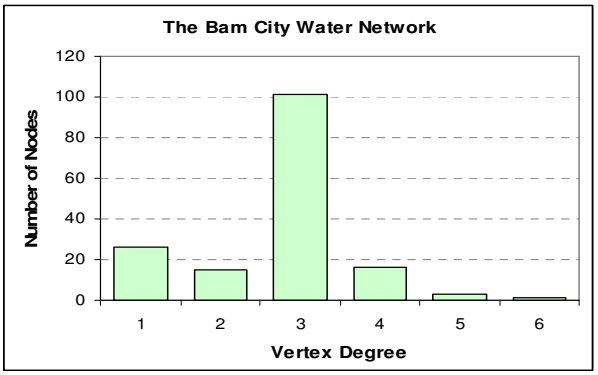

Fig 3.7 Abundance of the Bam city water network vertex degree

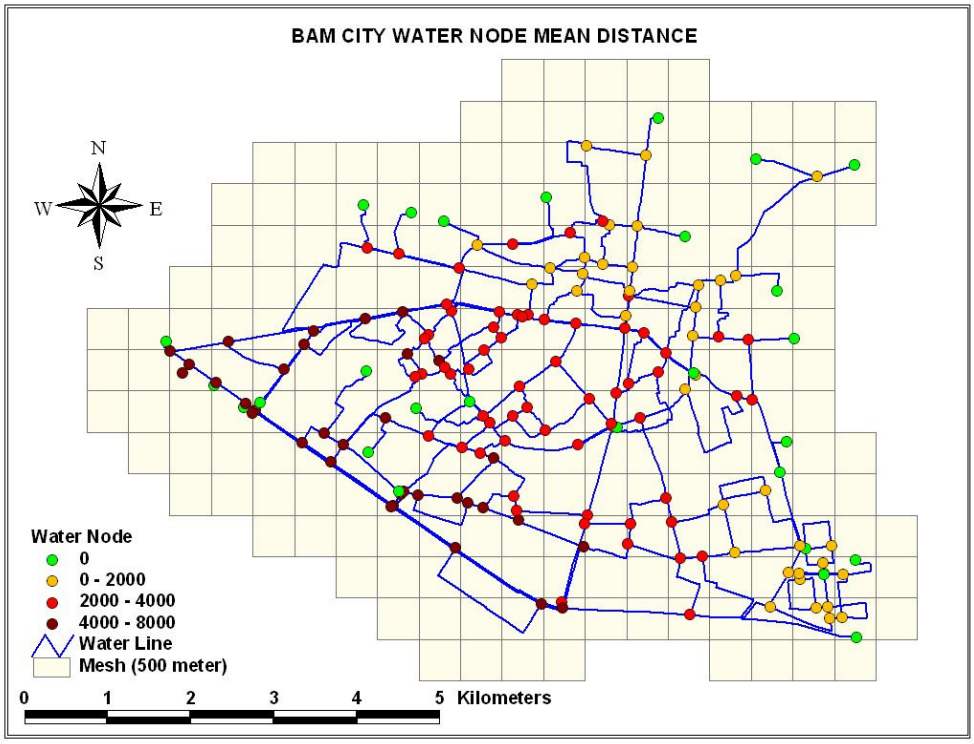

Fig 3.8 Bam water node mean distance

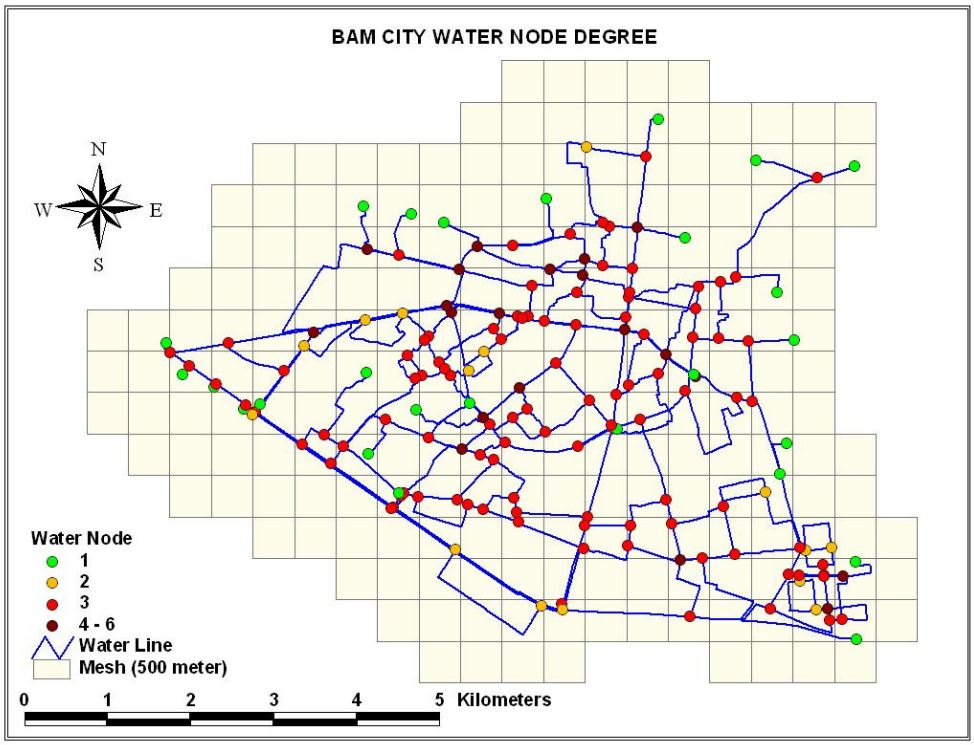

Fig 3.9 Bam water node degree

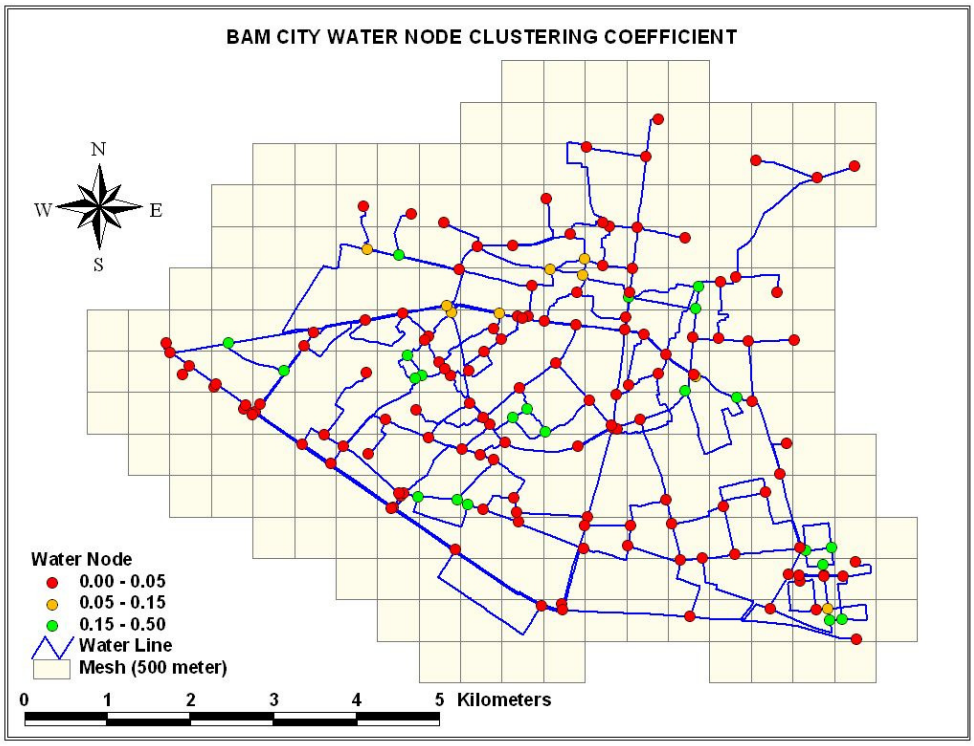

Fig 3.10 Bam water node clustering coefficient

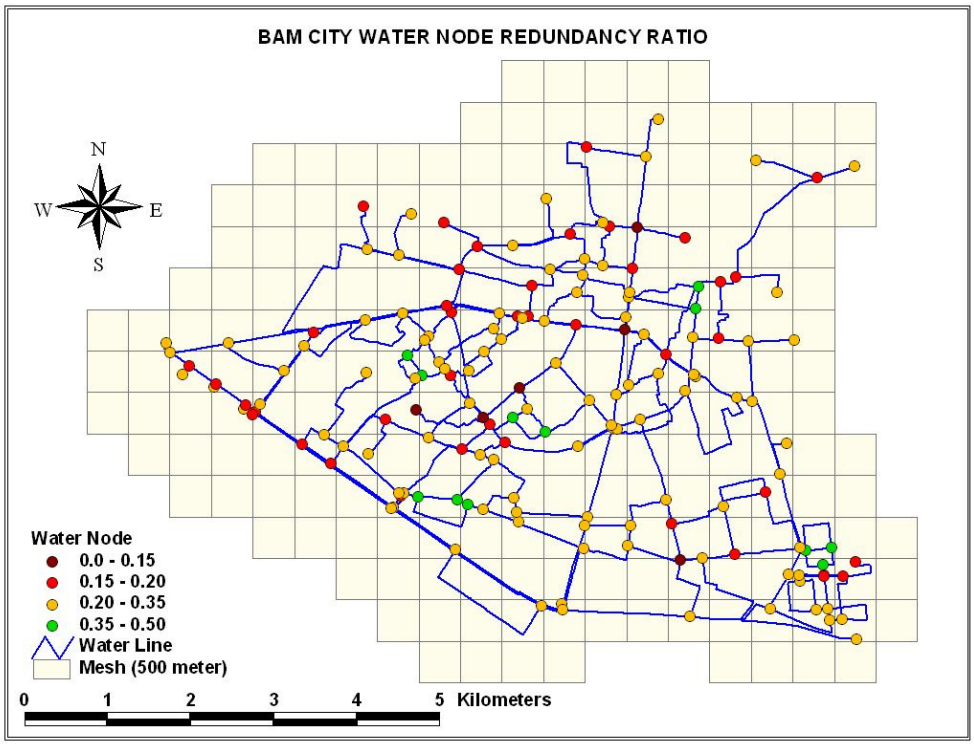

Fig 3.11 Bam water node redundancy ratio

3.5.2. Power main distribution grid

For the power main distribution grid, only the 230/132 kV substation and 20 kV areal transformer and at grade substations along with main distribution level facilities are identifiable from the data sources while the corresponding electric distribution network is not available for analysis due to *security concerns*; hence, except for power 230/132 kV substation, all other substations are regarded as load substations which provide power to customers including water facilities. Under this assumption, nodes represent high voltage substation and demand medium voltage substations, which are included in sets S_P and D_P, respectively, and in Bam city power network $S_P \cup T_P \cup D_P \subset V_P$. Links describe electrical main distribution lines between nodes, and are included in set E_P whose ends belong to V_P. A geographical representation of the main distribution power grid in Bam city is shown in **Fig 3.12** base on Kerman Province Electric Company (KREC) map in 2004. One example sheet of the map is put in **Appendix A**.

There are 80 nodes, where 1 of them is supply nodes and the rest are load nodes which 40 of them are as a leave. These nodes are connected by 88 links, with a total length of 73.1 km.

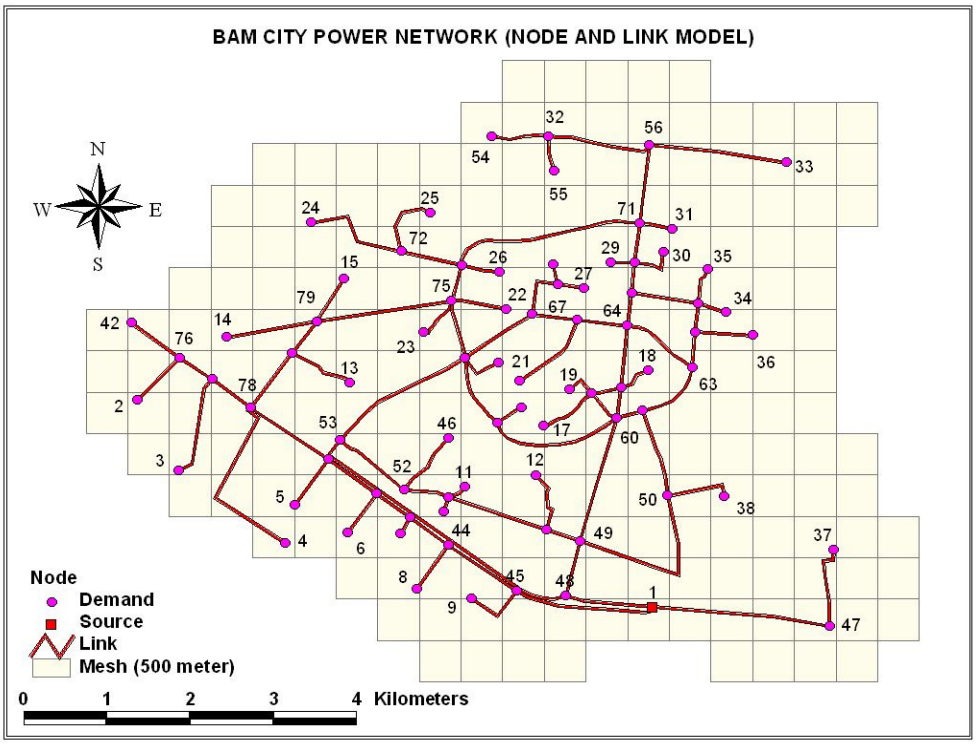

Fig 3.12 The geographical representation of the Bam city main distribution power network

The diameter of the network is 10654 m between nodes 35 and 54, the radius is 321 m between nodes 43 and 56. The maximum shortest path between source node and demand nodes

is related to demand node 24. The length of the shortest path is 9721 m. On the other words the demand node 24 is the farthest node to the sources which is the critical point in the network especially after earthquake. The maximum vertex degree is 5 in nodes number 60, 73 and 75, which are located in center of the network and they also have important role in network serviceability. The mean distance, degree, clustering coefficient and redundancy ratio of the Bam power network vertices are illustrated in **Figs 3.14 to 3.17** respectively.

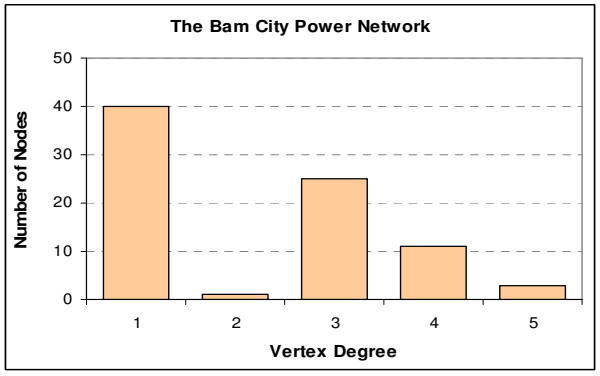

Fig 3.13 Abundance of the Bam city power network vertex degree

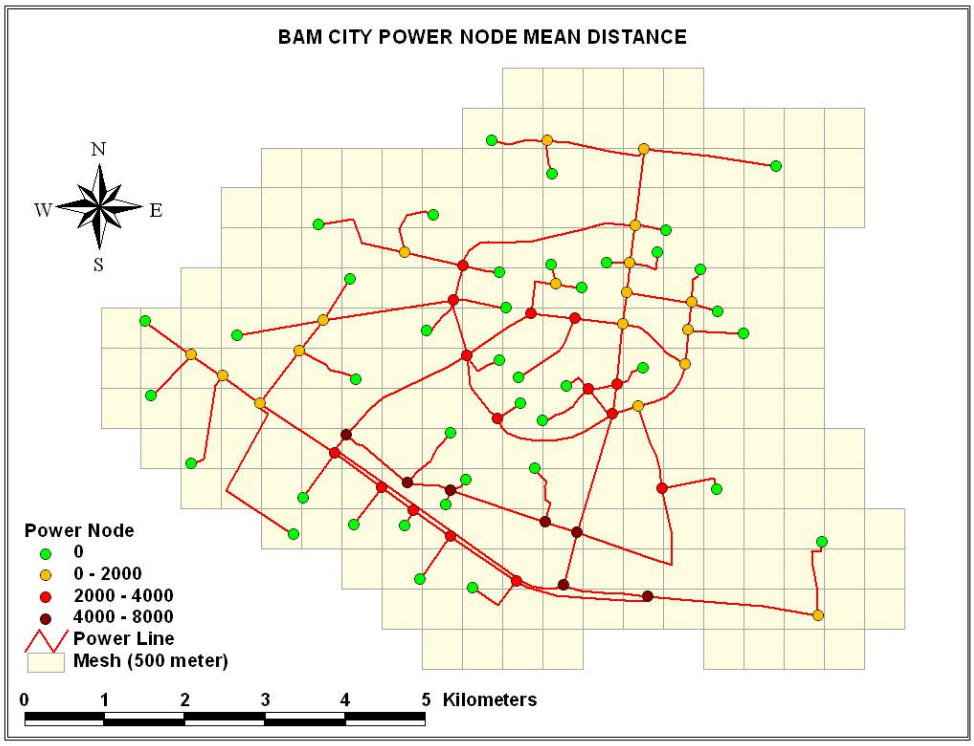

Fig 3.14 Bam power node mean distance

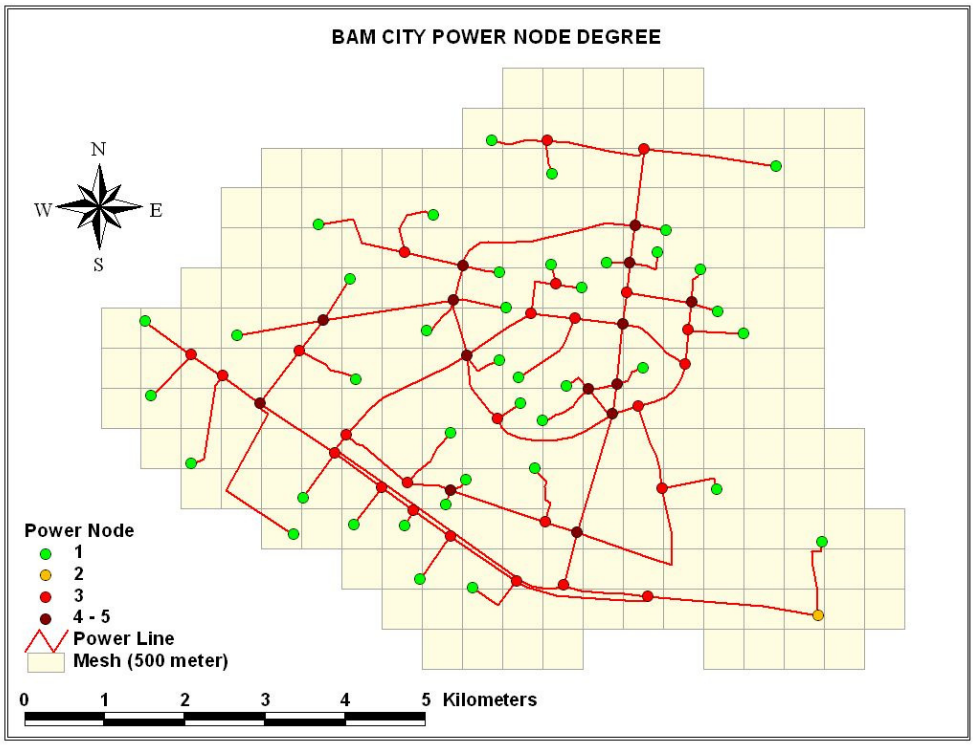

Fig 3.15 Bam power node degree

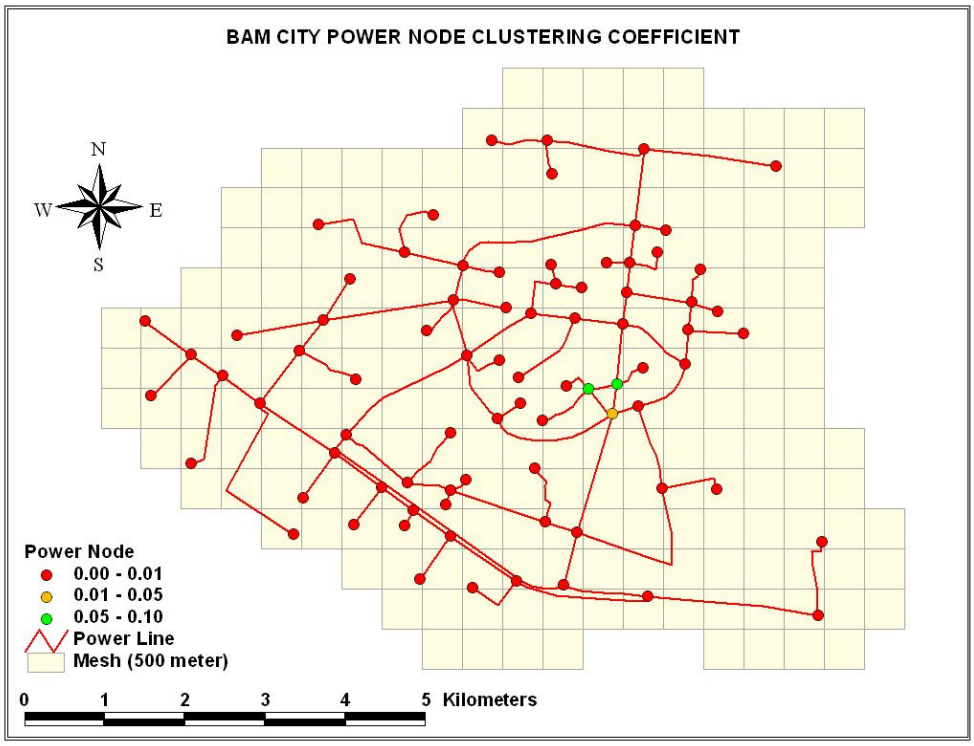

Fig 3.16 Bam power node clustering coefficient

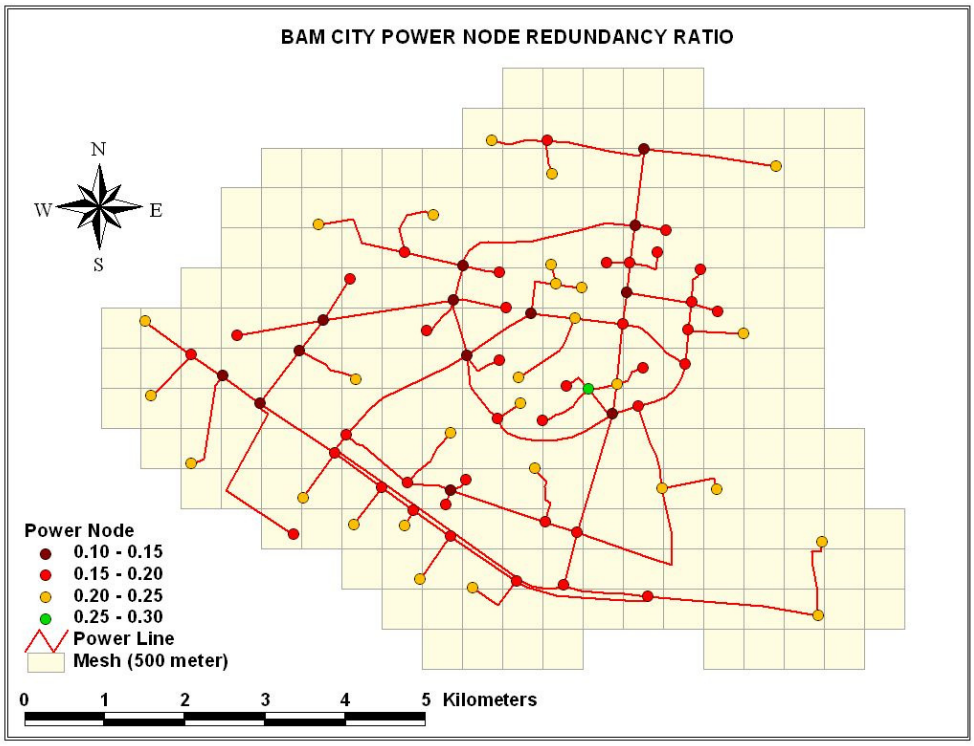

Fig 3.17 Bam power node redundancy ratio

3.6 Summary and Conclusion

The approaches for critical infrastructure modeling are illustrated in this chapter and the graph based method is considered which uses nodes to represent different types of system components and links to present the physical and relational connections among them, provides affordable and intuitive system representations along with detailed descriptions of their topology and flow patterns. This method can analyze the effects of system topology, element physical fragility, and attack intensity on system performance levels which are measured by connectivity and flow delivery. Therefore some of the most relevant parameters including mean distance, vertex degree, clustering coefficient and redundancy ratio are introduced. These mentioned parameters are computed for Bam critical infrastructures and their important nodes based on each parameter are defined. The obtained results will be used to estimate the potential resilience of networks in the next chapters.

CHAPTER 4

CRITICAL INFRASTRUCTURE SEISMIC HAZARD ANALYSIS

4.1 Introduction

Seismic risk assessment of distributed systems and infrastructures is considerably more complicated than that of a single structure on account of the geographical spread of lifelines. Lifeline risk assessment requires knowledge about ground-motion intensities at multiple sites. Seismic risk analysis of lifelines requires a different approach from the one commonly used for site-specific structures. One of the key issues, at least on the hazard side, is to account for the existence of a statistical correlation between ground motion intensity measures at the different sites where the segments spatially extend over long distances. Prediction of strong ground motion in a wide area has played a very important role in earthquake disaster prevention and damage mitigation, as well as in seismic design and assessment of infrastructures spatially spread. Earthquakes have regional characteristics: epicenters, magnitudes, seismic wave propagation characteristics and ground motions at specific sites. For structural design of new facilities and estimating damage to existing facilities, capturing these regional characteristics is important.

This chapter introduces fundamental characteristics and mathematical models of regional earthquake characteristics in the East Southern Iran (Bam), including earthquake sources, attenuation relationships, ground motion amplifications due to local soil characteristics, and spatial correlation of ground motions. Two methods for specifying seismic hazard are introduced: probabilistic seismic hazard analysis (PSHA) and scenario earthquake (SE) based seismic hazard analysis. The characterization of seismic hazard in this Chapter will be used subsequently to compute seismic intensities such as peak ground acceleration (PGA) and peak ground velocity (PGV) at sites of facilities and distribution elements comprising infrastructure systems after properly selected scenario earthquakes.

4.2 Seismic Hazard and Risk

A hazard is a situation, which possesses a level of threat to life, health, property, or environment caused by natural phenomena or human behavior (unintentional or intentional). Here it will be focused on natural hazards that could potentially be harmful to people's life, property or the environment. It is important to make a distinction between the risk and the

hazard because one can change the risk without changing the hazard. In general, the concept of risk combines the probability of occurrence of phenomena and the probabilistic evaluation of the economic and life loss associated with the phenomena. It is often expressed with the following mathematical relationship as **Eq 4.1**.

$$Risk = (likelihood\ of\ event) \times (consequences\ of\ the\ event) \tag{4.1}$$

As such, a risk is often expressed in measurable quantities such as the expected number of fatalities, injuries, extent of damage, failures, or economic loss. The whole process of measuring is called risk assessment, which must measure both the probability and consequences of all of the potential events that comprise the hazard. Risk assessments normally involve examining the factors or variables that combine to create the whole risk picture.

However the effects of hazards can mitigate by preparing for them. For example, seismic standards help to engineer earthquake-resistant buildings. Besides, the effectiveness of applied provisions can be improved with more accurate prediction of time, location, or intensity of the hazard occurrence. A set of provisions to control the risk is called risk management. Without risk assessment, it cannot be made decisions related to managing those risks. Because the additional provisions need extra financial investment, the risk management must deal with the judgment of the accepted risk and mitigation costs.

The case study of this research is focused on vulnerability of manmade networks to seismic hazards. Seismic hazard is defined as the probable level of ground shaking associated with the recurrence of earthquakes. The assessment of seismic hazard is only the first part in the evaluation of seismic risk, which is referred to as the likelihood of the event in the Eq 4.1. Seismic hazard is presented in seismic hazard maps with the expected earthquake ground motion at a given geographical location. When considering the local soil conditions and the other vulnerability factors of the affected infrastructures or population, it progresses to the second step in evaluation of seismic risk, referred to as consequences of the event in Eq 4.1.

It is possible that large earthquakes in remote areas result in high seismic hazard but show no risk; on the contrary, moderate earthquakes in densely populated areas result in small hazard but high risk.

4.3 Seismic Hazard Analysis

In order to assess risk to a structure or lifeline from earthquake shaking, it must first determine the annual probability or rate of exceeding some level of earthquake ground shaking

at a site, for a range of intensity levels. The somewhat complicated probabilistic evaluation could be avoided if it was possible to identify a "worst-case" ground motion and evaluate the facility of interest under that ground motion. This line of thinking motivates an approach known as deterministic hazard analysis. According to Boore (1987 and 2003), the spectrum of ground motion at a site can be evaluated from four ingredients (**Fig 4.1**): earthquake source (*E*), path (*P*), site (*G*) and type of motion (*I*) as **Eq. 4.2**:

$$Y(M_0, R, f) = E(M_0, f) \cdot P(R, f) \cdot G(f) \cdot I(f) \tag{4.2}$$

where M_0 is the seismic moment which is related to the moment magnitude of the earthquake, R is the distance from the source to the site and f is the frequency. The shape and the amplitude of the source spectrum $E(M_0, f)$ are specified from a single corner or double corner frequency spectrum and earthquake size. The path effect spectrum $P(R, f)$ is determined from the geometrical spreading of seismic waves and the epicentral distance to the site. The site effect spectrum $G(f)$ is determined from the local soil condition at the site. Finally, $I(f)$ is used to model the particular local ground motion evaluated from the other three spectra (Boore, 1987 and 2003; Fernandez and Rix, 2006).

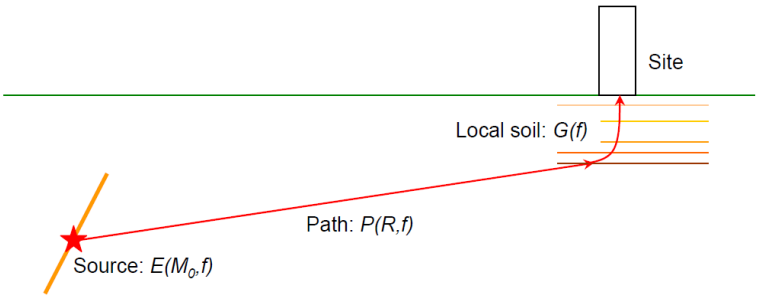

Fig 4.1 Seismic wave path from source to site (modified from Kramer, 1996)

From geological information and historical seismicity, seismic intensities at a site are determined using the following three factors: earthquake sources as a function of earthquake magnitude, attenuation relationships as a function of earthquake magnitude and epicentral distance to the site, and local soil amplification as a function of local soil condition and seismic intensity at the site. In addition, spatial correlation of seismic intensities is an important factor when analyzing response of an infrastructure system whose facilities and distribution elements are distributed over a wide area.

4.3.1 Earthquake Source

The earthquake source term depends on location of the earthquake epicenter and magnitude. The geographical distribution of epicenters is evaluated from earthquake records and fault locations. The recurrence of an earthquake with a certain magnitude level in a source zone is estimated by the Gutenberg-Richter recurrence law or the bounded Gutenberg-Richter recurrence law (Gutenberg and Richter, 1944; Kramer, 1996).

The Gutenberg-Richter recurrence law models a mean annual frequency of an earthquake whose magnitude is more than *m* (Kramer, 1996) by **Eq. 4.3**.

$$\lambda_m = 10^{a-b\cdot m} = \exp(\alpha - \beta \cdot m) \tag{4.3}$$

where $\alpha = \ln(10) \cdot a$ and $\beta = \ln(10) \cdot b$. The Gutenberg-Richter recurrence law implies that earthquake magnitudes are exponentially distributed when the range of possible earthquakes in large area are considered. The probability density function of magnitude *M* for the Gutenberg-Richter recurrence law is expressed by **Eq. 4.4**.

$$f_M(m) = \beta \cdot \exp(-\beta \cdot m) \tag{4.4}$$

The Gutenberg-Richter recurrence law often is bounded to capture the maximum event believed possible at a site or the minimum event of engineering significance. In this law, the distribution of magnitudes has a maximum ($m_{\max}$), which is determined from historical or geological evidence. According to historical data, maximum magnitude is considered 7.5 for Bam city. For engineering purposes, a lower threshold magnitude (m_0) is also implemented, which is defined as the magnitude of earthquake below which significant damage is unlikely to occur (Kramer, 1996). By considering both the lower threshold and maximum magnitude, the mean annual rate of exceedance of an earthquake of magnitude can obtain by **Eq. 4.5**.

$$\lambda_m = \nu \cdot \frac{\exp[-\beta(m - m_0)] - \exp[-\beta(m_{\max} - m_0)]}{1 - \exp[-\beta(m_{\max} - m_0)]} \tag{4.5}$$

where $\nu = \exp(\alpha - \beta \cdot m_0)$ and $m_0 \le m \le m_{\max}$. The probability density function of magnitude for the bounded Gutenberg-Richter recurrence law is expressed by **Eq. 4.6**.

$$f_M(m) = \frac{\beta \cdot \exp[-\beta(m - m_0)]}{1 - \exp[-\beta(m_{\max} - m_0)]} \tag{4.6}$$

4.3.2 Ground Motion Attenuation

The decay in seismic waves due to the seismic wave path from source to site is represented by an attenuation relationship, which is determined from many records of measured ground motions from earthquakes occurring in geologically similar zones. Attenuation relationships typically describe a mean or median value of a local ground motion intensity measure as a function of the magnitude of an earthquake and the epicentral distance. The uncertainty associated with these relationships is a major source of uncertainty in seismic risk assessment of civil infrastructure facilities. Several attenuation relationships are available which can be considered for estimating ground motions in Bam city as described below.

Toro and McGuire (1987) developed attenuation relationships for PGA, PGV and spectral velocities based on the proposed model by Hanks and McGuire (1981).

$$\ln(PGA) = 2.424 + 0.982 \cdot M_w - 1.004 \cdot \ln(R) - 0.00468 \cdot R \tag{4.7}$$

$$\ln(PGV) = -1.717 + 1.069 \cdot M_w - 1.000 \cdot \ln(R) - 0.00391 \cdot R \tag{4.8}$$

where M_W is moment magnitude and R is an epicentral distance. Atkinson and Boore (1990) proposed attenuation relationships for PGA and PGV, and spectral accelerations on hard rock which were derived from an empirically based stochastic ground motion model (**Eq. 4.2**).

$$\log_{10}(PGA) = 3.79 + 0.298 \cdot (M_w - 6) - 0.0536(M_w - 6)^2 - \log_{10}(R) - 0.00135R \tag{4.9}$$

$$\log_{10}(PGV) = 2.04 + 0.422 \cdot (M_w - 6) - 0.0373(M_w - 6)^2 - \log_{10}(R) \tag{4.10}$$

Toro et al. (1997) proposed the following attenuation relationships for PGA and spectral accelerations on rock based on predictions of a stochastic ground motion model and records;

$$\ln(PGA) = 2.2 + 0.81(M_w - 6) - 1.27 \cdot \ln\left(\sqrt{R^2 + 9.3^2}\right)$$
$$-(1.16 - 1.27) \cdot \max\left\{0, \ln\left(\frac{\sqrt{R^2 + 9.3^2}}{100}\right)\right\} - 0.0021 \cdot \sqrt{R^2 + 9.3^2} + \ln(1.52) \tag{4-11}$$

Toro (2003) later modified this relationship by including it as one of a weighted average of three attenuation relationships. The proposed attenuation for PGA on rock is as **Eq. 4.13**.

$$\ln(PGA) = 0.4 \cdot f_1 + 0.4 \cdot f_2 + 0.2 \cdot f_3$$

$$\ln(f_1) = 2.2 + 0.81(M_w - 6) - 1.27 \cdot \ln\left(\sqrt{R^2 + 9.3^2 \cdot e^{(-1.25+0.227M_w)^2}}\right) - (1.16 - 1.27) \cdot \max\left\{0, \ln\left(\frac{\sqrt{R^2 + 9.3^2 \cdot e^{(-1.25+0.227M_w)^2}}}{100}\right)\right\} - 0.0021 \cdot \sqrt{R^2 + 9.3^2 \cdot e^{(-1.25+0.227M_w)^2}} + \ln(1.52)$$

$$\ln(f_2) = 2.2 + 0.81(M_w - 6) - 1.27 \cdot \ln\left(R + 0.0089 \cdot e^{0.6 \cdot M_w}\right) - (1.16 - 1.27) \cdot \max\left\{0, \ln\left(\frac{R + 0.0089 \cdot e^{0.6 \cdot M_w}}{100}\right)\right\} - 0.0021 \cdot R + 0.0089 \cdot e^{0.6 \cdot M_w} + \ln(1.52)$$

$$\ln(f_3) = 2.2 + 0.81(M_w - 6) - 1.27 \cdot \ln\left(\sqrt{R^2 + 9.3^2}\right) - (1.16 - 1.27) \cdot \max\left\{0, \ln\left(\frac{\sqrt{R^2 + 9.3^2}}{100}\right)\right\} - 0.0021 \cdot \sqrt{R^2 + 9.3^2} + \ln(1.52) \quad (4.13)$$

Campbell (2003) employed a hybrid empirical method which includes the stochastic ground motion model. The attenuation relationship is bounded at epicentral distances of 70 km and 130 km considering the effect of the Mohorovicic discontinuity (Kramer, 1996):

$$\ln(PGA) = 0.0305 + 0.663 \cdot M_w - 0.0427 \cdot (8.5 - M_w)^2 - 1.591 \cdot \ln(R) + (-0.00428 + 0.000483 \cdot M_w) \cdot R + f$$

$$f = \begin{cases} 0 & R \le 70km \\ 0.683 \cdot \ln\left(\frac{R}{70}\right) & 70km < R \le 130km \\ 0.683 \cdot \ln\left(\frac{R}{70}\right) + 0.416 \cdot \ln\left(\frac{R}{130}\right) & 130km < R \end{cases} \quad (4.14)$$

Finally, the attenuations of PGA, PGV and spectral accelerations derived by Ghodrati et al. (2007) proposed predictive model especially for Iran seismic zones. The relationships for PGA and PGV on rock are;

$$\ln(PGA) = 4.15 + 0.623M_s - 0.96\ln(R) \tag{4.15}$$

$$\ln(PGV) = -0.71 + 0.894M_s - 0.875\ln(R) \tag{4.16}$$

The seven attenuation relationships for PGA and the three attenuation relationships for PGV shown above are plotted in **Fig 4.2** and **4.3** for $M_w = 6.5$. Each attenuation relationship leads the median values of PGA or PGV at specific epicentral distances. The aleatory uncertainty, which is due to the shortage of knowledge or data and yields the deviation from the attenuation relationship, must be included, as described subsequently.

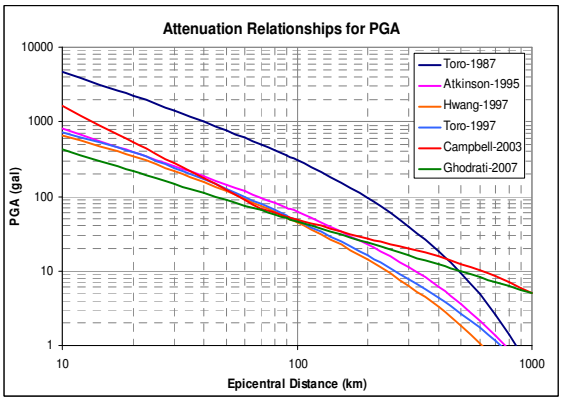

Fig 4.2 PGA Attenuation relations (Mw = 6.5)

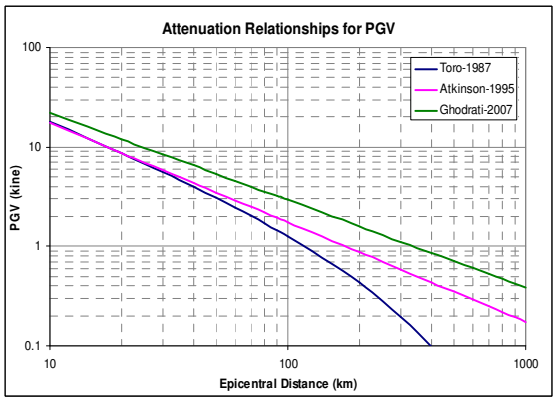

Fig 4.3 PGV Attenuation relations (Mw = 6.5)

Furthermore, the difference among the attenuation relationships leads an epistemic uncertainty, which is due to the differences in the modeling approaches on which the attenuation relationships are based.

4.3.3 Local Soil Amplification

Ground motions are amplified or damped as a result of local soil conditions at a site. This effect is captured from knowledge of the profile of local soil layers, the wave velocity in each layer of local soil, the plasticity index (PI) of each soil layer, the over consolidation ratio (OCR) of each soil layer and ground water level at the local site (Hwang et al, 1997; Dobry et al, 2000). The local amplification effects are represented numerically by soil amplification

factors with respect to the seismic intensity of interest, such as peak ground acceleration, peak ground velocity, spectral acceleration or spectral velocity.

Various researchers have proposed empirical relations between the average shear-wave velocity of surface deposits (averaged over a given depth) and relative amplification of ground motion. Some of these empirical relations which determine the average amplification ratio, AVR, proposed by Borcherdt and Gibbs (1976), Joyner et al. (1981), Borcherdt et al. (1978) show that this amplification factor is strongly correlated to the shear-wave velocity near the ground surface, especially the shear-wave velocity averaged over the upper 30 m, V_{s30} in m/s that is used as the key variable to represent site effects. Based on the data in the Kanto area in Japan, the empirical relationship for the site effect in terms of V_{s30} was proposed Midorikawa et al. (1994) as in **Eq. 4.17**.

$$\log_{10}(AVR) = 1.83 - 0.66 \cdot \log_{10}(V_{s30}) \tag{4.17}$$

The uncertainty associated with the site effect in Equation 8 is 0.37 in natural logarithmic standard deviation. But usefulness of such empirical relations is limited by the availability of shear-wave velocity data for the region under study. Various geophysical methods exist which allow direct measurement of the shear-wave velocity of the ground. Increasingly, measurements of low-amplitude ambient ground noise, *microtremors*, are being used in the characterization of local site effects spatially Shear wave velocity.

But In case, lack of data, the local soil amplification factors proposed in the 2003 NEHRP Provisions (FEMA, 2004) are widely used to estimate the amplification effects of ground motions due to local soil conditions. These factors are classified in six categories (A: hard rock, B: rock, C: dense soil, D: stiff soil, E: soft clay and F: soil requiring site-specific evaluation) mainly by shear wave velocity and standard penetration resistance. The local soil amplification factors for PGA proposed by the FEMA are shown in **Table 4.1**. In order to determine the local soil amplification factor for PGV, spectral acceleration, $S_a(T = 1.0\,\text{sec})$, is used. This is because of a relationship between $S_a(T = 1.0\,\text{sec})$ and PGV (**Eq. 4.18**) which is suggested in HAZUS (1997 and 2003). Therefore the amplification factors for PGV proposed by the FEMA are shown in **Table 4.2**.

$$PGV(in/\text{sec}) = \left(\frac{386.4}{2\pi} \cdot S_a(T = 1.0\,\text{sec}) \right) \Big/ 1.65 \tag{4.18}$$

According to the FEMA (2004), the local soil amplification factor for PGA and PGV are determined from **Tables 4.1** and **4.2**. Therefore by multiplying the attenuated seismic intensities by the local soil amplification factors, the, seismic intensities at the surface soil can be computed as **Eqs. 4.18** and **4.19**.

$$PGA_{surface} = PGA_{base}.F_a \tag{4.18}$$

$$PGV_{surface} = PGV_{base}.F_v \tag{4.19}$$

Table 4.1 Local soil amplification factor for PGA, (F_a)

Soil Type	PGA ≤ 0.25 g	PGA = 0.5 g	PGA = 0.75 g	PGA = 1.00 g	PGA ≥ 1.25 g
A	0.8	0.8	0.8	0.8	0.8
B	1.0	1.0	1.0	1.0	1.0
C	1.2	1.2	1.1	1.0	1.0
D	1.6	1.4	1.2	1.1	1.0
E	2.5	1.7	1.2	0.9	0.9

Table 4.2 Local soil amplification factor for PGV, (F_v)

Soil Type	S1 ≤ 0.1 g	S1 = 0.2 g	S1 = 0.3 g	S1 = 0.4 g	S1 ≥ 0.5 g
A	0.8	0.8	0.8	0.8	0.8
B	1.0	1.0	1.0	1.0	1.0
C	1.7	1.6	1.5	1.4	1.3
D	2.4	2.0	1.8	1.6	1.5
E	3.5	3.2	2.8	2.4	2.4

4.3.4 Correlation of Seismic Intensities

Since an infrastructure system is composed of many facilities and distributing elements which are distributed over a region, numerous seismic intensities scattered over that same region must be used for its serviceability assessment. When a single scenario earthquake is used for the serviceability assessment, the seismic intensities at sites of components are stochastically dependent to some degree due to the epicentral distances, local soil conditions and the proximity of components. In common engineering applications, such local variations in intensity are captured by the regional variation of first-order statistics of attenuation (e.g. mean or median). The covariance of seismic intensity (a second-order statistical property) is not considered in general. So the variance in seismic intensity is modeled by the standard error

associated with the attenuation relationship. The stochastic dependence of the seismic intensities at different sites is modeled by the spatial correlation of seismic intensities (Wesson and Perkins, 2001; Shimomura and Takada, 2004; Takada and Shimomura, 2003 and 2004; Wang and Takada, 2005). Unlike the regional variation captured by the first-order statistics (mean or median) of attenuation, the covariance of seismic intensity models the statistical association (correlation) between intensities in two sites. This covariance function clearly depends on the geographical distances between sites of components, and may depend on the magnitude and epicentral distances as well.

In order to make an auto correlation mode for ground motions, the observed data were firstly grouped into several bins with the same separation distance h between two sites (p,q) so that the separation distance in the same bin is within $h \pm \Delta h/2$. Therefore the auto-covariance function can be written by discrete expression.

$$C(h) = \frac{1}{N(h)} \sum_{i=1}^{N(h)} \left(L(x_{p_i}) - \mu_L\right) \cdot \left(L(x_{q_i}) - \mu_L\right) \tag{4.20}$$

$$\mu_L = \frac{1}{N_{all}} \sum_{i=1}^{N(h)} L(x_i) \tag{4.21}$$

$$L(x_{pi}) = \ln\left(\frac{y_{pi}}{\overline{Y_{pi}}}\right) \tag{4.22}$$

where N_{all} is the total number of observation sites; $N(h)$ is the number of pairs of sites (x_p , x_q) that meet the condition $h - \Delta h/2 < \left|x_p - x_q\right| < h + \Delta h/2$; h is the discrete distance whose interval is Δh. Assuming, $L(x)$ constitutes an isotropic two-dimensional stochastic field which can be approximately satisfied (Wang and Takada 2005), therefore auto-covariance function of $L(x)$ between different two sites depends only on the relative distance. Normalized auto-covariance function $R(h)$, is obtained from $C(h)$ as following which σ_L^2 is the variation of $L(x)$.

$$R(h) = C(h)/\sigma_L^2 \tag{4.23}$$

Now the spatial correlation model can be built up by modeling the discrete values of the normalized auto-covariance function $R(h)$ with an exponential decaying function as **Eq. 4.24**.

$$R(h) = \exp\left(-h/b\right) \tag{4.24}$$

where h is a separation distance between two observations and b is so-called a correlation length, which can characterize the degree of correlation of ground motions between two locations. It can be seen from **Eq. 4.24** that this exponential function satisfies the essential conditions $R(0)=1$, and $R(\infty)=0$. Therefore the co-variances between sites p and q meet the relations **Eq. 4.25**.

$$Cov(h)_{pq} = \sigma_L^2 \cdot R(h) \tag{4.25}$$

The studies by Shimomura and Takada (2004), Takada and Shimomura (2003 and 2004) and Wang and Takada (2005) using the ground motion records of six earthquakes that have occurred in Japan and Taiwan revealed that correlation lengths b typically are about 20 to 30 km for PGA and about 20 to 40 km for PGV.

In the new study which is done by the author, records of the 2011 Earthquake off the Pacific Coast of Tōhoku based on the database deployed by National Institute for Earth Science and Disaster Prevention (NIED) in Japan, is fully utilized to quantify the spatial correlation characteristics of the ground motions and compare with the previous models which are obtained by Wang and Takada (2005) and Jayaram and Baker (2009). Values of correlation lengths b can be obtained, and results are listed in **Table 4.3**. The auto covariance detailed data can be accessed in **Appendix B**.

Table 4.3. Correlation length b (km) of the 2011 Tōhoku earthquake with proposed model

Parameter / Direction	PGA (cm/s^2)	PGV (cm/s)	PGD (cm)	PGV/PGA (s)
East-West (E-W)	107.5	78.7	52.4	31.0
North-South (N-S)	97.1	77.5	53.8	30.3
Up-Down (U-D)	94.3	68.0	49.8	48.8

Because of the interpolate earthquakes are stronger than Intra plate (crustal) earthquakes and usually cause higher moment magnitudes, as it is shown in **Fig 4.4**, in the same moment magnitude, the correlation length of Intra plate earthquake is bigger than interpolate earthquakes. As it is shown in **Fig 4.5**, it seems that in case of PGV, both trend lines are in a direction at each other, therefore they can be considered as a continuous trend line.

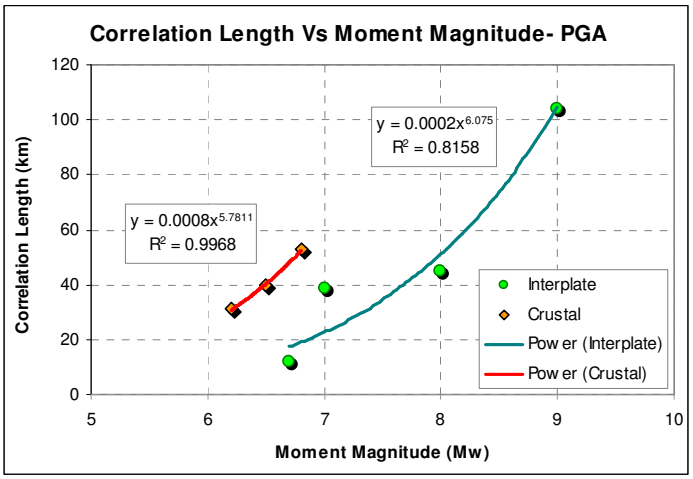

Fig 4.4 Relation between correlation length b and moment magnitude M_W for horizontal PGA

As can be seen, the correlation length and moment magnitude have a direct relationship so that correlation length further increases proportionally with moment magnitude. This is because of this fact that earthquake with large magnitudes affected the wider area and in this case, the correlation length will be increase.

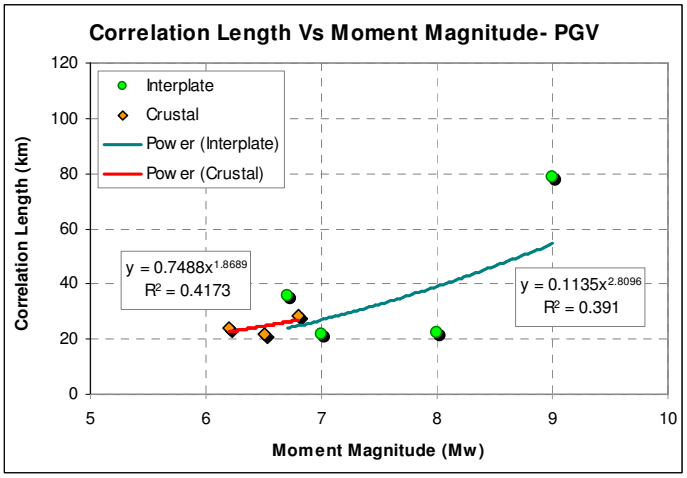

Fig 4.5 Relation between correlation length b and moment magnitude M_W for horizontal PGV

4.4 Deterministic Seismic Hazard Analysis

In order to assess risk to a structure from earthquake shaking, it must be first determined the annual probability or rate of exceeding some level of earthquake ground shaking at a site, for a range of intensity levels, Baker (2008). The somewhat complicated probabilistic evaluation could be avoided if it was possible to identify a *worst-case* ground motion and evaluate the facility of interest under that ground motion. This line of thinking motivates an approach known as deterministic hazard analysis. The deterministic method is the standard approach in which effects from the largest earthquake expected (MCE) are the primary focus. Note that a scenario earthquake is suggested as the central concept for the deterministic or maximum credible earthquake in seismic hazard assessment, Anderson (2000).

The use of the MCE ensures that effects from all other magnitudes are explicitly considered. In other words, by virtue of designing a structure to withstand the MCE, it will automatically withstand all other (smaller) earthquakes. MCEs from all faults in the region are considered. In the case of Bam city it is considered that Bam fault as a scenario earthquake, **Fig 4.6**. Bam fault caused the earthquake of 2003 is located 5 km far from city centre with magnitude 6.5.

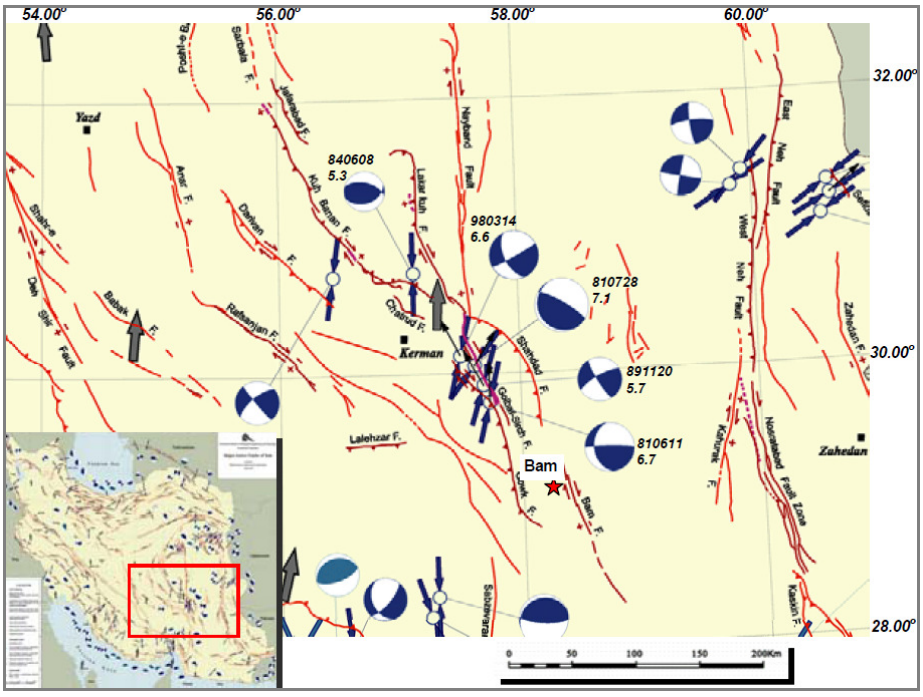

Fig 4.6 Regional seismology of Bam city (Courtesy of IIEES)

The estimated risk based on a scenario earthquake (SE) is conditioned on the occurrence of the scenario event. Appropriate scenario events can be determined by a process known as de-

aggregation (Bazzurro and Cornell, 1999), which identifies the dominant seismic events contributing to an earthquake hazard of 2% in 50 years, the current basis for building design in the United States (FEMA, 2004; ASCE, 2005), or some other hazard measure for the region being evaluated.

4.4.1 Characteristic Earthquake

Characteristic earthquakes, as well as large historical earthquakes, are often used as scenario earthquakes to assess the damage to facilities. Scenario earthquake based seismic hazard analysis is aimed at investigating the impact of a specific earthquake (usually stipulated in terms of magnitude and epicenter) on a facility or group of facilities. Such a specification of seismic hazard is useful as a communication tool (Adachi, 2007).

Furthermore, McGuire (2001) observed that the SE-based seismic hazard analysis is useful for high seismic regions since a deterministic scenario for this event will allow details to be examined such as ground motion effects caused by rupture propagation. McGuire also noted that, in moderate and low seismic regions, extreme deterministic scenarios will have probabilities of occurrence that are too low to be useful for most decision purposes.

4.4.2 Deaggregation Analysis

In a SE-based hazard analysis, one specific earthquake is selected from an examination of the seismicity surrounding the site or from a de-aggregation analysis of potential earthquakes. Most decision-making regarding public or private investment in seismic risk mitigation focuses on low probability /high consequence events. It seems that the return period of the selected scenario is more than 2000 years because the heritage in Bam is very old and it was without any heavy damage before the earthquake which it means that no severe quake occurred in the region during long time. In that case, the earthquake contributing most to the seismic hazard at a stipulated low probability level often is selected.

Occasionally, an earthquake is simply selected from recordings of severe ground motion. Although the scenario earthquake approach is very useful for investigating the damage to an infrastructure system when a specific earthquake occurs, it conveys no quantitative information on the probability of occurrence of the scenario event considered. Thus, the system reliability analysis is conditional in nature. The results of de-aggregation analyses of the city of Bam, is shown in **Fig 4.7**.

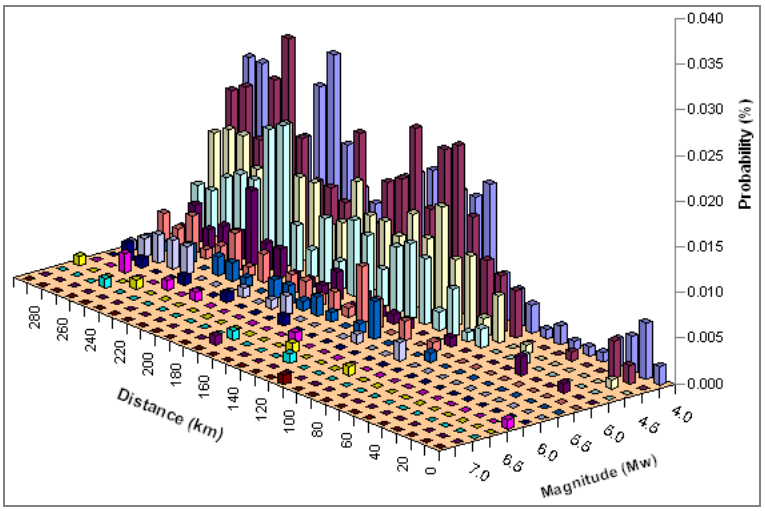

Fig 4.7 Deaggregation analysis for city of Bam

Based on the de-aggregation analysis it can be found that most of earthquake accorded in distance more than 100 km far from Bam city center and their magnitudes (Mw) often are less than 5. But the recent earthquake in 2003 with magnitude 6.5 is occurred near city center and considered as scenario for bam city. The seismograph and acceleration response spectra in three dimensions are shown in **Fig 4.8**.

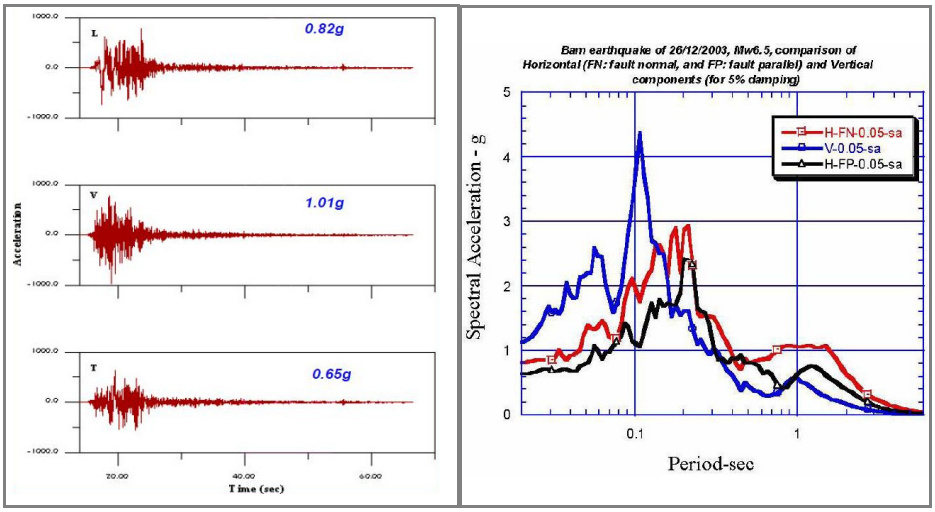

Fig 4.8 The seismograph and acceleration response spectra of 2003 bam earthquake ($M_W = 6.5$)

4.5 Probabilistic Seismic Hazard Analysis

While the choice of a *worst-case* earthquake can be difficult and subjective, an even greater problem with deterministic hazard analysis is the choice of worst-case ground motion intensity associated with that earthquake. With probabilistic seismic hazard analysis (PSHA) it

is no longer searching for elusive worst-case ground motion intensity. Rather, it will consider all possible earthquake events and resulting ground motions, along with their associated probabilities of occurrence, in order to find the level of ground motion intensity exceeded with some tolerably low rate, Baker (2008).

For the seismic hazard analysis, earthquake sources with the potential to affect the sites, seismic wave path from the sources to the sites and local soil conditions of the sites need to be evaluated. In general, the site may be affected by a number of seismic sources and the magnitudes of earthquakes from each seismic source are not deterministic. A probabilistic seismic hazard analysis (PSHA) determines the aggregated effect of the range of possible earthquakes in seismic source zones that are in proximity to a site, weighted by the probability of occurrence of each earthquake (McGuire, 1995; Kramer, 1996). The annual frequency of earthquakes whose seismic intensities IM at a site exceed a value x is evaluated by **Eq. 4.26**.

$$\lambda(IM > x) = \sum_{i=1}^{N_s} \nu_i \int_{m_{\min}}^{m_{\max}} \int_{0}^{r_{\max}} P(IM > x|m,r) \cdot f_{M_i}(m) \cdot f_{R_i}(r) dr \cdot dm \tag{4.26}$$

where $\lambda(IM > x)$ is the annual frequency rate of earthquakes, N_s is the number of earthquake sources, $\nu_i = \exp(\alpha_i - \beta_i \cdot m_0)$ at earthquake source *i* evaluated from **Eq. 4.3**, $P(IM > x|m,r)$ is the probability that seismic intensity generated from an earthquake whose magnitude is *m* and epicentral distance is *r* exceeds *x* which is the threshold seismic intensity, $f_{M_i}(m)$ and $f_R(r)$ are probability density functions of magnitude and epicentral distance of earthquake occurring at source *i*. Under the assumption that earthquake occurrence can be modeled as a Poisson process, the PSHA results in the probability that seismic intensities at a site exceed a threshold seismic intensity during a certain interval of time *T* (McGuire, 1995; Kramer, 1996) as **Eq. 4.27**.

$$P(IM_T > x) = 1 - \exp[-\lambda(IM > x) \cdot T] \tag{4.27}$$

A PSHA is particularly suited for designing individual facilities since the intensities can be represented at a probabilistically stipulated level of the seismic hazard in codes and other regulatory documents (e.g., 2% probability of exceedance in 50 years) (FEMA, 2004; ASCE, 2005). The seismic hazard maps are created under the assumptions that earthquake occurrence is a Poisson process, implying that earthquake occurrence is time homogeneous (Frankel et al., 1996). Since the spatial correlation of seismic intensities shown in the hazard map is lost in the

aggregation process of creating the map, the application of the mapped uniform hazard intensities to serviceability assessment of facilities and distribution elements that are spatially distributed over a region and are functionally dependent on each other is questionable.

A seismic source zone is identified from the historical record of earthquakes. The a and the b values of the Gutenberg-Richter law for a particular source are determined, in general, from the historical records. For the creation of a seismic hazard map of the Bam, the a and the b values of the background source zones are estimated by the earthquake records for a grid with spacing of 0.2 degree in latitude and longitude. The epicentral distances are determined as the distance between the grid and the site.

4.6 PSHA of the Bam City

It is interested in all earthquake sources capable of producing damaging ground motions at the site. These sources could be faults, which are typically planar surfaces identified through various means such as observations of past earthquake locations and geological evidence. If individual faults are not identifiable, then earthquake sources may be described by arial regions in which earthquakes may occur anywhere. Once all possible sources are identified, it can identify the distribution of magnitudes and source-to site distances associated with earthquakes from each source, **Fig 4.9**.

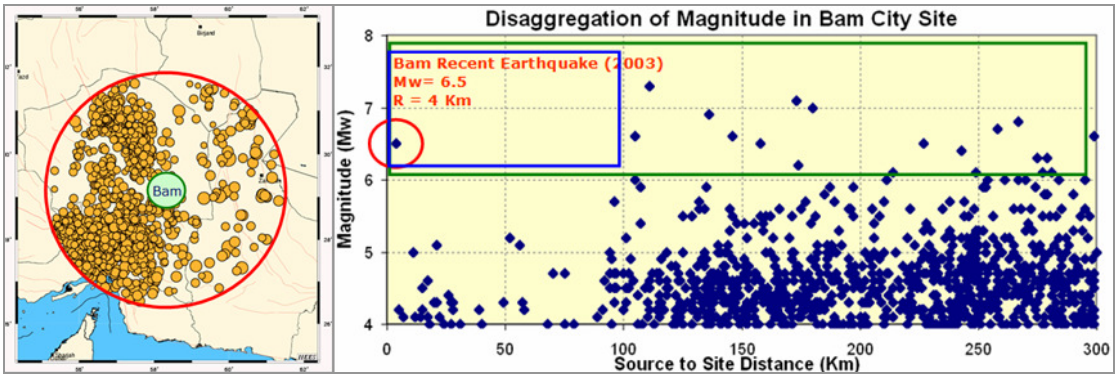

Fig 4.9 Eearthquakes in southeast Iran (Epicentres from online IIEES)

In this study it is consider an areal source, grid with spacing of 0.2 degree in latitude and longitude that is capable of producing earthquakes with a variety of magnitudes. The area source produces earthquakes randomly and with equal likelihood anywhere within the site. Area sources are often used in practice to account for background seismicity, or for earthquakes that are not associated with any specific fault. The number of 1789 records was gathered. It is

considered that the source produces events with M ≥ 4 (783 records). It is now quantified the distribution of potential earthquake magnitudes and locations, but it is interested in analyzing ground motions, not earthquakes. Therefore it is considered a suitable ground motion prediction model depending on study area. Ghodrati et al. (2007) attenuation relationship is considered to use. The relation is specified for Iran seismic zones, for PGA (**Eq. 4.15**) and PGV (**Eq. 4.16**). Finally it is used total probability theorem (**Eq. 4.26**) to perform the PSHA calculation. Bam district geology, seismicity is shown in **Fig 4.10**. The map is prepared base on the NGDIR map which can be accessed in **Appendix C**.

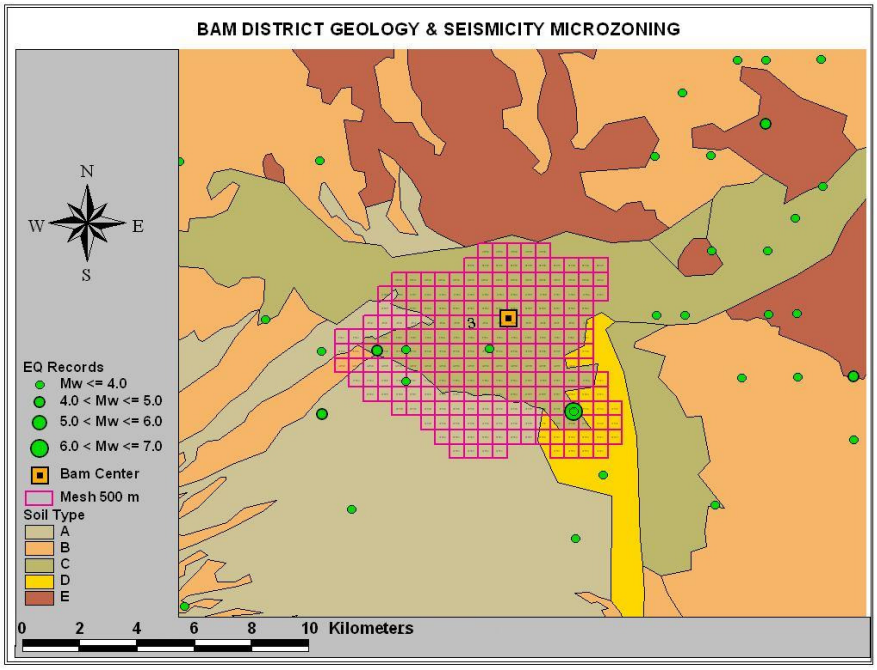

Fig 4.10 Bam district geology, seismicity and the city grid mesh in GIS

The description of the seismic hazard map is a monotonic function with the return period *T* and the exposure time *n*. The return period (or recurrence interval) is the average time span between two events of a given magnitude at a particular site. The exposure time usually equals the expected life of the structure. In order to calculate the design life expectation of the structure, both these parameters (as well as the return period of the event) must be employed when calculating the risk of the structure with respect to a given event. The risk assessment is thus the likelihood of at least one event that exceeds the design limits of the structure in its expected life. In this study, Bam seismic hazard maps calculated for 2475 return period and 50 years of exposure time corresponds to 2% probability of exceedence. PGA and PGV hazard map are shown in **Fig 4.11** and **Fig 4.12** respectively.

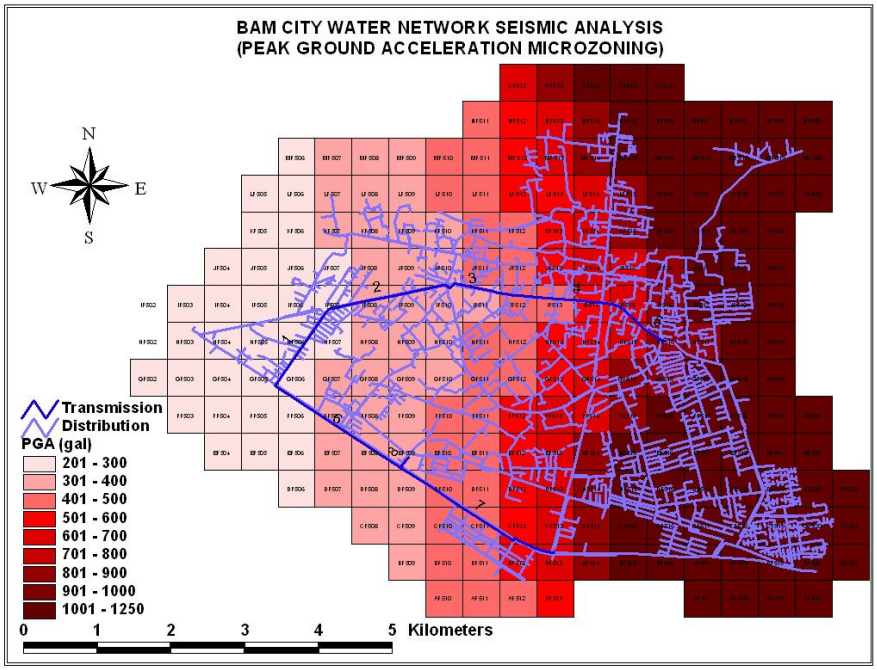

Fig 4.11 Bam city PGA hazard map calculated for 2475 return periods (2% in 50 years)

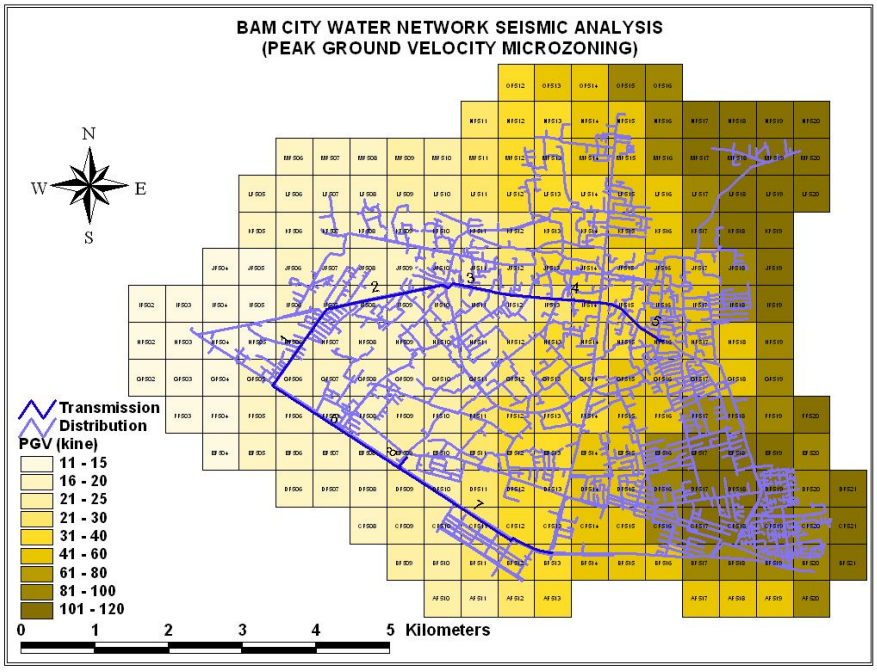

Fig 4.12 Bam city PGV hazard map calculated for 2475 return periods (2% in 50 years)

In fact, there is 98% chance that these ground motions will not be exceeded. This level of ground shaking has been used for designing important buildings in high seismic areas.

4.7 Damage Assessment of Critical Infrastructure

In the previous section it examined how to deal with the likelihood of the event characterized as a seismic hazard. Now evaluate the seismic vulnerability of each element of the network is illustrated and it fits in with the assessment of seismic vulnerability of the infrastructure network as a whole. For example, a substation is an element of the electricity network presented as a vertex; but from an engineering point of view, the same substation is a structure that can be damaged in the event of an earthquake. The seismic vulnerability of the structure is expressed by its associated fragility curves. In general, a fragility curve is a just the graphical representation of the conditional probability of exceeding a certain damage limit state at a given level of seismic hazard, which is dependant on the type of structure. Based on fragility curves, the functionality of the structure can be assessed whenever functionality is correlated to the damage state.

In this study, the fragility curves are taken from HAZUS Manual (FEMA, 2003) for lifeline facilities. These fragilities are described by log-normal distribution functions that define the probabilities of entering five damage states (*DS*), ranging from *I* (minor) to *V* (complete), as functions of ground motion parameter (e.g. PGA) as **Eq. 4.28**.

$$Pf_{\mathrm{PGA}}(pga) = \int_0^{pga} \frac{1}{\sqrt{2\pi}\xi \cdot s} \exp\left[\frac{-1}{2}\left\{\frac{\ln(s)-\lambda}{\xi}\right\}^2\right] ds \tag{4.28}$$

where $Pf_{\mathrm{PGA}}(pga)$ represents the failure probability given PGA, λ is the logarithmic mean of PGA and can be calculated by *ln(median(PGA))*, and ξ is the standard deviation of *ln(PGA)*.

4.7.1 Electric power network

In the case of electricity power system in medium and low voltage levels as Bam city, the fragility curves for the substations, transformers and poles are used. The shape of the fragility curve for the given element is dependant on the damage state. When the structure is defined as the vertex in the network, five damage states are defined; none (ds_1), slight/minor (ds_2), moderate (ds_3), extensive (ds_4) and complete (ds_5). More severe damage states correspond to the lower probability of exceedence at the same PGA. Damage states as defined in HAZUS are dependent on the type of element and the level of the damage of its subcomponents.

4.7.1.1 Substations

Fragility curves of the substations are classified according to the voltages assigned to the substation and according to whether all subcomponents of the substations are anchored or not. Based on HAZUS, substations are classified according to their voltage rating: from low voltage (<150 kV), medium voltage (150–350 kV) and high voltage (>350 kV). The classification is also a function of whether the subcomponents are anchored or typical (unanchored). The fragility curves of low and medium voltage substations which located in Bam, are shown in **Figs 4.13** and **4.14**.

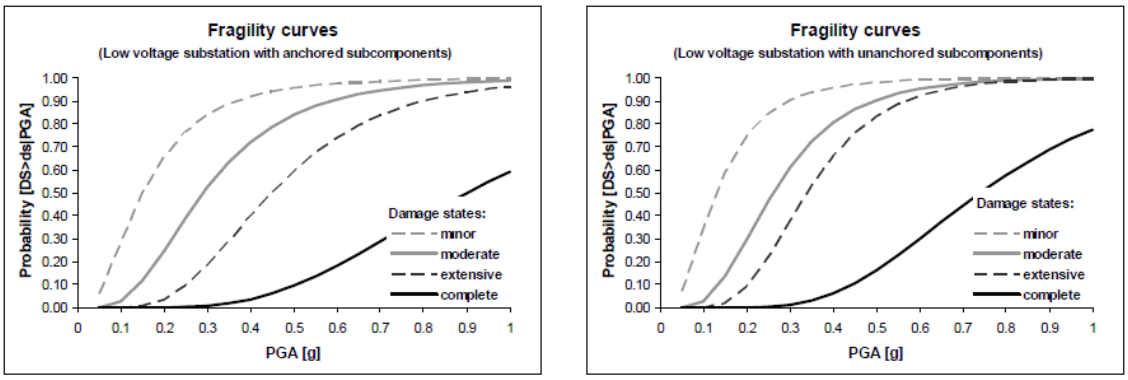

Fig 4.13 Fragility curves of low voltage substations (a) anchored (b) unanchored subcomponents

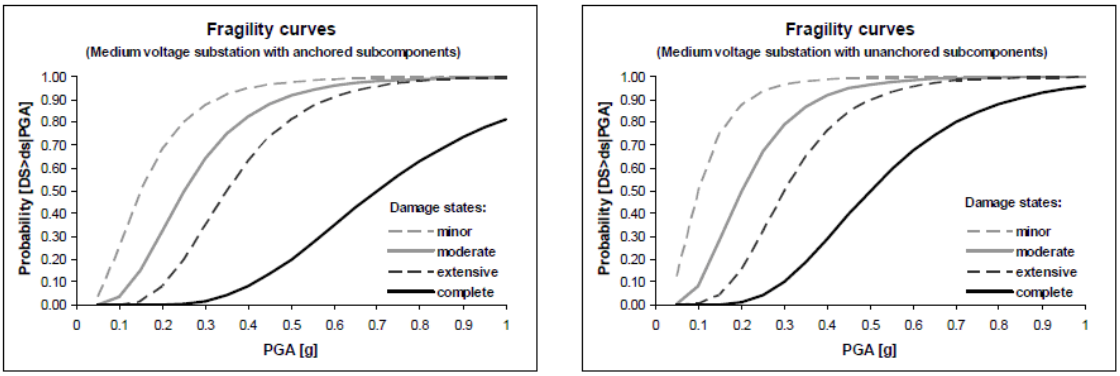

Fig 4.14 Fragility curves of medium voltage substations (a) anchored (b) unanchored subcomponent

First, the substation can be entirely enclosed in the building where all the equipment is assembled in one metal-clad unit and is treated as one anchored component. As it mentioned in chapter 2, other substations are usually compounded of subcomponents (transformers, disconnect switches, circuit breakers, lightning arrestors) that are located outside the substation's building. An anchored subcomponent in this classification refers to equipment that has been engineered to meet modern seismic design criteria.

In order to estimate the probability of exceeding a certain damage state of the substation, the following items are required as input: geographic location, PGA and Properties of the substation (voltage and design) for the classification. In the case of Bam city, there are three substations, 230 kV, 132 kV. Based on HAZUS, the 230 kV is classified as medium voltage, and another two 132 kV are classified as low voltage because both of them are under 150 kV.

4.7.1.2 20 kV substations and transformers

Fragility curves of the transformer are classified according to the installation type (TREC, 2006). There are three types, underground, surface and aerial on pole.

As for 20kV substation of underground pit type, it makes no sense that pit collapses with earthquakes. Therefore, it is enough to consider the damage mode only for a transformer. As a result, fragility curve of this underground substation in major mode is shown in **Fig 4.15**.

Fragility of 20kV class substation of surface type is calculated from fragilities of transformer and housing structures. As this housing structure usually is made by bricks with steel frames, fragility studied in past research project for Tehran area was employed. As damage modes, collapse (complete) is supposed. **Fig 4.16** shows the fragility curve of 20 kV substations on surface which is based on supposition that above transformer and housing structure are connected in series (TREC, 2006).

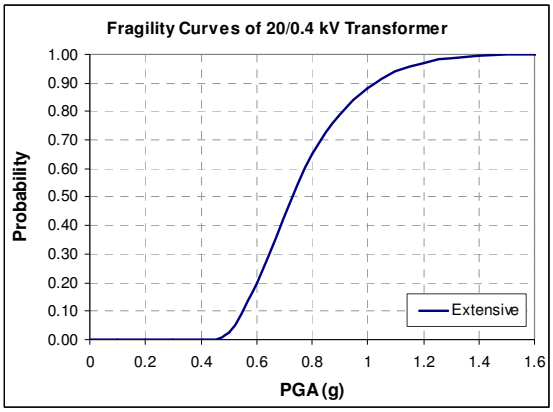

Fig 4.15 Fragility curve of 20 kV transformer

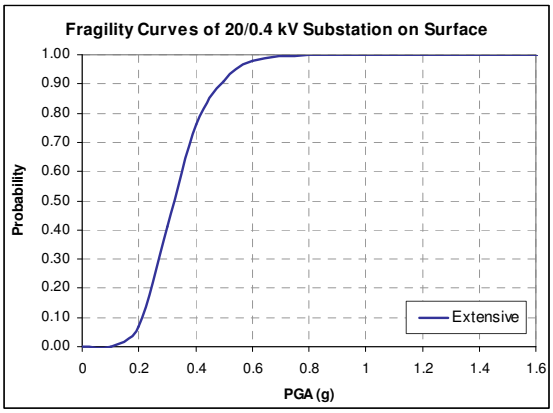

Fig 4.16 Fragility curve of 20 kV surface substation

Aerial 20/0.4 kV substations are included a transformer which is put on two girders of channels and fixed with bolts to them on poles as shown in **Fig 2.22**. This type of substation is most popular one in Iran cities especially Bam. In the case of 0.4 kV class, two channels combine poles at the height of 6m. Cross beams fixing channels into poles and members holding the transformer are supposed as channels. Weight of transformer of 0.4 kV class is

supposed as 0.75 ton. In case of 20 kV class, height of transformer is supposed as 8m. Weight of transformer of 20 kV is supposed as 1.5 ton. These beams and crossbeams are supposed as absolute rigid. Span of two poles is supposed as 2m (TREC, 2006). The fragility curves of 20 kV and 0.4 kV aerial substations are shown in **Fig 4.17** and **Fig 4.18**.

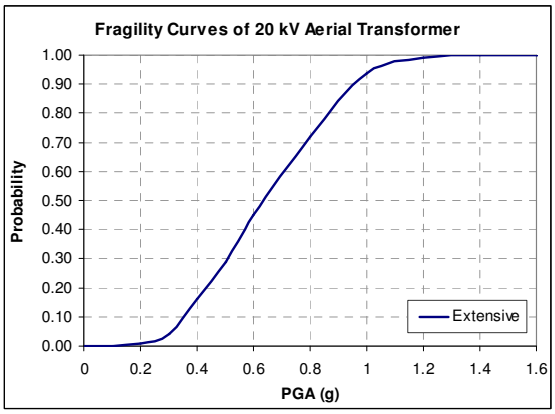

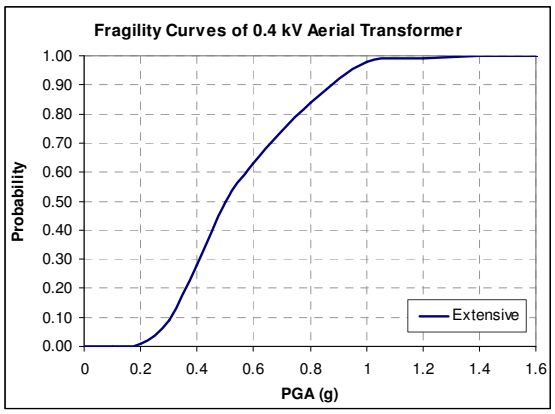

Fig 4.17 Fragility curve of 20 kV aerial transformer **Fig 4.18** Fragility of 0.4 kV aerial transformer

4.7.1.3 Distribution network poles

In this project, RC pole is employed as typical model which were often used in Bam city during the 2003 earthquake. There are 3 kinds of entire length which are 9m, 12m and 15m. In this study, 12m and 15m length are employed for 0.4 kV and 20 kV respectively.

Embedded length (setting depth) is supposed as 1.5m of entire length of 12m. As a pole has tapered wall, dimension of section becomes smaller in higher section (TREC, 2006). Section is basically H-shape and there are some rectangular sections called foot step. The fragility curves of 20 kV and 0.4 kV poles are shown in **Fig 4.19** and **Fig 4.20**.

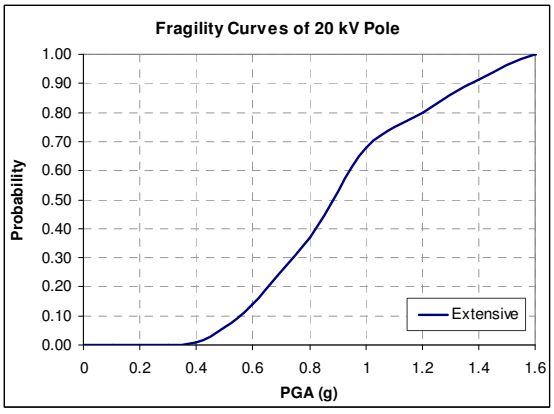

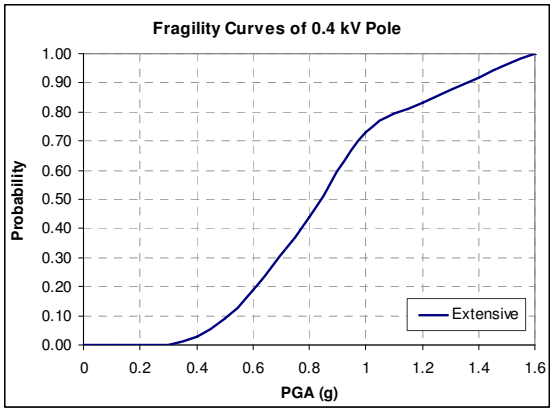

Fig 4.19 Fragility curve of 20 kV pole **Fig 4.20** Fragility curve of 0.4 kV pole

In this study assume that the line damage is related to its poles damage and the distance between two poles is about 50 meters. Therefore, in order to obtain the damage probability of 20 kV electric power lines, they are simulated as 50 meter length series sub-segments.

4.7.2 Potable water network

In the case of potable water network in main distribution level as Bam city, the fragility curves for the wells, pump stations, reservoirs and pipelines are used. The approach for the wells, pump stations and reservoirs is fragility curve but in case of pipeline is different.

4.7.2.1 Wells and water resources

Fragility curves of the water wells are presented as a total of four PGA-related damage functions based on HAZUS. In developing these damage functions, it is assumed that equipment in wells is anchored. Fragility curve of well damage is shown in **Fig 4.21**.

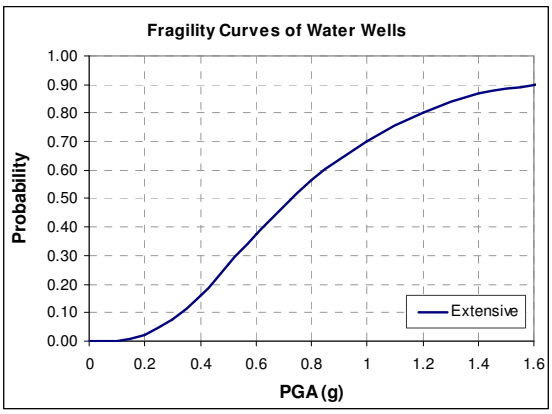

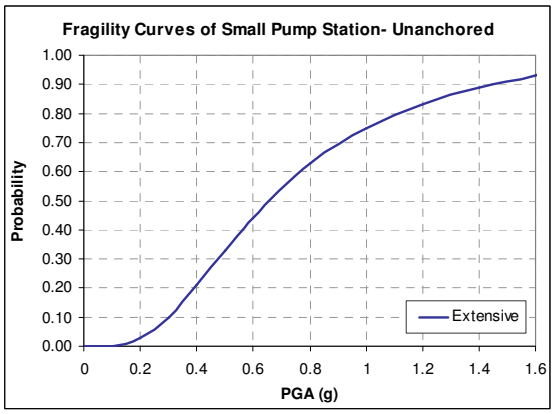

Fig 4.21 Fragility curve of water well **Fig 4.22** Fragility curve of unanchored pump station

4.7.2.2 Pump stations

PGA related damage functions for pump stations are developed with respect to their classification (small and large). Fragility curves of the pump stations are presented a total of 16 damage functions based on HAZUS. Half of these damage functions correspond to pump stations with anchored subcomponents, while the other half corresponds to pump stations with unanchored subcomponents. Because of Bam city pump station is small size, only the fragility curve of unanchored small pump stations is presented in **Fig 4.22**.

4.7.2.3 Reservoirs

Fragility curves of the pump stations are developed a total of 24 PGA related damage functions based on HAZUS. These correspond to on ground concrete, on ground steel, elevated

steel, and on ground wood reservoirs for anchored and unanchored. Anchored and unanchored refers to connection between reservoir wall and the ring wall. The fragility curves of unanchored and anchored concrete reservoirs are presented in **Fig 4.23** and **Fig 4.24**.

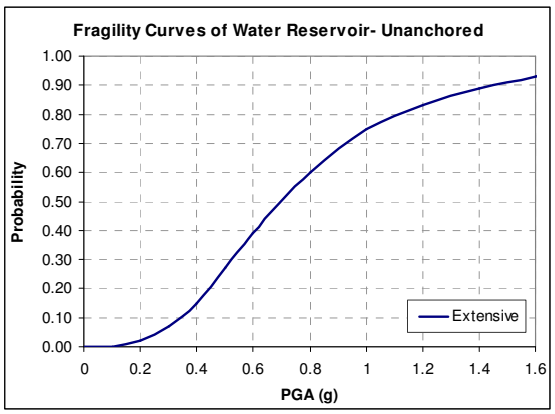

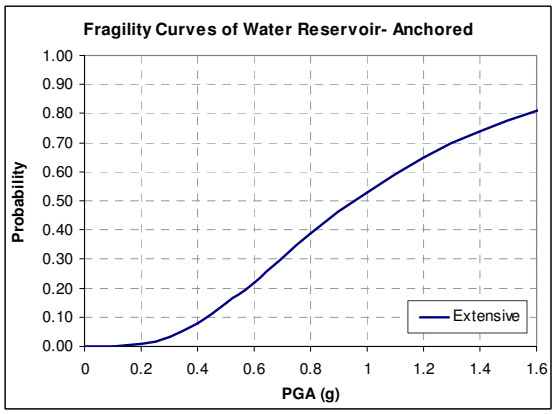

Fig 4.23 Fragility curve of unanchored RC reservoir **Fig 4.24** Fragility of anchored RC reservoir

4.7.2.4 Pipelines

For pipelines, two damage states must be considered: namely, leaks and breaks. Generally, when a pipeline is damaged due to ground failure, type of damage is likely to be a break. This type of damage is correlated to the permanent ground displacement (PGD). When the pipe is damaged due to the seismic wave propagation, the type of damage is likely to be due to leakage. It has been reported by O'Rourke and Ayala (1993), that the earthquake damage statistics give close correlation of pipeline leaks with peak ground velocity (PGV). Different fragility curves of pipelines are presented, while the HAZUS methodology incorporates the fragility relationship of O'Rourke and Ayala (1993). The pipe diameter is not considered as an influential factor. Their function (**Eq. 4.29**) estimates expected number of repairs per unit length dependant on the PGV (cm/s). By the HAZUS definition, this repair rate function covers damage mechanism that results in 20% of breaks and 80% of leaks.

$$RR = K \times (0.0001) \times PGV^{2.25} \tag{4.29}$$

where the constant factor $k = 1$ in the case of brittle pipes, and $k = 0.3$ in case of ductile pipes.

The another relation proposed by the American Lifeline Alliance (ALA) (2001) suggest that damage to water pipe caused by strong ground motion can be expressed as a function of PGV as **Eq. 4.30**.

$$RR = K \times (0.00187) \times PGV \tag{4.30}$$

where RR is the repair ratio, which is the number of pipe breaks per 1000 feet (305 m) of pipe length, K is a coefficient determined by the pipe material, pipe joint type, pipe diameter and soil condition, and PGV has the units of *in/sec*.

Classification of pipes is made according to the material and the joint type. Brittle pipes are usually made from asbestos cement, concrete, cast iron, and pre-1935 steel. Ductile pipe types are usually made from steel, ductile iron or PVC. Steel pipes with gas-welded joints and those where information on the joining process are considered brittle, whereas steel pipes with arc-welded joints are considered ductile. Although most pipelines are typically made of ductile steel, we classify all the pipelines as brittle because in our database there is no information on the type of joining between pipe segments.

Repair rate function is a useful indicator to characterize the probability of having link (pipeline) ruptures since it allows estimation of the mean occurrence rate of the break. Supposing that the ruptures occur continuously and independently of one another, the Poisson process can be used. If the water main connecting two facilities is short, it may be assumed that the seismic demand on that water main connecting two facilities is essentially uniform. In that case, the number of pipe breaks can be expressed by **Eq. 4.31**.

$$P[N=n]=\frac{(RR\times L)^n}{n!}\cdot e^{-RR\times L} \tag{4.31}$$

where n is the number of pipe breaks, RR is the repair ratio evaluated by the Eq. 4.28 or 4.29, and L is the length of pipe segment. If, in addition, it is assumed that a pipe segment cannot deliver water when the segment has at least one pipe break, the failure probability of the pipe segment can be expressed by the exponential distribution as **Eq. 4.32**.

$$P_f=1-P[N=0]=1-\exp(-RR\times L) \tag{4.32}$$

More generally, the water main is modeled as a line superposed on the stochastic field describing seismic intensity, and the PGV varies over its length. Thus, the failure probability of a water line can be computed by generalizing the above formulation by modeling the number of breaks by a non-homogeneous Poisson process, Rausand et al. (2004) as **Eq. 4.33**.

$$P_f=1-\exp\left(-\int_L RR(PGV(s))ds\right) \tag{4.33}$$

where $RR(\bullet)$ is repair ratio expressed as a function of $PGV(s)$, which is a function of site s, and L is the length of the water main. As $PGV(s)$ is a continuous function along the length of the pipe, PGV values at discrete points must be used.

4.7.3 Failure probability of the link

The lifelines are infrastructures which extend spatially over large geographical regions. For the assessment of the failure of linearly extending elements, two models are developed in previous studies.

In the first model, the probability distribution of the appropriate seismicity parameter is computed at a number of points along each spatially extending segment of the system and the highest seismic demand for each segment is identified. In this model the lengths of the segments do not appear in the safety evaluation. Such an approach is justified in the case of perfectly correlated seismic load and seismic capacity along the full length of a segment, where failure is expected to occur at the point of maximum seismic load assuming seismic capacity is homogeneous along the total length of the spatially extending segment.

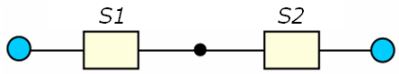

Fig 4.25 Simple link model as a series system with two segments

In the other model, the spatial correlation within segments is modeled and the length effect on the vulnerability of a segment is taken into consideration (Wang et al, 2005). In this model, each member of the lifeline is divided into segments and seismic demand is identified at the midpoints of each segment. The survival of the element requires the survival of each segment; in other words, it may be represented as a series system (**Fig 4.25**).

The failure events of the segments on the same member are expected to be highly correlated because of the fact that they are subjected to the same earthquake excitation and the same material properties are expected to exist along the total length of the element. But the assessment of the exact value of the reliability of an element consisting of m connected segments is computationally difficult yet; besides it is generally not possible to quantify the true value of the correlation among the segments. The probabilities of series system failure can be expressed as **Eq. 4.34**. The system reliability can be analyzed subsequently (Wang, 2004).

$$\text{Prob} = P\{y_1 > a_1 \cap y_2 > a_2\} \tag{4.34}$$

In which y_1, y_2 are seismic ground motion and a_1, a_2 the seismic level. As can be seen from Eq. 4.33, the joint probability density function is necessary for the link as a series system. Notice the Eq. 4.22, the joint CDF can be rewritten into **Eq. 4.35**.

$$\text{Prob} = P\{L_1 > l_1 \cap L_2 > l_2\} \tag{4.35}$$

As it is mentioned above, the correlation of between different L_is can be obtained from Eq. 4.25 given the correlation lengths. Then the joint probability of two segments of the link can easily be calculated by **Eq. 4.36**, where λ_{link} is the joint exceedance probability of two segments.

$$P_{\lambda_{link}} = 1 - \exp\left(- \int_{-\infty}^{l_1} \int_{-\infty}^{l_2} \lambda_{link}(L_1, L_2) dL_1 dL_2 \right) \tag{4.36}$$

By expanding the above equation, the joint probability distribution of m segments of the link can be considered a multivariate normal distribution characterized by the covariance matrix Γ, where the inter-event variability produces fully correlated residuals and the intra-event variability produces correlated residuals. One of the most important applications of the model is in the link hazard curve assessment. So annual exceedance probability of the link $P_{\lambda_{link}}(y)$, which the earthquake ground motion intensity exceeds y, can estimate by **Eq. 4.37**.

$$P_{\lambda_{link}}(y) = 1 - \exp\left\{ - \sum_{i=1}^{N} \nu_i \left(1 - \frac{1}{\sqrt{|\Gamma|(2\pi)^m}} \int_{-\infty}^{l_1} \ldots \int_{-\infty}^{l_m} \exp\left[-\frac{1}{2} Y^T \Gamma^{-1} Y \right] dX \right) \right\} \tag{4.37}$$

where, N is the number of is observed points and m the number of link segments. In this model it is assumed that, under specific hypotheses, the spatial variability of intra-event residuals can be assumed as a function only of the inter-site separation distance, b, and as the separation distance increases, the correlation asymptotically tends to disappear.

The number of link segments required to achieve an accurate estimate of P_λ (optimum number of the link segments) depends on the correlation length, b, of the seismic intensity. If b=0 km, the seismic intensities at the two sites are statistically independent. **Fig 4.26** illustrates the relation between the number of segments of the link and failure probability of the link with five correlation lengths: b=0, 20, 50, 100 and 107 km that is calculated based on 2011 great east Japan Earthquake data. As it can be seen in the figures, failure probability increases when the

number of segments goes up, and this trend holds for all four correlation lengths. In better express, if the number of segments is small, there is a potential risk that failure probability will be underestimated. Thus, a larger number of segments should be chosen to avoid underestimating failure probability. As it can be seen in **Fig 4.26**, it seems that there is the inverse relation between correlation length *b*, and the optimum number of link segments. Whereas increasing the correlation length b, the optimum number of link segments decrease. In the other words increasing the correlation length *b*, seismic hazard of the link converge to the fix level at smaller number of the link segments.

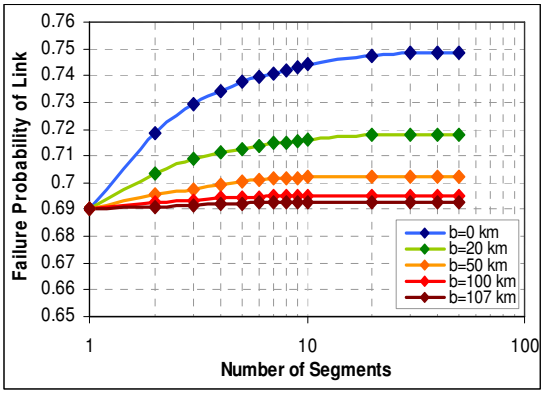

Fig 4.26 Failure probability of the link

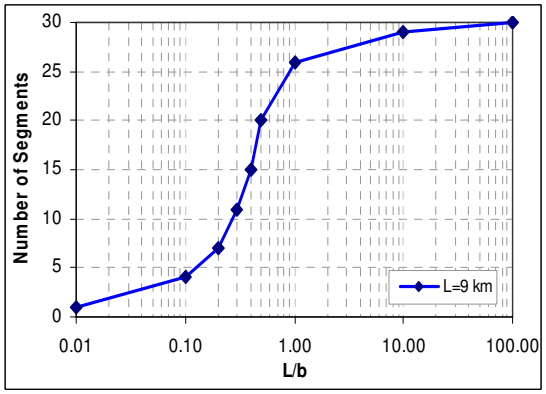

Fig 4.27 Relation between *m* and *L/b*

It is represented in **Fig 4.27** that the rate of convergence depends on the ratio of link length and the correlation length. The rate of the convergence is fast in the small ratio. Therefore in this case, the optimum number of the link segments which it should be consider in calculation goes down. With regard to the conventional transmission line approximately 10-20 km and correlation length about 20-40 km, it can be assumed that the logical amount of *L/b* is about 0.5. In this case the optimum number of the link segments is about 20. It sees that maximum amount of the link segments required to achieve an accurate estimate of P_λ is about 30-50 when the length of the link is too long.

As regards the length of the critical infrastructure links is usually less than one kilometer in distribution and main distribution level, and considering the normal proposed correlation length is about 20 km, the optimum number of link segments is obtained less than 5 based on Fig 4.26. Therefore it seems that taking into account the correlation ground motion is not useful in failure probability calculation of distribution and main distribution links. Although it should be used in transmission level because the length of the links is too long considering correlation length. In this case *L/b* goes up and as a result, the optimum number of link segments increased proportionally.

When a single PGV value is used to compute P_f of a water main of length L (as is shown in **Fig. 4.28.a**), the spatial distribution of PGV for that water main may not be modeled correctly if the pipe length L is too long for the segment to be considered as one discrete component. In this case, L should be divided into a sufficient number of short-length water main segments (**Fig 4.28.b**), with PGV assigned to each segment, to compute P_f of the pipe, (Adachi et al. 2009).

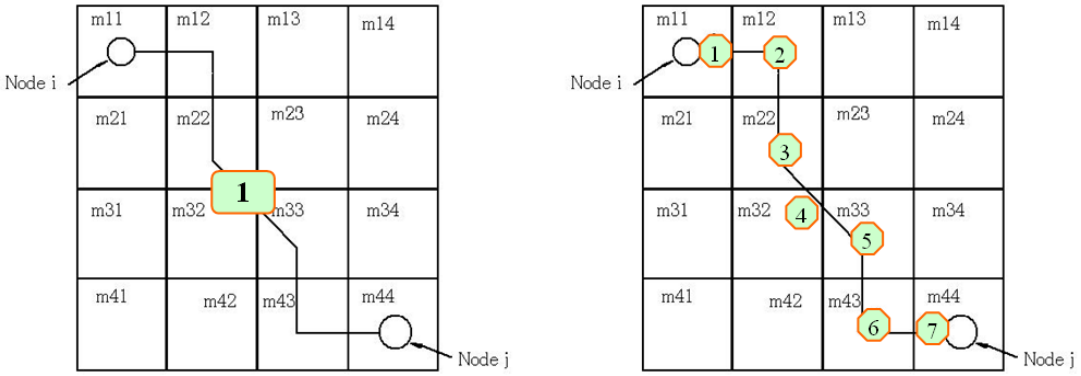

Fig 4.28 PGV distribution along a water main (GTGC 2002)
(a) an original water pipe, and (b) a mesh grid segmented water pipe

The failure probability of the pipe then becomes as **Eq. 4.38**.

$$P_f = 1 - \exp\left(- \sum_{i=1}^{m} RR(PGV_i) \times \Delta L_i \right) \qquad 4.38)$$

where PGV_i is the PGV value for water main segment i, ΔL_i is the length of segment i, and m is the number of segments and in this study it is equal to number of meshes that the pipeline passed on them.

4.8 Damage Assessment of Bam Critical Infrastructure

4.8.1 Damage of water network

For the damage assessment of components within the Bam water network, wells, reservoirs and pump stations, the HAZUS extensive damage State (ds_4) fragilities are used. Generally water pipes installed in the Bam area were Cement-asbestos and some of them were PVC and polyethylene. Only large-diameter water mains, with diameters from 10 inches to 25 inches (300–800 mm), were concrete, cast and ductile iron. Considering the typical water pipes, pipe material, pipe joint type, pipe diameter and soil conditions in Bam, it is assumed various *K* in **Eqs. 4.28** and **4.29** based on HAZUS and ALA. The result of Bam water network pipelines damage ratio are shown in **Fig. 4.29** and **Fig 4.30**.

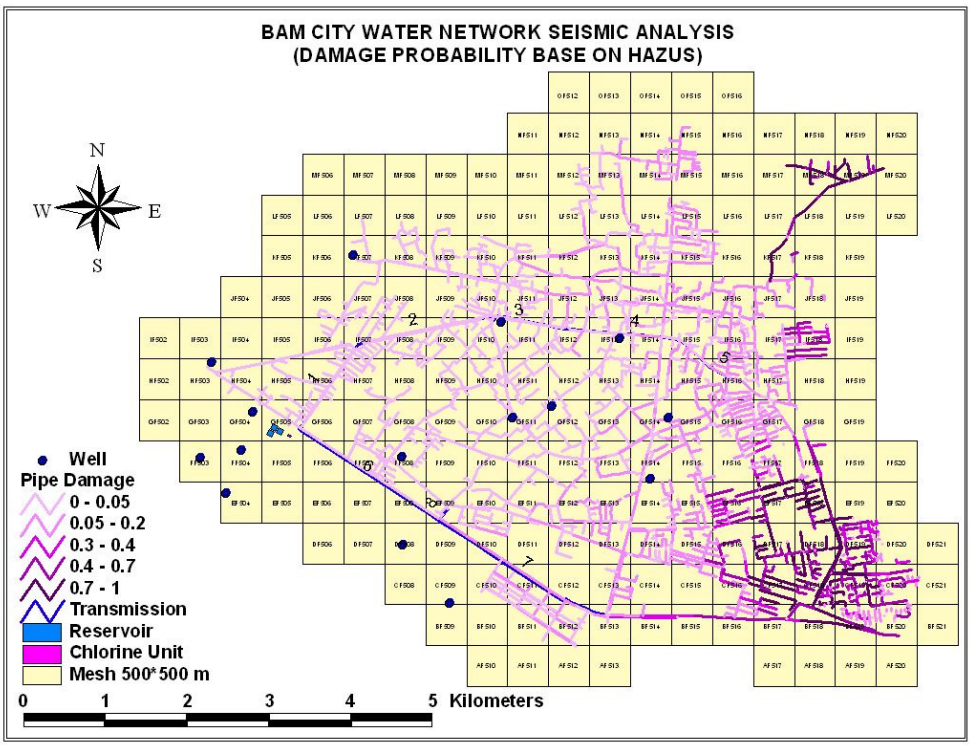

Fig 4.29 Bam water network damage probability based on HAZUS-2003

Water main pipelines also can be damaged due to permanent ground displacement due to liquefaction, ALA, (2001). Although there are areas in Bam city may be prone to liquefaction, according to post earthquake survey Wilkinson et al. (2009). The area with very high liquefaction susceptibility in Bam is only a small fraction of the area of the city and Furthermore, liquefaction data from the Northridge earthquake, O'Rourke et al. (2000),

indicated that permanent ground displacements (PGD) due to liquefaction occurred only in zones where the PGV exceeded 45 cm/s, and in this study, the PGV exceed approximately at any point in Bam city but considering the soil type, the possibility of pipe break caused by permanent ground deformation due to liquefaction is neglected.

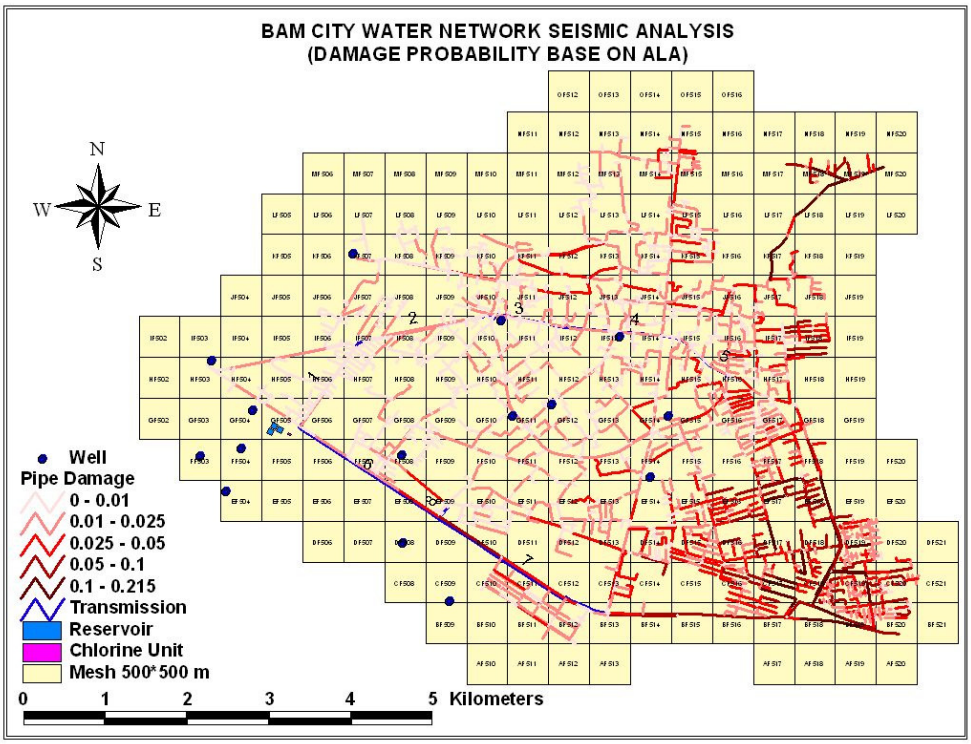

Fig 4.30 Bam water network damage probability based on ALA-2001

4.8.2 Damage of power network

Electricity power network of Bam city is supplied by a 230 kV transmission line. There is a 230/132 kV substation in the south part of the city (**Fig. 4.31**). Bam power distribution network is about 600 km length and divided to two levels, medium (20 kv) and low voltage. Because of lack of data, in this study only the high voltage substation and main distribution network (medium voltage) are considered to damage assessment.

For the damage assessment of Bam power network components such as substations, the HAZUS extensive damage State (ds_4) fragilities are used. In case of Bam electricity power substation, it is considered medium voltage and unanchored. According to the location of the substation, affected PGA is about 574 gal. Thus by using medium voltage and unanchored fragility curve, fig. 8, the probability of physical damage is about 0.98.

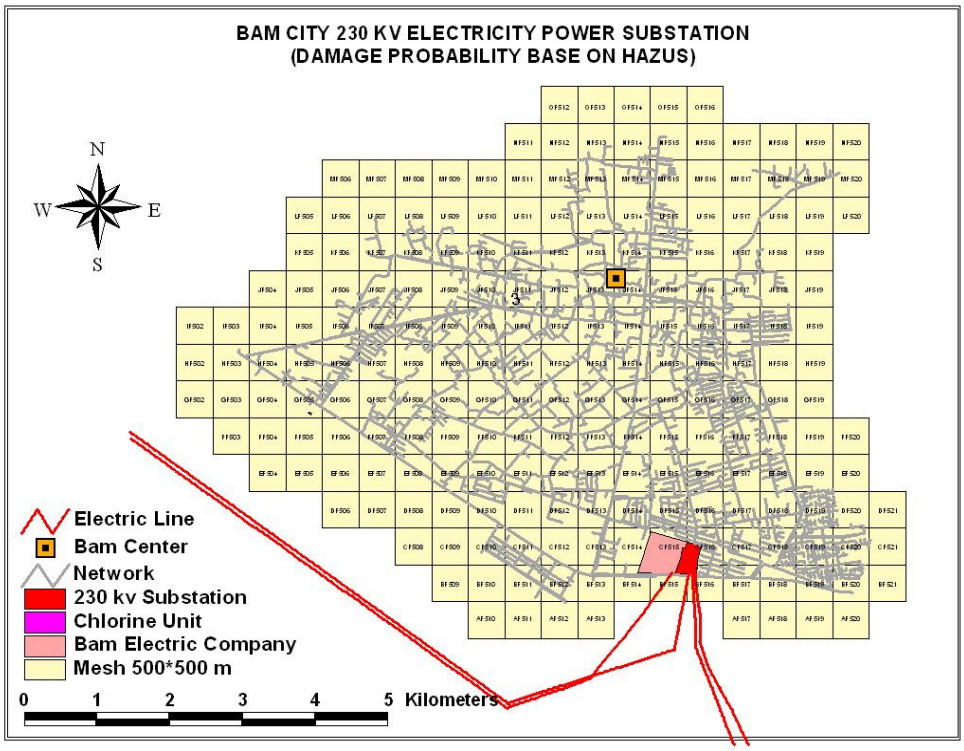

Fig 4.31 Bam 230/132 kV main power electric substation and main transmission lines

In this study, the electric main distribution network (20 kV) of Bam is considered which consist of concrete poles with aerial transformers. In this study it is assumed that the damage of electric power nodes is depend on their transformers and damage of lines is depend on their poles. Therefore, each link is divided to 50-meter length segments and damage of each segment is considered equal to damage of its related pole. In this way, damage probability of typical poles is calculated based on the fragility curves of TREC (2006). The damage probability of Bam power network nodes and lines are shown in **Fig. 4.32** and **Fig 4.33** respectively.

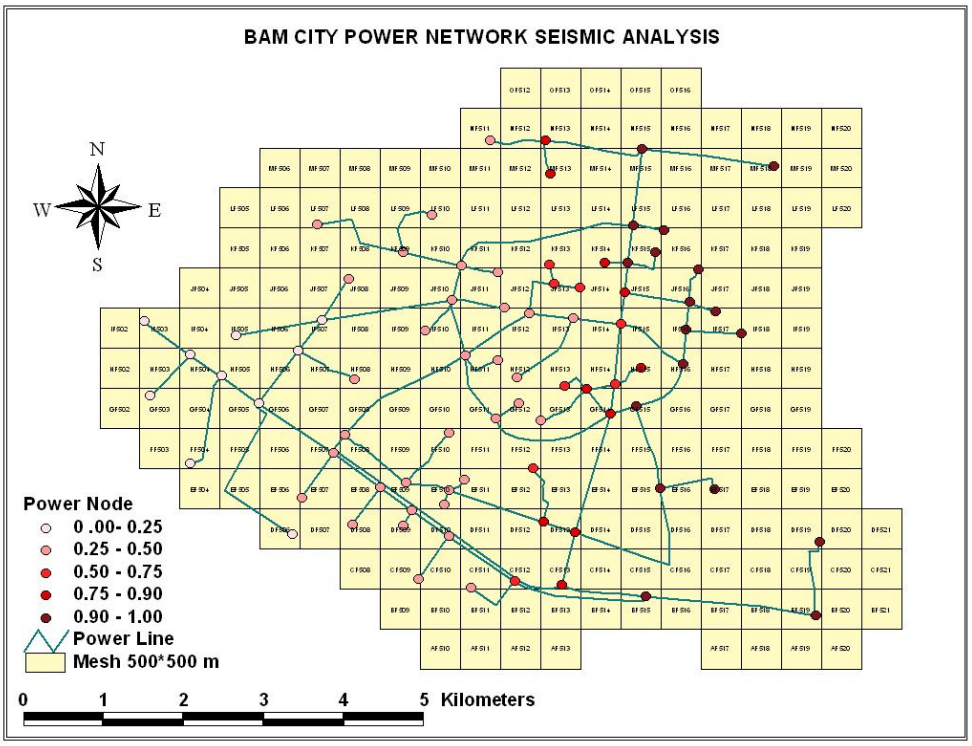

Fig 4.32 Bam power network transformer damage probability based on TREC

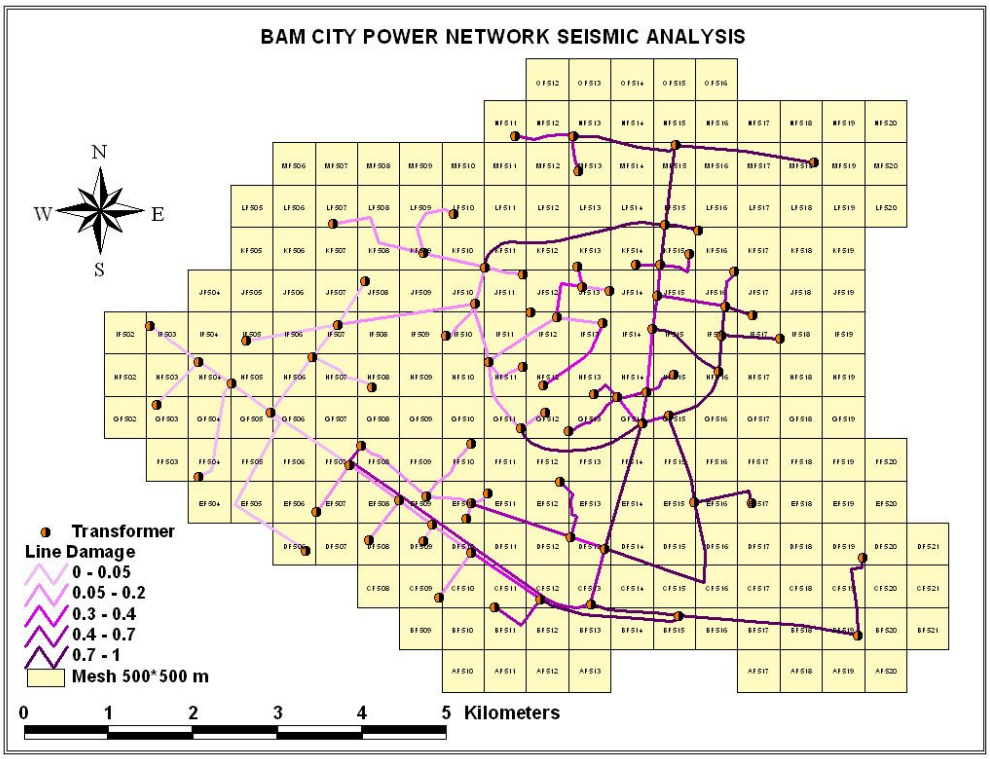

Fig 4.33 Bam power network circuit damage probability based on TREC

4.9 Summary and Conclusion

The framework of lifeline seismic analysis especially *PSHA* methodology is summarized in this chapter and the probabilistic seismic hazard maps of Bam city is obtained. After considering the active fault and considering appropriate attenuation relationships, *PGA* and *PGV* were calculated in 2475-year return period for 500 m grid mesh. The repair ratio of buried pipelines is computed for each cell based on ALA-2001, and after that damage probability of pipelines is derived. The results consistent with happened damages after the earthquake. Based on the results, most of high probable damaged pipelines are located in west part of Bam in coast area. Density of damaged pipelines and power electric lines especially in east and southern east part of the city is more than another. Results of vulnerability analysis appropriately are consistent with reality and actual damages. However in this study, only main distribution lines are analyzed and also the exact materials of lines such as joint types were not clear. Therefore, some differences are due to those matters. The results can be used as an important input data for network reliability analysis, disaster management and post earthquake activities such as emergency water supply.

CHAPTER 5

RELIABILITY ASSESSMENT OF CRITICAL INFRASTRUCTURES

5.1 Introduction

The advancement in science and technology has made the critical infrastructures of a society tightly interconnected and mutually dependent. Some aspects of this interdependency include physical factors, human behavior and information sharing; however, all these are vulnerable to disasters. Natural or man-made disasters happen and can cause thousands of severe casualties. These disasters have made the protection and restoration of critical infrastructures, such as health care, utilities, transportation and communication, a serious national concern.

In fact, individual critical infrastructure elements are a part of the whole interconnected system. The system functionality changes when one of the components does not work properly (much in the same way as organs in the human body) and the consequences of the failure of one facility may spread through the whole system. All of a sudden it is not talking only about the vulnerability of one facility, but also about the vulnerability of the system (Poljansek, 2010). Furthermore, it is clear that systems do not work in isolation. On the contrary, they are interdependent with other critical infrastructure systems. What does this mean? The propagation of the failure in one system can spread among systems; therefore such behavior introduces an extra vulnerability into the functioning of each particular system by virtue of its dependence on others.

However, society expects that the infrastructure service will continue with minimal disruptions, even during and after the emergency situation. Such expectations have probably been reinforced by reliable availability of the infrastructure service in the past where small disturbances have been successfully locally absorbed by the system. This perception may be eroded as large-scale accidents may become more frequent and the repercussions more complicated. Interdependencies enhance the overall system performance while also increasing the potential for cascading failures and amplifying the impact of small failures into catastrophic events. For instance, the major North American power blackout on August 14, 2003, initially triggered by some overhead transmission lines contacting with trees, lasted up to 4 days and affected several other infrastructure systems, where the estimated direct costs ranged from US$4 to US$10 billion (U.S.–Canada Power System Outage Task Force, 2006).

The most likely trigging factors are probably due to increasing demands combined with constant growth, imposed upon aging processes and equipment, and stressed by unusual environmental and operating conditions. These are probably only the symptoms of the fact that the management of critical infrastructure systems is not completely controllable for any contingency.

Rinaldi, (2001) has defined four primary classes of interdependencies: the physical, cyber, geographical and logical. Two infrastructures are physically interdependent if the state of each is dependent on the material output(s) of the other. An infrastructure has cyber interdependency if its state depends on data transmitted through the information system. Infrastructures are geographically interdependent if a local environmental event can create state changes in all of them. Two infrastructures are logically interdependent if the state of each depends on the state of the other via a mechanism that is not a physical, cyber, or geographical connection. The emphasis in this thesis is on the physical layer.

.

5.2 System Reliability Theory

As was stated in chapter 2, civil infrastructure systems are modeled as consisting of facilities and distributing elements. A water distribution system consists of dams, storage tanks and pumping stations as facilities and pipes as distributing element. An electrical power transmission system involves generating plants, substations and transmission towers as facilities and transmission lines as distributing elements. The performance of such systems can be assessed using methods of system reliability analysis.

System reliability theory is used in a variety of engineering fields and has a central role in risk analysis, quality management, maintenance and operation optimization and engineering design. As a tool for evaluating infrastructure systems, system reliability theory can be used to assess potential risks of natural hazards for infrastructure systems, to improve redundancy of infrastructure systems efficiently, to create maintenance plans at lower cost and higher efficiency, and to design the layout of facilities and distributing elements of infrastructure systems. There are several approaches to quantifying the failure modes of an infrastructure system. These include fault tree models, reliability block diagrams and event tree analysis (Adachi, 2007).

A fault tree model is a logic diagram that displays the interrelationships between a potential critical event (accident) in a system and the causes for this event (Rausand and Hoyland, 2004). The fault tree model can deal with both qualitative and quantitative analysis. The primary (or top) failure event of interest is situated at the top of the fault tree; below the

top event are located, in turn, the immediate causal failure events. The primary failure event and the immediate causal failure events are connected through logic gates (AND or OR gates). The process is continued until the top event is expressed as a combination of basic events which are located at the bottom of the fault tree, so the structure of the fault tree is deductive in nature. In a fault tree model, all failure events from primary to basic failure events are binary in nature: occurs or does not occur, fails or does not fail, etc. Events with intermediate states cannot be analyzed (U.S. Nuclear Regulatory Commission, 1981).

Fig 5.1 illustrates three simple fault tree models. In **Fig 5.1(a)**, the top event is the result of three basic events 1-3, linked through an OR-gate. Thus, the top event occurs if any of the basic events occur. In **Fig 5.1(b)**, the top event is the result of three basic events 1-3, linked through an AND-gate. Here, the top event occurs only if all three basic events occur at the same time. In **Fig 5.1(c)**, the top event is the result of basic event 1 or a sub-event, while the sub-event requires the occurrence of both events 2 and 3.

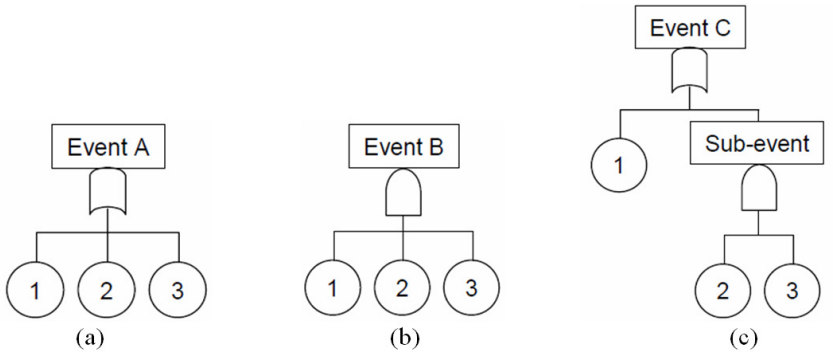

Fig 5.1 Fault tree model using; (a) OR gate, (b) AND gate and (c) OR and AND gates

Quantitative analysis of a fault tree model requires the identification of minimal cut-sets or minimal path-sets after the fault tree is constructed. A minimal cut-set is defined as an essential set of basic events whose occurrence must result in occurrence of the top event. A minimal path-set is defined as an essential set of basic events whose non-occurrence results in the non-occurrence of the top event. **Table 5.1** describes the minimal path-sets and the minimal cut-sets of three events shown in **Figs 5.1(a)** to **5.1(c)**. In **Table 5.1**, the {○} represents a set of basic events. For example, the occurrence of any of the basic events 1, 2 or 3 results in the occurrence of top event A, thus, each basic event 1, 2 or 3 is a minimal cut-set of event A. On the other hand, top event A does not occur when basic events 1, 2 or 3 does not occur at the same time, which is a minimal path-set of event A.

Table 5.1 Minimal cut-sets and minimal path-sets of three events A, B and C

	Event A	**Event B**	**Event C**
Minimal cut-set	{1}{2}{3}	{1,2,3}	{1}{2,3}
Minimal path-set	{1,2,3}	{1}{2}{3}	{1,2}{1,3}

In a reliability block diagram, the function of a system is illustrated as a logical combination of functioning components which are not repairable. Thus, a reliability block diagram is the graphical representation of how components are connected in such a way as to comprise a system. The combinations of functioning components in a reliability block diagram are classified into series and parallel structures. A series system is defined as a system whose components are linked in a single row. Thus, a series system maintains its function only when all components maintain their function. A parallel system is defined as a system whose components cannot be linked together in a row. Thus, a parallel system maintains its function as long as at least one component maintains its function.

For quantitative analysis of a system described by a reliability block diagram, a structure function must be constructed. A structure function $\phi(x)$ is a binary function assumed to take on values *1.0* if the system is functioning and *0.0* if the system is in a failed state. The structure function is a function of a state vector (x), whose coefficients (x_i) are binary variables representing the two states of the components that comprise the system; *1.0* if component *i* is functioning, *0.0* if component *i* is in a failed state. The structure function of a series system is expressed as a product of all coefficients in a state vector (**Eq.5.1**), and the structure function of a parallel system is expressed as the maximum of the coefficients of the state vector (**Eq.5.2**) (Ross, 2003; Rausand and Hoyland, 2004).

$$\phi(x) = \prod_{i=1}^{n} x_i \tag{5.1}$$

$$\phi(x) = \max_{i=1}^{n}(x_i) \tag{5.2}$$

The failure probability of a system can be calculated (at least conceptually) when failure probabilities of the components of the system can be determined. When failure events of components are statistically independent, the failure probability of a series system is computed as **Eq.5.3** and the failure probability of a parallel system is computed as **Eq.5.4**.

$$P_f = 1 - \prod_{i=1}^{n} \left(1 - P_{f_i}\right) \tag{5.3}$$

$$P_f = \prod_{i=1}^{n} P_{f_i} \tag{5.4}$$

If the component failures are not statistically independent, the failure probability of a system can be computed from an integral of the joint probability density function describing the random variables over the domain defined by the limit state function of a system failure (Thoft-Christensen and Baker, 1982; Ang and Tang, 1984; Thoft-Christensen and Muratsu, 1986; Melchers, 1999). Monte Carlo simulation may be used to perform this integral when the system behavior or limit state are complex or the component failure events are not statistically independent (Ang and Tang, 1984; Melchers, 1999).

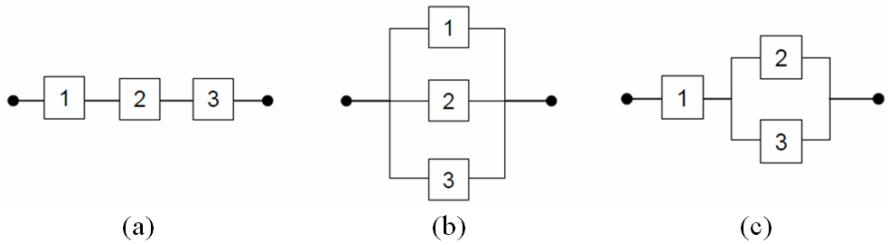

Fig 5.2 Reliability block diagram of a; (a) series, (b) parallel and (c) series and parallel system

Figs 5.2(a) to **5.2(c)** illustrate three simple and typical reliability block diagrams. These diagrams represent the same events illustrated by the fault tree models in **Figs 5.1(a)** to **5.1(c)**. By determining that there is at least one connection between the two ends, the system is identified as being functioning. For example, when any one of the three components shown in **Fig 5.2(a)** fails, there is no connection between the ends, and the system fails. In **Fig 5.2(b)**, the system loses its function only when all three components fail. In **Fig 5.2(c)**, there is no connection between two ends when either component 1 fails or components 2 and 3 fail. The structure functions of these three systems are given by **Eqs.5.5** to **5.7**, respectively.

$$\phi(x) = x_1 \cdot x_2 \cdot x_3 \tag{5.5}$$

$$\phi(x) = 1 - (1 - x_1) \cdot (1 - x_2) \cdot (1 - x_3) \tag{5.6}$$

$$\phi(x) = 1 - (1 - x_1) \cdot (1 - x_2 \cdot x_3) \tag{5.7}$$

An initiating event generally leads to a sequence of other events. For example, when a building fire occurs (an initializing event), fire alarms may warn the building residents (one consequential event) or they may fail to operate (the second consequential event). If the fire alarms function, residents may either escape from the building safely or wait for firefighters to assist them in evacuation (third events following the preceding second event). Such event progressions can be modeled by an event tree analysis. Each event in an event tree has two or more outcomes, and each outcome is conditioned on the occurrence of a previous event. Thus, the initiating event is connected inductively with the final outcomes through the sequences of events depicted in the event tree. Since each outcome has a probability of occurrence, the probability of each final outcome can be calculated by multiplying the conditional probabilities of the sequential events on the path from the initiating event to the final outcome. Event trees also can be used to describe the multiplicity of choices involved in decision analysis, in which case the event tree model is called a decision tree model. Both models are used to compute the probability of occurrence of final outcomes and their consequences (Ang and Tang, 1984; Rausand and Hoyland, 2004).

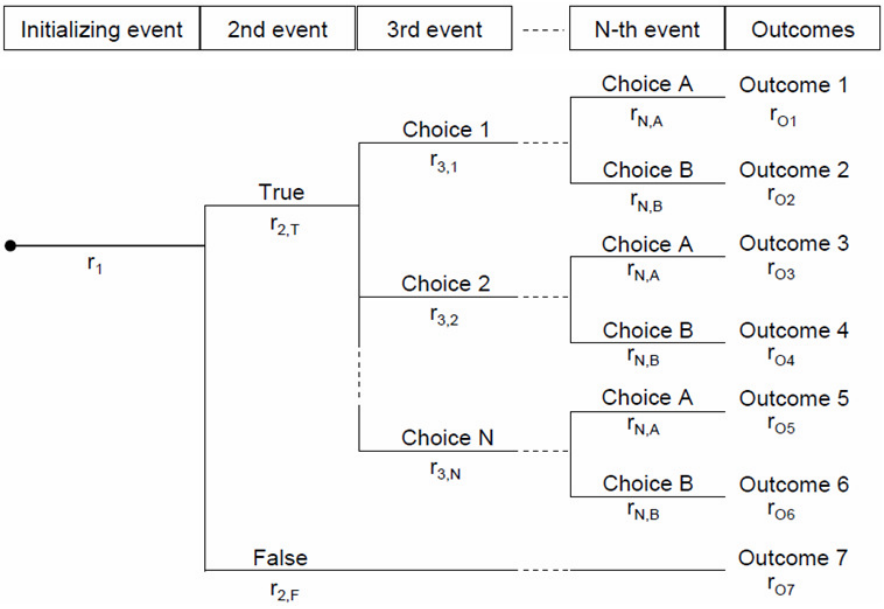

Fig 5.3 An event tree model

An example of an event tree and its probabilistic analysis is illustrated in **Fig 5.3**. Here, the initiating event occurs with probability r_1. Once the initiating event occurs, the second event occurs. The outcomes of the second event are True or False. The probability that the second event is True is $r_{2,T}$, and the probability that the it outputs False is $r_{2,F}$, . If the second event

results in False, no other events occur and the final outcome 7 is evaluated at the probability of $(r_1 \cdot r_{2,T})$. If the second event results in True, the third event occurs and *N* outcomes (*Choice 1, Choice 2, ···, Choice N*) are possible with the probabilities of $r_{3,1}$, $r_{3,2}$ and $r_{3,N}$ respectively. By continuing the procedure, the probability of each outcome is evaluated. For example, the probability of Outcome 1 is computed as $r_{o1} = r_1 \cdot r_{2,T} \cdot r_{3,1} \cdot r_{N,A}$. By comparing the probabilities of final outcomes, the most probable outcome can be identified. Furthermore, if the outcomes are expenses or casualties, the consequences can be measured by the weighted average, **Eq. 5.8**.

$$(r_{o1} \cdot outcome1) + (r_{o2} \cdot outcome2) + \cdots + (r_{o7} \cdot outcome7) \tag{5.8}$$

5.3 Probabilistic Reliability Model

Every element of a network experiences different seismic demand depending on its geographical location and its dynamical characteristics. The damage probability of Bam water and power network links and nodes are shown in **Figs. 5.5**, **5.6**, **5.7** and **5.8** respectively. The main interest is how the seismic damage of each the vulnerable network's elements affects the overall network performance (Poljansek 2010). In this model only seismic damage that causes evident mechanical element failure which could be detrimental to the operability of the other elements in the network is considered. It is presumed that, eventually, the topological deterioration of the overall connectivity due to the failure of any of the element/s compromises the functionality of the entire network.

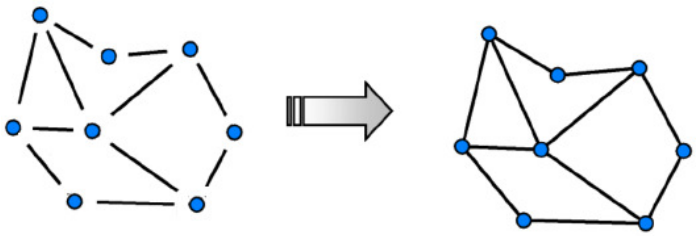

Fig 5.4 Propagation of probabilities failure of elements in overall analysis.

Therefore, the determination of element failure implies the generation of a damaged network. In principle, the connectivity analysis of the damaged network assesses the extent to which it is capable of operating functionally, but this study does not consider dynamic processes like simulation of cascading failure. Detection and development of cascading failures is possible to track down using power flow analyses; however, such an analysis requires an extensive dataset of possible flows and existent capacities.

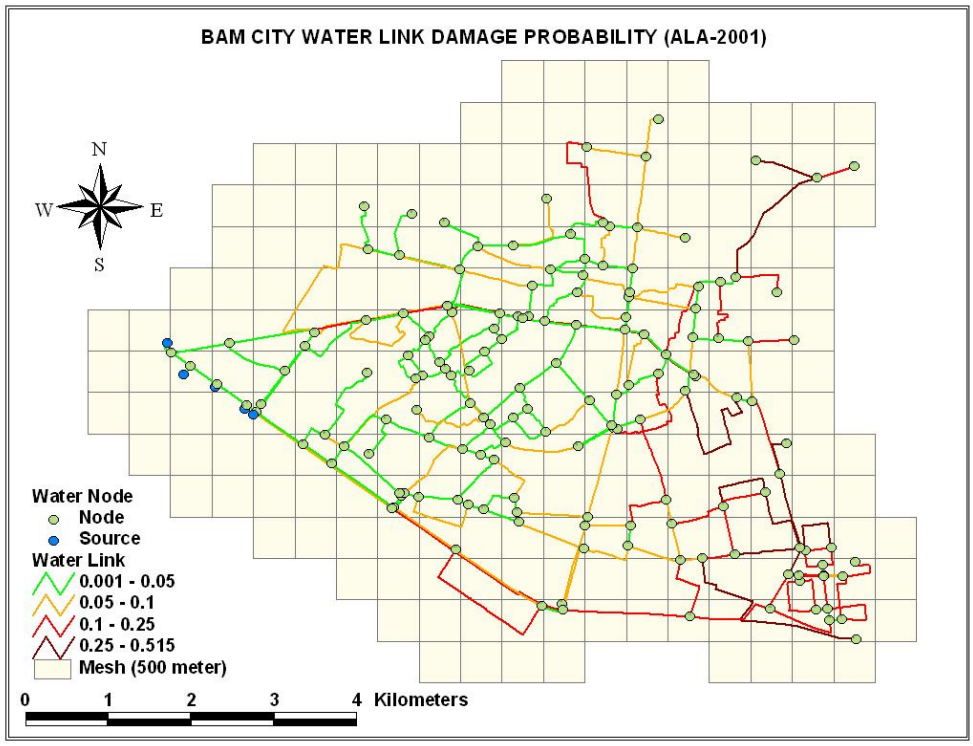

Fig 5.5 Bam water links damage probability based on ALA-2001

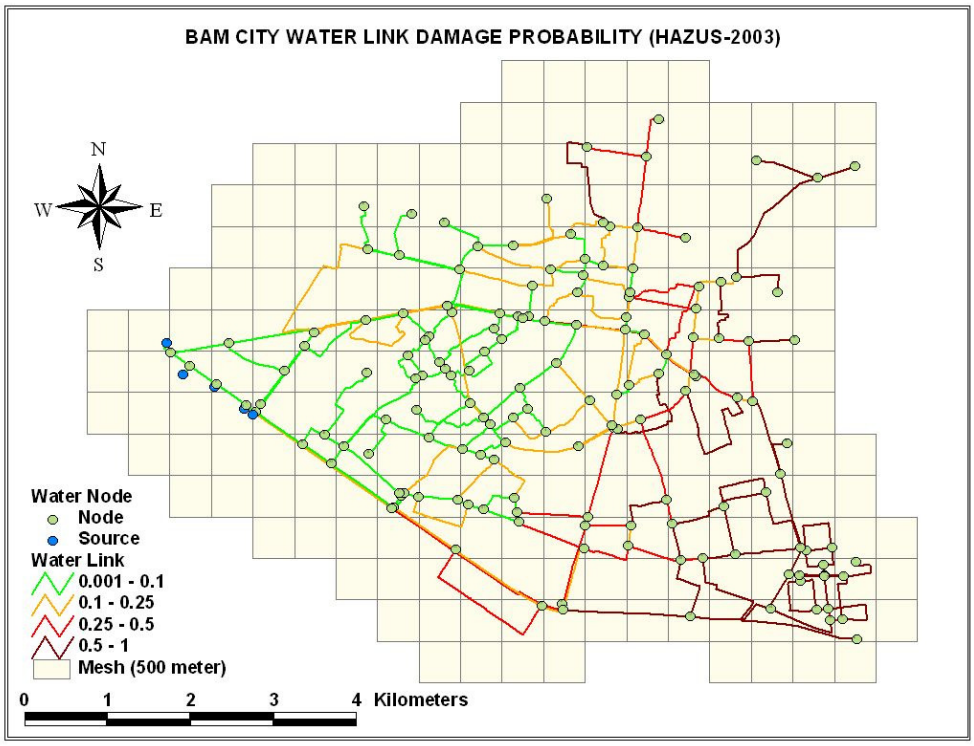

Fig 5.6 Bam water links damage probability based on HAZUS-2003

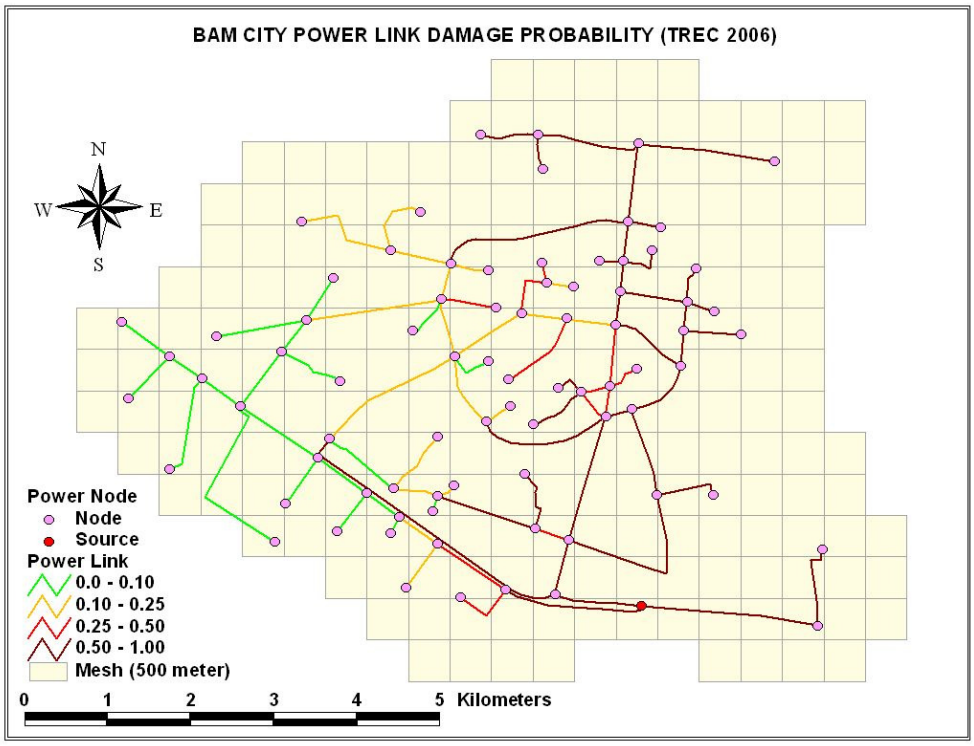

Fig 5.7 Bam power links damage probability based on TREC-2006

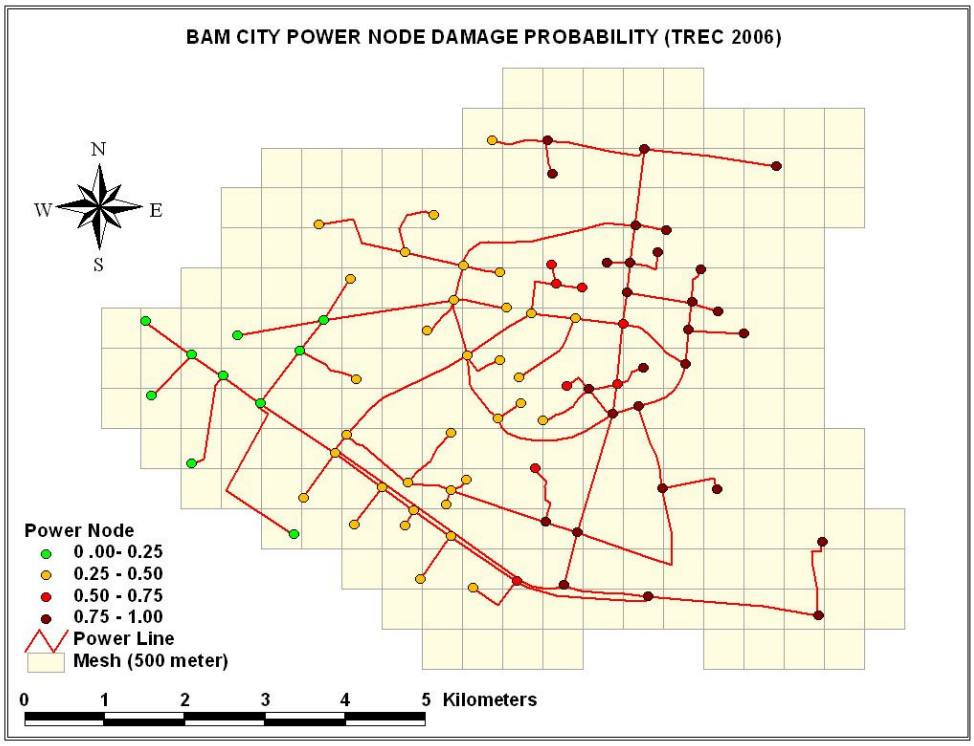

Fig 5.8 Bam power nodes damage probability based on TREC-2006

Earlier, the probability of failure for each element is illustrated, so now the model must be able to propagate all these singular probabilities of failure through the network and present the result as the probability of failure or probability of exceeding any other defined damage state of the whole network. This transformation from element level to the network level was performed using Monte Carlo simulations.

5.4 Network Performance Properties

Independent of the nature of the disruption and the mechanism by which it propagates either by overloading the most connected vertices, or the vertices most in between other vertices, or the most instrumental to flow circulation, or by random malfunction, overall network functionality needs to be characterized (Deunus-Osorio, 2005). So, before proceeding with the network analysis, network performance measures should be introduced. If it is to compare the robustness of the network to the quality of the network's performance, various parameters are necessary that quantify the network's performance regardless of the hazard type.

Such measures must have two important attributes. First, they should be a representative characteristic of the whole network, and secondly they should be able to quantifiable. Consequently, the definition of damage states can be introduced in relation to the various descriptive parameters chosen to quantify damage (i.e. undelivered water or the population affected). Finally when the performance measures are presented as the probability estimation in the form of network fragility curves, they can be used as surrogate measures for risk indicators. However, they also directly reflect the response of the network under the chosen hazard. Five network performance measures are introduced in this section. They are based upon the topological properties taken from graph theory, but the last two measures, serviceability loss and impact factor on the population, can be exported to GIS database in order to evaluate actual impact of the seismic disruption of the (dependant) water network on the water supply to the population.

5.4.1 Efficiency, *E*

Network efficiency generalizes the concept of the reciprocal harmonic mean, L', of a graph *G*. The fundamental difference is that *E* drops the restriction of edge unweightedness and undirectedness. As originally formulated, L' relies upon calculation of distance $d(i, j)$ between any two vertices of the graph. The distance $d(i, j)$ was defined as the length of the shortest path between *i* and *j*, and this length corresponds to the number of edges in the path.

Also, L' assumes the graphs to be undirected. The generalization introduces a matrix *D*, with non-zero entries identical to the adjacency matrix *A*, and d_{ij} elements that represent the physical distance between them. Hence, the new distances $d(i, j)$ calculated using *A* and *D* reflect the physical separation between vertices *i* and *j*, and $d(i, j) \geq d_{ij}$ for all $i, j \in V(G)$. The equality is valid if there is an edge joining *i* and *j*. The parameter *E* can be calculated as **Eq. 5.9** (Latora and Marchiori, 2002).

$$E = \frac{\sum_{i \neq j} \frac{1}{d(i, j)}}{\sum_{i \neq j} \frac{1}{d_{ij}}} \tag{5.9}$$

where the denominator normalizes the numerator with respect to the most efficient of all possible simple graphs: a complete graph with same order n as the original graph. Therefore, $0 \leq E(G) \leq 1$. This parameter, as its names suggests, can be regarded as a global indicator of efficiency in network connectivity. It represents the ease with which any two vertices can communicate or share flow. The input information requirements are limited to the Euclidean distances between adjacent vertices. The efficiency coefficient of Bam water and power network nodes are shown in **Figs. 5.9** and **5.10** respectively.

5.4.2 Betweenness loss, B_v

The betweenness, B_v, of a vertex *v* is defined as the total number of shortest paths that pass through vertex *v*, when the shortest paths are calculated between every pair of vertices and *v* is not considered an end of any shortest path (Newman, 2001; Borgatti, 2005).

In the context of technological networks, such as electric power or water distribution, the vertex betweenness can be measured for paths going from a generation subset *S*, to a distribution subset *D* passing through a transmission subset *T* (Albert et al., 2004).

Assuming that network flows are routed through the most direct path (i.e., shortest), which is consistent with optimal engineering systems design, the betweenness, B_v, of a vertex *v* represents the load or total flow that traverses it. Its calculation reduces to finding every shortest path from *S* to *D* and keeping the score of the nodes linked by each path.

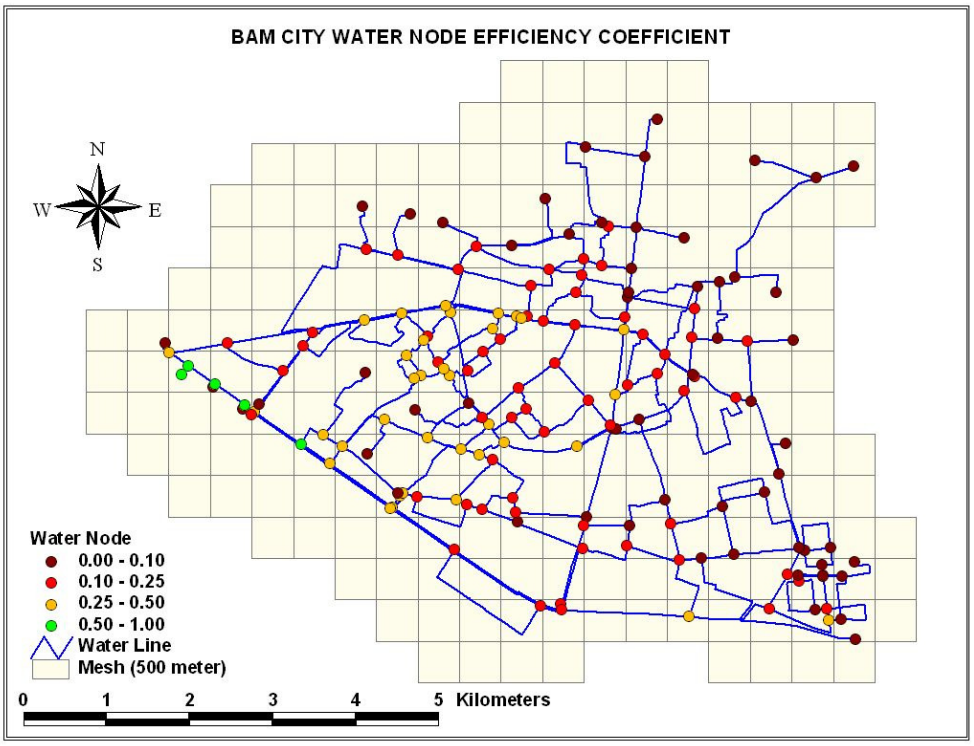

Fig 5.9 Bam water nodes efficiency coefficient

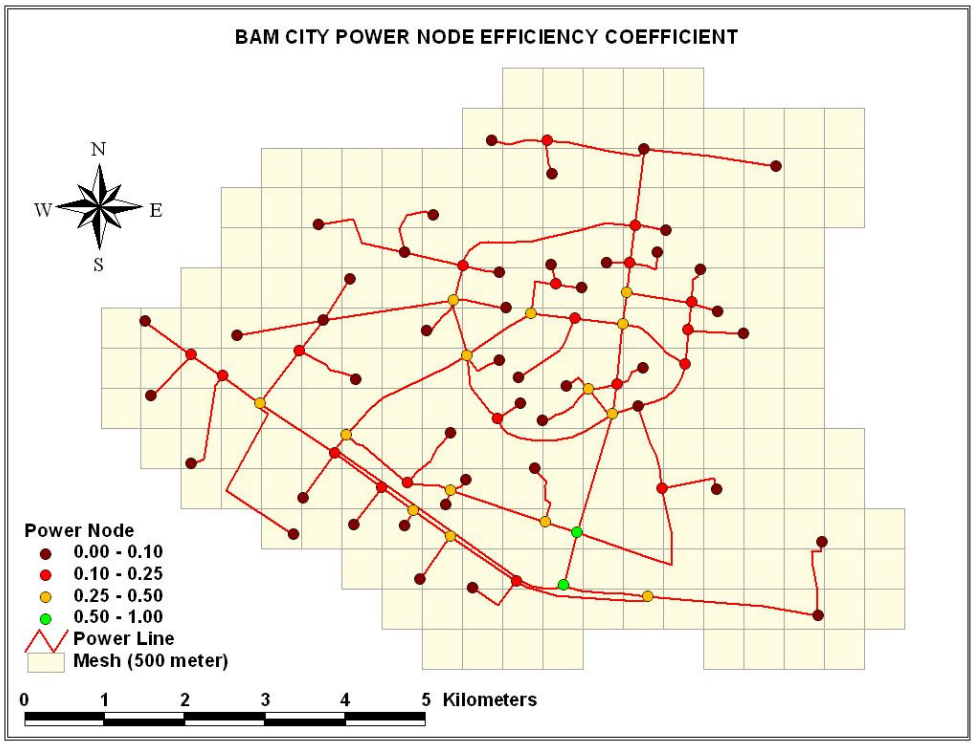

Fig 5.10 Bam power nodes efficiency coefficient

Given a graph $G = \{S \cup T \cup D\}$, the concept of betweenness loss, B_{v_L}, is useful to quantify the average decrease of the flow passing through transmission vertices elements of the T subset due to reduced number of damaged distribution vertices. Denoting N_T^i, the number of shortest paths that pass through vertex i of transmission subset $T \subseteq G$, at normal condition of network, and N_t^i, the number of shortest paths that pass through vertex i after a damage takes place. The betweenness loss of vertex v, B_{v_L} can be calculated as **Eq. 5.10**.

$$B_{v_L} = 1 - \left\langle \frac{N_t^i}{N_T^i} \right\rangle_i \tag{5.10}$$

where the averaging $\langle\ \rangle$ is done over the transmission vertices i of transmission subset $T \subseteq G$. Rank ordering by vertex betweenness takes into account information beyond network topology. It accounts for the potential flow patterns within the network. This parameter requires distinctions between vertices' roles and functions. Its investigation provides information about the effect on network performance induced by removing the nodes that are in between most other nodes. These nodes are not necessarily the most connected ones. The betweenness loss ratio of Bam water and power network nodes are shown in **Figs. 5.11** and **5.12** respectively.

5.4.3 Connectivity loss, C_L

The concept of connectivity loss, C_L, is useful to quantify the average decrease of the ability of distribution vertices those belonging to the D subset to receive flow from the generation vertices elements of the S subset passing through transmission vertices elements of the T subset. In other words C_L quantifies the decrease in the number of generators with connecting paths to the distribution vertices (Albert et al., 2004). Denoting N_S^i, the number of generation units, $S \subseteq G$, able to supply flow to distribution vertex i, in normal condition of the network and N_s^i, the number of generation units able to supply flow to distribution vertex i, after damage takes place. The connectivity loss, C_L, can be calculated as **Eq. 5.11**.

$$C_L = 1 - \left\langle \frac{N_s^i}{N_S^i} \right\rangle_i \tag{5.11}$$

where the averaging $\langle\ \rangle$ is done over the distribution vertices i of distribution subset $D \subseteq G$.

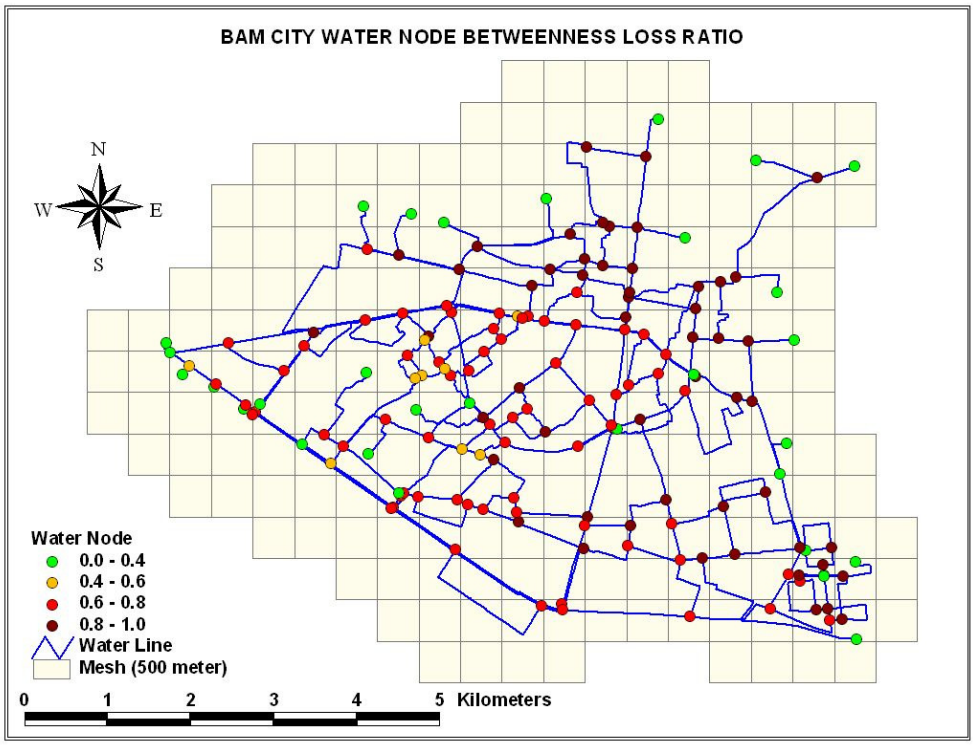

Fig 5.11 Bam water node betweenness loss ratio

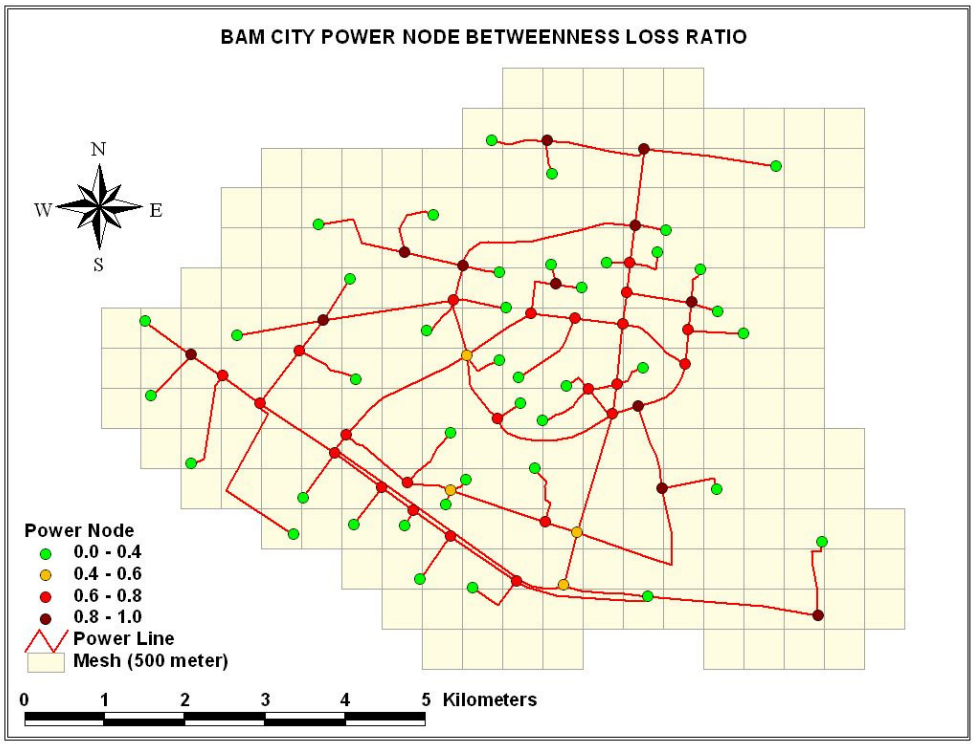

Fig 5.12 Bam power nodes betweenness loss ratio

The calculation of this parameter clearly relies on the topological structure of the network, and on the existence of paths connecting supply and demand elements. The input information requires distinction on the types of vertices. The connectivity loss ratio of Bam water and power network nodes are shown in **Figs. 5.13** and **5.14** respectively.

The final calculation of the connectivity loss measure goes through the counting process of the relevant shortest paths. Since connectivity loss is a network characteristic, it can be used for definition of network damage states. Deunus-Osorio et al. (2007) used the connectivity losss for evaluating the overall network damage states, so that 20%, 50% and 80% connectivity loss for minor, moderate and extensive respectively.

5.4.4 Serviceability loss, S_L

The capacity of source node in terms of operating supply (e.g. power substation (MW) and water reservoir (m^3)) is employed and define the serviceability loss *SL* (%) as the performance measure. It follows a similar concept to connectivity loss as **Eq. 5.12**.

$$S_L = 1 - \left\langle \frac{S_s^i}{S_S^i} \right\rangle_i \tag{5.12}$$

where S_S^i and S_s^i are the sums of the supply capacity of all the sources connected to *i*-th demand (load) node in the undamaged and damaged network, respectively. Therefore serviceability loss of undamaged state is $S_L = 0$. In case of Bam city, water and power has only one source node, therefore the serviceability loss ratio of nodes is the same as their connectivity loss ratio.

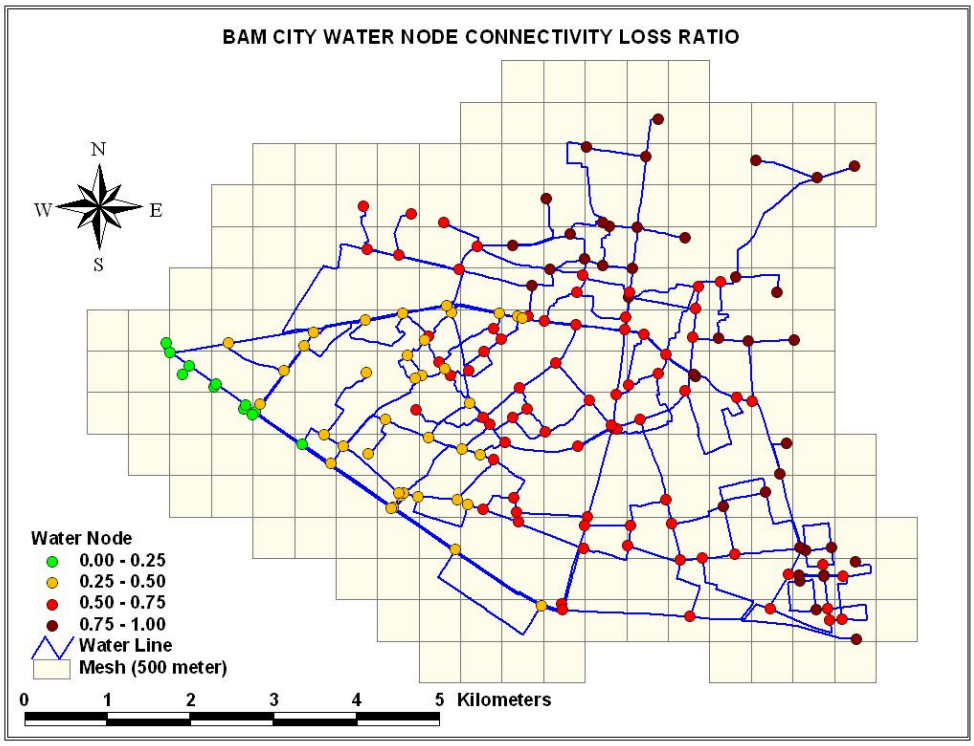

Fig 5.13 Bam water node connectivity loss ratio

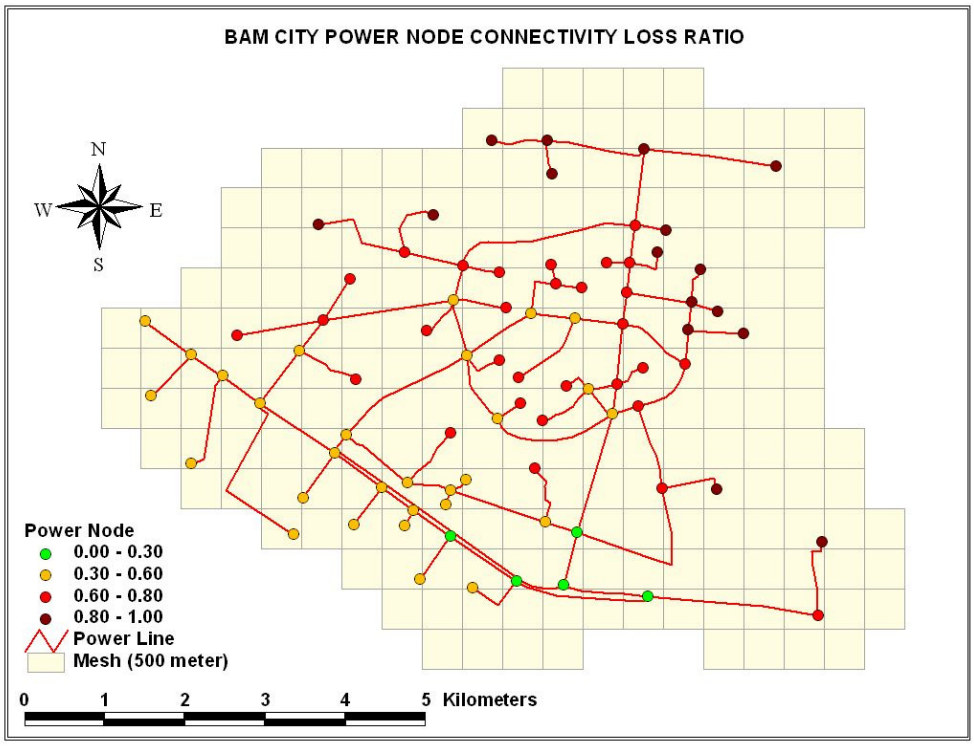

Fig 5.14 Bam power nodes connectivity loss ratio

5.4.5 Population impact factor, I_P

Considering that each demand (load) node supplies service to an assigned population area (**Fig 5.15**), the impact of the disruption of the network under seismic hazard on the population can be evaluated.

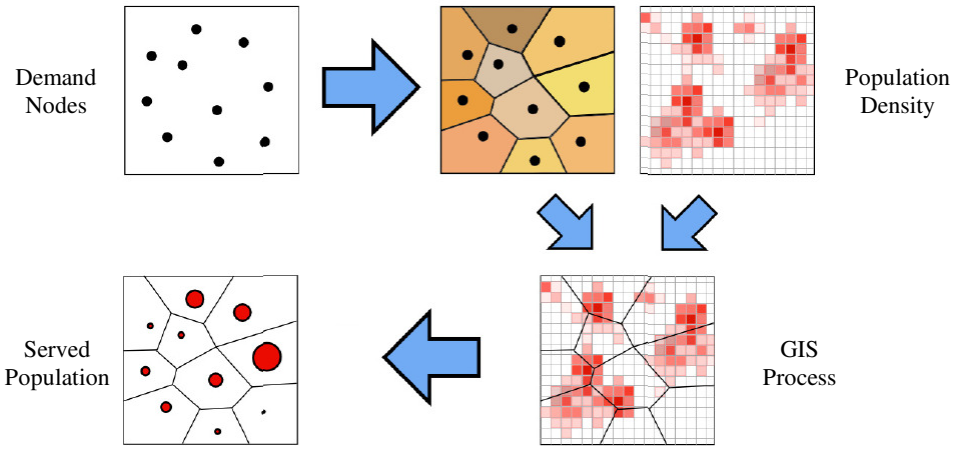

Fig 5.15 GIS processing for demand nodes' served population definition

So, consider the number of people P_i that are assigned to each demand node, and also the decreased service supply for each demand node $\left(S_s^i / S_S^i\right)$. It can assume that part of the population is still supplied by demand node while another part undergoes shortage. The division between supplied and affected population is executed in the ratio of still-disposable to lost serviceability. Therefore the part of supplied population covered by the i -th demand node equals the normalized service supply of the i -th demand node in the damaged network. Finally, the overall population impact factor $I_P(\%)$ is calculated as the normalized value of affected population. It equals 0.0 in the case of undamaged network.

$$I_P = 1 - \frac{\sum_{i=1\cdots N_D} \frac{S_s^i}{S_S^i} \cdot P_i}{P_{all}} \tag{5.13}$$

Like connectivity loss, serviceability loss and population impact factor are also network characteristic ranging from 0 to 100%, and they can be used for the definition of network damage states. The number of affected population in each node of Bam water and power network is shown in **Figs. 5.16** and **5.17** respectively. The overall population factor is 0.64 for Bam water network and 0.73 for Bam power network.

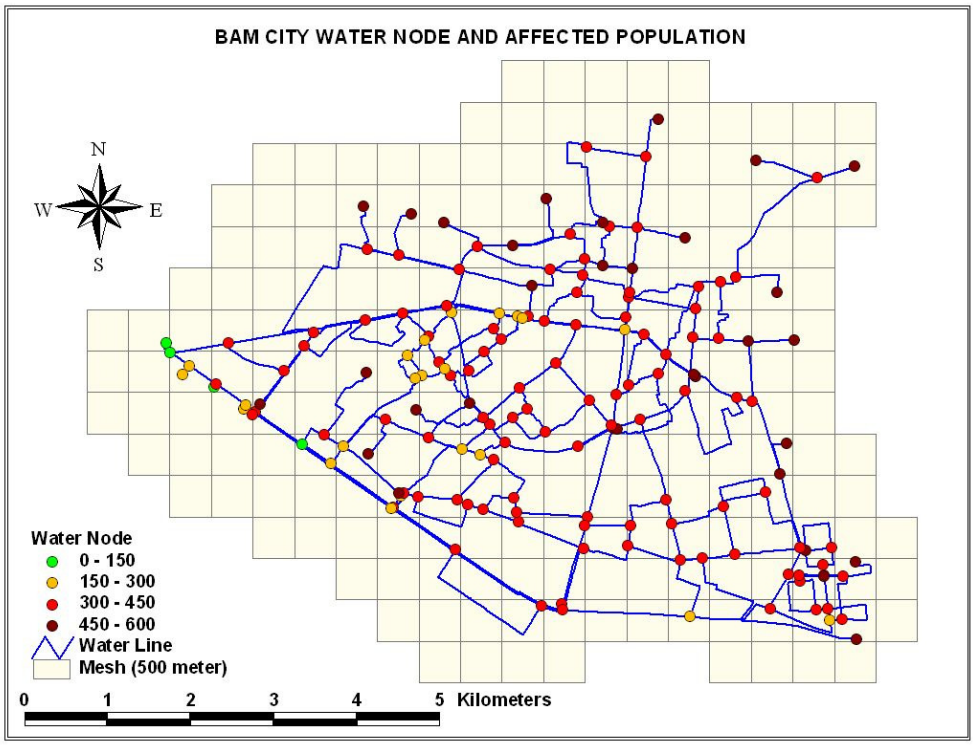

Fig 5.16 Bam water node and affected population

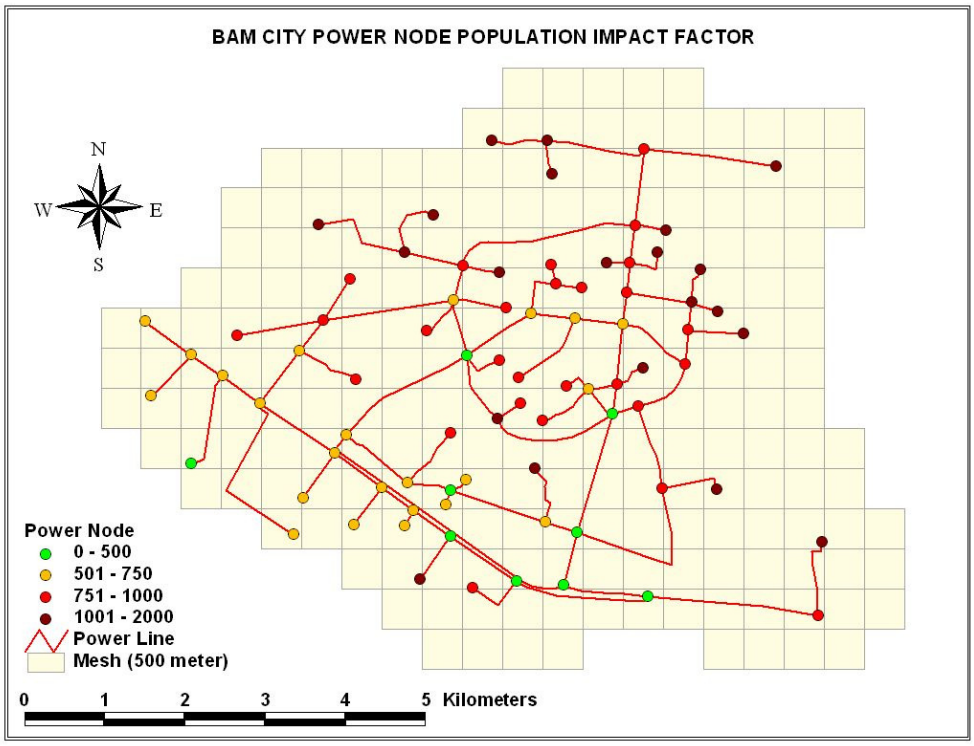

Fig 5.17 Bam power nodes and affected population

5.5 Discussion about Results

Five performance measures are calculated for the Bam water and power networks individually. The calculation of these parameters clearly relies on the topological structure of the network, and on the existence of paths connecting supply and demand elements.

As it is shown in **Fig 5.18(a)**, the efficiency coefficient of end user nodes are zero because they don't connect to other nodes (directed network) and in the other words their shortest paths to other nodes is infinity. In contrast, the efficiency coefficients of source nodes usually are the highest. It is for this reason that generally the source nodes are connected to most of nodes in the networks more than another. However there are some cases that the efficiency coefficients of among network nodes are higher than some source nodes. Its usually occurs in the transmission nodes of the networks which one source node supports most part of the network than other source nodes. For example, as it can be seen in **Fig 5.19(a),** in the Bam city power network, the efficiency coefficients of two transmission nodes are higher than source nodes. It is worth noting that the power network of the Bam city is supported by only one source node.

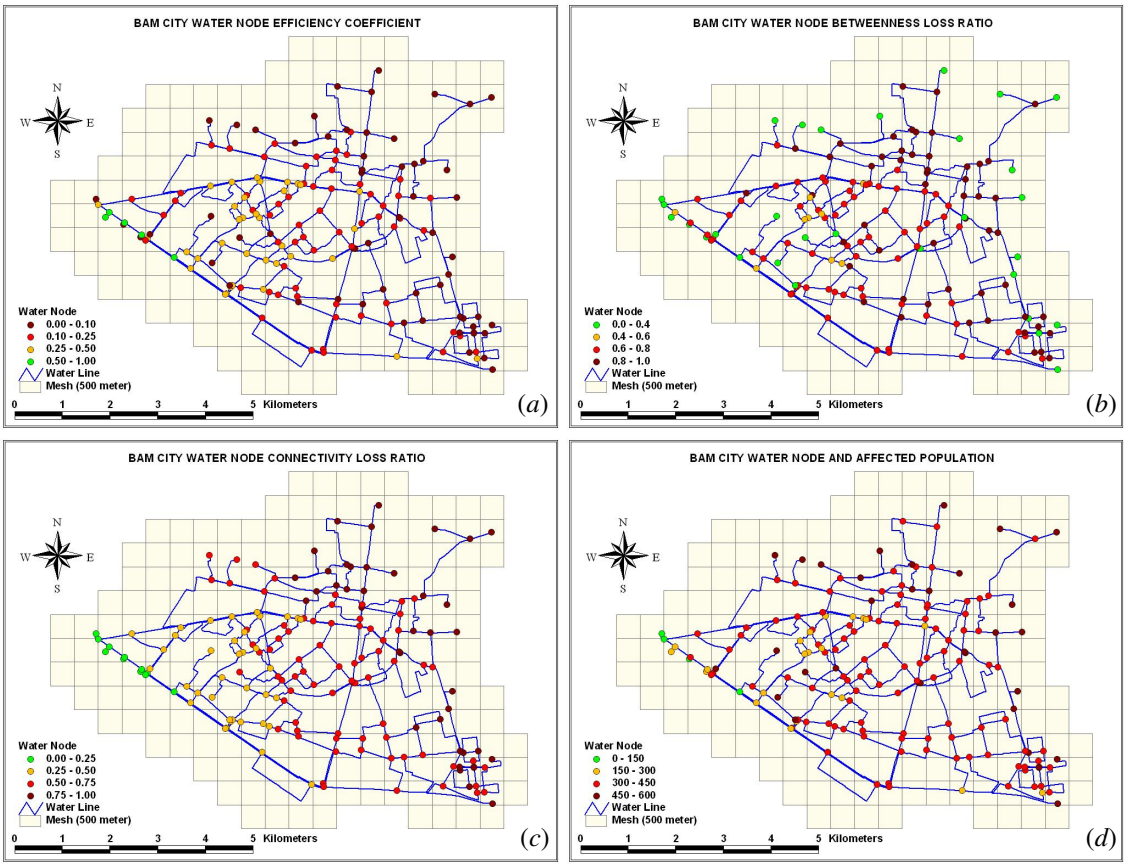

Fig 5.18 Performance measures of the Bam water network
(a) efficiency, (b) betweenness loss, (c) connectivity loss and (d) affected population

The efficiency can be regarded as a global indicator of efficiency in network connectivity. It represents the ease with which any two vertices can communicate or share flow. As a result it can be said that the nodes with higher efficiency coefficient are important than others because they are connected to other nodes with the most optimum shortest paths. Therefore they are a higher priority in strengthening, replacement and restoration than other nodes.

The second performance measure is betweenness loss ratio. As it is illustrated in **Fig 5.18(b)** like the efficiency coefficient, the betweenness loss ratios of end user nodes are zero because as it is said they don't connect to other nodes (directed network) and in the other words the number of shortest paths that pass through them are zero in both cases (damaged and undamaged network). Therefore the betweenness loss ratios for the end user nodes are actually undefined but it is assumed equal zero. However the highest betweenness loss ratios are usually belongs to the nodes before end user nodes because they are generally connected only to one or two (end user) nodes (**Fig 5.19.b**). In this way, the betweenness loss ratios of among network nodes are usually less than them.

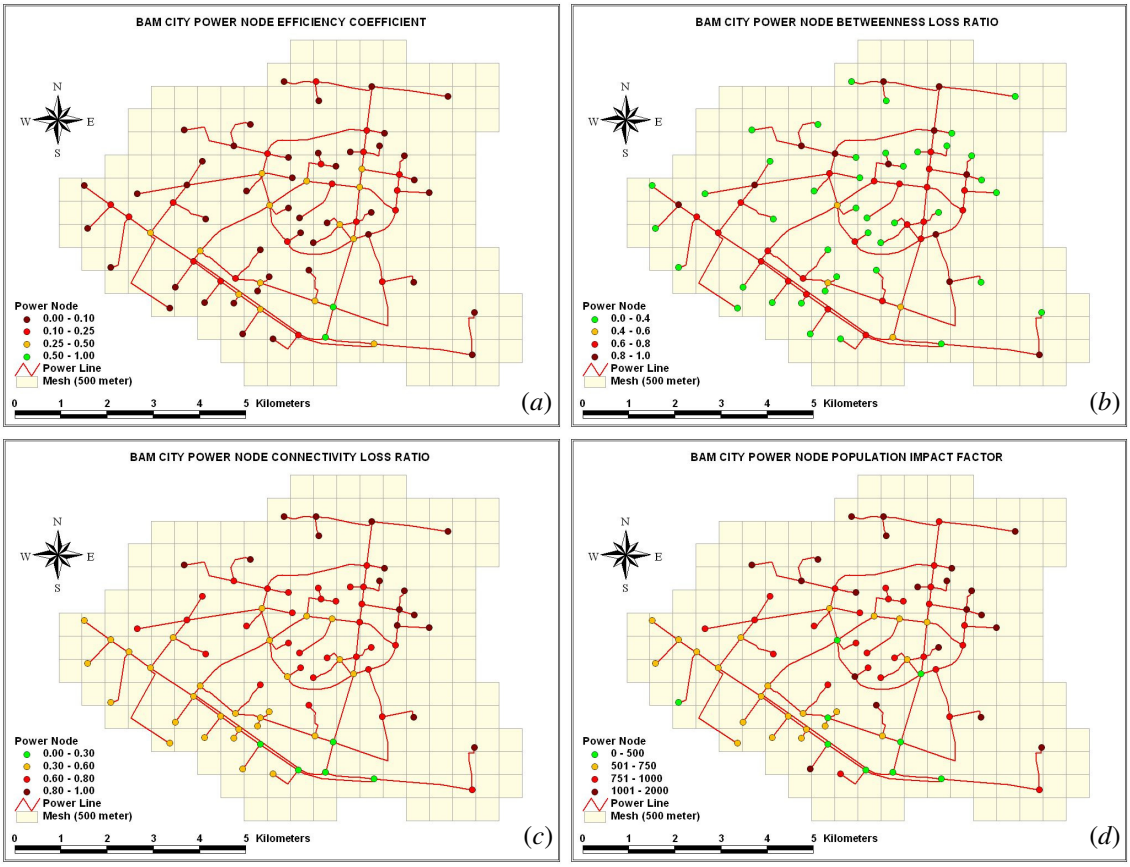

Fig 5.19 Performance measures of the Bam power network
(a) efficiency, (b) betweenness loss, (c) connectivity loss and (d) affected population

As the result, the nodes with high betweenness should be considered as important points which high flow pass through them. In contrast, the high betweenness loss ratio in a node means that the down-stream of the node doesn't have good situation. In the other words this ratio is equal to the demand loss of the node. Therefore the nodes with high betweenness loss ratios are lower priority because the higher loss of their down stream demands. In this way the nodes with lower betweenness loss ratios such as source nodes are higher priority.

The third measure is connectivity loss ratio. As it is presented in **Fig 5.18(c)** unlike the past two measures, the connectivity loss ratios of the end user nodes are higher than others. These loss ratios of the nodes are decreased approaching to the source nodes (**Fig 5.19.c**). The high connectivity loss ratio in a node means that the up-stream of the node doesn't have good situation. In the other words this ratio is equal to the supply loss of the node. Therefore nodes with high connectivity loss ratios are lower priority because the higher loss of their supply. In this way the nodes with lower connectivity loss ratios such as source nodes are higher priority.

The forth measure, serviceability loss ratio is the same as connectivity loss, the only difference is that the source nodes capacity which connected to the nodes. Therefore same as the connectivity loss ratio, the nodes with lower serviceability loss are high priority.

The last measure is population impact factor. The nodes with high population impact factor are usually located in populated area (**Fig 5.18.d**). It seems that the nodes with higher population impact factors and lower serviceability loss ratios are high priority (**Fig 5.19.d**).

In conclusion, it seems that the high betweenness nodes with the lower connectivity loss are the first priority and the demand nodes with low serviceability loss ratio and high population impact factor are the second priority.

5.6 Summary and Conclusions

It is presumed that, eventually, the topological deterioration of the overall connectivity due to the failure of any of the elements compromises the functionality of the entire network. Five network performance measures, efficiency, betweenness loss, connectivity loss, serviceability loss and impact factor on the population are described. All of these measures are based upon the topological properties taken from graph theory.

Based on the measures, the fundamental concepts of reliability are introduced and the reliability analysis of individual infrastructure systems is done. The results are used to assess potential risks of earthquake for infrastructure systems, to improve redundancy of infrastructure systems efficiently, to create restoration plans at lower cost and higher efficiency, and to design the layout of facilities and distributing elements of infrastructure systems.

CHAPTER 6

SYATEM MODELING OF INTERDEPENDENT CRITICAL INFRASTRUCTURES

6.1 Introduction

Recent research has assessed the response of a complex urban lifeline system under seismic conditions. Some approaches rely on simulation models to estimate seismic performance of a lifeline system (Hwang 1998, Kim 2007 and Shinozuka 2007), while others adopt system reliability frameworks to estimate the probabilities of complex system events (Vazni 1996, Li 2002, Kang 2007). These approaches generally incorporate the vulnerability of components represented by fragility curves in a system level analysis.

Although these approaches are important advances in the understanding of the seismic response of a lifeline system, consideration of interdependencies (i.e., the influence from the failures of other networks) in modeling and analyzing lifeline systems accordingly is still a significant challenge. The need of accounting for this *interdependency effect* is seen by looking at the importance of a functioning power grid to the water and gas distribution systems. Water and gas distribution systems must have power for proper operation. When a power station is damaged by significant seismic forces, the likelihood that water and gas systems dependent on that power station can continue to function properly is reduced. Therefore, there has been an emerging need of modeling complex and interdependent critical infrastructure to better understand their susceptibility against potential hazards.

Recently, an approach is presented to assess the seismic performance of interdependent lifeline systems. In this approach, a probabilistic model is developed to characterize network interdependency. This probabilistic model is then incorporated into network flow algorithms to assess the seismic performance of the interdependent lifeline systems.

6.2 Dimensions of Interdependencies

For a given a geographically bounded system, determination of what constitutes interdependencies among infrastructures is a nontrivial problem because factors of different nature contribute to the observed coupling characteristics. Ideally, interdependencies could be quantified by weighting each of the following dimensions: type of interdependency, coupling and response behavior, infrastructure characteristics, infrastructure environment, type of failure,

and network state of operation (Rinaldi et al., 2001). A brief description of these dimensions is presented by Deunus-Osorio, 2005 as below.

6.2.1 Types of interdependency

There are four main types of interdependencies: physical, geographical, informational, and logical. Physical interdependencies arise when the state of the infrastructures depends on tangible or material linkages among them. This type of interdependency is suitable for quantification with low uncertainty. Visual inspection would be the simplest procedure for determining physical coupling. Geographical interdependencies are also quantifiable because they depend on the spatial proximity among network elements. Informational interdependencies emerge due to the contemporary need for exchange of data, and the computerized control of infrastructure performance. Finally, logical interdependencies appear when human decisions intervene, or when the connection is not physical, geographical, or informational.

6.2.2 Coupling and response behavior

This dimension is characterized by the degree of coupling, the coupling order, and the complexity of the connections. The degree of coupling refers to the "tightness or looseness" of the interdependency. In highly coupled infrastructures disturbances tend to propagate rapidly through and across them. Hence, tight coupling implies time dependent processes with little slack. Coupling order defines whether or not two infrastructures are directly connected to one another or indirectly coupled through one or more intervening infrastructures. For instance, if the power grid fails, there is a supply / demand imbalance whose first-order effects could be disruption in gas supply, oil extraction, and water distribution. Second-order effects manifest as reduced cogeneration for oil production, inventory buildup in refineries, inventory drawdown in storage terminals, and crop losses in agriculture. Third-order effects can also be quantified by reduced oil production, shortages of gasoline for road transportation, disruption of flight schedules, financial losses, etc. This type of analysis can be extended to nth-order effects, at the expense of introducing additional complexity and uncertainty. Complexity of the links represents the linearity or nonlinearity of the interactions among critical infrastructures.

6.2.3 Infrastructure characteristics

This dimension considers the scale of the infrastructure in spatial, temporal aspects and the hierarchy of the elements that constitute an infrastructure. Scale brings into consideration the

size of the problem analysis (i.e., level of granularity). Different temporal scales for network functionality are illustrated in the case of unforeseen network element perturbation: in power grids disruption travels in milliseconds; in gas, water and transportation networks, disruptions propagate in hours; and in most networked systems, interruptions due to maintenance, upgrading, or capacity increase, propagate disruptive effects during years.

Spatial scales reflect the level in the hierarchy of network elements, at which the analysis is defined. Typical hierarchical levels, illustrated with a power grid, are:

- ✓ Part: smallest component identifiable in power analysis.
- ✓ Unit: functionally related collection of parts (e.g., steam generator).
- ✓ Subsystem: array of units (e.g., secondary cooling system).
- ✓ System: grouping of subsystems (e.g., nuclear power plant).
- ✓ Infrastructure: complete collection of like systems (e.g., electric power infrastructure).

A network *G*, as represented in this research by its adjacency matrix, is a collection of systems. The functionality of infrastructures is established from the performance of systems, subsystems, units, and parts.

6.2.4 Infrastructure environment

This dimension refers to the impact on network interconnectedness due to economic concerns, government decisions, legal regulations, public health and safety, technical limitations, and social and political decisions. These types of factors are highly subjective, and can introduce large uncertainties in the definition of network interdependencies.

6.2.5 Types of failures

Failure modes influence interdependent behavior through the way networks propagate or absorb disruptive effects. Cascading, escalating, and parallel failures are feasible modes of failure. Cascading failures are a manifestation of the potential vulnerability of otherwise highly robust networks. Blackouts are examples of such propagation mode, where disturbances can initiate and propagate in a variety of ways that are difficult to foresee. Escalating failures occur when an existing disruption in one infrastructure exacerbates an independent disruption of a second infrastructure, generally in the form of increasing the severity or the time for recovery or restoration. A parallel failure occurs when two or more infrastructure networks are disrupted at the same time and elements within each network fail because of some common triggering event. This case represents simultaneous effects, either because the elements occupy the same physical space, or because the root problem is widespread.

6.2.6 State of operation

The state of operation of an infrastructure exhibits different behaviors during normal operating conditions (i.e, varying from peak to off-peak conditions), during times of severe stress or disruption, and during times when repair and restoration activities are underway. The state of operation of a unit, subsystem, or system at the time of failure affects the extent and duration of the disruption of the entire infrastructure.

Even though the six dimensions for describing infrastructure interdependencies are conceptually simple, the amount of data required for their characterization makes their systematic evaluation impractical. Fewer fundamental parameters are necessary to capture the essential mechanism for coupling networked systems. In this study, three aspects are selected for establishing the model of network interdependencies. Accessibility to data, objectivity, and possibility to explore their domain are the criteria for their selection.

6.3 Probabilistic Model for Interdependency

Interdependence among infrastructure systems is a nontrivial problem because factors of different nature contribute to their coupling characteristics. As described in the last section, Rinaldi et al. (2001) define interdependency as a bidirectional relationship between two critical infrastructures through which the state of each infrastructure influences or is correlated to the state of the other. The dimensions could be considered as interdependent coupling terms: type of interdependency (physical, cyber, geographic, logical), coupling and response behavior (degree of coupling, the coupling order, and the complexity of the connections), infrastructure characteristic (organizational, operational, temporal range of infrastructure dynamics, spatial scales), infrastructure environment, type of failure (common cause, cascading, escalating) and network state operation (normal, disruption or restoration mode).

Such a thorough quantification of networks interdependency is practically impossible due to insufficient or ill-defined parametric data; therefore, the concept of multidimensional coupling dimensions is currently accepted only for generic description and identification of the interconnectedness behavior (Poljansek, 2010). From this point of view, it can be a useful tool for a qualitative overview of the problem in order to find out representative mechanisms that trigger interconnectedness. The interdependent networks of Bam city is shown in **Fig 6.1**. The interdependent part of the networks in south west of the city is indicated by the dashed red line where the water wells and pumps are located. Totally 5 water source nodes is considered in bam water network which connected to power demand nodes.

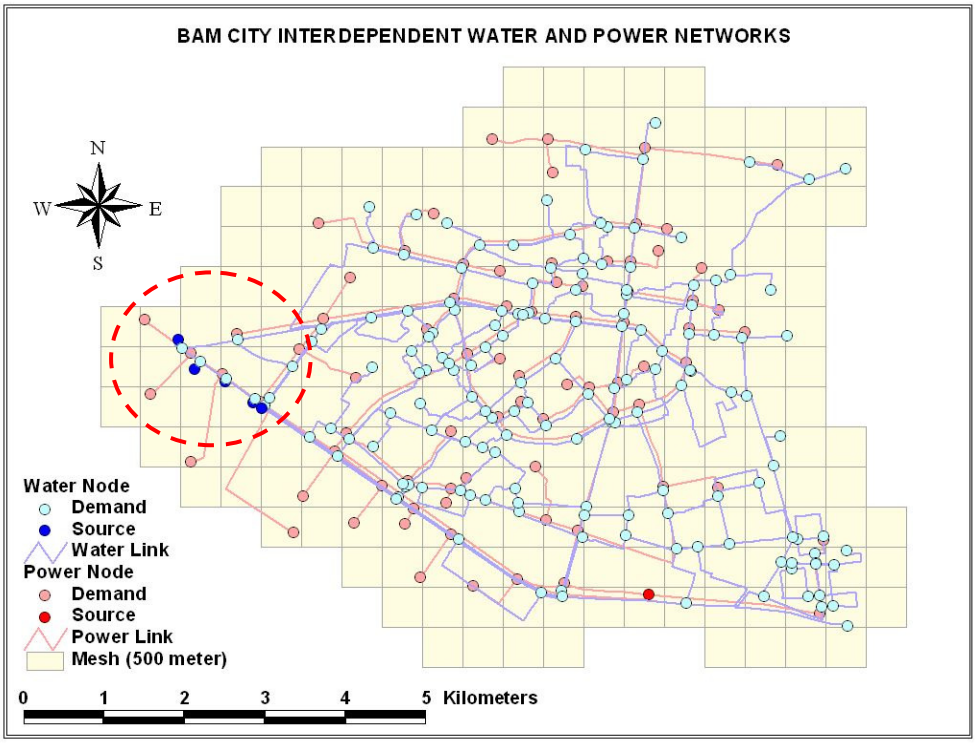

Fig 6.1 Bam interdependent water and power networks

In general, fewer fundamental parameters are necessary to capture the essential mechanisms of coupled networks. The criteria for selecting them depend on how difficult it is to obtain pertinent data and the possibility to explore their behavior in a mathematical sense.

6.3.1 Fundamental Interdependence

It is selected three aspects for establishing the model of network interdependencies. These are physical interdependence, direction of the interaction, and degree of coupling.

6.3.1.1 Physical interdependence

Two infrastructures are physically interdependent if the state of each depends upon the material output of the other. For the water network it may consider that part of the network is transmitted by pump stations which need electricity. Of course, there are other examples implicitly related to the flow of gas; for example, if no gas is available for home heating, end users tend to use electricity appliances. In this analysis it shall only consider the explicit coupling related to major water source nodes.

6.3.1.2 Direction of the interaction

As defined by Rinaldi et al. (2001), interdependency refers to the relation when each of the infrastructures is dependent on the other. In this study, the direction of interconnection is one way only: with dependence of water network on power network, whereas the supply of water to cooling the power stations is not taken into account. Therefore, the power network is independent while the water network is partially dependent. The interdependent critical path between power source (substation) and water sources of Bam city is shown in **Fig 6.2**.

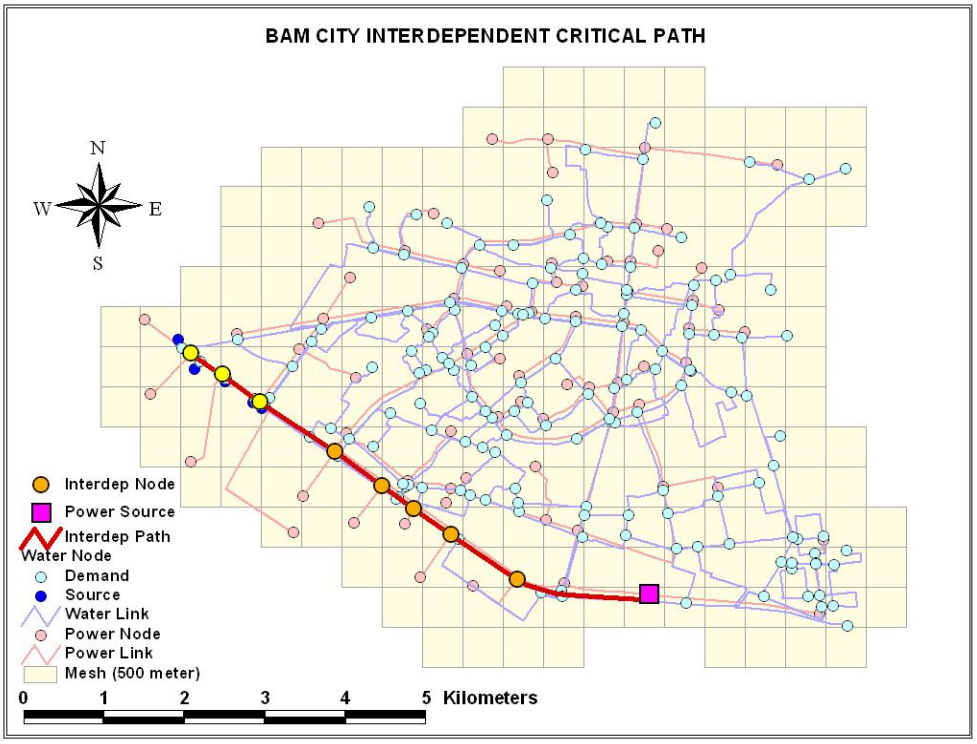

Fig 6.2 Bam interdependent critical path between power substation and water sources

6.3.1.3 Degree of coupling

Whenever there is interaction between two systems, the question arises: what is the degree of coupling. Perrow (1984), classified interactions as either tightly coupled or loosely coupled. Furthermore, the degree of coupling is measured by the strength of coupling which quantitatively implies how fast the disturbances propagate from one network to the other: the higher the strength coupling the tighter the coupling. Tightly coupled interactions are those that do not tolerate delay; i.e., the process of interaction is time-dependant with little slack. So, disturbances in the electric supply would have an almost immediate effect on potable water supply. On the other hand, loose coupling implies that the infrastructures are relatively independent from each other and the state of one infrastructure is weakly correlated to, or even

independent from, the state of another. Slack is present in the system because the propagation of the disturbances from one network to another is very slow.

There are even more possibilities of the regulation of the strength of coupling depending on how slow the propagation of the disturbances is; for example, a power substation could have local backup system or could even switch to alternative diesel generator. Such situations imply different levels of loose coupling of the power substation to the power network. In short, tight and loose couplings refer to the relative degree of dependencies among infrastructures.

6.3.2 Interoperability matrix

This study is modeled all three aspects of power network dependency on the water network with the interoperability matrix. A similar approach was adopted by Deunus-Osorio (2007). A set of conditional probabilities of failure are compiled and put together in such a way that the interoperability matrix reflects the physical interdependence, direction of interaction and strength of coupling of the dependency behavior.

Generally, it needs two interoperability matrices to capture the bidirectional relationship between two networks. With one interoperability matrix it can simulate only the coupling behavior in one direction. The size of interoperability matrix is always $N_{independent} \times N_{dependent}$ where $N_{independent}$ refers to the size of the independent network and $N_{dependent}$ is the size of dependent network. Two possible interoperability matrices arise by switching the roles between dependent and independent networks.

For example $I_{W/E}$ is an $N_E \times N_W$ interoperability matrix which captures the effect of power network on water network, and $I_{E/W}$ is an $N_W \times N_E$ interoperability matrix which captures the effect of water network on electricity network (N_E , size of the power network, N_W , size of the water network). In this study, $I_{E/W}$ will have only zero entries, therefore the direction of the interaction is immediately defined.

The type of dependency, in this case physical dependence, helps to define the inter adjacency matrix which is a simpler version of interoperability matrix because it contains only 0.0 and 1.0. If the node *i* from the power network and the node *j* from the water network are adjacent, the (i, j) element in appertain inter-adjacency matrix receives the value 1.0 and presents the directed link between two networks. The inter-adjacent nodes are clearly defined because common elements of power and water networks are pump stations. They play a double role, the role of demand nodes in the power network and the role of source nodes in the water

network. So the power electricity transmitted along the circuit lines of the power network is needed as electric energy for the water pump stations and reservoirs. The physical interdependent link between 3 power demand nodes (number 76, 77 and 78) and 5 water sources (9, 11, 13, 49 and 162) of Bam city is shown in **Fig 6.3**.

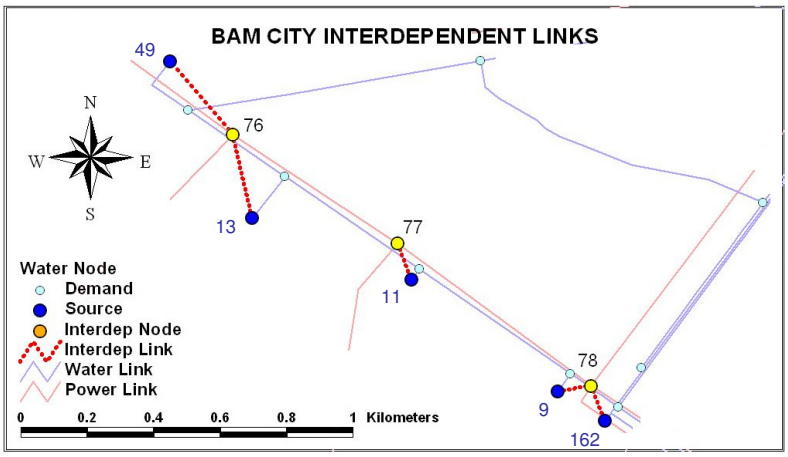

Fig 6.3 Bam interdependent link between power demand nodes and water sources

Therefore the connections of pump stations with both of the networks are unambiguously defined. Only one (nearest) power node feeds each pump station with the power electricity, whereas each pump station may have more than one connection to the transmission water network (**Fig 6.3**). Since all nodes in one network usually do not couple to all nodes in the other, the inter-adjacency matrix is very sparse. Furthermore, the interoperability matrix is a weighted inter-adjacency matrix, where weights describe the strength of coupling. The strength of coupling is defined as the conditional probability of failure of water node at the given failure of adjacent power node as **Eq. 6.1**.

$$P\left(FailureW_j^{dep} \middle| FailureE_i\right) = p_{W_j|E_i} \quad \text{for all } i \text{ adjacent to } j \tag{6.1}$$

To be more precise, in the equation above, W_j^{dep} represents failure of the j-th element of the water network due to its dependency on the power network and E_i represents failure of the i-th element of the power network. In this study, the failure of node E_i (the node from the power network that is adjacent to water pump station) conditions the failure of pump station W_j^{dep} with the probability $p_{W_j|E_i}$. In such a manner it can capture the effect of element failure in the power network on the overall response (seismic hazard and interdependency effect) of the water network using the interoperability matrix.

6.3.3 Strength of coupling

The seismic performance network analysis always starts at the element level of the network. First, the seismic response of each vulnerable element is calculated, and then the evaluation of the seismic response of the whole network is performed. Simultaneously the probabilities of failure of each element are propagated through the analysis in order to represent the final result with the probabilities of networks' damage states. But it also clear that the seismic response of water network is partly dependent on the seismic response of the power network. So, the overall response of the water network should reflect the vulnerability of the water network under seismic hazard and the influence of the damaged power network on the functionality of the water network. In order to introduce this extra vulnerability of the network due to interdependency, it has to return to the element level. Before repeating the seismic performance network analysis, it must first introduce additional information of coupling behavior into the network definition and, then again, calculate the seismic response of each vulnerable element (Poljansek, 2010). This study, apply the dependency effect directly on the pump stations which it also considers to be nodes of the water network.

To consider interdependency behavior with the probabilistic reliability model it needs the updated probability of failure of electricity node. In general, the failure of the *j*-th node of the water network, denoted W_j, can occur due to an earthquake or due to the failure of the power supply, denoted W_j^{EQ} and W_j^{dep}, respectively. Therefore, the event W_j can be defined as the union of the events W_j^{EQ} and W_j^{dep}:

$$W_j = W_j^{EQ} \cup W_j^{dep} \tag{6.2}$$

Because $W_j^{EQ} \cap W_j^{dep} \neq 0$, these two events are not mutually exclusive (**Fig 6.4**) and the probability of the water node failure can be formulated as **Eq. 6.3**.

$$P\left(W_j^{EQ} \cup W_j^{dep}\right) = P\left(W_j^{EQ}\right) + P\left(W_j^{dep}\right) - P\left(W_j^{EQ} \cap W_j^{dep}\right) \tag{6.3}$$

Since that W_j^{EQ} and W_j^{dep} are statistically independent, the joint probability of W_j^{EQ} and W_j^{dep} equals to **Eq. 6.4**.

$$P\left(W_j^{EQ} \cap W_j^{dep}\right) = P\left(W_j^{EQ}\right) \cdot P\left(W_j^{dep}\right) \tag{6.4}$$

If Eq. 6.4 inserts into Eq. 6.3, the result is obtained by **Eq. 6.5**.

$$P\left(W_j^{EQ} \cup W_j^{dep}\right) = P\left(W_j^{EQ}\right) + P\left(W_j^{dep}\right) - P\left(W_j^{EQ}\right) \cdot P\left(W_j^{dep}\right) \tag{6.5}$$

Now, all the probabilities in **Eq. 6.5** should be defined. $P\left(W_j^{EQ}\right)$ is determined from the fragility curves of the elements' vulnerability under seismic hazard.

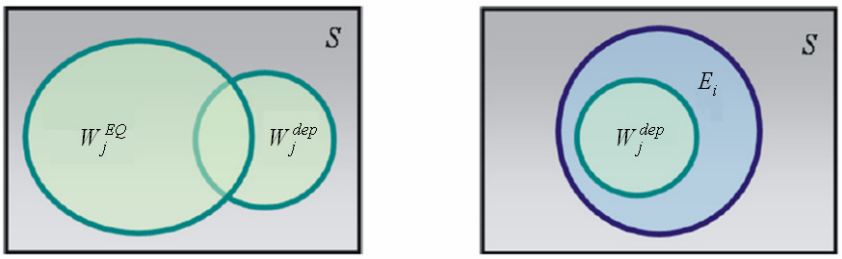

(a) (b)

Fig 6.4 Venn diagram: (a) failure of the water node and (b) conditional probability of failure of water node because of dependency on power network due to the power node failure

As far as $P\left(W_j^{dep}\right)$ is concerned, event W_j^{dep} will occur only after the occurrence of the failure of the adjacent power node denoted as event E_i . So, events W_j^{dep} and E_i are statistically dependent. The relationship among the probabilities of their occurrences is defined with the conditional probability that expresses the probability of event W_j^{dep} given the occurrence of E_i:

$$P\left(W_j^{dep} \middle| E_i\right) = \frac{P\left(W_j^{dep} \cap E_i\right)}{P\left(E_i\right)} \tag{6.6}$$

It is convenient for the analysis that it deals with the extreme case of the dependent events where one set contains the other (Poljansek, 2010). Therefore the intersection of E_i and W_j^{dep} is explicitly defined as $W_j^{dep} \cap E_i$ (**Fig 6.4.b**). In a similar way, it can express the probabilities of occurrence follow the **Eq. 6.7**.

$$P\left(W_j^{dep} \cap E_i\right) = P\left(W_j^{dep}\right) \tag{6.7}$$

Now, it can simplify the general Eq. 6.6 for conditional probability by considering in Eq. 6.7, which $P\left(W_j^{dep}\right)$ can be obtained by **Eq. 6.8**.

$$P\left(W_j^{dep}\right) = P\left(W_j^{dep} \middle| E_i\right) \cdot P\left(E_i\right) \tag{6.8}$$

Eventually, for the realization of the $P\left(W_j^{dep}\right)$, it needs to know $P\left(W_j^{dep}|E_i\right)$ and $P(E_i)$, and $P\left(W_j^{dep}|E_i\right)$ is defined as the strength of coupling $p_{W_j|E_i}$ written in the interoperability matrix. Setting the value of the strength of coupling can either be done by setting it to be equal for all the pump stations, or individually setting coupling strength for each pump station. In the first approach the strength of coupling reflects a general vulnerability of the water network to any kind of failures in the power network. While for the second approach, individual strength of coupling can reflect a vulnerability of each pump station to shortage of power supply. In this study, there is not sufficient information to set individual coupling strengths, and so it uses a single strength of coupling throughout, but which can be tuned from complete independence $P\left(W_j^{dep}|E_i\right)=0$, to complete interdependence $P\left(W_j^{dep}|E_i\right)=1$ (**Fig 6.5**).

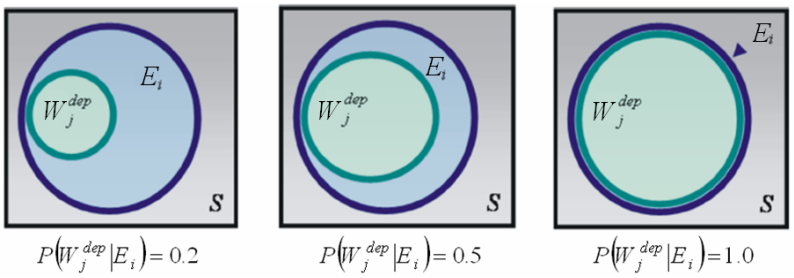

Fig 6.5 Strength of coupling in Venn's diagrams

In order to compute $P(E_i)$, it considers that the failure of the power electric node, event E_i, can be induced by an earthquake E_i^{EQ} or by the disconnection from the sources E_i^{CL}. So, event E_i is defined as the union of E_i^{EQ} and E_i^{CL}.

$$E_i = E_i^{EQ} \cup E_i^{CL} \tag{4.9}$$

In this way, $P\left(E_i^{EQ}\right)$ are determined from the elements' fragility curves for the seismic hazard. While disconnection of power nodes from the sources $P\left(E_i^{CL}\right)$ reflects the seismic response of the whole water network (**Fig 6.6**) and can be measured with the connectivity loss as the network performance criteria.

It is impossible to compute $P\left(E_i^{CL}\right)$ analytically because it is associated with the probability of failure of other components in the power electric network. But it can determine the probability of failure due to both causes $P\left(E_i\right)$ as a part of the seismic response analysis of

the gas network using the Monte Carlo simulation. For each power node adjacent to a water source node or pump station, the fragility curves are constructed in terms of connectivity loss and PGA. These fragility curves describe the vulnerability of the whole power source supply under seismic hazard while taking into account the whole topology of the power network as well. The power source supply failure is defined with exceedence of the damage state defined with the 80% of connectivity loss of the power node *i* that is adjacent to water pump station.

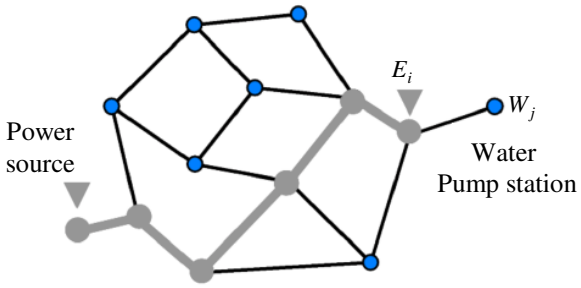

Fig 6.6 Schema of power source supply of the water pump station

Whenever the power node *i* fails because of the earthquake hazard (event E_i^{EQ}), the result of the simulation is 100% of connectivity loss for the power node *i*. When disconnection is the cause of the failure the connectivity loss of *i*-th power node is defined as **Eq. 6.10**.

$$C_L^{E_i} = 1 - \frac{N_{dam}^i}{N_{norm}^i} \tag{6.10}$$

where N_{norm}^i and N_{dam}^i is the number of sources connected to the *i*-th power node adjacent to water pump station in the original and in the damaged network, respectively. Both events E_i^{EQ} and E_i^{CL} can happen simultaneously since they are not mutually exclusive and it can be write $\left(E_i^{EQ} \cap E_i^{CL} \neq 0\right)$, but must not be considered twice (**Eq. 6.11**).

$$P\left(E_i^{EQ} \cup E_i^{CL}\right) = P\left(E_i^{EQ}\right) + P\left(E_i^{CL}\right) - P\left(E_i^{EQ} \cap E_i^{CL}\right) \tag{6.11}$$

Finally, the seismic performance of network can evaluate taking into account also the effect of the network dependency. $P\left(E_i\right)$ is completely determined with $P\left(W_j^{EQ}\right)$, $P\left(W_j^{dep} | E_i\right)$ and $P\left(E_i\right)$. With the Monte Carlo simulation of element failures, the dependent network fragility curves are constructed. In this study, two levels of random number generator in the

range 0.0 to 1.0 execute to define the damaged network. In the first level, the damaged vertices are defined due to the earthquake hazard checking if the random number is smaller than $P\left(W_j^{EQ}\right)$. In the second level, the damaged vertices are defined due to the dependency effect checking if the random number is smaller than $P\left(W_j^{dep}\right)$. The vertices whose failure arises by at least one of the two, above described, causes are eliminated.

The output from the Monte Carlo simulations consists of network fragility curves expressed in terms of performance measures which are described in chapter 5. Performance measures try to capture two important issues of the interconnected system. First, the response of the system exposed to the seismic hazard and then the influence of interdependency effect. In this study, the power electric network plays the role of independent network while the water network takes over the role of dependent network where the degree of coupling is regulated with the strength of coupling. In order to develop fragility curves for independent and dependent networks it is necessary to evaluate the network performance under several hazard levels and different strength of coupling.

6.4 Simulation Methodology

When the interdependency effect is included, one series of trials is characterized not only by the hazard level but also by the strength of coupling. Three different values of strength of coupling are considered to model the total independence $P\left(W_j^{dep}\middle|E_i\right)=0.0$, the partial dependence $P\left(W_j^{dep}\middle|E_i\right)=0.5$ and the complete dependence $P\left(W_j^{dep}\middle|E_i\right)=1.0$. In order to construct the damaged network the same strength of coupling is used for all water pump stations. Nevertheless, more detailed information were need on the response of each water pump station to the disturbances of the power electric supply, the value of the strength of coupling could performed on a station by station basis.

The results of the Monte Carlo simulations, i.e. performance measures of the damaged network under one hazard level and strength of coupling, are presented in statistical terms in the form of complementary cumulative distribution functions. For a certain damage state, one probability of exceedence for construction of the network fragility curves is obtained from each complementary cumulative distribution function. Network fragility curves are presented as the lognormal distribution function dependent on the maximum PGA in the network as the best fit to collected probabilities. In this way, three damage states of network, i.e. minor, moderate and extensive is employed, that are defined with the limiting value of the performance measure:

20%, 50% and 80% of connectivity loss (power loss or impact factor on the population), respectively. The probability of occurrence of each damage state is described by one network fragility curve. In the case of the power electric network 10000 Monte Carlo simulations were executed, whereas in the case of water network it is confined to 1000 simulations in one series of trials. This is because the water network has not only more vertices, but also more than five times more source vertices. For this reason, the computational capacity in the case of the analysis of water network is in greatly increased.

First, the seismic response the power electric and water networks are investigated as if they were independent. This is then followed by an additional analysis of the water network in order to obtain the fragility curves of the water source (this introduces the interdependency behavior). Afterwards, the results of the seismic response of the dependent water network are presented. Finally, the geographical spread of damage is visualized in terms of the water loss and affected population.

6.5 Bam Interdependent CI Simulation

The Bam power electric network has two types of vulnerable elements, power circuit lines (defined as links) and power substation (defined as node) as expressed in chapter 3. Probabilities of failure of the node element are always a reflection of the seismic hazard map. This is because the fragility curves of the vertices are mostly dependent on the PGA of the node location. The higher the PGA the higher the probability of failure calculated from the fragility curves for the same type of facility.

This is not the case for link elements, where the fragility is not only dependent on the PGA of the end vertices but also on the length of the links. Therefore, the links that are the most vulnerable to earthquake hazard do not appear only in the areas with the high PGA. This is because the majority of lines, which transport the flow directly from the sources to the areas of the high consumption, are long. In particular, the elimination of those connections in the damaged networks causes the fastest rise in the connectivity loss due to disconnection of the source nodes.

On the other hand, in the electricity network the vulnerability of nodes and link has been analyzed. But preliminary studies of this network's fragmentation show that link elimination is no more harmful than node elimination. However, it is the length dependency of the link fragility. Because as mentioned before, in this study it is assumed that the damage of electric power links is depend on their poles. In this way, each link is divided to 50-meter length

segments and considered that damage of pole is equal to damage of its related segment. Therefore the probabilities of the link failure could be much higher than those of node failure.

The dependent network in this study interconnected system is the water network. The influence of the strength of coupling on connectivity loss of water network is calculated as the performance measure of this network. Considering the interdependency effect, the fragility curves of the power source supply are used, which are calculated out of whole power network, but is extracted according to the water source nodes or pump stations under consideration. So, the set of fragility curves of the power source supply is the same irrespective of the analyzed water network. **Fig 6.7** clearly shows the consistent increase in system vulnerability as the strength of coupling grows. The extent of dependency effect is neither dependent on damage state nor the performance measure.

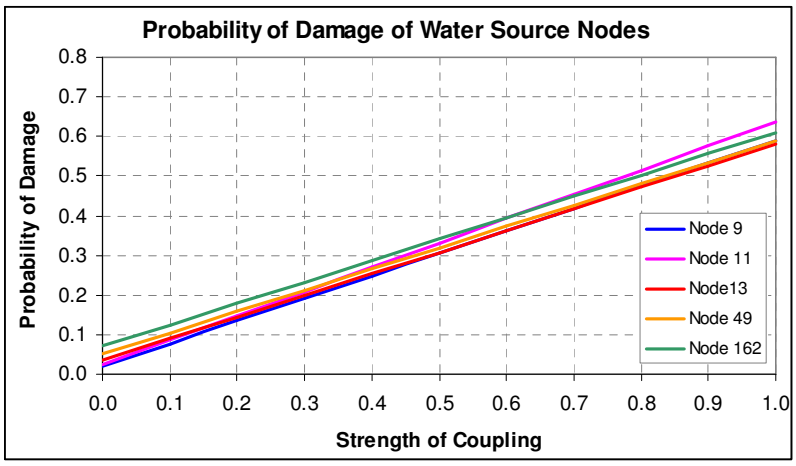

Fig 6.7 Probability of damage of the water source nodes vs. strength of coupling

Extreme values in the tail of the frequency distribution are rare, and as such tend to disappear in the averaging process when calculating the network performance measure. However, if the performance measures observed at the local level, those extreme values can cause anomalies. For example, there are distribution substations with high power loss but low impact factor on the population if the demographics have a scattered geographical nature. Such discrepancies among different performance measures are therefore geographically dependent. The connectivity loss analysis is done for strength of coupling 0.0, 0.2, 0.5, 0.8 and 1.0, and the results are illustrated in **Figs 6.8** to **6.13** respectively.

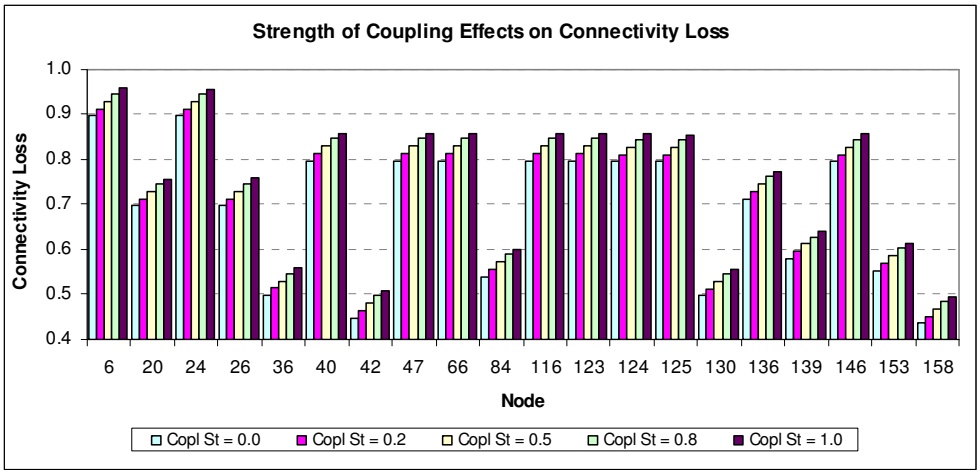

Fig 6.8 Probability of damage of the water demand nodes vs. strength of coupling

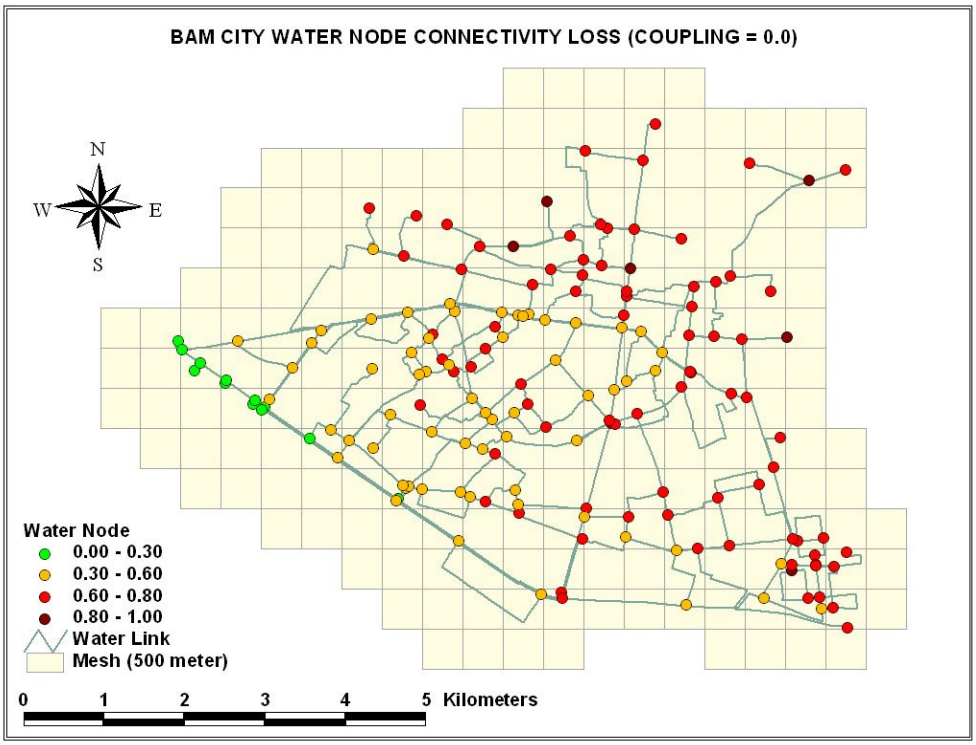

Fig 6.9 Probability of damage of the water demand nodes with 0.0 strength of coupling

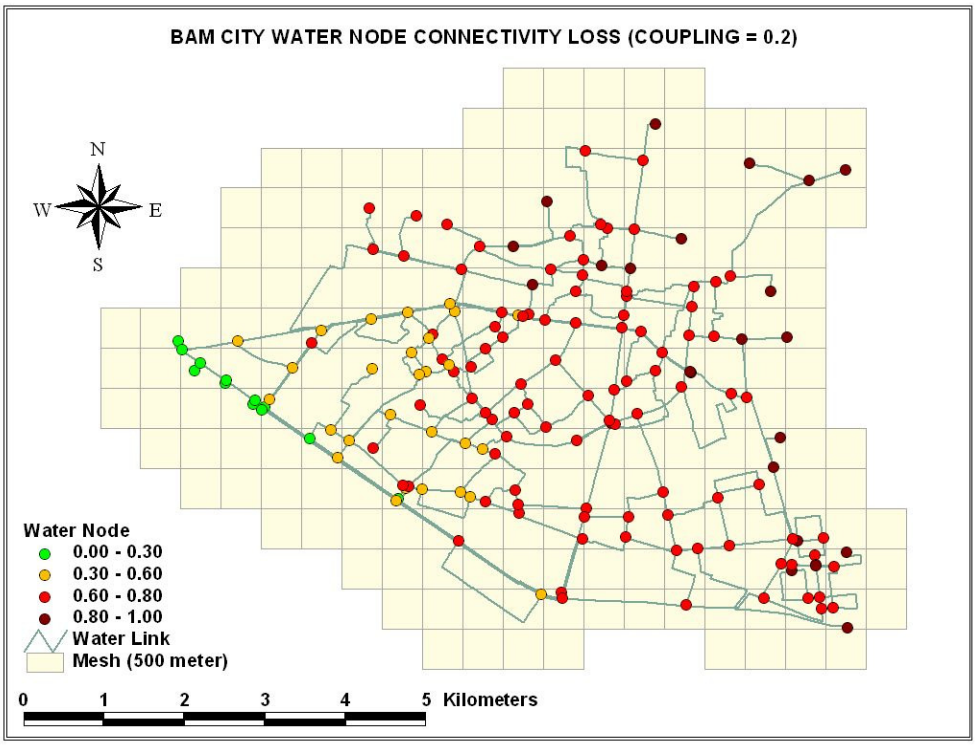

Fig 6.10 Probability of damage of the water demand nodes with 0.2 strength of coupling

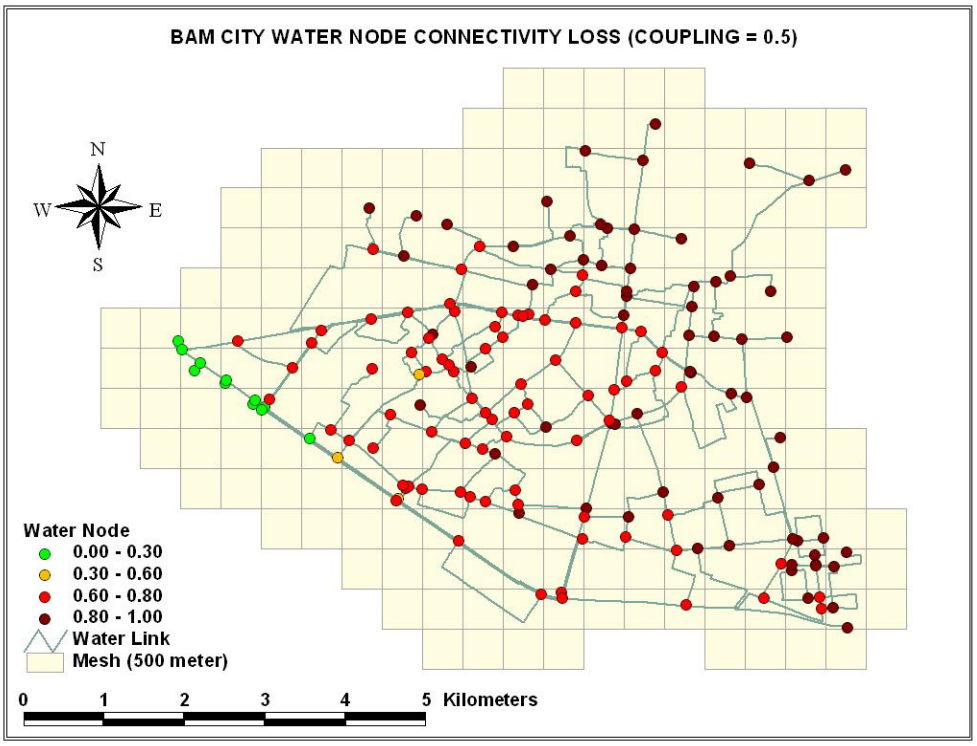

Fig 6.11 Probability of damage of the water demand nodes with 0.5 strength of coupling

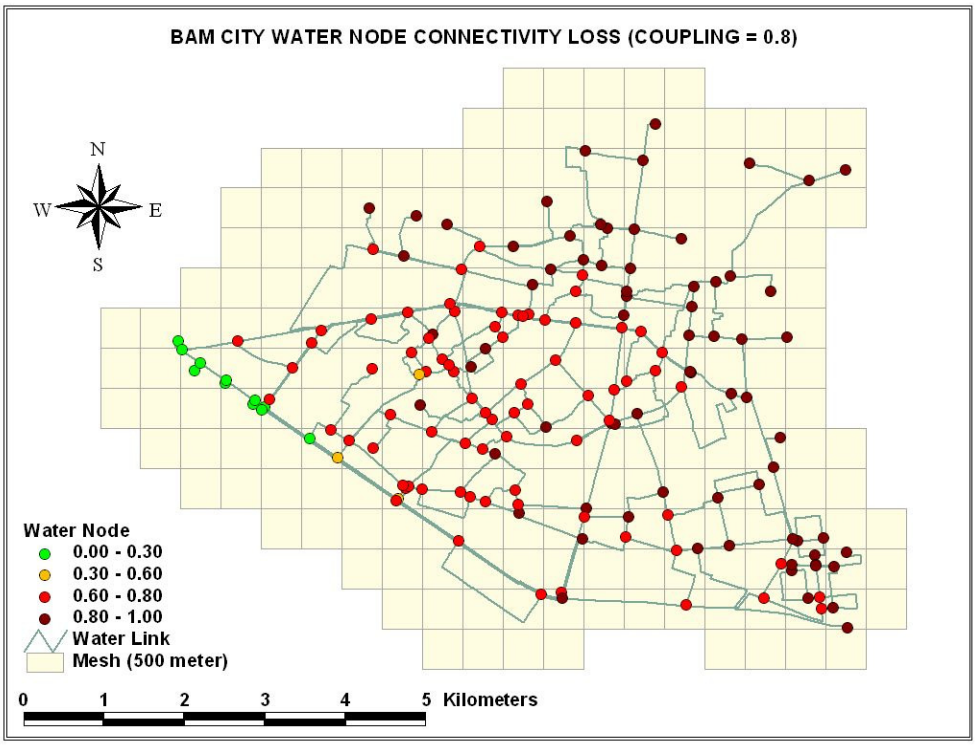

Fig 6.12 Probability of damage of the water demand nodes with 0.8 strength of coupling

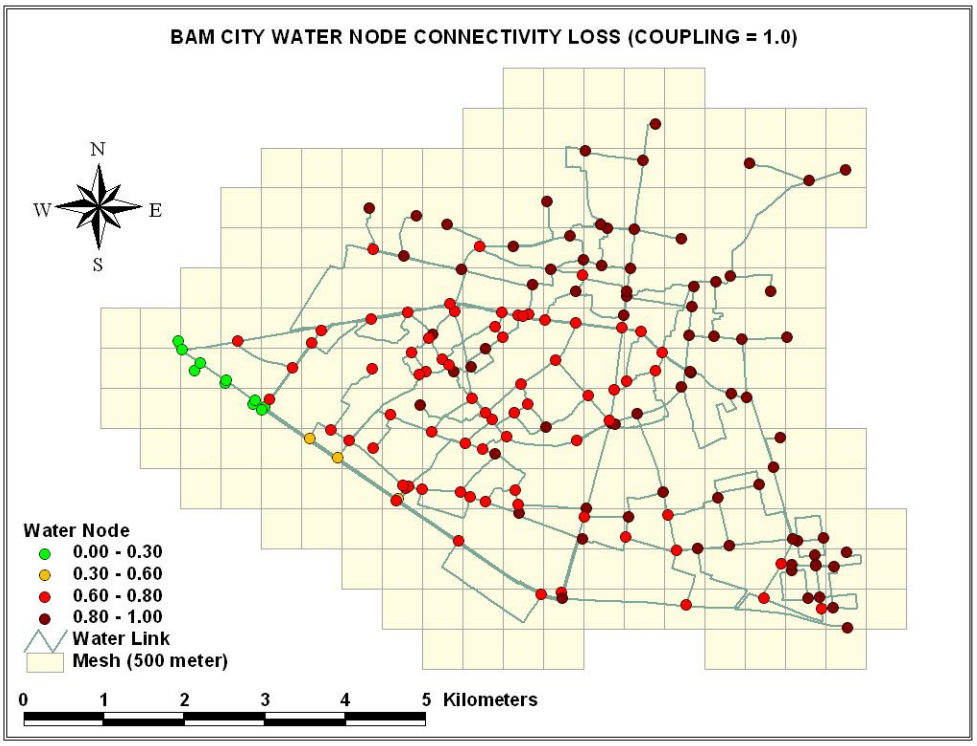

Fig 6.13 Probability of damage of the water demand nodes with 1.0 strength of coupling

6.6 Discussion about Results

This chapter began with an investigation of the dependency effect of power network on water network. It is found that the dependency effect introduces an extra vulnerability to the water network response under seismic hazard, but this effect is relatively small. This finding raises an obvious question, why is this influence so small? To understand the phenomena better it must be aware that the response of the system is strongly dependent on the topology of the individual networks and modeling of the interdependency behavior. There are probably more reasons for such results among which, physical interdependency, water source nodes or pump stations are in general one degree vertices, and in some case electric dependence water sources are a minor part of water source nodes.

In order to the first reason, physical interdependency, a question comes up that how intense is the propagation of earthquake induced damage in the power network on the water network? It would appear that it is certainly dependent on the quantity of the connection among the network. The larger the number of nodes whose functionality is closely dependent on the performance of the power network, the faster is the spread of damage that can be seen in higher connectivity loss. In our case only the water source nodes suffer the disturbances in power supply, which is dictated by the disconnection from the adjacent power node. Such a one to one connection is typical for the physical dependency that is characterized by slow damage propagation. If one were to define interdependency based on geographical proximity, then one node of independent network would influence more than one node in dependent network; in that case the propagation of damage would be faster and cause more extensive damage.

The second reason cites to the fact that the water source nodes are in general one degree nodes. One degree nodes have zero betweenness centrality. It is certainly true that the elimination of such node will not cause the fragmentation of the network in the sense of the increase in the number of components, but will raise the connectivity loss.

Since the connectivity loss measures the decrease in the number of sources reached by each demand node, it is obvious that failure of one source out of many will not cause a noticeable change. What about the node which has the highest betweenness centrality? Elimination of this node, which is on the path of many connections between the sources and the demand nodes can cause that certain demand nodes may be disconnected from more than one source at once. So, such an attack does, not only, quickly fragment the network, but can also cause a large increase of the connectivity loss. In the case of the earthquake hazard, more than one node is bound to fail and, statistically, most of these will have a value of betwenness centrality closer zero (**Figs 5.11** and **5.12**). Therefore, the elimination of the water nodes due to

earthquake failure can mask the increase of the connectivity loss due to interdependency, i.e., the failure of water source node or pump station because of the disturbances in the power supply.

Finally the third reason maybe refers to the fact that power network dependence water nodes are a minor part of water source nodes. The problem of elimination of the sources from the network it has already encountered in the power network. Power source nodes play a role in the power network equivalent to the water source nodes in the water network, but their disconnections due to the high probability of failure of the long power electric transmission lines cause high connectivity loss. The higher the proportion of the sources in the network, the smaller is the effect of failure of one source on the connectivity loss. In case of Bam city only one power source is available; therefore effect of failure of this source can cause high connectivity loss in power demand nodes spatially water network interdependent nodes.

6.7 Uncertainty and Sensitivity Assessment

The serviceability assessment of the water distribution and electrical power transmission systems is based on numerous assumptions and modeling parameters: the attenuation relationships for PGA and PGV, the local soil amplification factors for PGA and PGV, the spatial correlation of PGA and PGV, the water pipe break ratios and the fragility curves for the water storage tanks, the water pumping stations, the electrical power substations and backup systems. These modeling parameters affect the serviceability and the functionality ratios, and their selection contributes uncertainty to the results of the network analysis. Such uncertainties are classified into two types: aleatory uncertainty (inherent randomness) and epistemic uncertainty (knowledge-based uncertainty) (Ang and Tang, 2006).

6.7.1 Aleatory and epistemic uncertainties

The aleatory uncertainty arises from naturally occurring random factors. The aleatory uncertainty generally cannot be reduced through more information or data, but it can be estimated more accurately (with higher confidence) with additional information. On the other hand, the source of epistemic uncertainty is incomplete knowledge; such uncertainties can be reduced when more information is collected (Adachi, 2007). The epistemic uncertainty contains modeling uncertainty, which represents difference between the actual physical process and the simplified model used to predict the physical process, and parametric uncertainty, which represents uncertainty in the values of the parameters that are used in the model, respectively (Toro et al., 1997; Ang and Tang, 2006).

In seismic hazard analysis, a major source of aleatory uncertainty is the variability in the ground motion attenuation with respect to the estimated mean or median; this uncertainty is modeled by a log-normal distribution, as described previously. The uncertainty is represented numerically by the standard deviation or coefficient of variation of the probability distribution. On the other hand, the epistemic uncertainty can be depicted by an event tree model, which represents the different modeling assumptions and decisions made by the analyst. The branches extending from each node are assigned weights in such a way that they sum to unity. The weights are assigned by the analyst to reflect the relative confidence in each option.

6.7.2 Source of uncertainty

The case studies in the previous chapters included the aleatory uncertainties arising from the attenuation of seismic intensity from source to site and the fragility curves. Both uncertainties are modeled by log-normal distributions whose median values are determined by the attenuation relationships or the fragility curves. The log-standard deviation is defined to be 60% for the attenuation relationships and is set equal to the values for the fragility curves. The epistemic uncertainties due to the modeling assumptions made in the previous analyses can be analyzed by the event tree models.

In the process the event tree model for evaluating the PGA at a site, four steps are required. First, the scenario earthquake is determined. For the scenario earthquake-based seismic hazard analysis, the magnitude and the epicenter are assumed to be unique, and no other choice is considered. Second, the attenuation relationship must be selected. For the Bam city, at least six attenuation relationships have been proposed in chapter 4. The local amplification factors for the Bam city are taken from the FEMA, 2004 and Midorikawa et al. (1994). However the amplification factor proposed by the FEMA is more widely used for the seismic hazard analysis. The spatial correlation of PGA is characterized by the correlation length. The correlation length (km) is determined from the 0 km to infinity which implying perfect independence and dependence in ground motion intensity at two sites respectively.

Similarly, the event tree can use for evaluating the PGV at a site. Here, three attenuation relationships have been proposed for the Bam city. The other modeling parameters are defined as same as those for PGA.

In the modeling process the event tree for evaluating the serviceability ratio of the network, five steps are required. First, an infrastructure system is selected. Second, a set of fragility curves to support the system analysis are determined. For example, HAZUS (2003) provides the fragility curve for a water reservoir and pumping station. The ALA (2001) and HAZUS (2003)

developed alternate water pipe break ratio functions. Fragilities for specific electrical power substations have been developed by Pires et al. (1996), Ang et al. (1996) and Jin et al. (2002), Hwang and Chou (1998) and Dong and Shinozuka (2003); however, since these studies all focus on a specific power substation, only the substation fragilities provided by HAZUS (2003) are used. Third, for the seismic assessment of the water distribution system, whether the infrastructure interdependency effect due to electrical power availability is, or is not, considered is selected. Fourth, when infrastructure interdependency effect is considered, whether or not the power backup system is installed must be selected. Fifth, only the shortest path algorithm is used for the accessibility assessment method. The last three steps ("Power availability", "Backup system installation" and "Accessibility assessment") are not the sources of epistemic uncertainty. However, they are included in the event trees since they are necessary to complete the accessibility assessment of a water distribution system and an electrical power transmission system.

The weighting factor for each attenuation relationship is assumed. This assumption may be controversial. In any event, this assignment of weights can reflect the judgment of the analyst and allows variations in the serviceability estimates to be traceable directly to this assumption and subsequently revised, if necessary.

The mentioned serviceability assessment involves numerous modeling parameters such as attenuation equations for PGA and PGV, local soil amplification factors for PGA and PGV, correlation distance of PGA and PGV, component fragilities, and water pipe break ratios. Engineers and decision makers may wish to know which factors are the most influential on the serviceability or functionality ratios in order to select proper modeling parameters or to target investments in additional data acquisition or risk management.

6.8 Summary and Conclusions

For modeling the interdependency between critical infrastructures, two important issues of modern interdependent critical infrastructure systems are studied in this research. First the network response under seismic hazard is assessed; then the increased vulnerability due to coupling between networks is analyzed. The coupling behavior among networks is characterized as a physical dependency of the potable water network on the electricity grid through the water source nodes and pump stations. The dependence of one network on the other is modeled with an interoperability matrix, which is defined in terms of the strength of coupling; additionally it is considered how the mechanical structural fragility of the substations and poles of the electric power supply contributes to this dependence.

In a topological sense, the network interdependency model manages to follow the propagation of failures resulting from seismic vulnerability of the power network and how they affect the topology of the water network. The partial dependence of the water network on the power network introduces an additional implicit seismic vulnerability of the water network over and above the explicit structural seismic vulnerability of the components of the water network.

Network damage was measured in terms of connectivity loss, power loss and impact factor on the affected population. Damage was evaluated at both macroscopic (for the whole network) and at a local levels by examining the damage status of each and every water demand node in the water network. The seismic vulnerability of power and water networks, having been condensed in the form of fragility curves of the independent and dependent systems. Results is expected, that the highest direct damages are occurred in east and southeast of Bam city. However, this does not imply that the Bam power network is only locally vulnerable to seismic hazards. The results are used for the disaster management of interdependent network activities spatially in restoration process modeling in next chapter.

CHAPTER 7

DISASTER MAMANGEMENT OF INTERDEPENDENT CRITICAL INFRASTRUCTURES

7.1 Introduction

Disaster risk management seeks to comprehensively reduce the disaster risk to which people are exposed in disaster-prone regions. The top priority is to reduce the population's vulnerability to earthquake, floods or storms, and prevent the emergence of new risks (Kohler and Schaef, 2004). Risk management is a systematic management of the process exposures to achieve its objectives in a manner consistent with public interest, human safety, environmental factors, and the law. It consists of planning, organizing, leading, coordinating, and controlling activities undertaken with the intent of providing an efficient pre-loss plan the minimizes the adverse impact on risk on the organization's resources, earnings, and cash flows (Tusler, 2005).

Risk management comprises two key elements: risk assessment and risk control. Risk assessment can take place at any time during the implementation of a project, though the sooner the better. However, risk control cannot be effective without a previous risk assessment. Similarly, most people tend to thing that having performed a risk assessment, they have done all that is needed. Far too many projects spend a great deal of effort on risk assessment and then ignore risk control completely.

A city can be easily considered as a system which can be studied from several points of view. It can be seen as a place of heterogeneous groups of humans congregating, a place of living, a place of economic, cultural, and administrative activities, and a place of power and decision-making (Ancas et al, 2006). It is a place that also provides a certain number of services and occupies a specific place within a given geographical and decision-making environment. It is place where different systems converge, assuming specific shapes, and marking the urban identity and image, by radiating its influence.

Urban development and functioning are dependent of a numerous internal relations between its urban components spatially critical infrastructures. The damage caused by an earthquake to the same elements of risk in two different cities, will not create the same disruptions and consequences for the whole system. The corresponding impact of the disaster will depend on internal and external relationships, and possible functional substitutions of damage elements. This means that the risk analysis must not only consider the vulnerability of

elements at risk (**Figs 7.1 and 7.2**), but should also assess the failure and resistance chains due to interdependency of the main functions, activities, decision making, and human behavior in an urban system. Thus, a city is the place of numerous social, economic, political, and physical exchanges (Atanasiu, 2006). The urban system is not only dependent on inner flows, but also on its external environment and relationship at regional, national and international levels.

7.2 Outline of Critical Infrastructure Protection Countermeasures

On the bases of better understanding of seismic behavior of critical infrastructures spatially lifelines, earthquake countermeasures have been developed and implemented in actual systems by many lifeline sectors (Kameda, 2000). Earthquake countermeasures for lifelines are aimed at abating outcome of an earthquake; specifically, they are;

- ✓ Preventing and mitigating physical damage,
- ✓ Minimizing service malfunction,
- ✓ Mitigation of secondary disasters, and
- ✓ Executing an expeditious recovery.

To realize these objectives, various disaster mitigation measures have been established, which may be classified in the following four categories:

- ✓ Upgrading structural performance of network components such as pipelines, liquefaction, fault offset, structural interface.
- ✓ Improvement of network organization including redundant systems, fault-crossing elements.
- ✓ Implementing system automation such as shutdown valves, automated backup generators.
- ✓ Disaster operation under earthquake emergency which consist of block separation systems, information management systems, monitoring systems, mutual-aid agreements, expert systems.

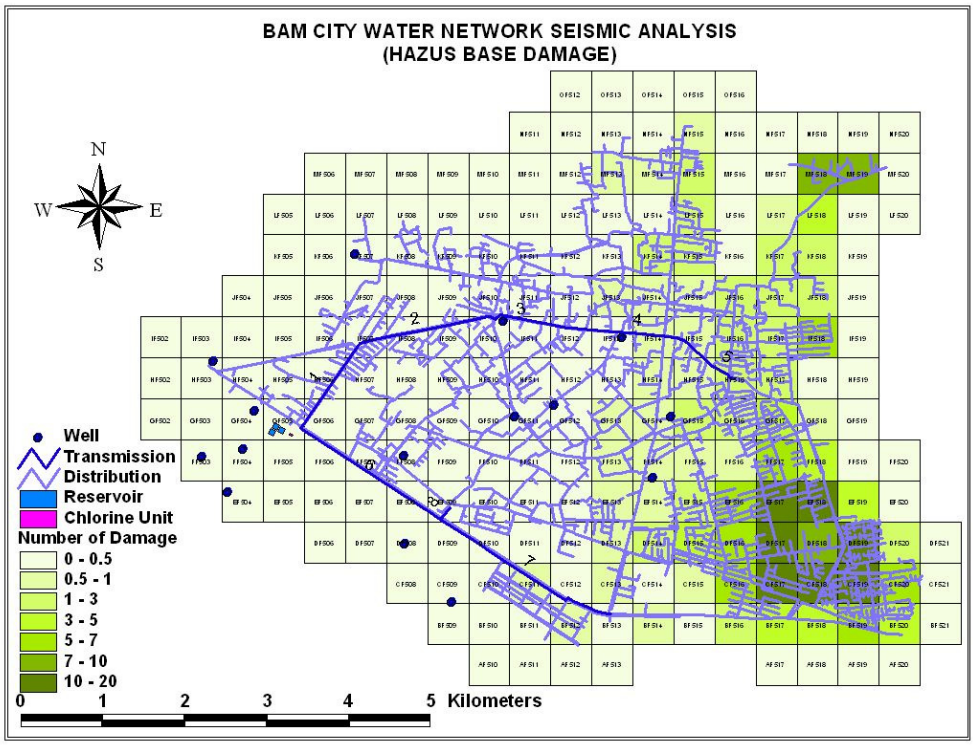

Fig 7.1 Bam potable water network (number of damage in each mesh)

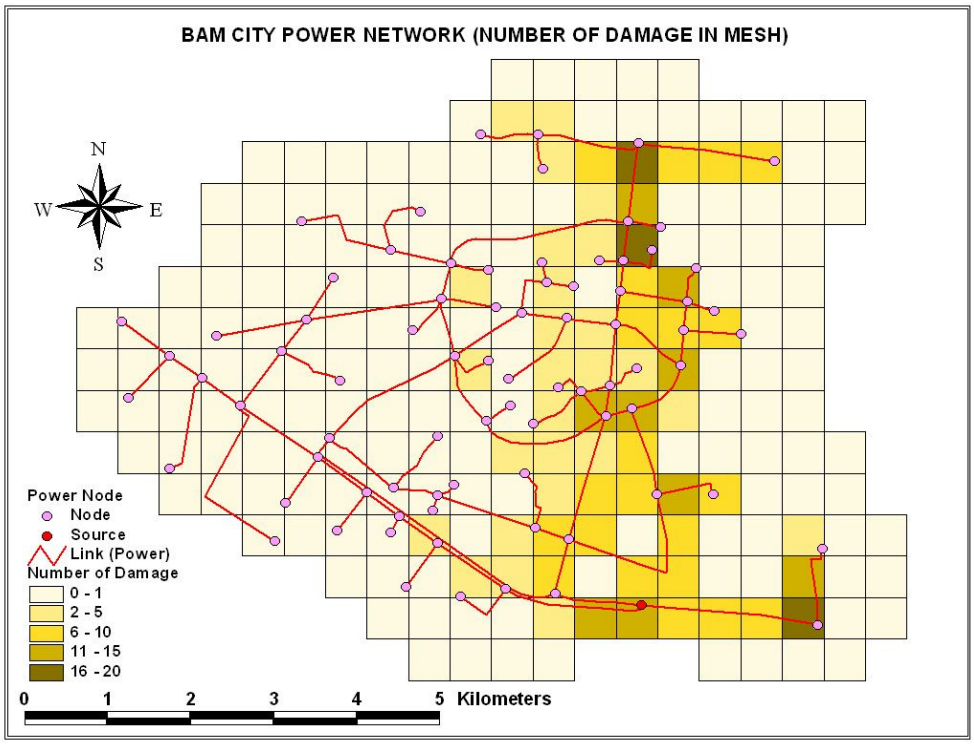

Fig 7.2 Bam electric power network (number of damage in each mesh)

On which categories of these four emphases are placed depends on the system characteristics of individual infrastructures. It is noted that the set of earthquake countermeasures are the consequences of basic studies in lifeline earthquake engineering as well as creative technology developments in the each lifeline sectors and related industries. Their typical examples are found in the development of ductile iron pipes with earthquake proof joints, construction of redundant networks, zonal block separation for isolation of damaged networks, installation of earthquake monitoring for effective emergency shutdown and operation, implementation of expert systems to aid post-earthquake operation, etc.

7.3 Critical Infrastructure Restoration Models

As mentioned before, following an earthquake, loss of infrastructure system functionality can significantly disrupt normal economic activity. The duration of this loss of service is a critical determinant of the ultimate magnitude of economic disruption. It can especially affect, for example, business interruption and indirect economic loss. Quantitative models of the post-earthquake restoration process, therefore, are important in evaluating the total economic loss caused by an earthquake.

Different approaches have been used previously in modeling post-earthquake lifeline restoration. The first method is based on statistical restoration curves. The other empirical approach is based on resource constraints. There also exist more theoretical approaches, such as, the Markov process approach and the network approach. The latter is mainly used for developing optimum restoration strategies. The basic goal of all these approaches is to develop a curve or curves that represent the functionality of a lifeline system versus time. Each of these approaches is explained in more detail below.

In the statistical restoration curves approach, data obtained from previous earthquakes and/or from expert opinion are employed to fit restoration curves. This approach has been used in previous studies, such as, ATC-25-1 (1992), Chang et al. (1996) and Nojima et al. (2001). In ATC-25, restoration curves are constructed by using data sources excerpted from ATC-13 (1985) that are based on regression analysis of expert-opinion data obtained through an iterative questionnaire process. In Nojima et al. (2001), Gamma distributions are used as restoration curves and parameters of the distributions are estimated as a function of damage level using data from previous earthquakes. Nojima et al. (2001) enables breaking down the single “system restoration curve” into many restoration curves depending on seismic intensity, and hence, spatially disaggregates the restoration process. In the statistical restoration curves approach, the primary determinant of system restoration time is ground shaking intensity. Issues such as

personnel constraints and opportunities to reduce losses by speeding up or optimizing restoration are not considered (Chang et al., 1999).

In the deterministic resource constraint approach, the evolution of the restoration is modeled in a simplified way. The number of repairs that can be made in any time period is specified according to the number of repair personnel available. This approach allows depiction of restoration progress across both time and space, and enables exploring earthquake loss reduction in a variety of new directions, such as, speeding up total restoration times, prioritizing spatial sequencing of restoration, and developing mutual aid agreements (Chang et al., 1999). This approach has been employed in Isumi and Shibuya (1985), Ballantyne (1990), HAZUS – water distribution system section (NIBS 1997), and in Chang et al. (2002). In these studies, restoration processes are modeled deterministically, so the uncertainty associated with expected restoration time is not estimated. It has also been assumed that restoration processes involve only the repair phase. However, restoration processes are more complex than that in reality; they include phases such as damage assessment, and initial inspection as well.

Hoshiya (1981) and Isoyama et al. (1985) model an individual lifeline's functional performance in the post-earthquake period using discrete-state, discrete-transition Markov processes. In later studies, such as Kozin and Zhou (1990) and Zhang (1992), a discrete-state, discrete-transition Markov process is employed to model evolutionary restoration process of various lifelines together as a system. Zhang (1992) takes into account the effects of interactions between various lifelines as well, by considering the transition probability of each subsystem not only as function of allocated resource but also as a function of the states of other subsystems. The Markov processes approach requires that the model parameters and probability values are estimated accurately. Even if adequate databases are established for this purpose, converting available data into model parameters and probability values can be a real challenge.

In the network approach, a system consists of a supply node and a number of demand nodes. These are connected to each other via links that can be damaged or fully functional. In Nojima and Kameda (1992), graph theory (Minimum Spanning Tree and Shortest Path Tree) and optimization theory (Horn's Algorithm (Horn 1972)) are combined to develop an optimal restoration plan. In Okumura (1994), the proposed optimal repair sequencing method is based on the connectivity of a tree-shaped network and involves simplified flow analysis of the network as an approximate global optimization strategy. The network approach enables both spatial and temporal desegregations of restoration processes and consideration of the effects of resource constraints. The main disadvantage is that the system and restoration process have to be simplified to be able to model the evolution of restoration with this approach.

7.4 Critical Infrastructure Restoration Analysis

As noted earlier, infrastructure service provides the key link between the infrastructure system and the economy in the model. Economic loss depends not only on initial service outage of network but also on the duration and spatial pattern of restoration. The restoration model usually simulates repair progress over the restoration period according to specified algorithms. A resource constraint approach is adopted in the restoration model, and this specifies the number of repairs that can be made in any time period according to the number of repair personnel available. The damage state *d* (damaged or undamaged) for element *i* at time *t* can be characterized as **Eq. 7.1**.

$$d_i(t) = R[d_i(t-1), n(t-1), \rho_u, h_i] \tag{7.1}$$

where *t* is the time period index (in weeks), *R* the repair and restoration function, *n* the number of repair personnel available, ρ_u the repair rate for damage type *u* (in worker-days per repair), h_i the repair priority assigned to element *i*.

The damage state of element *i* at time *t* depends upon the damage state in previous time period and whether or not the element got repaired. The latter depends upon how many repair workers were available in the previous time period, the number of repairs each worker can make in a week and the priority of element *i* in repair sequence.

Note that the worker-days per repair vary with type of damage. Specifically, repairs to large pipes require more worker-days than do repairs to smaller pipes. Model parameters are based on a survey of previous lifeline restoration models and data from the Kobe earthquake (Chang et al. (1999), Takada et al. (2003)). In case of water network, pipes of diameter greater than 20 inches are assumed to require 14 worker-days to repair if damaged, and smaller pipes are assumed to require 2.5 worker-days. Another study which is done by Koike (2006), it is assumed that the restoration team can repair two damaged pipeline joints per day. It should be given that pre-disaster mutual maneuvers between main and its backup cities are very useful and can increase the number of repairs by each worker in day and decrease the restoration time consequently.

Following HAZUS, the number of repair workers available is assumed to be 0.02% of the county population. These numbers would undoubtedly be somewhat variable in an actual disaster. As seen in the Northridge earthquake and in other events, worker-days per repair could vary according to damage circumstances as well as financial incentives for speedier work. The number of workers would depend on such factors as temporary in migration of labor, timeframe

after the earthquake, and mutual aid agreements that the responsible company had established with other utility agencies.

The parameters n and ρ in Eq. 7.1 dictate the total number of repairs that can be made in any time period. Repair priorities h determine which damaged elements are actually repaired in that time period. The restoration model specifies the repair sequence on the basis of engineering priorities and observations from the 1995 Kobe and 1994 Northridge earthquakes. Specifically, in case of water network, any damage to large pipes (diameter >20 inches) is repaired first, in order to bring the transmission backbone of the system online before repairing service pipes. But based on functionality criteria, damaged nodes and links with high betweenness ratio should be selected as first priority for repair. The restoration of smaller pipes then occurs in spatial sequence, from census tracts with the least amount of damage to those with the highest. Initial damage patterns are updated on a weekly basis until repairs have been completed. At each weekly interval, system flow or connectivity analysis is conducted on the updated network and flow ratio results for each node i are updated.

7.5 Restoration Model of Bam City Critical Infrastructures

The 2003 Bam earthquake mainly affected power and water networks in the epicentral regions. The earthquake causes total 467 damaged points in water network and 495 damaged points in power network. Most of damaged points are located in east, south east of Bam. In order to basic concepts of disaster management and for restoration analysis, Bam city is divided to eight restoration zones (**Fig 7.3**) based on the topology of the city. It should be mentioned that usually the boundary of these zones are the main streets which are the same as water company sub regions boundary or districts of municipality and ward office limits.

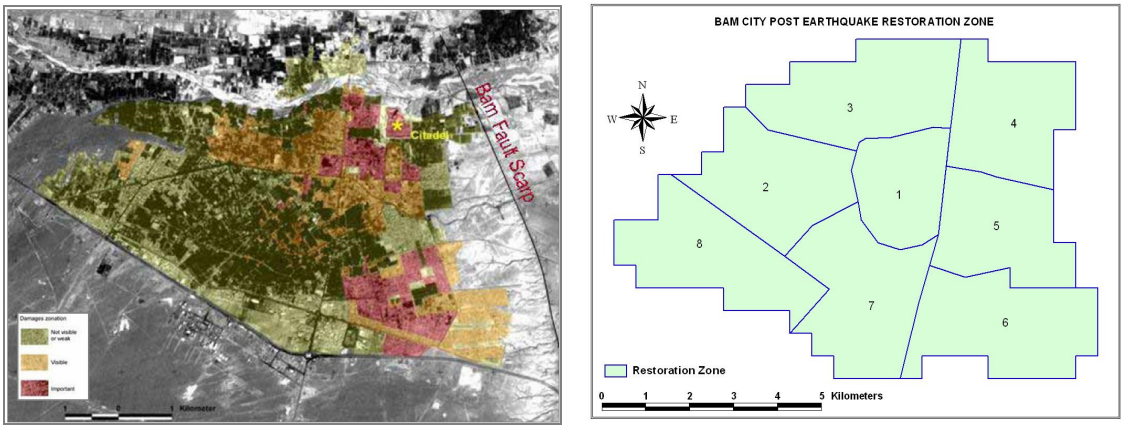

Fig 7.3 Bam city topology and post earthquake restoration zones

7.5.1 Water network restoration model

There are 467 damaged points in water links. Most of these damages are occurred in small diameter asbestos cement pipelines in east of Bam. However the main distribution 20-inch steel pipelines are damaged in 3 points. These pipelines connect the water source nodes in west Bam to the city center pass through south east and center of city (**Fig 7.4**). As mentioned in last section, in water network, pipes of diameter greater than 20 inches are assumed to require 14 worker-days to repair and smaller pipes are assumed to require 2.5 worker-days.

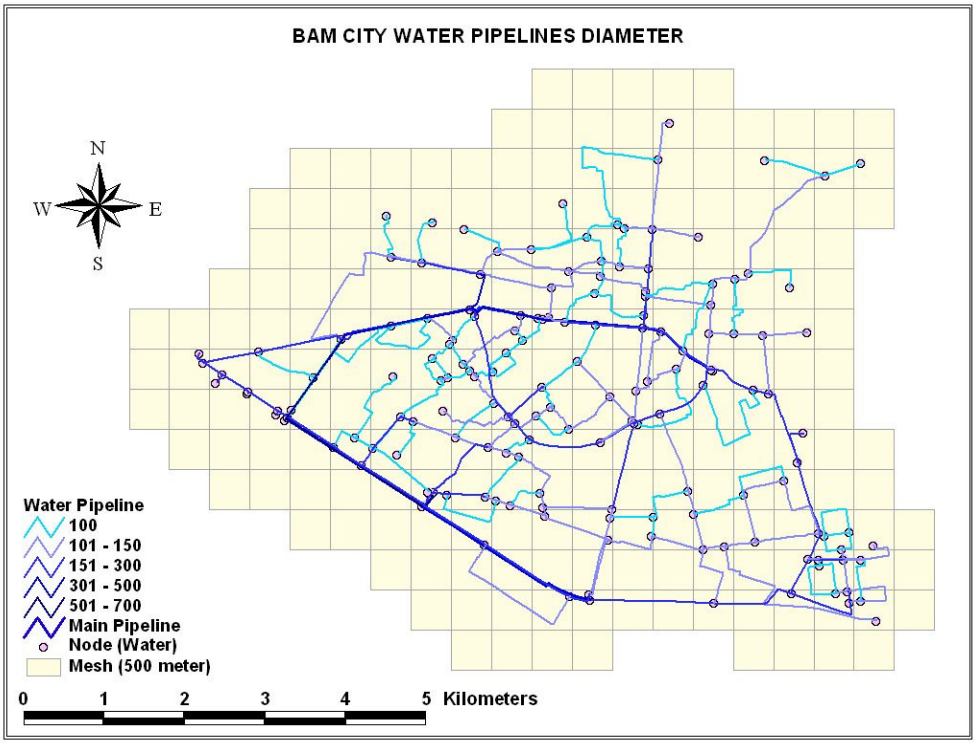

Fig 7.4 Bam city water pipelines diameter and main 20-inch pipelines

In ideal situation, the numbers of workers who can repair main pipelines and also all small diameter pipelines in a day are 70 and 185 respectively. But manage this amount of man power during the disaster period is very difficult, or to better express, it is impossible. Because they need accommodation, food and above all tools and utilities for pipeline repair. However, regardless of all these cases, finding these numbers of skill workers who are dominant to the city water network is not easy during the disaster spatially earthquake.

Therefore, in fact the limited numbers of skill workers are available or dispatched from backup cities. Following HAZUS, the number of repair workers available is assumed to be 0.02% of the city population, which in case of Bam with population of 92800, the number of available repair workers is predicted about 18. But in fact, there were only 2 water repair

workers in Bam just after the earthquake because numbers of workers or their relatives are died or injured and because of that they were absent in restoration period. So it is assumed that 36 workers are dispatched from backup cities of Bam. The restoration analysis is done by the assumption. The number of water pipeline damage in each restoration zone just after earthquake is shown in **Fig 7.5**.

7.5.2 Pawer network restoration model

There are 495 damaged points in power network which 50 damages out of them is occurred in power nodes (aerial transformers) and 445 in the links. Most of the link damages are occurred in main distribution poles those are power link representatives. Same as the Bam water network, most failures of power networks are happened in the east of the city. However the main 230/132 kV Bam electric power substation is heavy damaged because of near field effects. But the main transmission lines didn't have any damages. The number of networks damage in each restoration zone just after earthquake is shown in **Figs 7.5** and **7.6**.

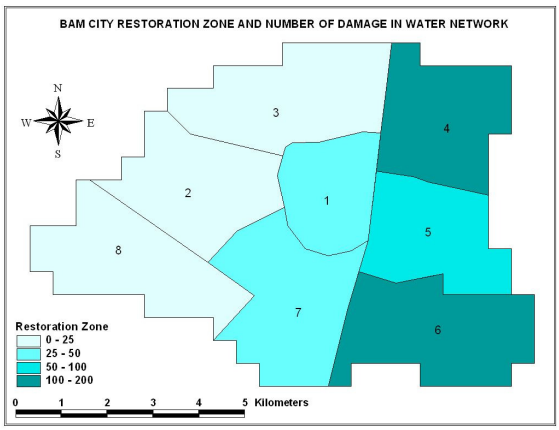

Fig 7.5 Number of damage in water network

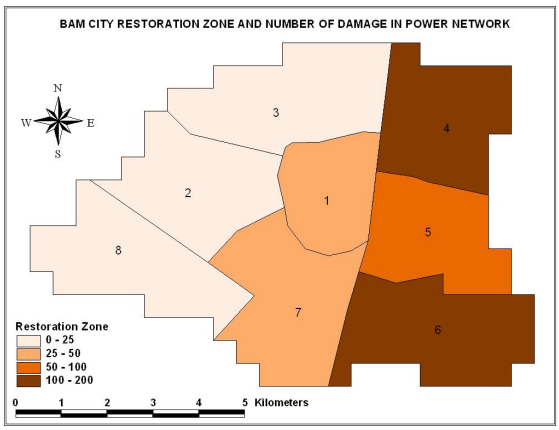

Fig 7.6 Number of damage in power network

In order to restoration model of bam power network, damage for aerial line (pole) is considered as basic index. The efficiency of repair work for the damage against this aerial line is supposed below and required repair worker man for 0.4 kV class and 20 kV class is supposed as equal. But the required worker for the repair work for aerial transformer is supposed as 30% large of the repair work for aerial line (TREC 2006). So, in calculation, one damage for aerial transformer is counted as 1.3 damages for 0.4kV line. In the district where heavy building damage occurs, collapse of building becomes obstacles for restoration work. Therefore, in the district that the rate of major building damage exceeds 50%, number of the damage is assumed 30% larger.

Required number of workers for restoration work of aerial line (pole) was supposed as follows by considering same calculation of Kansai electric company (ADEP 1986).

- ✓ Number of workers per team: 6 workers
- ✓ Time necessary for one damage: 7.3 hours
- ✓ Working hours per day: 16 hours

So it is assumed that 40 power repair workers are dispatched from backup cities of Bam.

There are two cases of strategies for selecting restoration target district. If there are one or more unfinished districts around finished district, first priority for rescue is placed on the district contains maximum number of unfinished damage (Case A) and on the district contains minimum number of unfinished damage (Case B). It means latter policy is giving priority for increasing the number of districts resumed.

The spatial patterns of water and power outage severity are shown in **Figs 7.7** and **7.8** respectively**.** The figures are illustrated for the initial damage state and after one week of repairs have been completed for the Bam power electric network and 3 months for the Bam potable water network.

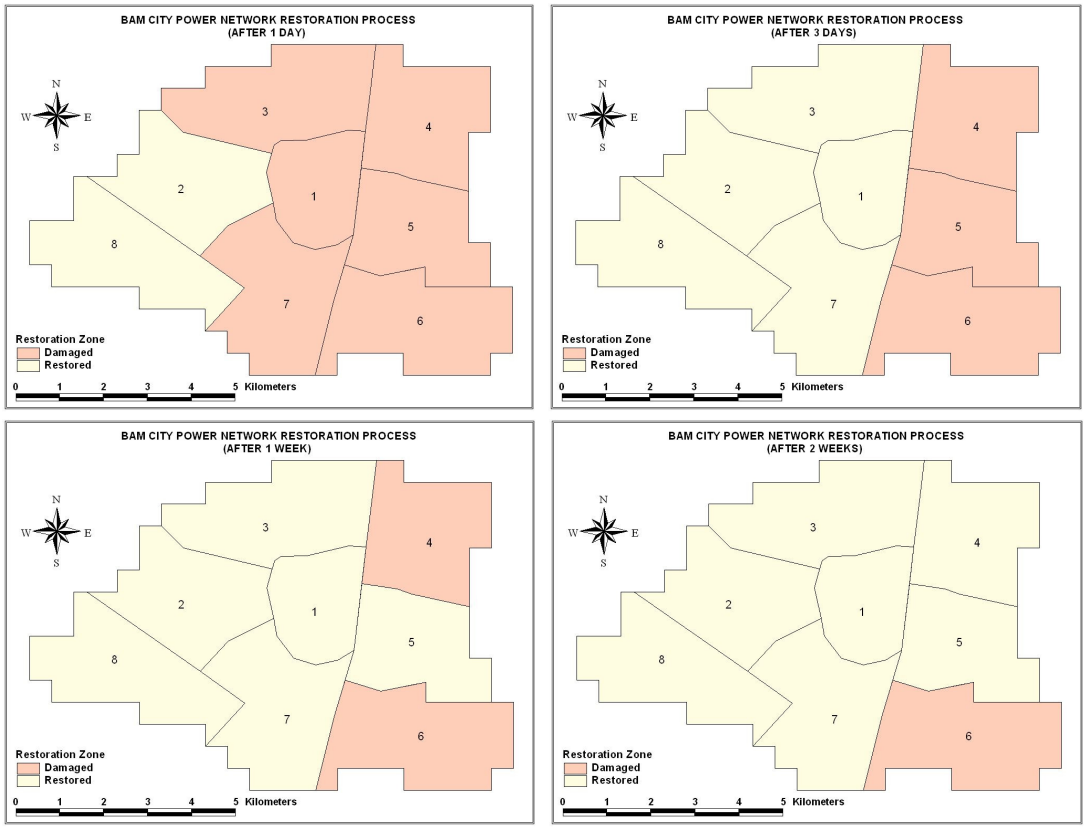

Fig 7.7 Bam city power network restoration process (from first day to 3 weeks)

It is mentioned that because of interdependency effect, the restoration period of water network should be add to the restoration time of main electric power substation and interdependent path between power source to water sources. As mentioned in chapter 2, the main substation is heavy damaged and 3 and 21 damaged occurred in nodes and links of the interdependent path (equally 25 damages).

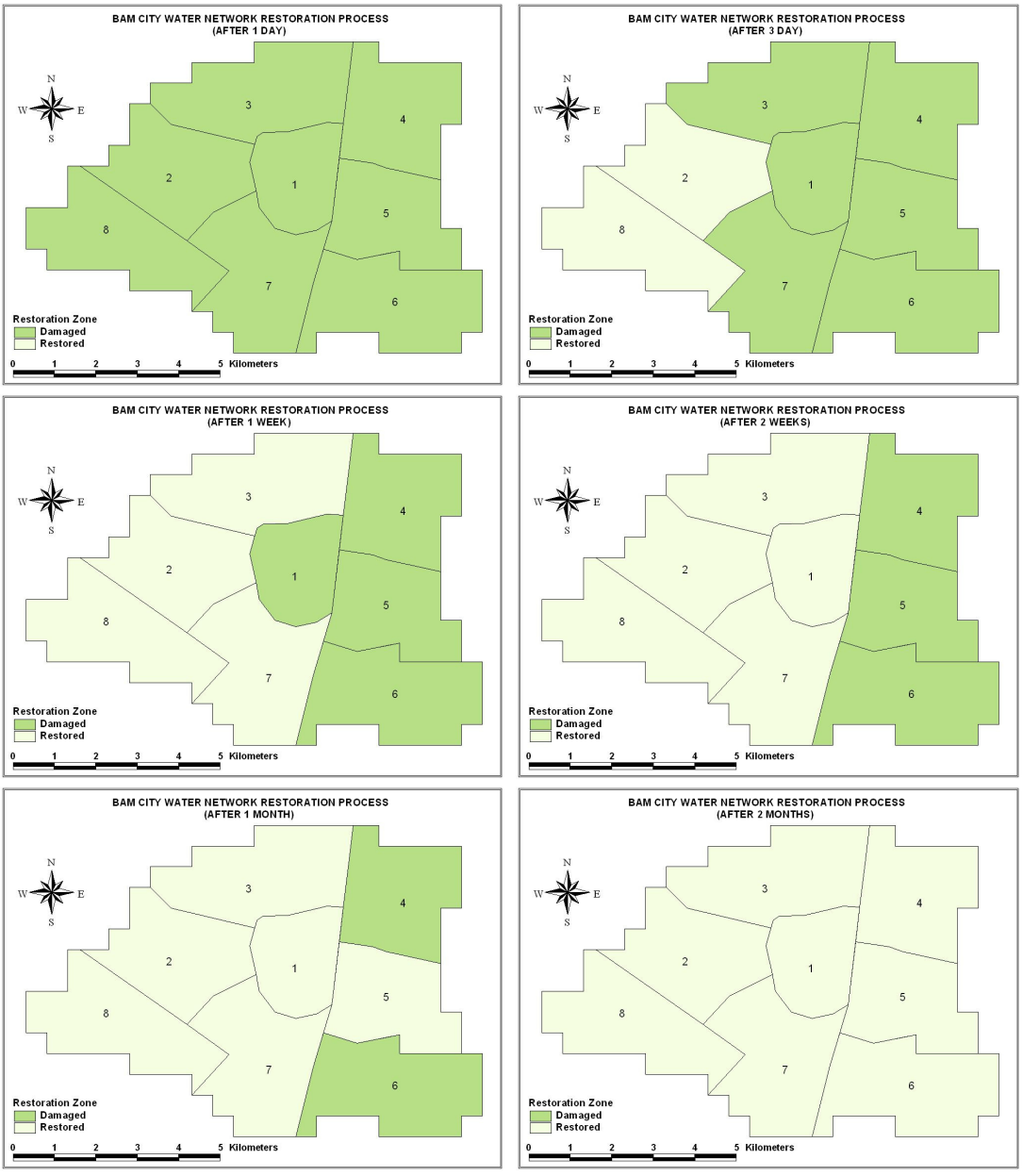

Fig 7.8 Bam city water network restoration process (from first day to 3 months)

Although the restoration function adopted here is reasonable given experience in recent urban earthquakes, it should be noted that other restoration algorithms could also be simulated.

For example, one alternative could seek to minimize employment losses by giving priority to those sub areas that utilize the lowest amounts of service, directly and indirectly, per worker (Rose et al, 1997). Another alternative would be to give highest priority to restoring service in eastern Bam.

7.6 Critical Infrastructure Acceptance Criteria

The structural performance of a group of a large number of components is shown in constitute fine lifeline networks are evaluated by using *fragility curves*, while critical components should be evaluated by event tree, fault tree and reliability assessment for individual subsystems. For the post earthquake recovery phase, *restoration curves* are common tools for overall post event system performance evaluation, and engineering measures for supply to critical facilities under earthquake emergency are key factors for dealing with specific lifeline components. A practical criterion is how to minimize the area above the restoration curve within constraints of resources for post earthquake activities.

It should be noted the target reliability for earthquake protection of lifelines cannot be determined only from engineering measures. Questions are often raised from lifeline engineers that a rational basis should be provided by which post earthquake performance of lifelines can be evaluated in a way that societal consensus or acceptance is realized. To do this, it is indispensable to incorporate evaluation of lifeline performance in an appropriate manner from the users' side.

The conceptual illustration of a scheme to evaluate users' inconvenience under lifeline disruption is shown in **Fig 7.9** (Kameda, 1994). In this context, it is also used restoration curves, but it needs restoration curves for various levels of lifeline services. Conventional restoration curves are normally defined as the time variation of the proportion of the served section in entire service area, where the situation is judged from served or not served. It should be noted that considering different levels of service will lead to different restoration curves.

Consider a case of water supply. It may classify the levels of water supply into the following typical cases.

- ✓ 3 litters per capital per day (*lcd*) is specified as a minimum standard of water supply under disaster emergencies. In the Japanese post-earthquake activities, local governments conduct emergency water deliveries aimed at supplying at least this amount of water.
- ✓ 10-100 *lcd* is said to be a minimum requirement to be able to cook foods and prepare daily meals. This level is considered as a target of supply during the second stage of restoration.

- ✓ In the third stage, water supply is aimed at delivering 100-180 *lcd*, which is not enough for normal activity levels but basic demands are met.
- ✓ Then, finally, normal levels are to be recovered at which water consumption in Japanese urban regions is 200-400 *lcd*.

These four levels may be typically defined as the corresponding service levels, level 0 to level 3, respectively, and corresponding restoration curves for these levels can be considered and corresponding restoration curves can be drawn as in **Fig 7.6**.

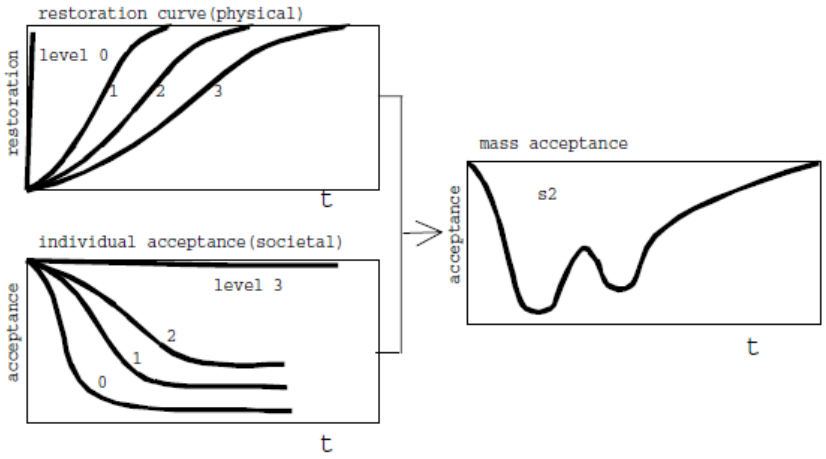

Fig 7.9 The conceptual illustration to evaluate users' inconvenience under lifeline disruption

While these restoration curves are an engineering measure, the users' perception of lifeline disruption may be represented by the time variation of the degree of acceptance. People can stand lifeline disruptions for some period immediately following the earthquake. But as a reduced level of supply is sustained, their demand will increase and the individual users' *acceptance curve* decreases with time, and converges to a certain lower level. The speed of decrease and the reduced level of convergence would be different for different service levels. It is emphasized that the acceptance curves should be understood as a measure not only of lifeline users' physical environments but also their psychological situations (Kameda 2000). Therefore, definition of the acceptance curves must be done on the basis of a rational combination of evaluations both from engineering and social psychology.

Once the restoration curves and the acceptance curves are defined for various service levels, the rate of acceptance or the *overall acceptance* by the people in the entire service area, denoted by $D(t)$ can be defined as the weighted mean of these curves as **Eq. 7.2**.

$$D(t) = \frac{\sum_i R_i(t) \cdot A_i(t)}{T_P} \tag{7.2}$$

where $R_i(t)$ is restoration curve at service level *i*, $A_i(t)$ individual users' acceptance curve, and T_P duration of the total post-earthquake period. The summation is performed for all supply levels at time *t*.

The overall acceptance curve is a single curve that can be used as a comprehensive measure of evaluation of post earthquake performance of lifeline systems. The area of the section above the overall acceptance curve $D(t)$ and below the horizontal line of unity may be used as a utility index of lifeline performance incorporating users' evaluation. In case of Kobe water network in earthquake 1995, a very long period of time, 82 days, was needed for recovery of water supply. The experience was quite severe if compared to the cases of other earthquakes. For this reason, the time needed for functional restoration played a role of a quantitative index for measuring water customers' difficulties coming from sustained water loss, which are basically qualitative or judgmental issues. An evidence this situation is reflected is seen in the telephone calls from individual customers to the Municipal Water Supply Headquarters that were made throughout the restoration period (Matsushita, 1999).

There were a total of approximately 2,400 calls. The number of calls per day generally decreased with time, as restoration works progressed and the total number of people without water supply decreased. In contrast, the number of calls per day normalized by the number of customers without water remained nearly constant during the first four weeks of restoration period, and increased drastically after four weeks had passed. This demonstrates that the people who had to spend more than four weeks without water had excessive difficulties of leading their lives. Indeed, the contents of conversation in these calls varied from those of inquiry type in earlier stages to strong complaint, anger and desperation in the post four week phase. On the basis of this experience, the Kobe Municipal Waterworks Bureau has established a long term reconstruction plan for its system in a way that emergency recovery to all customers should be finished within four weeks under any heavy urban earthquake disaster. Construction of redundant and robust transmission and distribution networks is the major feature of the reconstruction plan. So, the quantification of the users' acceptance level can be a feasible concept. By doing so and combining them with engineering technology, it is expected that reasonable framework and methodologies be established for general risk management of lifeline systems under earthquake environment.

7.7 Emergency Water Supply Plan

The target of emergency water supply after earthquake is that 3 litters of water shall be supplied at every 1 km to all the people in water outage area for initial three days and then 20 litters of water up to 2 weeks. As shown in the **Fig 7.10**, main water supply base are exiting reservoirs and existing wells. The number of the base will be increased by setting emergency water supply taps to fire hydrant on restored distribution line.

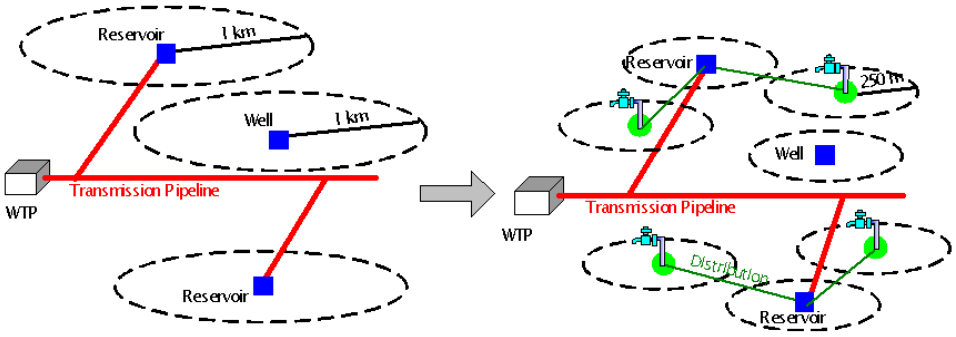

Fig 7.10 Overview of emergency water supply

7.7.1 Methods of emergency water supply

7.7.1.1 Preparation of emergency water supply

It is important for smooth execution of emergency water supply to prepare emergency water supply beforehand. The proposed methods for emergency water supply, mobilization of staffs, receiving of assistants form other provinces, and allocation of teams is described herein (TWWC 2006). For preparation of the plan of emergency water supply, following shall be paid attentions:

- ✓ Estimation of water supply interrupted population
- ✓ Securing methods of drinking water
- ✓ Selection of materials and equipment for emergency water supply
- ✓ Selection of high priority in emergency water supply (Evacuation places, general hospitals, welfare facilities and other places executing emergency activities)
- ✓ Initial activities and deployment of required personnel, vehicles etc.

7.7.1.2 Water supply at emergency water supply bases

Supply interrupted consumers will get water from emergency water supply base, which will be prepared in every one kilometer. Since existing reservoirs are selected as emergency

water base, water shall be stored there until treated water is transmitted. When water transmission lines are reinforced, water will be transmitted to all the reservoirs just after recovery of power suspension, which period is assumed as one week. The amount to be stored in reservoirs for each person is calculated as:

$$(3litters \times 3days) + (20litters \times 4days) = 89\,litters/person$$

Two third of the volume of water reservoir is assumed to be remain in the reservoir after earthquake since the capacity of the reservoir is about 24 hours of daily demand and one third of the capacity will be enough for daily demand fluctuation and other daily urgent purpose. The remaining one third of the volume will be used for urgent work mainly fire fighting and the other one third is stored for emergency water supply to people. The total capacity of Bam water reservoirs are about 30000 m^3 which base on above assumption one third of the volume (10000 m^3) can be used for emergency water supply. The water requested population of Bam city and rescue dispatched personals are around 100000. Therefore the required amount of water for the first week is about 9000 m^3 which is less than available water (10000 m^3). But in case of water shortage, the water supply base other than existing reservoir is well, which has sufficient yield capacity for emergency water supply and to be equipped with generator. Drinking water shall be stored in emergency tank in the poor water quality of groundwater area.

7.7.1.3 Water Tanker

Water shall be supplied by water tanker in the area of insufficient water supply bases. When traffic of road is secured after earthquake, water tanker is useful to transmit water from emergency water supply base to temporary tanks to be installed. It is also helpful in the area of poor water quality or insufficient water supply. When small sized water tanker of 1-2 m^3 capacity is used for narrow road area, water will be directly supplied to consumers from water tanker. The location of water tanker is shown in **Fig 7.11**. Totally 20 water tanker in the first day can supply the bam city area by the assumption that each people can walk less than 1.0 km to access to the drinking water. But one month after earthquake for prevents decreasing the acceptance level of customers, the number of water bases increase in non restored area (restoration zone no. 4 and 6). Therefore as shown in **Fig 7.12**, the total 20 water bases are used and the target distance is decrease to 500 meter. These water tankers should be replaced by temporary water taps which connected to the water network. In this case the target distance can be reduced to 250 meter.

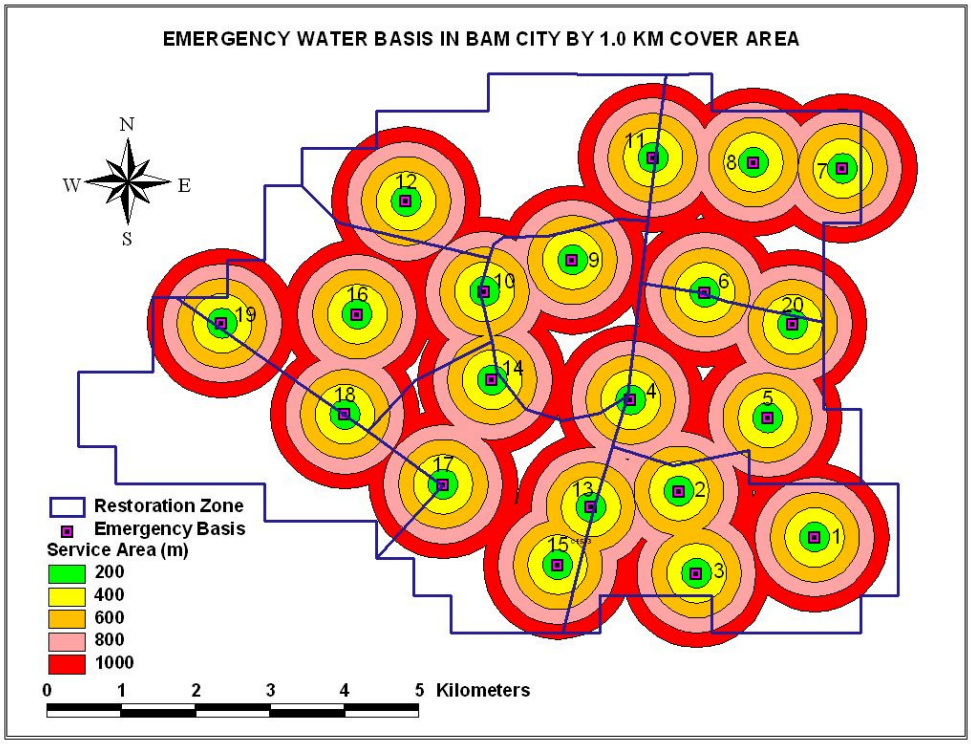

Fig 7.11 Emergency water bases in Bam city with 1.0 km cover area (first week)

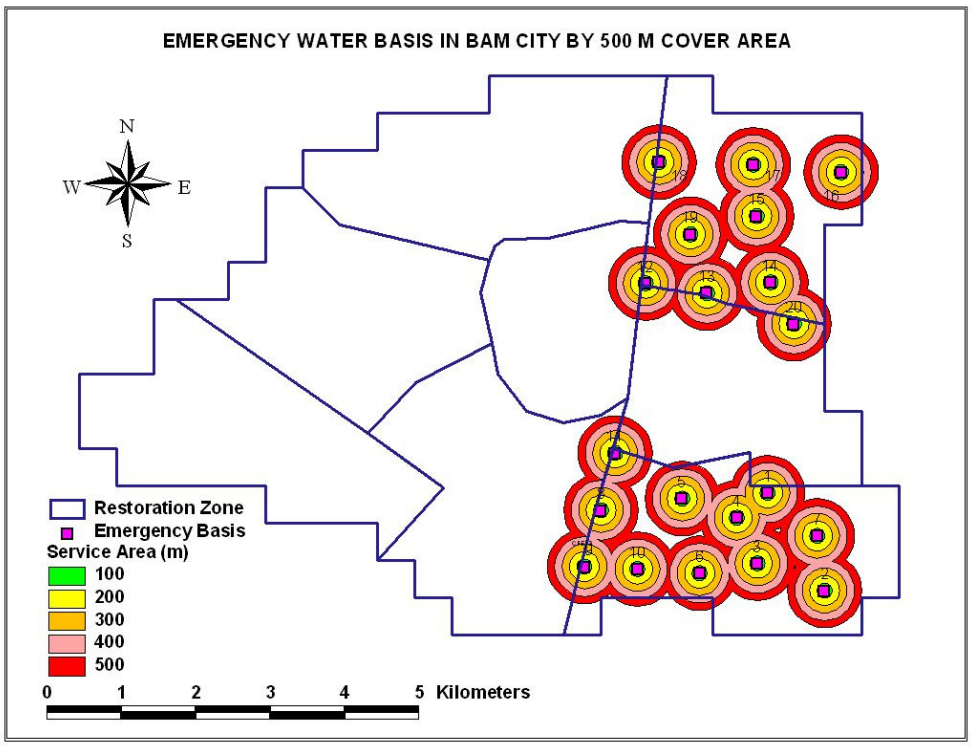

Fig 7.12 Emergency water bases in Bam city with 500 m cover area (after one month)

7.7.2 Safety of water quality

Maximum attention shall be paid to safety of water quality for usage of emergency water base under the responsibility of laboratories. Simple chlorination facilities and guideline for chlorination shall be prepared at the site considering that unaccustomed assistants also handle it. Water quality shall be checked before water supply by using simple kit for checking residual chlorine. After the efforts, when there is possibility of insufficient disinfection, consumers shall be instructed to boil water before drinking.

Some groundwater contain high nitrate, which might cause cyanosis to infant. If water quality of groundwater found to be unsuitable for drinking after testing, drinking water shall be supplied by tanker. Emergency water tanks are required to be installed to supplement well water for drinking purpose where water supply by tanker is not suitable. The same arrangement will be required if the wells locate near factories and there is a possibility of pollution after earthquake.

7.7.3 Storage of materials and equipment

Required materials and equipment shall be listed up and prepared as much as possible. It is required to prepare maintenance methods of procured tools and equipment especially the ones which will be used only after earthquakes.

It is necessary to distribute the material and equipment at several locations for quick and easy start of the emergency activities. It is recommended to equip at gathering places with some materials such as cameras, cotton work gloves, flashlights, keys for valve, manhole opener, flashlights with generator, fire fighting horse, motor bikes and emergency medical kit. Maps, pipeline drawings, canned food, cooking tools, folding bed and blanket are also required especially for assistants form other provinces and far resident. Warehouse is required to be constructed at emergency water base and store;

- ✓ Manual for emergency water supply
- ✓ Chlorine (Calcium hypochlorite)
- ✓ Simple residual chlorine meter
- ✓ Engine pump for water supply
- ✓ Temporary pipes and temporary water supply taps

Water supply bases shall be prepared by water supply responsible company and consumer shall be instructed to secure some amount of water. In addition, emergency distribution of

bottled water will be also very useful to supplement the activities. It is recommended to consider introduction of water packing machine for water bag or bottling. It is also better to consider introduction of portable water treatment equipment, which can treat water at emergency sites. The method of maintenance during the ordinal time shall be carefully studied especially when it is membrane filter type.

7.8 Summary and Conclusions

Following an earthquake, loss of infrastructure system functionality can significantly disrupt normal economic activity. The duration of this loss of service is a critical determinant of the ultimate magnitude of economic disruption. Therefore quantitative models of the post-earthquake restoration process are important in evaluating the total economic loss caused by an earthquake. So, the restoration models of Bam interdependent critical infrastructures are analyzed in this chapter. The results of model are mentioned that the duration of water network restoration depends on the power network. For example, water network restoration process in the first day doesn't have any significant progress and that is because of required damage repair period in power network. On the other hand, during the restoration work, emergency water supply should be done to achieve the customer's acceptance criteria. The restoration period of Bam power network is about one week but in case of water network is increased to two months. The total numbers of required emergency water bases are 20 which distributed in Bam city area in the first week after earthquake and they are concentrated to non restored area (zone 4 and 6) after one month.

CHAPTER 8

SUMMARY AND CONCLUSIONS

8.1 Introduction

Modern societies are becoming increasingly dependent on critical infrastructure systems specially lifelines to provide essential services that support economic prosperity and quality of life. Water distribution systems, electrical power transmission systems, and other lifeline systems are not alone but interdependent at multiple levels. Interdependencies enhance the overall system performance while also increasing the potential for cascading failures and amplifying the impact of small failures into catastrophic events. To understand the cascading failures among infrastructure systems under random incidents, man made attacks and natural hazards, many researchers have proposed different methods for modeling and simulation of interdependent infrastructure systems. Notable examples include Agent Based Methods (ABM), Inoperability Input output Methods (IIM), System Dynamics Methods (SDM), Network or Graph Based Methods (NBM) and Data Driven Methods (DDM).

8.2 Conclusions

In order to better understand the critical infrastructure role in a society and also learn more about components of interdependent critical infrastructure and their seismic performance, the characteristics of critical infrastructures are illustrated in chapter 2 and a literature review on the recent advances is presented in the fields of complex networks, network topology, network dynamics, and interconnected systems. For each of the main typologies, the different damage states are related to serviceability of the whole network or the single component, depending on the considered analysis level. Therefore damage scales for network components are defined here for using in seismic performance analysis.

As a case study, the city of Bam in south east of Iran is considered where is affected by an earthquake in 2003. The earthquake was by far the most devastating earthquake in the history of the region around Bam which destroyed most of the city and nearby villages.

In order to compare the real situation with analytical results which obtain in the research, the characteristics of Bam city infrastructures and their performance during the earthquake are investigated. Water network in Bam experienced heavy damage and the water supply was cut off for a long duration due to extensive pipe breaks. Power electric substation and numerous

electrical concrete poles are damaged which caused blackouts in city within hours following the earthquake and power had not been restored for several days.

The approaches for critical infrastructure modeling are illustrated in chapter 3 and the graph based method is considered which uses nodes to represent different types of system components and links to present the physical and relational connections among them, provides affordable and intuitive system representations along with detailed descriptions of their topology and flow patterns. This method can analyze the effects of system topology, element physical fragility, and attack intensity on system performance levels which are measured by connectivity and flow delivery. Therefore some of the most relevant parameters including mean distance, vertex degree, clustering coefficient and redundancy ratio are introduced. These mentioned parameters are computed for Bam critical infrastructures and their important nodes based on each parameter are defined. The obtained results will be used to estimate the potential resilience of networks in the research.

The framework of lifeline seismic analysis especially *PSHA* methodology is summarized in chapter 4 and the probabilistic seismic hazard maps of Bam city is obtained. After considering the active fault and considering appropriate attenuation relationships, PGA and PGV were calculated in 2475-year return period for 500 m grid mesh. The repair ratio of buried pipelines is computed for each cell based on ALA-2001, and after that damage probability of pipelines is derived. The results consistent with happened damages after the earthquake. Based on the results, density of damaged pipelines and power electric lines especially in east and southern east part of the city is more than another. Results of vulnerability analysis appropriately are consistent with reality and actual damages. However in this study, only main distribution lines are analyzed and also the exact materials of lines such as joint types were not clear. Therefore, some differences are due to those matters. The results can be used as an important input data for network reliability analysis, disaster management and post earthquake activities such as emergency water supply.

It is presumed that, eventually, the topological deterioration of the overall connectivity due to the failure of any of the element/s compromises the functionality of the entire network. Independent of the nature of the disruption and the mechanism by which it propagates either by overloading the most connected vertices, or the vertices most in between other vertices, or the most instrumental to flow circulation, or by random malfunction, overall network functionality needs to be characterized. Therefore before proceeding with the network analysis, performance measures are introduced for quantified the performance of the network regardless of the hazard type. Five network performance measures, efficiency, betweenness loss, connectivity loss,

serviceability loss and impact factor on the population are described. All of these measures are based upon the topological properties taken from graph theory.

Based on the measures, the fundamental concepts of reliability are introduced and the reliability analysis of individual infrastructure systems subjected to spatially correlated seismic demands is done. The results are used to assess potential risks of earthquake for infrastructure systems, to improve redundancy of infrastructure systems efficiently, to create restoration plans at lower cost and higher efficiency, and to design the layout of facilities and distributing elements of infrastructure systems.

For modeling the interdependency between critical infrastructures, two important issues of modern interdependent critical infrastructure systems are studied in this research. First the network response under seismic hazard is assessed; then the increased vulnerability due to coupling between networks is analyzed. The coupling behavior among networks is characterized as a physical dependency of the potable water network on the electricity grid through the water source nodes and pump stations. The dependence of one network on the other is modeled with an interoperability matrix, which is defined in terms of the strength of coupling; additionally it is considered how the mechanical structural fragility of the substations and poles of the electric power supply contributes to this dependence.

In a topological sense, the network interdependency model manages to follow the propagation of failures resulting from seismic vulnerability of the power network and how they affect the topology of the water network. The partial dependence of the water network on the power network introduces an additional implicit seismic vulnerability of the water network over and above the explicit structural seismic vulnerability of the components of the water network.

Network damage was measured in terms of connectivity loss, power loss and impact factor on the affected population. Damage was evaluated at both macroscopic (for the whole network) and at a local levels by examining the damage status of each and every water demand node in the water network. The seismic vulnerability of power and water networks, having been condensed in the form of fragility curves of the independent and dependent systems. Results is expected, that the highest direct damages are occurred in east and southeast of Bam city. However, this does not imply that the Bam power network is only locally vulnerable to seismic hazards. The results are used for the disaster management of interdependent network activities spatially in restoration process modeling in the research.

Following an earthquake, loss of infrastructure system functionality can significantly disrupt normal economic activity. The duration of this loss of service is a critical determinant of the ultimate magnitude of economic disruption. Therefore quantitative models of the post-

earthquake restoration process are important in evaluating the total economic loss caused by an earthquake. So, the restoration models of Bam interdependent critical infrastructures are analyzed in last chapter. The results of model are mentioned that the duration of water network restoration depends on the power network. For example, water network restoration process in the first day doesn’t have any significant progress and that is because of required damage repair period in power network. On the other hand, during the restoration work, emergency water supply should be done to achieve the customer's acceptance criteria.

REFERENCES

[1] Ancas D., Doniga C, Atanasiu G.(2006). Current state of the art for existing critical systems in urban seismic area, Bulletin of technical University of Iasi, 1-2, in print

[2] Adachi, Takao and Ellingwood, Bruce R. (2007). Assessment of probabilistic seismic hazard analysis applied to the networked civil infrastructure systems. Manuscript under review by Journal of Infrastructure Systems, American Society of Civil Engineers (ASCE).

[3] Adachi T, Ellingwood BR. (2008). Serviceability of earthquake damaged water systems: effects of electrical power availability and power backup systems on system vulnerability. Reliability Engineering and System Safety 93: 78–88.

[4] Association for Development of Earthquake Prediction (1986). Seismic Assessment and Restoration Method of Electric Power System and its components. Technical Report from ADEP.

[5] Axelroad R, Cohen M. (1999). Harnessing complexity: Organizational implications of a scientific frontier. Published by Simon and Schuster Inc.

[6] Basu N, Pryor R, Quint T. (1998). ASPEN: a micro simulation model of the economy. Computational Economics, 12(2): 23–41.

[7] Brown, T., Beyeler, W., Barton, D. (2004). Assessing infrastructure interdependencies: the challenge of risk analysis for complex adaptive systems, International Journal of Critical Infrastructures 1(1): 108–117.

[8] Bush, B., Dauelsberg, L., LeClaire, R., Powell, D., DeLand, S., Samsa, M. (2005). Critical infrastructure protection decision support system project overview. Technical Report LA-UR-05-1870. Los Alamos National Laboratory.

[9] Chang, S.E.; Seligson, H.A. and Eguchi, R.T. (1996). Estimation of the Economic Impact of Multiple Lifeline Disruption: Memphis Light, Gas and Water Division Case Study (NCEER-96-0011). Buffalo, N.Y.: The Multidisciplinary Center for Earthquake Engineering Center (MCEER).

[10] Chou CC, Tseng SM. (2010). Collection and analysis of critical infrastructure interdependency relationships. Journal of Computing in Civil Engineering, (ASCE) CP.1943-5487.

[11] Conrad, K. (1997). Traffic, transportation, infrastructure and externalities: a theoretical framework for a CGE analysis. The Annals of Regional Science 31(4): 369–389.

[12] Conrad, K., Heng, S. (2002). Financing road infrastructure by savings in congestion costs: a CGE analysis. The Annals of Regional Science 36(1): 107–122.

[13] Conrad SH, LeClaire RJ, O'Reilly GP, Uzunalioglu H. (2006). Critical national infrastructure reliability modeling and analysis. Bell Labs Technical Journal 11(3): 57–71.

[14] Crowther KG, Haimes YY. (2010). Development of the multiregional inoperability input–output model (MRIIM) for spatial explicitness in preparedness of interdependent regions. Systems Engineering 13(1): 28–46.

[15] Dudenhoeffer, D., Permann, M., Manic, M. (2006). CIMS: a framework for infrastructure interdependency modeling and analysis. In: Proceedings of the 2006 Winter Simulation Conference, Monterey, CA, 478–485.

[16] Duenas-Osorio, L., Craig, J., Goodno, B. (2004). Probabilistic response of interdependent infrastructure networks. In: Proceedings of the 2nd Annual Meeting of the Asian-Pacific Network of Centers for Earthquake Engineering Research (ANCER), Honolulu, Hawaii.

[17] Duenas-Osorio, (2005). Interdependent response of networked systems to natural hazards and intentional disruptions. Chapter 4: Network models. Dissertation, Georgia Institute of Technology. Atlanta: Georgia Tech Library, UMI 3198529.

[18] Duenas-Osorio, L., Craig, J., Goodno, B., Bostrom, A. (2007). Interdependent response of networked systems. ASCE Journal of Infrastructure Systems 13(3); 185–194.

[19] Ehlen MA, Scholand AJ. (2005). Modeling interdependencies between power and economic sectors using the N-ABLE agent based model. In: Proceedings of the IEEE conference on power systems, San Francisco.

[20] Eusgeld I, Nan C. (2009). Creating a simulation environment for critical infrastructure interdependencies study. In: Proceedings of the IEEE international conference on industrial engineering and engineering management, Hong Kong, 8–11 December 2009. 2104–2108.

[21] Eusgeld I, Nan C, Dietz S. (2011). System-of-systems approach for interdependent critical infrastructures. Reliability Engineering and System Safety 96: 679–86.

[22] Fedora, Philip A. (2004). Reliability Review of North American Gas and Electric System Interdependency. Proceedings of the 37th Hawaii International Conference on System Sciences, IEEE.

[23] Federal Emergency Management Agency (1997). HAZUS 97 Technical Manual. Washington D.C.: Federal Emergency Management Agency (FEMA).

[24] Federal Emergency Management Agency (2003). HAZUS MH MR1 Technical Manual. Washington D.C.: Federal Emergency Management Agency (FEMA).

[25] Friesz, T.L., Peeta, S., Bernstein, D.H. (2001). Multi-layer infrastructure networks and capital budgeting. Working Paper TF0801A. George Mason University and Purdue University.

[26] Gillette, J. L., Fisher, R. E., Peerenboom, J. P., Whitfield, R. G. (2002). Analyzing water and wastewater infrastructure interdependencies. 6th International Conference on Probabilistic Safety Assessment and Management. San Juan.

[27] Haimes YY, Jiang P. (2001). Leonief based model of risk in complex interconnected infrastructures. Journal of Infrastructure Systems. 7(1): 1–12.

[28] Haimes, Y.Y., Horowitz, B.M., Lambert, J.H., Santos, J.R., Crowther, K.G., Lian, C. (2005a). Inoperability input–output model for interdependent infrastructure sectors. II: Case studies. Journal of Infrastructure Systems 11(2): 80–92.

[29] Haimes, Y.Y., Horowitz, B.M., Lambert, J.H., Santos, J.R., Lian, C., Crowther, K.G. (2005b). Inoperability input–output model for interdependent infrastructure sectors. I: Theory and methodology. Journal of Infrastructure Systems 11(2): 67–79.

[30] Hines P, Cotilla-Sanchez E, Blumsack S. (2010). Do topological models provide good information about vulnerability in electric power networks? Physics and Society 1002.2268.

[31] Hwang H, Shinozuka M. (1998). Seismic performance assessment of water delivery systems. Journal of Infrastructure Systems 4(3);118-125

[32] Jeong, H., Qiao, J., Abraham, D., Lawley, M., Richard, J.P., Yih, Y. (2006). Minimizing the consequences of intentional attack on water infrastructure. Computer- Aided Civil and Infrastructure Engineering 21(2): 79–92.

[33] Johansson J, Hassel H. (2010). An approach for modeling interdependent infrastructures in the context of vulnerability analysis. Reliability Engineering System Safety 95(13): 35–44.

[34] Kang WH, Song J, Gardoni P. (2007). Matrix-based system reliability and applications to bridge networks. Proceedings of 10th International Conference on Applications of Statistics and Probability in Civil Engineering (ICASP), Tokyo, Japan, July 31-August 3

[35] Kameda, H. (1999). Recent developments and research initiatives for urban earthquake disaster mitigation. Keynote Address, Proceedings of the 6th Japan/United States Workshop on Urban Earthquake Hazard Reduction, ISSS/EERI, Kobe, 17-30.

[36] Kim YS, Spencer BF, Elnashai AS, Ukkusuri S, Waller ST. (2006). Seismic performance assessment of highway networks. The 8th National Conference for Earthquake Engineering, San Francisco, U.S.A., April 18-22.

[37] Kim Y, Spencer BF, Elnashai AS, Song J. (2009). Seismic performance assessment of interdependent lifeline systems. International Journal of Engineering Under Uncertainty: Hazards, Assessment and Mitigation. 1(3–4); 173–180.

[38] Koike T. (2006). Seismic risk assessment of a water supply lifeline system in Baku. The report of Baku water project.

[39] Kroger W. (2008). Critical infrastructures at risk: a need for a new conceptual approach and extended analytical tools. Reliability Engineering and System Safety 93; 1781–1787.

[40] Leontief WW. (1951). Input–output economics. Scientific American 10: 15–21.

[41] Li J, He J. (2002). A recursive decomposition algorithm for network seismic reliability evaluation. Earthquake Engineering and Structural Dynamics 31(8): 1525- 1539.

[42] Little, Rachel A, Huan Zhao, and Vineet Kumar. (2002). Controlling cascading failure: A systems approach to addressing multiple hazards. Presented to the natural disasters roundtable, The national academies, Feb 28th.

[43] Macal, C.M., North, M.J. (2002). Simulating energy markets and infrastructure interdependencies with agent based models. In: Proceedings of the Workshop on Social Agents: Ecology, Exchange and Evolution, Chicago, IL, 195–214.

[44] Matsushita, M. (1999a). The 1995 Kobe Earthquake and the new JWWA seismic design guideline for water facilities," Proceedings of the 7th US/Japan Workshop on Seismic Resistant Design of Lifeline Facilities and Countermeasures Against Liquefaction, Seattle.

[45] Mc Daniels T, Chang S, Peterson K, Mikawoz J, Reed D. (2007). Empirical framework for characterizing infrastructure failure interdependencies. Journal of Infrastructure Systems 13(3): 175–184.

[46] Nagurney, A., Dong, J. (2002). Supernetworks: Decision-making for the Information Age. Edward Edgar Publishing, Cheltenham, England.

[47] North American Electric Reliability Council (NERC). (2004). Gas and Electricity Interdependencies and Recommendations. Prinston, NJ: North American Electric Reliability Council.

[48] North, M.J. (2001). Multi-agent social and organizational modeling of electric power and natural gas markets. Computational Mathematical Organization Theory 7(4): 331–337.

[49] North MJ. (2001). Toward strength and stability: agent-based modeling of infrastructure markets. Social Science Computer Review 19(3): 307–329.

[50] Nozick, L.K., Turnquist, M.A., Jones, D.A., Davis, J.R., Lawton, C.R. (2005). Assessing the performance of interdependent infrastructures and optimizing investments. International Journal of Critical Infrastructures 1(2/3): 144–154.

[51] Qiao, J., Jeong, D., Lawley, M., Richard, J.P., Abraham, D., Yih, Y. (2007). Allocating security resources to a water supply network. IIE Transactions, Special Issue on Homeland Security 39(1): 95–109.

[52] Quimpo, Rafael G. and Wu, Sue-Jen (1997). Condition assessment of water supply infrastructure. Journal of Infrastructure Systems 3(1): 15-22.

[53] Ouyang M, Hong L, Mao ZJ, Yu MH, Fei Q. (2009). A methodological approach to analyze vulnerability of interdependent infrastructures. Simulation Modeling Practice and Theory 17(8): 17–28.

[54] Ouyang M, Duenas-Osorio L. (2011). An efficient approach to compute the generalized interdependent effects between infrastructure systems. ASCE Journal of Computing in Civil Engineering, doi: 10.1061/ (ASCE)CP.1943- 5487.0000103.

[55] Pederson, P., Dudenhoeffer, D., Hartley, S., Permann, M. (2006). Critical infrastructure interdependency modeling: a survey of US and international research. Technical Report INL/EXT-06-11464. Idaho National Laboratory.

[56] Poljansek, K., Bono, F., Gutierrez, T.E. (2010). GIS-based method to assess seismic vulnerability of interconnected infrastructure: A case of EU gas and electricity networksEUR - Scientific and Technical Research Reports.

[57] Peerenboom, James P., Fisher, Ronald E., Rinaldi, Steven M. and Kelly, Terrance K. (2002). Studying the Chain Reaction.

[58] Rinaldi SM, Peerenboom JP, Kelly TK. (2001). Identifying, understanding, and analyzing critical infrastructure interdependencies. IEEE Control Systems Magazine 12: 11–25.

[59] Robert, Benoit (2004). A method for the study of cascading effects within lifeline networks. International Journal of Critical Infrastructures 1(1): 86-99.

[60] Rosato V, Issacharoff L, Tiriticco F, Meloni S. (2008). Modeling interdependent infrastructures using interacting dynamical models. International Journal of Critical Infrastructure (IJCI) 4(1–2): 63–79.

[61] Rose, Adam; Benavides, J; Chang S.E.; Szczesniak, P and Lim,D. (1997). The Regional Economic Impact of an Earthquake: Direct and Indirect Effects of Electricity Lifeline Disruptions. Journal of Regional Science. 37(3): 437-458.

[62] Santos JR, Haimes YY. (2004). Modeling the demand reduction input–output inoperability due to terrorism of interconnected infrastructures. Risk Analysis 24(6): 1437–1451.

[63] Santella N, Steinberg LJ, Parks K. (2009). Decision making for extreme events: modeling critical infrastructure interdependencies to aid mitigation and response planning. Review of Policy Research 26(4): 409–422.

[64] Satyanarayana, A. and Wood, R. Kevin (1985). A linear-time algorithm for computing K-terminal reliability in series-parallel networks. SIAM Journal of Computing 14(4); 818-832.

[65] Shinozuka, M.: Hwang, H. and Murata, M. (1992). "Impact on Water Supply of a Seismically Damaged Water Delivery System." Lifeline Earthquake Engineering in the Central and Eastern U.S.: 43-57.

[66] Shinozuka, Masanobu; Chang, Stephanie E.; Eguchi, Ronald T.; Abrams, Daniel P.; Hwang, Howard H.M. and Rose, Adam (1997). Advances in Earthquake Loss Estimation and Application to Memphis, Tennessee." Earthquake Spectra. 13(4): 739-758.

[67] Shinozuka, M.; Rose, A. and Eguchi, R.T. (1998). Engineering and Socioeconomic Impact of Earthquake –an analysis of electricity lifeline disruptions in the New Madrid area- (MCEER Monograph Series 2). Buffalo, NY: Multidiciplinary Center for Earthquake Engineering Research.

[68] Shinozuka, M; Cheng, Tsen-Chung; Feng, Maria Q. and Mau, Sheng-Taur (1999). "Seismic Performance Analysis of Electric Power Systems." MCEER Research Progress and Accomplishments 1997-1999; 61-69.

[69] Shinozuka M, Dong X, Chen TC, Jin X. (2007). Seismic performance of electric transmission network under component failures. Journal of Earthquake Engineering and Structural Dynamics 36(2): 227-244.

[70] Takada, Shiro and Imanishi, Tatsuhiko (2003). "Time and Space Restoration Process and Prediction of Recovery Period for Damaged Water Supply Systems Based on GIS Data of The 1995 Kobe Earthquake." Technical Council on Lifeline Earthquake Engineering Monograph 25: 39-48.

[71] Thomas, W.H., North, M.J., Macal, C.M., Peerenboom, J.P. (2003). Complex adaptive systems representation of infrastructure interdependencies. Naval Surface Warfare Center Technical Digest, Naval Surface Warfare Center, Dahlgren, VA. 58–67.

[72] Tolone, W.J., Wilson, D., Raja, A., Xiang, W.N., Hao, H., Phelps, S., Johnson, E.W. (2004). Critical infrastructure integration modeling and simulation. In: Proceedings of the 2nd Symposium on Intelligence and Security Informatics, 214–225.

[73] U.S.–Canada Power System Outage Task Force (2006). Final report on the August 14, 2003 blackout in the United States and Canada: causes and recommendations.

[74] Vanzi I. (1996). Seismic reliability of electric power networks: methodology and application. Structural Safety 18(4): 311– 327.

[75] Wagner, Janet M.; Shamir, Uri; Marks, David H. (1988a). Water Distribution Reliability: Analytical Methods. Journal of Water Resources Planning Management: 114(3); 253-275.

[76] Wagner, Janet M.; Shamir, Uri; Marks, David H. (1988b). Water Distribution Reliability: Simulation Methods. Journal of Water Resources Planning Management 114(3): 276-294.

[77] Winkler J, Duenas-Osorio L, Stein R (2012). Subramanian D. Interface network models for complex urban infrastructure systems. ASCE Journal of Infrastructure Systems, doi:10.1061 (ASCE)IS.1943-555X.0000068.

[78] Yang, Han and Shaoping, Sun (2003). Seismic Reliability of Urban Pipeline Network Systems. Proceedings of the Sixth U.S. Conference and Workshop on Lifeline Earthquake Engineering: 445-454.

[79] Zhang, P., Peeta, S., Friesz, T.L. (2005). Dynamic game theoretic model of multi-layer infrastructure networks. Networks and Spatial Economics 5(2): 147–178.

[80] Zhang, P., Peeta, S. (2010). Implementation and computation issues in interdependent infrastructure systems analysis. Working Paper. Purdue University, West Lafayette, IN.

[81] Zhang, P., Peeta, S. (2011). Dynamic analysis of interdependent infrastructure systems. In: Proceedings of the 90th Annual Meeting of the Transportation Research Board, Washington, DC.

[82] Zhang PC, Peeta S. (2011). A generalized modeling framework to analyze interdependencis among infrastructure system. Transportation Research PartB 45: 553–579.

APPENDIX

Appendix A.1

Example sheet of the Bam city water network

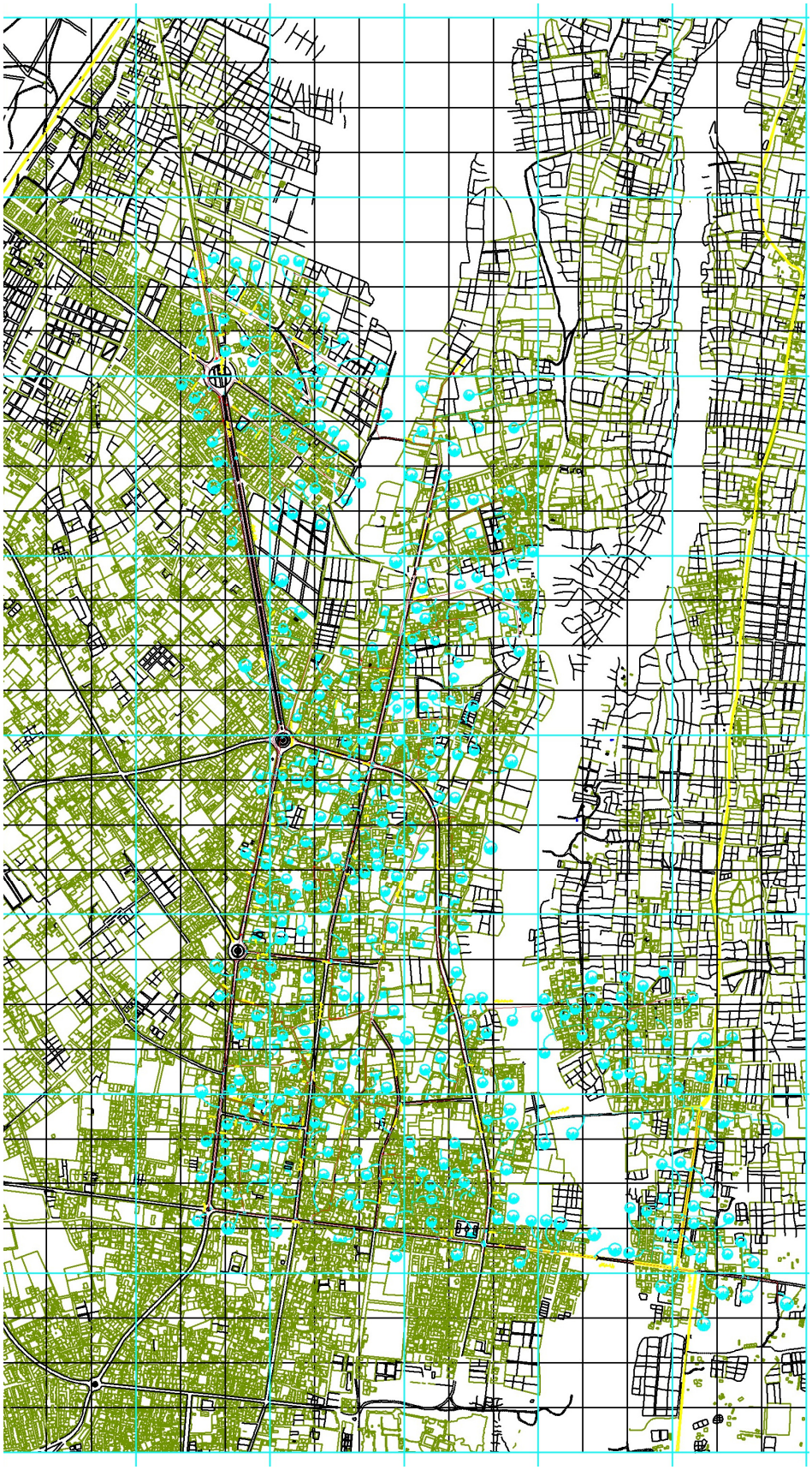

Appendix A.2

Example sheet of the Bam city power network

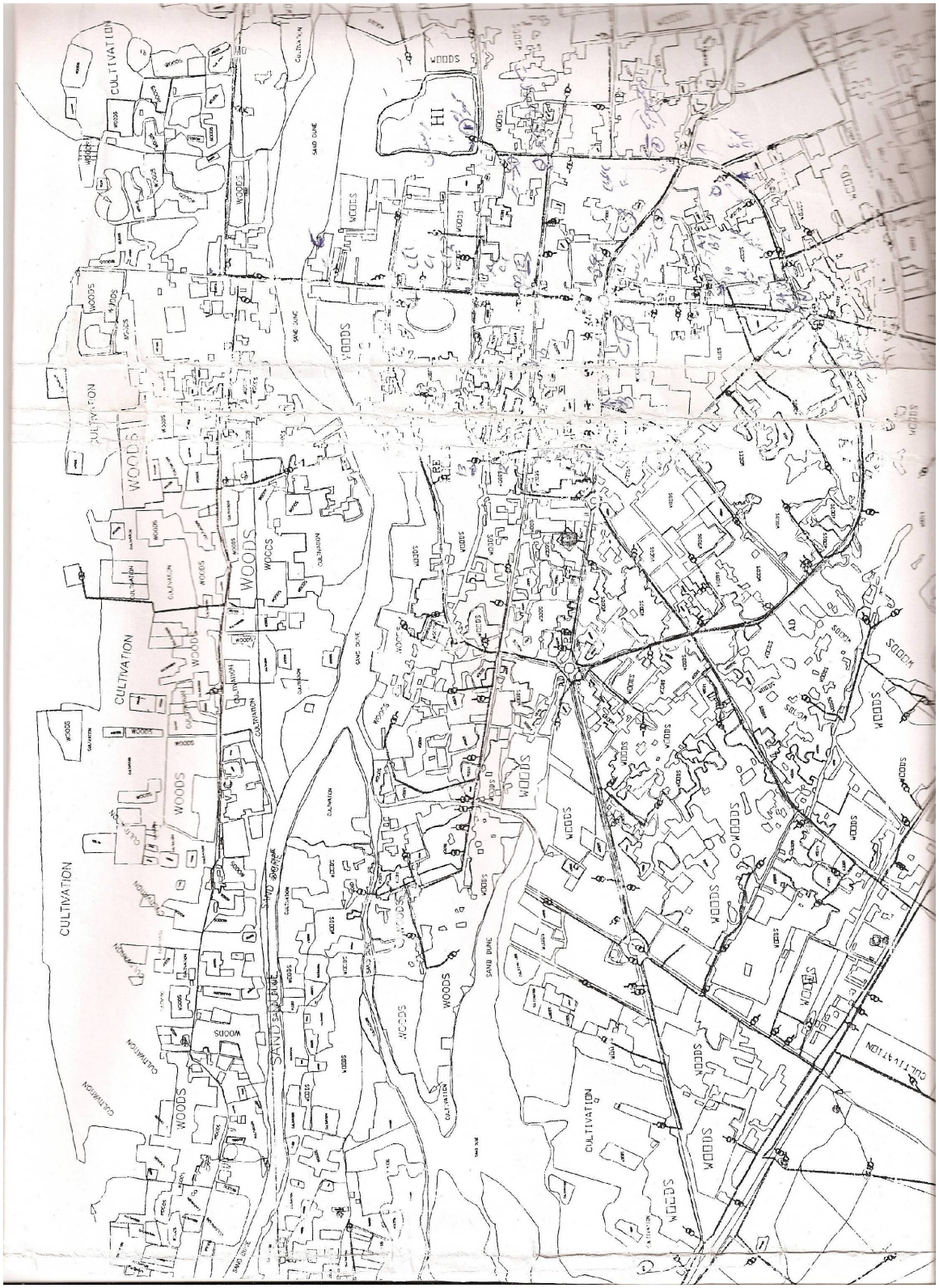

Appendix B.1

Normalized auto-covariance model of the 2011 Tohuku earthquake
(E-W direction)

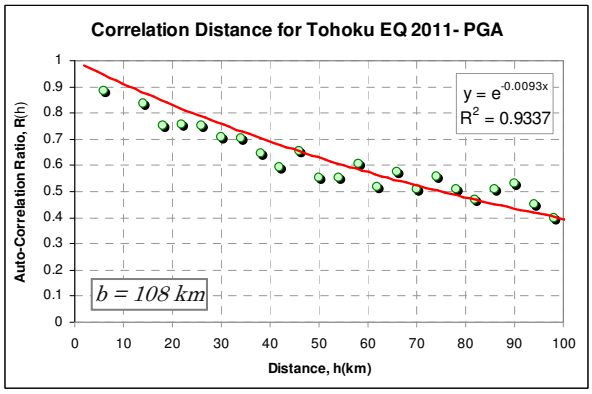

(a)

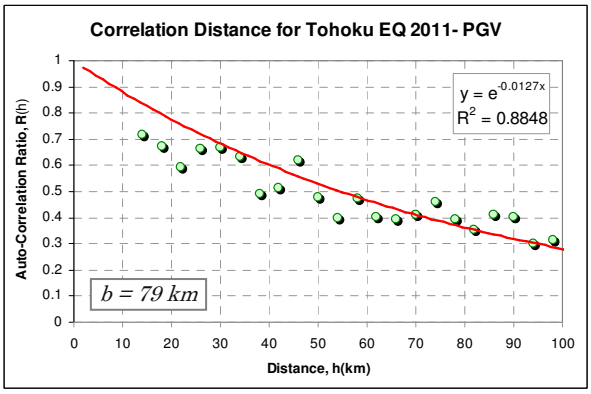

(b)

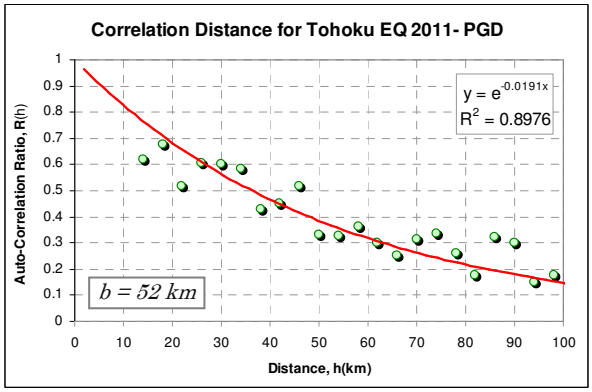

(c)

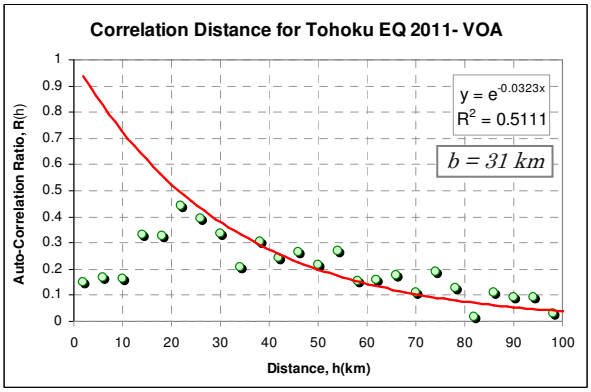

(d)

Normalized auto-covariance function in E-W direction
(a) PGA, (b) PGV, (c) PGD, (d) PGV/PGA

Appendix B.1

Normalized auto-covariance model of the 2011 Tohuku earthquake
(N-S direction)

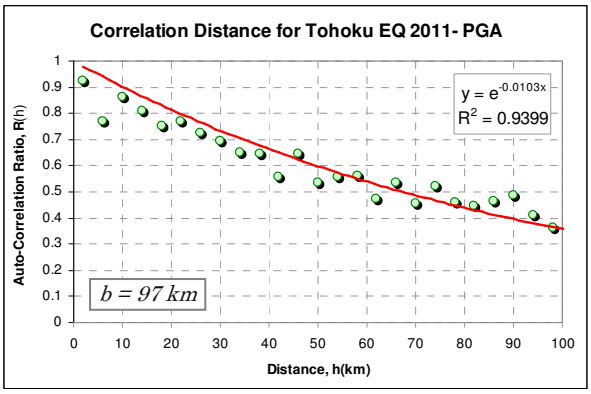

(a)

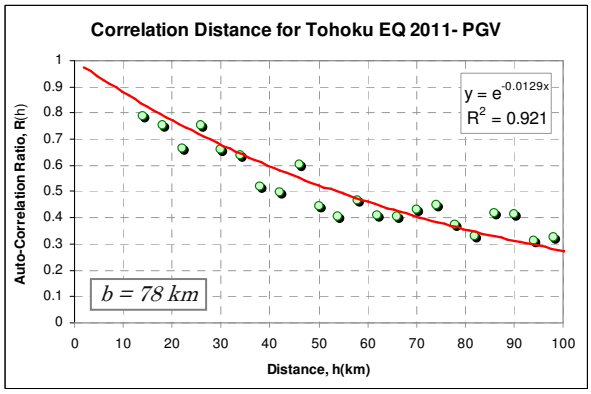

(b)

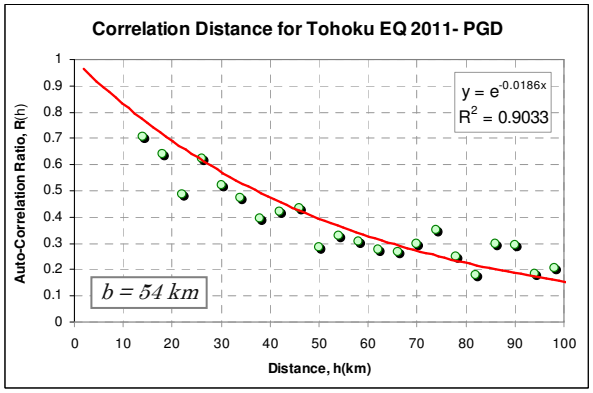

(c)

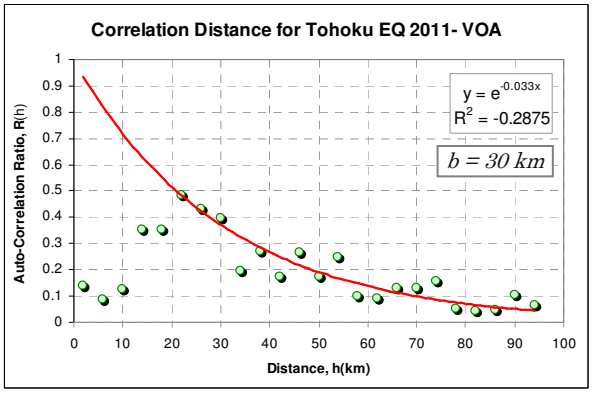

(d)

Normalized auto-covariance function in N-S direction
(a) PGA, (b) PGV, (c) PGD, (d) PGV/PGA

Appendix B.1

Normalized auto-covariance model of the 2011 Tohuku earthquake
(U-D direction)

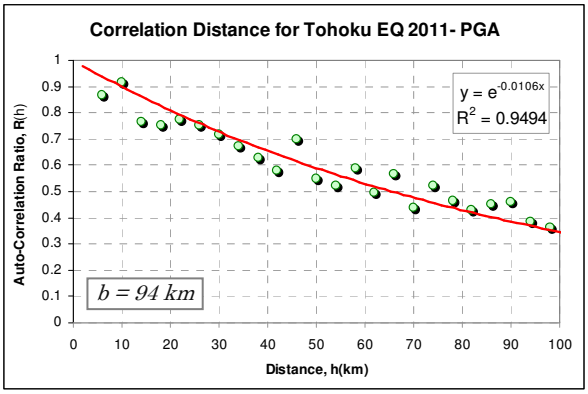

(a)

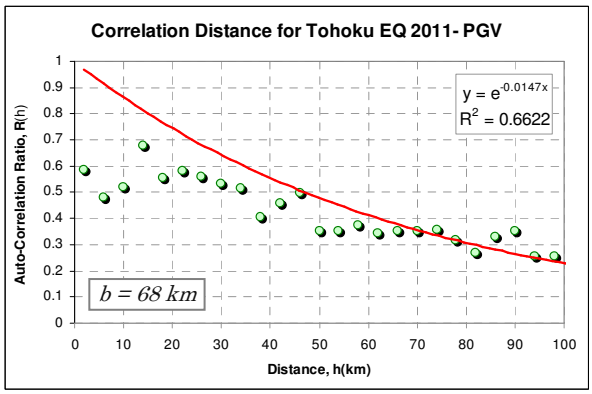

(b)

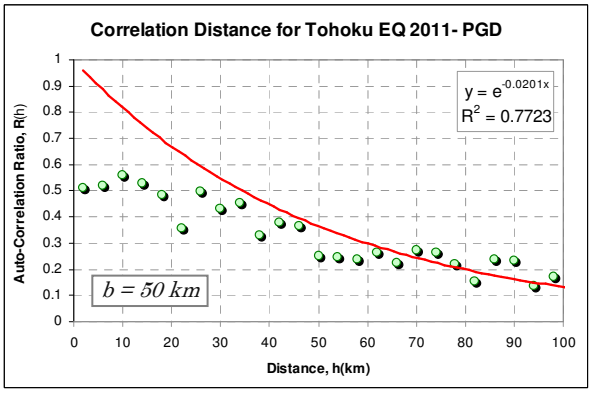

(c)

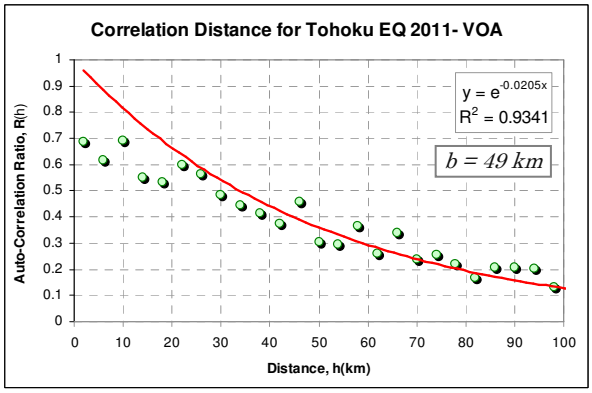

(d)

Normalized auto-covariance function in U-D direction
(a) PGA, (b) PGV, (c) PGD, (d) PGV/PGA

Appendix C.1

The Bam city geology map